



University of Milan
Ph. D. thesis

Development of analytical techniques for the characterization of natural and anthropogenic compounds in fine particulate matter

Tutor:

Dott.ssa Paola Fermo

Dep. of Inorg., Metall. and Analytical Chemistry, University of Milan

Dott.ssa Roberta Vecchi

Inst. of Applied General Physics, University of Milan

Coordinator

Prof. Franco Cozzi

Andrea Piazzalunga

Matr.n. R06068

XX cycle

a.a. 2006/07

«Se si escludono istanti prodigiosi e singoli che il destino ci può donare, l'amare il proprio lavoro (che purtroppo è privilegio di pochi) costituisce la migliore approssimazione alla felicità sulla terra. Ma questa è una verità che non molti conoscono.»

Primo Levi

Index

Part 1

Development of analytical techniques

1. Introduction.....	9
1.1. Carbonaceous Aerosol Components	10
1.2. Primary and Secondary Organic Aerosol Components	13
1.3. Climate and Health Effects	14
2. Set-up of Extraction Procedures for Ions Quantification in Aerosol Samples.....	21
2.1. Introduction	21
2.2. Experimental procedures	22
2.3. Results and discussion	23
2.4. Conclusions	27
3. A TGA/FT-IR study for measuring OC and EC in aerosol samples.	29
3.1. Introduction	29
3.2. Experimental	32
3.3. Analytical techniques	34
3.4. Results and discussion	38
3.5. Conclusions	50
4. Intercomparison between two different analytical techniques for Organic and Elemental Carbon in Atmospheric Aerosol Samples	53
4.1. Introduction	53
4.2. Experimental procedures	54
4.3. Results and discussion	55
4.4. Conclusions	59
5. Development of a novel technique for WSOC (Water Soluble Organic Carbon) quantification by Sunset Instrument and discussion about an hypothetical error in EC quantification.....	61
5.1. Introduction	61
5.2. WSOC quantification with TOT instrument	61
5.3. An hypothetical error in EC quantification	64
5.4. Conclusions	68

6. Identification and estimation of atmospheric aerosol main components: hit the target by means of a single analytical method.....	71
6.1. Introduction	71
6.2. Methods	71
6.3. Result and discussion	72
6.4. Conclusion	77
7. New analytical technique for levoglucosan quantification	79
7.1. Introduction	79
7.2. Analytical techniques	80
7.3. Conclusions	84
Part 2	
Field campaigns	
8. Carbonaceous particles in Lombardy region: the results of a two years campaign.....	89
8.1. Material and methods	91
8.2. PM and carbonaceous particles concentration	94
8.3. The contribution of wood combustion to particulate matter concentration	105
8.4. Estimation of secondary OC and preliminary apportionment of primary OC	109
8.5. Conclusions	112
9. PM mass concentration and chemical composition in the alpine remote site Bormio – San Colombano (N. Italy; 2,200 m a.s.l.).....	115
9.1. Introduction	115
9.2. Experimental settings	116
9.3. The mass of PM	117
9.4. The chemical composition of PM	118
9.5. Conclusions	120
10. Characterization of atmospheric aerosols at Monte Cimone, Italy, during summer 2004	123
10.1. Introduction	123
10.2. Sampling and Methods	125
10.3. Campaign Results	129
10.4. Discussion	136
10.5. Conclusions	137

11. A mass closure on the sub-micron sized aerosol fraction at urban sites in Italy.....	141
11.1. Introduction	141
11.2. Materials and methods	142
11.3. Results and discussion	145
11.4. Conclusions	152
12. PM ₁₀ physical and chemical characterisation using high-time resolved samplings in an air pollution “hot-spot” area in Europe.....	155
12.1. Introduction	155
12.2. Experimental	156
12.3. Results and discussion	158
12.4. Conclusions	168
13. Identification of secondary inorganic and organic aerosol components in urban particulate matter samples	171
13.1. EC tracer method	172
13.2. Comparison of SOC derived from EC tracer method and the PMF model	184
13.3. Secondary aerosol	186
13.4. Conclusions	188
14. Chemical and physical measurements for indoor air quality assessment at the Ca’ Granda historical archive, Milan (italy).....	191
14.1. Introduction	191
14.2. Materials and Methods	193
14.3. Results	196
14.4. Discussion	199
14.5. Conclusions	201
15. Particulate matter in Pietà Rondanini (by Michelangelo) storage room - Castello Sforzesco Museum, Milan	203
15.1. Introduction	203
15.2. Experimental	204
15.3. Results and discussion	205
15.4. Conclusion	213
16. Conclusions.....	215
[publications]	219
[congress comunactions]	221
Acknowledgment.....	225

1. Introduction

The effects of aerosols on the atmosphere, climate, and public health are among the central topics in current environmental research. Aerosol particles scatter and absorb solar and terrestrial radiation, they are involved in the formation of clouds and precipitation as cloud condensation and ice nuclei, and they affect the abundance and distribution of atmospheric trace gases by heterogeneous chemical reactions and other multiphase processes (Finlayson-Pitts et al., 2005; Houghton et al., 2001; Lohmann et al., 2005; Seinfeld and Pandis, 1998). Moreover, airborne particles play an important role in the spreading of biological organisms, reproductive materials, and pathogens (pollen, bacteria, spores, viruses, etc.), and they can cause or enhance respiratory, cardiovascular, infectious, and allergic diseases (Finlayson-Pitts et al., 2005; Bernstein et al., 2004; Finlayson-Pitts et al., 1997; Hinds, 1999).

Atmospheric aerosol particles originate from a wide variety of natural and anthropogenic sources. Primary particles are directly emitted as liquids or solids from sources such as biomass burning, incomplete combustion of fossil fuels, volcanic eruptions, and wind-driven or traffic-related suspension of road, soil, and mineral dust, sea salt and biological materials (plant fragments, microorganisms, pollen, etc.). Secondary particles, on the other hand, are formed by gas-to-particle conversion in the atmosphere (new particle formation by nucleation and condensation of gaseous precursors). As illustrated in Figure 1-1, airborne particles undergo various physical and chemical interactions and transformations (atmospheric aging), that is, changes of particle size, structure, and composition (coagulation, restructuring, gas uptake, chemical reaction). Particularly efficient particle aging occurs in clouds, which are formed by condensation of water vapor on preexisting aerosol particles (cloud condensation-CCN and ice nucleiIN).

The concentration, composition, and size distribution of atmospheric aerosol particles are temporally and spatially highly variable. In the lower atmosphere (troposphere) the total particle number and mass concentrations typically vary in the range of about 10^2 - 10^5 cm^{-3} and 1-100 $\mu\text{g}/\text{m}^3$, respectively (Raes et al., 2000; Williams et al., 2002; Van Dingenen et al., 2004). In general, the predominant chemical components of air particulate matter (PM) are sulfate, nitrate, ammonium, sea salt, mineral dust, organic compounds, and black or elemental carbon, each of which typically contribute about 10-30% of the overall mass load. At different locations, times, meteorological conditions, and particle size fractions, however,

the relative abundance of different chemical components can vary by an order of magnitude or more (Finlayson-Pitts et al., 2005; Seinfeld and Pandis, 1998; Raes et al., 2000; Putaud et al., 2004). In atmospheric research the term “fine air particulate matter” is usually restricted to particles with aerodynamic diameters $\leq 1\mu\text{m}$ (PM1) or $\leq 2.5\mu\text{m}$ (PM2.5). In air pollution control it sometimes also includes larger particles up to $10\mu\text{m}$ (PM10).

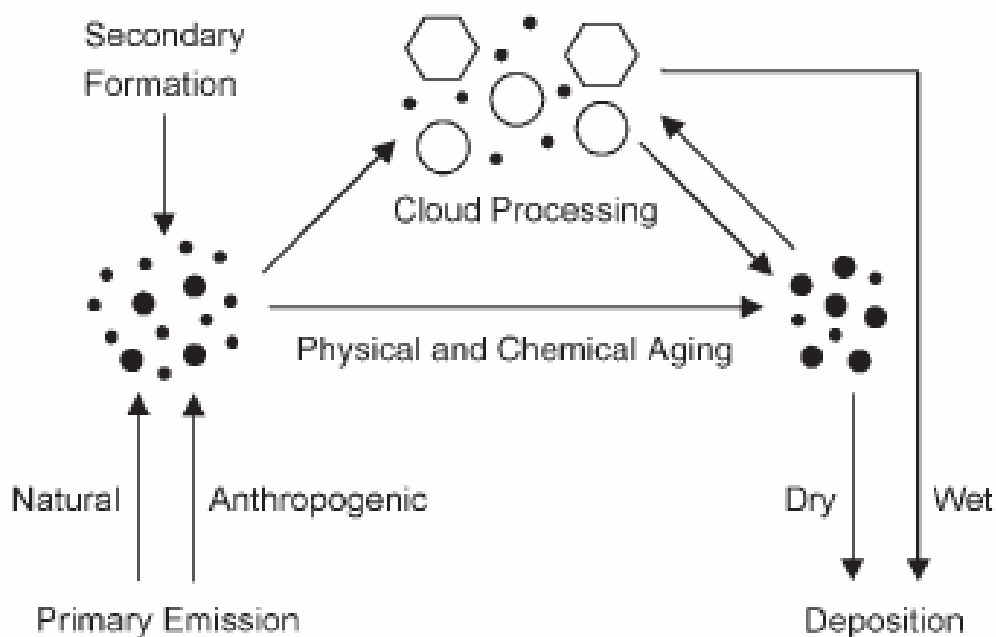


Figure 1-1: Atmospheric cycling of aerosols.

Figure 1-2 illustrates the interdependence of composition, composition-dependent properties, atmospheric interactions and transformation, climate and health effects, and aerosol sources. The resulting feedback loops are of central importance in the science and policy of environmental pollution and global change. Thus a comprehensive characterization (climatology) and mechanistic understanding of particle sources, properties, and transformation is required for the quantitative assessment, reliable prediction, and efficient control of natural and anthropogenic aerosol effects on climate and public health.

1.1. Carbonaceous Aerosol Components

Carbonaceous aerosol components (organic compounds and black or elemental carbon) account for a large fraction of air particulate matter, exhibit a wide range of molecular structures, and have a strong influence on the physicochemical,

biological, climate- and health-related properties, and effects of atmospheric aerosols (Finlayson-Pitts et al., 2005; Seinfeld and Pandis, 1998; Gelencser, 2004; Henning et al., 2005; Kulmala et al., 2004; Kanakidou et al., 2005).

Traditionally the total carbon (TC) content of air particulate matter is defined as the sum of all carbon contained in the particles, except in the form of inorganic carbonates. TC is usually determined by thermochemical oxidation and evolved gas analysis (CO₂ detection), and divided into an organic carbon (OC) fraction and a black carbon (BC) or elemental carbon (EC) fraction. Measurements of BC and EC are generally based on optical and thermochemical techniques, and OC is operationally defined as the difference between TC and BC or EC (TC=BC + OC or TC=EC + OC) (Gelencser, 2004). As illustrated in Figure 1-3, however, there is no real sharp boundary but a continuous decrease of thermochemical refractiveness and specific optical absorption going from graphite-like structures to nonrefractive and colorless organic compounds, respectively (Pöschel, 2003). Both BC and EC consist of the carbon content of the graphite-like material usually contained in soot (technically defined as the black product of incomplete hydrocarbon combustion or pyrolysis) and other combustion aerosol particles, which can be pictured as more or less disordered stacks of graphene layers or large polycyclic aromatics (Homann, 1998; Sadezky, 2005). Depending on the applied optical or thermochemical methods (absorption wavelength, temperature gradient, etc.), however, BC and EC measurements also include the carbon content of colored and refractory organic compounds, which can lead to substantially different results and strongly limits the comparability and suitability of BC, EC, and OC data for the determination of mass balances and physicochemical properties of air particulate matter.

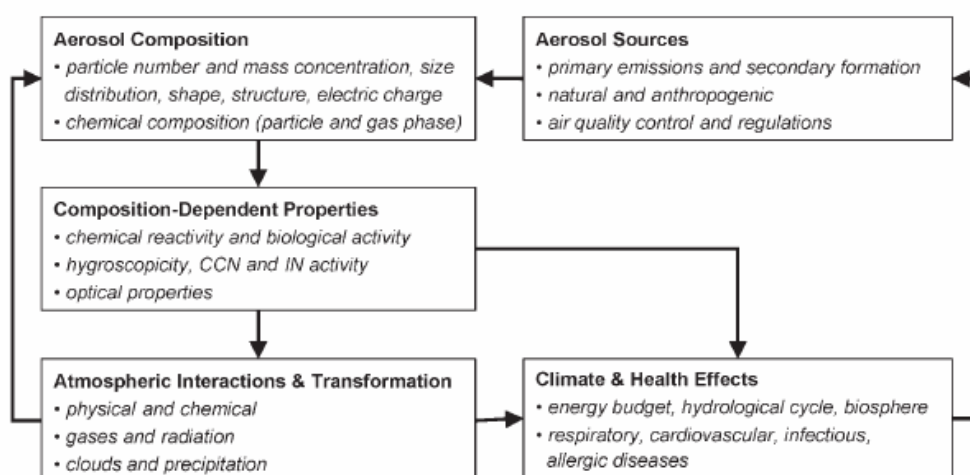


Figure 1-2: Interdependence and feedback between atmospheric aerosol composition, properties, interactions and transformation, climate and health effects, and sources (Pöschel et al., 2005)

Nevertheless, most information available on the abundance, properties, and effects of carbonaceous aerosol components so far is based on measurement data of TC, OC, and BC or EC (Gelencser, 2004; Kanakidou, 2005). These data are now increasingly complemented by measurements of water-soluble organic carbon (WSOC), its macromolecular fraction (MWSOC), and individual organic compounds. Moreover, the combination of thermochemical oxidation with ^{14}C isotope analysis (radiocarbon determination in evolved CO_2 by accelerator mass spectrometry) allows a differentiation between fossil-fuel combustion and other sources of carbonaceous aerosol components. Recent results confirm that the EC is dominated by fossil-fuel combustion and indicate highly variable anthropogenic and biogenic sources and proportions of OC (Szidat et al., 2004).

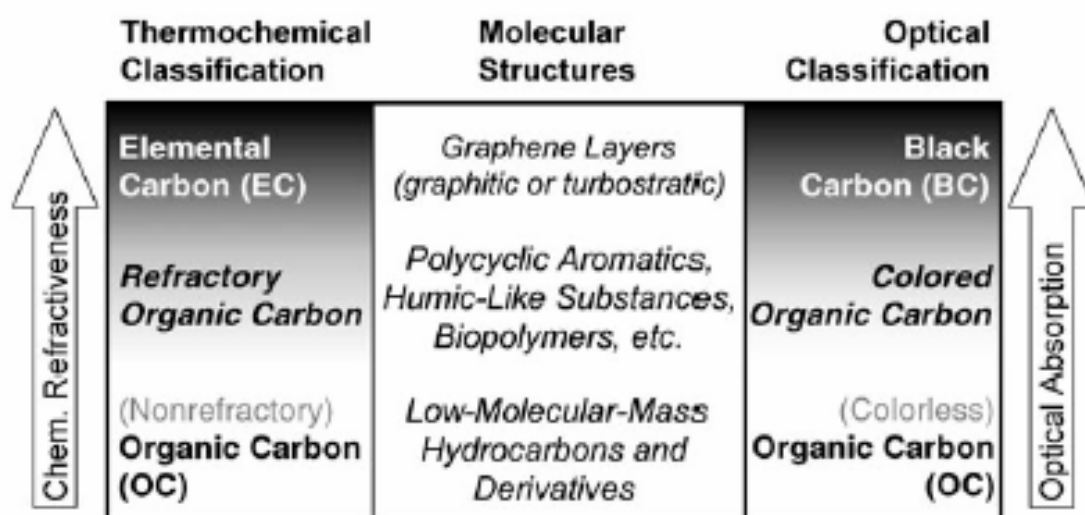


Figure 1-3 Optical and thermochemical classification and molecular structures of black carbon (BC), elemental carbon (EC), and organic carbon (OC=TC-BC or TC-EC) (Pöschel et al., 2003). Depending on the method of analysis, different amounts of carbon from refractory and colored organic compounds are included in OC and BC or EC

On average, the total $\text{PM}_{2.5}$ mass concentration decreases by about a factor of 2 from urban to rural and from rural to alpine air, whereas the TC mass fraction decreases from around 40% to 20%. The EC/TC ratios in $\text{PM}_{2.5}$ are as high as 50% in the urban air samples taken close to a major traffic junction and on the order of approximately 30% in rural and high alpine air, demonstrating the strong impact of diesel soot and other fossil-fuel combustion or biomass-burning emissions on the atmospheric aerosol burden and composition. The water-soluble fraction of organic carbon (WSOC in OC), on the other hand, exhibits a pronounced increase from urban (~20 %) to rural (~40 %) and high alpine (~60 %) samples of air particulate

matter. This observation can be attributed to different aerosol sources (e.g. water-insoluble combustion particle components versus water-soluble biogenic and secondary organic particle components) but also to chemical aging and oxidative transformation of organic aerosol components, which generally increases the number of functional groups and thus the water solubility of organic molecules.

Black or elemental carbon accounts for most of the light absorption by atmospheric aerosols and is therefore of crucial importance for the direct radiative effect of aerosols on climate (Hendricks et al, 2004; Kirkevåg et al, 1999). Despite a long tradition of soot and aerosol research, however, there is still no universally accepted and applied operational definition of BC and EC. Several studies have compared the different optical and thermal methods applied by atmospheric research groups to measure BC and EC. Depending on techniques and measurement locations, fair agreement has been found in some cases, but mostly the results deviated considerably (up to 100 % and more) (Schmid et al., 2001; Hitzenberger et al., 1999; Wittmaak, 2005) .

1.2. Primary and Secondary Organic Aerosol Components

The total mass of organic air particulate matter (OM), that is, the sum of organic aerosol components, is usually estimated by multiplication of OC with a factor of about 1.5-2, depending on the assumed average molecular composition and accounting for the contribution of elements other than carbon contained in organic substances (H, O, N, S, etc.) (Gelencser, 2004; Russell, 2003).

Depending on their origin, organic aerosol components can be classified as primary or secondary. Primary organic aerosol (POA) components are directly emitted in the condensed phase (liquid or solid particles) or as semivolatile vapors, which are condensable under atmospheric conditions. The main sources of POA particles and components are natural and anthropogenic biomass burning (forest fires, slashing and burning, domestic heating), fossil-fuel combustion (domestic, industrial, traffic), and wind-driven or traffic-related suspension of soil and road dust, biological materials (plant and animal debris, microorganisms, pollen, spores, etc.), sea spray, and spray from other surface waters with dissolved organic compounds.

Secondary organic aerosol (SOA) components are formed by chemical reaction and gas-to-particle conversion of volatile organic compounds (VOCs) in the atmosphere. The formation of new aerosol particles from the gas phase generally proceeds through the nucleation of nanometer-sized molecular clusters and subsequent growth by condensation of condensable vapor molecules. Experimental evidence from field measurements and model simulations suggests that new particle formation in the atmosphere is most likely dominated by ternary nucleation

of $\text{H}_2\text{SO}_4\text{-H}_2\text{O-NH}_3$ and subsequent condensation of SVOCs (Kulmala et al., 2004a, b; Antilla et al., 2004). The formation of new particles exhibits a strong and nonlinear dependence on atmospheric composition and meteorological conditions, may be influenced by ions and electric-charge effects, and competes with gas-particle partitioning and heterogeneous or multiphase reactions (Laasko et al., 2004). Among the principal parameters governing secondary particle formation are temperature, relative humidity, and the concentrations of organic and inorganic nucleating and condensing vapors, which depend on atmospheric transport as well as local sources and sinks such as photochemistry and preexisting aerosol or cloud particles (Kulmala et al., 2004a, b; Kamakidou et al., 2005).

1.3. Climate and Health Effects

Anthropogenic emissions are major sources of atmospheric aerosols. In particular, the emissions of particles and precursor gases from biomass burning and fossil-fuel combustion have massively increased since preindustrial times and account for a major fraction of fine air particulate matter in polluted urban environments as well as in the global atmosphere (carbonaceous components, sulfates, etc.) (Finlayson-Pitts et al., 2005; Houghton et al., 2001; Seinfeld and Pandis, 1998; Raes et al., 2000; Bond et al., 2004). Numerous studies have shown that both natural and anthropogenic aerosols have a strong impact on climate and human health. Due to the limited knowledge of aerosol sources, composition, properties, and processes outlined above, however, the actual effects of aerosols on climate and health are still far from being fully understood and quantified. Some of the most important aspects and recent developments will be addressed in the following sections.

1.3.1. Direct and Indirect Aerosol Effects on Climate

Aerosol effects on climate are generally classified as direct or indirect with respect to radiative forcing of the climate system. Radiative forcings are changes in the energy fluxes of solar radiation (maximum intensity in the spectral range of visible light) and terrestrial radiation (maximum intensity in the infrared spectral range) in the atmosphere, induced by anthropogenic or natural changes in atmospheric composition, Earth surface properties, or solar activity. Negative forcings such as the scattering and reflection of solar radiation by aerosols and clouds tend to cool the Earth's surface, whereas positive forcings such as the absorption of terrestrial radiation by greenhouse gases and clouds tend to warm it (greenhouse effect) (Houghton et al. 2001). Figure 1-3 illustrates the distinction between direct and indirect aerosol effects and some major feedback loops in the climate system. Direct effects result from the scattering and absorption of radiation by aerosol

particles, whereas indirect effects result from their CCN and IN activity (influence on clouds and precipitation), or from their chemical and biological activity (influence on aerosol and trace gas emissions and transformation).

The optical properties relevant for the direct effects (scattering and absorption coefficient or extinction cross-section and single scattering albedo, etc.) as well as the CCN, IN, chemical and biological activities relevant for indirect effects are determined by aerosol particle size, structure, and chemical composition. Thus they are strongly influenced by the atmospheric processes outlined above (coagulation, chemical transformation, water interactions).

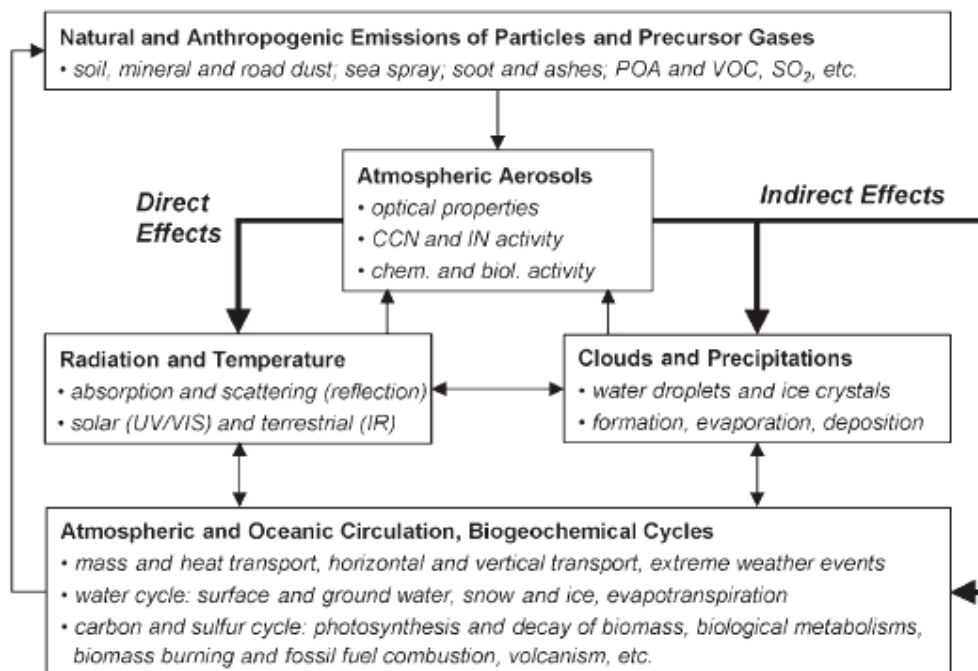


Figure 1-4: Direct and indirect aerosol effects and major feedback loops in the climate system (Pöschel et al., 2005)

The climate feedback loops illustrated in Figure 1-3 involve the interaction of atmospheric aerosols with solar and terrestrial radiation, clouds and precipitation, general circulation and hydrological cycle, and with natural and anthropogenic aerosol and trace gas sources on global and regional scales. On microscopic and molecular scales, each of the interactions outlined in Figure 1-3 comprises a multitude of physicochemical processes that depend on atmospheric composition and meteorological conditions and are largely not quantitatively characterized. Thus the actual climate system responses and feedback to natural or anthropogenic perturbations such as industrial and traffic-related greenhouse gas and aerosol

emissions, volcanic eruptions, etc. are highly uncertain. In many cases, even the sign or direction of the feedback effect is unknown, that is, it is not clear whether a perturbation will be reinforced (positive feedback) or dampened (negative feedback).

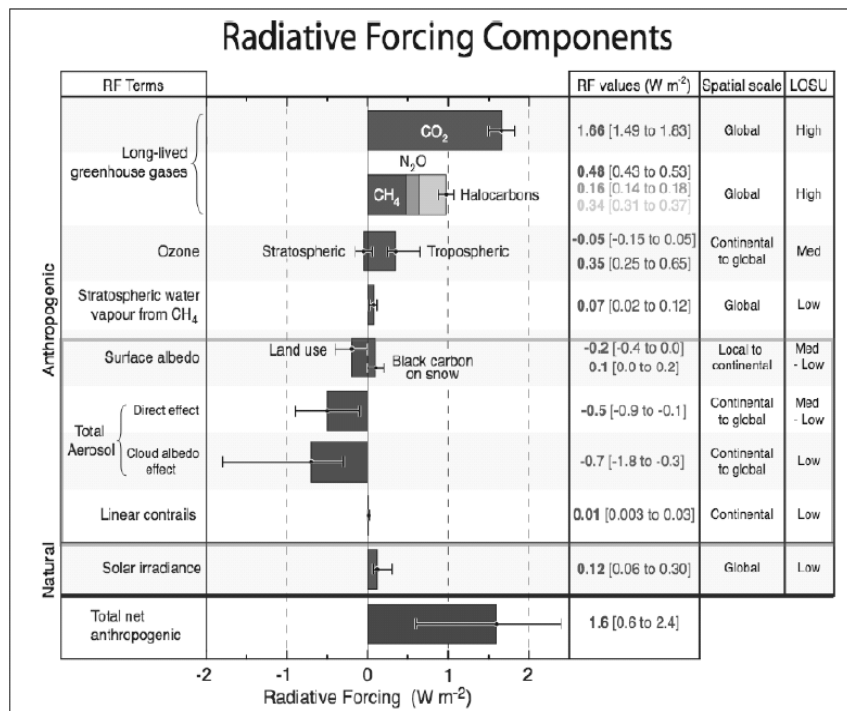


Figure 1-5: Global annual mean radiative forcing (W/m^2) for the year 2000, relative to 1750 (source: IPCC 2007).

Overall, the current aerosol radiative forcing relative to that in preindustrial times is estimated to be around -1 to $-2W/m^2$, as opposed to a greenhouse gas forcing of about $+2.4W/m^2$ (Houghton et al., 2001; Lohmann et al., 2005; Andreae et al., 2004). Owing to the limited understanding of the underlying physicochemical processes, however, it is still unclear if clouds provide a positive or negative feedback to an increase in atmospheric carbon dioxide and other greenhouse gases. The uncertainties of aerosol, cloud, and precipitation interactions and feedback effects are among the main reasons for the high uncertainty of climate sensitivities and for the projected global mean surface temperature increase over the next century ($1-6$ °C or more) (Houghton et al., 2001; Lohmann et al., 2005; Kanakidou et al., 2005).

References

Andreae (2005) *Nature* 435, 1187

- Andreae (2004) *Science* 303, 1337
- Anttila et al. (2004) *Atmos. Chem. Phys.* 4, 1071
- Bernstein (2004) *J. Allergy Clin. Immunol.* 114, 1116.
- Bond et al. (2004) *J. Geophys. Res.* 109
- Finlayson-Pitts and Pitts, (2000) *Chemistry of the Upper and Lower Atmosphere*, Academic Press, San Diego,
- Finlayson-Pitts, J. N. Pitts (1997) *Science* 276, 1045.
- Gelencser (2004) *Carbonaceous Aerosol*, Springer, Dordrecht
- Henning et al. (2005) *Atmos. Chem. Phys.* 5, 575
- Hinds (1999) *Aerosol Technology*, Wiley, New York,
- Hitzenberger et al. (1999) *Atmos. Environ.* 33, 2823.
- Homann (1998) *Angew. Chem* 110, 2572, *Angew. Chem. Int. Ed.* 37, 2435.
- Houghton et al. (2001), *Climate Change 2001: The Scientific Basis (Contribution of Working Group I to the Third Assessment Report of the Intergovernmental Panel on Climate Change)*, Cambridge University Press, Cambridge
- Jacobson (2002) *J. Geophys. Res.* 107, 4410
- Kanakidou et al. (2005) *Atmos. Chem. Phys.* 5, 1053.
- Kirkevåg et al. (1999) *Atmos. Environ.* 33, 2621
- Kulmala (2004) *Atmos. Chem. Phys.* 4, 557
- Kulmala et al. (2004a) *Atmos. Chem. Phys.* 4, 2553
- Kulmala et al. (2004b) *J. Aerosol Sci.* 35, 143
- Lohmann and Feichter (2005) *Atmos. Chem. Phys.* 5, 715.
- Pöschl (2002) *J. Aerosol Med.* 15, 203
- Pöschl (2003) *Anal. Bioanal. Chem.* 375, 30
- Pöschl (2005) *Angew. Chem. Int. Ed.* 44, 7520.
- Pruppacher and Klett (1997) *Microphysics of clouds and precipitation*, Kluwer, Dordrecht
- Putaud et al. (2004) *Atmos. Environ.* 38, 2579
- Russell (2003) *Environ. Sci. Technol.* 37, 2982
- Sadezky et al. (2005) *Carbon* 43, 1731
- Schmid et al. (2001) *Atmos. Environ.* 35, 2111.
- Seinfeld, S. N. Pandis, (1998) *Atmospheric Chemistry and Physics*, Wiley, New York
- Szidat et al. (2004) *Radiocarbon* 46, 475
- Wittmaack (2005) *Atmos. Chem. Phys.* 5, 1905.

Part 1

Development of analytical techniques

2. Set-up of Extraction Procedures for Ions Quantification in Aerosol Samples

Ions quantification in aerosol samples is commonly achieved by means of Ion Chromatography (IC) after extraction of the analytes from the filter generally using MQ water and operating in an ultra-sound bath. Although this sample preparation system is widely employed in the literature, some important aspects such as ions recovery percentages after the extraction are often not taken into consideration.

The aim of this work was to focus on the optimization of the extraction method for different types of filter supports (i.e. PTFE and quartz-fibre filters), which are commonly used for aerosol sampling.

For $\text{SO}_4^{=}$, NO_3^- and NH_4^+ the best recoveries, after a single extraction step, were achieved with PTFE while chlorides recovery was quite low and not reproducible. When quartz is employed and a single extraction step used, in order to give a correct quantification of ions concentration it is generally necessary to apply a correction factor but for chloride quantification three subsequent steps are mandatory.

Both techniques and extraction procedure uncertainties have been evaluated and resulted to be within 10%. Limit of detection (LOD) for all the analysed species were determined and it was found that they were within the ranges reported in the literature.

2.1. Introduction

Ions represent a major component in airborne particulate matter (PM). In some cases these species (mainly $\text{SO}_4^{=}$, NO_3^- , Cl^- and NH_4^+) account for more than 40% of the total PM mass. Furthermore ions are ubiquitous pollutants with numerous adverse effects on the environment. In this study IC (Ion Chromatography), performed on solution obtained after ultrasonic extraction, is used for ions quantification. Our aim was to deeply investigate the whole analytical method paying particular attention to the filter extraction procedure, which is the most tricky point. In fact a unique method for sample preparation doesn't exist and, in the literature, quite different procedures are employed.

The aim of the present work is to set-up a reliable extraction procedure for ions quantification in particulate matter (PM). Since quartz and PTFE filters are among

the most employed supports for PM sampling, both of them have been examined. The reliability of the set-up procedure was verified comparing the results obtained by IC, on a series of PM10 samples, with those previously obtained analyzing the same filters by XRF (X-ray Fluorescence).

2.2. Experimental procedures

The water-soluble inorganic fraction was determined by ion chromatography (IC) using an ICS-1000 Ion Chromatograph (Dionex). Solutions obtained after extraction of inorganic ions from particulate matter were analysed. Major ionic species (NO_3^- , SO_4^{2-} , F^- , Cl^- , NO_2^- , Br^- , NH_4^+ , Na^+ , K^+ , Ca^{2+}) were determined. Both techniques and overall uncertainties for all the ions determined, were estimated (including also the error that could be performed during sample preparation, see paragraph 2.3).

2.2.1. Extraction procedure

A quarter of each fibre filter (cut using a home-made precision cutter equipped with two orthogonal blades) was extracted in Milli-Q water. The extractions were carried out in a Branson MTH 2510 ultrasonic bath with frequency of 42 kHz. The sample was put in a plastic tube, 2 mL of MQ water were added and the tube submitted to a first extraction for 20 minutes. It is worth noting that plastic must be used since in this way the releasing by the tube of ions, which are the same of interest for the analysis, is avoided; in fact these ions can be released if glass tubes are employed. Since it was observed that one extraction was not enough to obtain a complete recovery (see paragraph 2.3), the filter was submitted to a second and to a third extraction (20 minutes each) with the renewal of the water at each step. After each extraction the filter was placed in a new tube and 2 mL of MQ water added. For each of the three solutions obtained, an aliquot of 1.5 mL was drawn and the three aliquots joined in a clean tube from which the solution for ions determination (100 μL) was withdrawn. For the ions extraction from PTFE, as it is suggested in the literature (Chow and Watson, 1999), the filter surface (1/4) was previously wetted with 50 μL methanol because of its hygroscopicity. In order to verify if three subsequent extractions were always needed, independently from the support type, quartz and PTFE were tested and the recovery percentages after each step calculated. Both sampled and blank filters were submitted to the set-up extraction procedure. All the solutions were maintained at a temperature of about 5°C until the analysis.

2.2.2. Instrumentation

Anions analysis was carried out by means of a Ion Pac AS14A (Dionex) column using 8 mM Na₂CO₃/ 1 mM NaHCO₃ as eluent at 1mL/min flow rate and, for the detection, a conductivity system equipped with a ASRS-ULTRA suppression mode (Dionex). Cations determination was performed by means of a CS12A (Dionex) column using 20 mM MSA (Methanesulfonic Acid) as eluent at 1mL/min flow rate and, for the detection, a conductivity system equipped with a CSRS-ULTRA suppression mode (Dionex).

The instrument was daily calibrated with standard solutions. Solutions obtained after particulate matter extraction, solutions prepared extracting blank filters and blank solutions of MQ were analysed.

2.2.3. PM sampling

Atmospheric particulate matter samples were collected on both quartz and PTFE filters. A set of 6 samples (3 on quartz and 3 on PTFE filters) were collected during winter 2005 in Milan using low volume CEN-equivalent samplers (flow rate: 2.3 m³/h) equipped with PM10, PM2.5 or PM1 (particulate matter with aerodynamic diameter smaller than 10, 2.5 and 1 µm, respectively) inlets. Sampling duration was 24 hours. These filters were employed to calculate major ions recovery percentages and to check the sample preparation procedure uncertainty.

Furthermore a complete series of PM1 samples collected on quartz and PTFE filters during a previous campaign, were also analyzed (F. Marengo, et al., 2006). All the masses were gravimetrically determined.

2.3. Results and discussion

The frame of the present work consists of different points such as the evaluation of the technique uncertainty, the optimization of particulate matter extraction procedure, the evaluation of the detection limits and, finally, the comparability of the results obtained by ion chromatography with those determined by a different technique.

First of all a standard solution containing all the ions of interest (a solution having a concentration of 0.5 ppm for all the ions with the exception of sulphates and nitrites which were present in concentration of 1 ppm) was analysed (9 measurements) in order to estimate the uncertainty of our chromatographic system. The results are reported as percentages in

Table 2-1.

Generally PM samples are extracted in a single step in MQ water using an ultrasonic bath or a shaker (Chow and Watson, 1999; Wieprecht et al., 2004). Nevertheless, the conditions employed are very different: quite long extraction times together with refrigeration (up to 12 h) or, on the contrary, shorter time with heating. To clarify this point some experiments were carried out varying both extraction duration and number of subsequent extraction steps in order to obtain the best recovery percentages. Three quartz and three PTFE filters were extracted, as described in the experimental section, and each solution obtained (i.e. after the first, the second and the third extraction) injected. Thereafter the recovery percentages for the major ions were calculated. As it can be observed (Table 2-2, Figure 2-1), the ions recoveries are higher for PTFE, with the exception of chloride. What we concluded was that, independently from the filter type, for chlorides determination 3 steps are necessary.

	F ⁻	Cl ⁻	NO ₃ ⁻	PO ₄ ³⁻	SO ₄ ⁻	Na ⁺	NH ₄ ⁺	K ⁺	Mg ⁺	Ca ⁺⁺
Uncertainty % (n=9)	0.4%	7.0%	1.9%	1.7%	0.8%	2.0%	1.3%	4.3%	1.0%	3.5%

Table 2-1: Technique uncertainty obtained analysing a standard solution containing all the ions

	PTFE filter					
	1° extraction		2° extraction		3° extraction	
	average	s	average	s	average	s
Cl ⁻	29% ± 15%		55% ± 15%		16% ± 5%	
NO ₃ ⁻	95% ± 1%		3% ± 1%		2% ± 1%	
SO ₄ ⁻	93% ± 4%		4% ± 3%		3% ± 1%	
NH ₄ ⁺	91% ± 6%		9% ± 5%		-- ± --	

	Quartz filter					
	1° extraction		2° extraction		3° extraction	
	average	s	average	s	average	s
Cl ⁻	49% ± 15%		36% ± 27%		14% ± 12%	
NO ₃ ⁻	85% ± 3%		11% ± 3%		4% ± 2%	
SO ₄ ⁻	83% ± 4%		13% ± 2%		5% ± 2%	
NH ₄ ⁺	80% ± 6%		15% ± 4%		5% ± 3%	

Table 2-2: Recovery percentages for major ions obtained analyzing quartz and PTFE filters

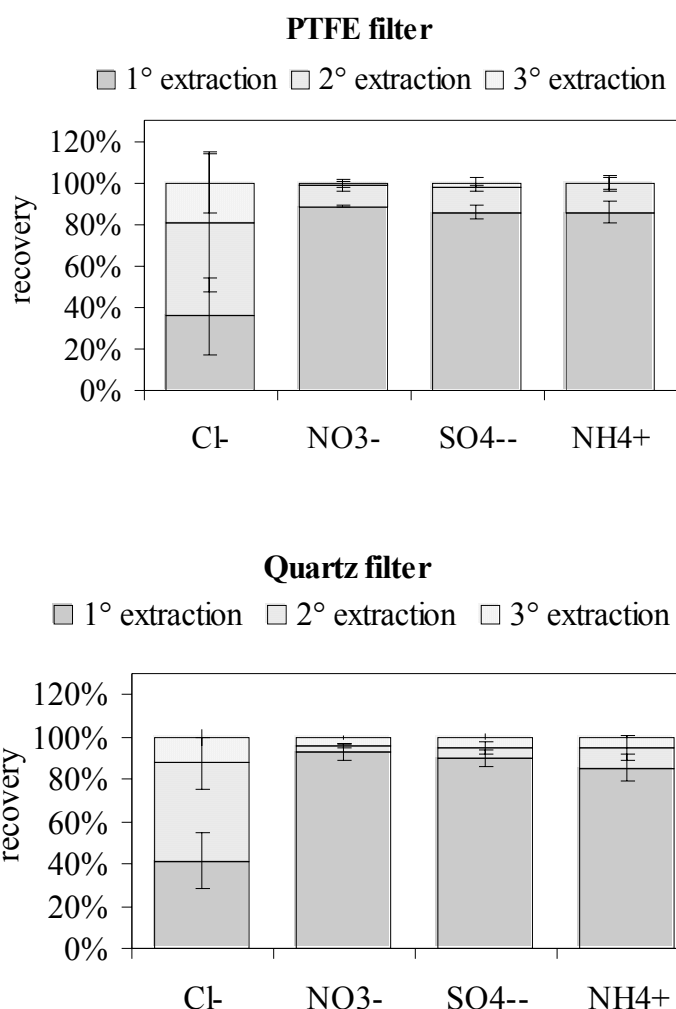


Figure 2-1: Recovery percentages for major ions obtained analyzing quartz and PTFE filters

Limits of detection (LOD) were calculated, according to Desimoni et al., 2004, as:

$$\text{LOD} = \frac{\mu_B + k \cdot \sigma_B - a}{b} \quad k=3$$

where b =slope, a =intercept,
 μ_B = blank signal and σ_B = standard deviation

The blank concentrations are represented by the values obtained analyzing both MQ water submitted to the extraction procedure ($n=8$) and the blank filters. The LOD values reported in Table 2-3 have been converted to “blank” air concentration values taking into account a standard 24-hours sampling carried out at 2.3 m³/h flow rate. It can be observed that values obtained are within the ranges reported in the literature for LOD if a normalization to both volumes and areas used in our work is performed (Wieprecht et al., 2004; Karthikeyan and Balasubramanian,

2006). The data obtained referring to water as blank are interesting since in this way the filter contribution can be clearly singled out.

	Calibration curve parameters				Water	Quartz filter	PTFE filter
	slope	slope 2	intercept	R ²	LOD k=3 (ng/m ³) n=4	LOD k=3 (ng/m ³) n=3	LOD k=3 (ng/m ³) n=3
F⁻	0.87		0.00	99.28	0.4	0.7	0.8
Cl⁻	0.72		0.00	99.87	7.6	25.3	6.0
NO₂⁻	0.34		0.00	99.87	16.0	8.0	8.6
NO₃⁻	0.43		0.00	99.87	6.6	60.8	14.5
SO₄⁻	0.52		0.00	99.86	1.8	28.3	14.5
Na⁺	1.14		0.00	99.99	22.8	89.3	47.4
NH₄⁺	0.64	-0.02	0.00	99.27	4.3	7.7	3.4
K⁺	0.75		0.00	99.98	13.5	39.9	24.5
Mg⁺	1.91		0.00	100.00	1.1	1.5	1.4
Ca⁺⁺	1.33		0.00	99.95	12.3	27.1	14.9

Table 2-3: LOD of the analytical technique obtained analyzing MQ water, blank quartz fibre filters and PTFE filters.

Finally, the procedure reliability has been verified comparing data obtained by IC and by XRF on the same PM1 filters and for those elements/ions detectable by both techniques. After the XRF analysis carried out on the whole filters, 1/4 was cut and extracted. The good agreement between the techniques can be observed in Figure 2-2 where the concentration trends are reported for sulphates and calcium.

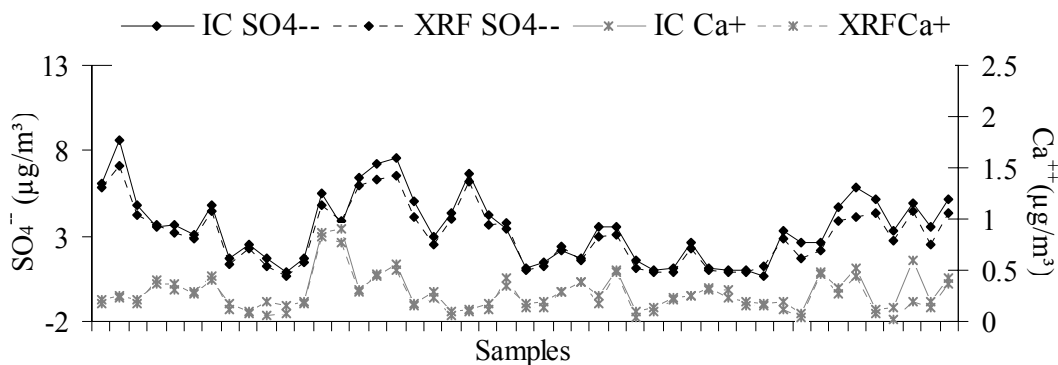


Figure 2-2 Comparison between IC and XRF data, obtained analyzing PM1 filters, for Ca²⁺ and SO₄²⁻

2.4. Conclusions

The extraction procedure for the determination of ions in particulate matter by ion chromatography has been studied. Two different types of filters have been examined (quartz and PTFE). The method is characterized by a good reproducibility and also by low limits of detection.

From the calculation of recovery percentages it has been pointed out that, for the determination of chlorides, a three steps extraction procedure is mandatory. For sulphates, nitrates and ammonium, when the collecting support is quartz and if a single step extraction is performed, correction factors must be calculated and applied in order to avoid an underestimation of these ions concentrations.

The set-up method is suitable for the analysis of ions in PM samples and has been employed for ions quantification in PM samples. The technique reliability is also checked by the comparison with the results obtained for the same filters with an independent method (XRF).

Acknowledgment

I would like to acknowledge dr. F.Abballe, G.Ferracin, L.Casagrande and C.Reschiotto from Dionex (Italia) for their precious contribution to this research.

References

- Chow J. C. and J. G. Watson, (1999), *Elemental Analysis of Airborne Particles*, vol. 1: Ion chromatography in elemental analysis of airborne particles, Eds. S. Landsberger and M. Creatchman, Gordon and Breach Science Publishers, Australia
- Desimoni, et al., (1994) *Annali Di Chimica* 94, 555
- F. Marengo, et al., (2006) *J. Geophysical Research*, 111, D24202, 2006
- Karthikeyan and Balasubramanian, (2006), *Microchem. J.* 82, 49
- Skoog et al., (2005) *Fondamenti di Chimica Analitica*, second edition EdiSES s.r.l., Napoli
- Wieprecht W., et al., (2004) *Atmos. Environ.* 38, 6477

3. A TGA/FT-IR study for measuring OC and EC in aerosol samples

Carbon analysis consists in the evaluation of the carbonaceous content of the aerosol (TC) but, more importantly, of its distribution between the two components EC (Elemental Carbon) and OC (Organic Carbon) that are characterized by different physical-chemical properties. In spite of the numerous studies focused on this topic, nowadays

a universal methodology for the determination of the two components EC and OC is not available. In fact OC and EC (also known as black carbon or soot) are operationally defined by the method of analysis and, as a consequence, different methods can produce different results.

In this paper we present results on the application of TGA/FT-IR (Thermogravimetric Analysis/Fourier Transformed Infrared Spectroscopy) to the characterization of carbonaceous aerosols. The analytical methodology was applied to PM₁₀ (particulate matter with aerodynamic diameter smaller than 10 μm) four-hour time resolution samples collected in Milan urban area. The method is a two-steps thermal one and it is based on the different thermal behaviour of OC and EC. It has been set up analyzing suitable standards containing both organic and elemental carbon. Carbon quantification is achieved by on-line, continuous monitoring of CO₂ infrared absorption at 2361 cm^{-1} . A good separation between OC and EC on particulate matter (PM) samples has been obtained. Ranges and average values were 12-70 $\mu\text{g}/\text{m}^3$ and 20 $\mu\text{g}/\text{m}^3$ for OC and 0.2-6 $\mu\text{g}/\text{m}^3$ and 2 $\mu\text{g}/\text{m}^3$ for EC. On average OC and EC made up 29 (± 13) % and 2.5 (± 1.8) % of the PM₁₀ fraction, respectively. The method reliability has been verified by a preliminary comparison with TOT (Thermal Optical Transmission) technique. OC and EC values determined for ambient samples of PM₁₀ were correlated with meteorological parameters as well as with Radon concentrations.

3.1. Introduction

The overall composition of the particulate matter (PM) has become one of the fundamental topics in the field of environmental chemistry. One of the main topics is represented by carbonaceous fraction quantification since this component makes up about the 50% of the particulate mass concentration.

The total carbon content (TC) includes elemental carbon (EC) and organic carbon (OC) as well as a small percentage (less than 5%) of inorganic carbon mainly present as carbonate.

EC is essentially a primary pollutant (Seinfeld and Pandis, 1998) emitted during incomplete combustion of fossil and biomass carbonaceous fuels. In urban areas, diesel emissions are one of the major sources for black carbon, which is often used as a marker for urban pollution (Delumyea et al., 1980; Salma et al., 2004); furthermore, its temporal pattern could be related to traffic intensity (Ruellan and Cachier, 2001).

OC has both primary and secondary origin. Primary OC is mainly formed during combustion processes such as unleaded gasoline combustion in urban area or biomass and field agricultural burning (Duan et al., 2004). It is also directly emitted as plant spores, pollens and soil organic matter. Secondary OC can originate from different processes such as gas to particle conversion of low vapour pressure volatile organic compounds, condensation and physical and chemical adsorption. The presence of secondary organic aerosol (SOA) is suggested by an increase of the OC/EC ratio. Secondary organic aerosol can be easily estimated using EC as tracer of OC primary emission (Turpin and Huntzicker, 1995; Salma et al., 2004). As for OC chemical composition, this fraction contains a large amount of organic substances belonging to different classes (aliphatic or aromatic compounds, acids, etc.) the majority of which has not yet been identified.

EC is also indicated as black carbon (BC) because of its color. It has a graphitic-like structure with the presence of some functional groups containing elements such as oxygen, sulphur, hydrogen and nitrogen, which are able to enhance catalytic processes. EC is sometimes referred as *soot* when carbon to oxygen ratio during the combustion process is less than 1. Indeed soot, that represents the dark component of the carbonaceous aerosol, is a very complex mixture of both elemental carbon and highly polymerized organic substances.

The large concern on elemental carbon (EC) concentrations in PM samples is due to the adverse health effects (Summerhays, 1991; Oberdörster and Yu, 1990) and soiling of surfaces. At a global scale, EC might also play a role in radiative forcing effects, as it is the dominant light-absorbing component of atmospheric aerosols. As regards to the organic carbon (OC) the increasing awareness has to be attributed to the fact that it typically constitutes up to 70 % of the total dry fine particle mass in atmosphere. Moreover, OC is an aggregate of hundreds of individual compounds, which can modify the thermodynamic and chemical properties of the atmosphere (Turpin et al., 2000).

The large number of studies carried out in the last years and devoted to OC and EC quantification, have demonstrated that, because of the carbonaceous aerosol

complex nature, it is difficult to compare results produced by means of different techniques (Schmid et al., 2001; Chow et al., 2001; Chow et al., 2004). In fact, these methods gave results in fairly good agreement just with respect to TC concentration while difficulties have been encountered in the determination of the two fractions i.e. EC and OC.

It is worthy to note that up to now a reference method of analysis is not available and there is a significant disagreement in the experimental results (Schmidt et al., 2001).

The methods most commonly applied are based on thermal evolution and reflectance/transmission measurements. Amongst them the IMPROVE (Chow et al., 1993) and the NIOSH (Birch and Cary, 1996) protocols are widely employed. Both methods involve the sample (PM deposited on a filter support) first heating to 600°C in pure He and, after the temperature has decreased to 400 °C, a second heating to 600°C in He containing a small percentage of O₂. During the first step organic substances are removed since OC is less thermally resistant than EC. However, at the same time OC can partially be converted into EC through a pyrolysis. Because of this process, known as *charring*, OC would be underestimated. In order to overcome this problem, a pyrolysis correction is applied monitoring a laser beam transmitted or reflected by the filter. The IMPROVE protocol adopts the thermo-optical reflection (TOR) method while the NIOSH protocol uses the thermo-optical transmission (TOT) method. The comparison of NIOSH and IMPROVE carbon measurements has shown that they are equivalent as concerns TC while NIOSH EC is lower than IMPROVE EC (Chow et al., 2001). The discrepancy is mainly due to differences in the temperature steps and to the different correction system. Moreover, a recent comparison between TOR and TOT methods has shown that the EC concentration determined by TOT is often a factor two lower than the corresponding value determined by TOR (Chow et al., 2004).

Another well-established thermal method for OC/EC analysis has been proposed by Cachier et al. (1989). In this procedure inorganic carbon is preliminarily eliminated by exposure of the filter to HCl vapours. Afterwards, half a filter is heated at 340°C in oxygen in order to decompose the whole OC. The remaining carbon, i.e. EC, is then determined by coulometric titration. The remaining half of the filter is directly analyzed without the pre-treatment. OC concentration is determined by difference. This protocol is known as LSCE (Laboratoire des Sciences du Climat et de l'Environnement, Cachier et al., 1989).

A thermal method quite similar for some aspects to the LSCE protocol has been proposed in a preliminary work carried out by Fermo et al. (2003). In this study the carbonaceous component in the Milan urban particulate matter was estimated by means of a thermo-gravimetric analyzer combined with an infrared

spectrophotometer (TGA/FT-IR). In the present paper the employed technique is the same but the protocol has been partially modified in order to overcome some drawbacks of the previous methodology such as a not satisfactory OC/EC separation and, in some cases, a not sufficient sensitivity.

The aims of this study are:

- to test the reliability of TGA/FT-IR technique for the detection of the carbonaceous component in particulate matter samples;
- to quantify OC and EC concentrations on PM samples collected in Milan (Italy) in a field campaign carried out during winter 2003.

The method set up has involved the analysis of both standard samples prepared in our laboratory and ambient samples of Milan urban particulate matter.

3.2. Experimental

3.2.1. Standards preparation

To optimize and calibrate the analytical methodology applied in this study, some "standard samples" (carbon black or graphite mixed with SiO₂ and some suitable compounds) were generated. These standard mixtures have been prepared so that their carbon concentration, both for organic and elemental carbon, was similar to the one expected in the atmospheric aerosol samples.

For this reason, among the organic substances, some of those present in the particulate matter in higher concentration were chosen (Seinfeld and Pandis, 1998).

The following mixtures were prepared:

- *standard a* containing: SiO₂ (80%) and Na₂C₂O₄ (20%)
- *standard b* containing: SiO₂ (85%) - palmitic acid (5%) – stearic acid (5%) and benzoic acid (5%)
- *standard c* containing: SiO₂ 70% - Na₂C₂O₄ 5% - palmitic acid (5%) – stearic acid (5%) - benzoic acid (5%) – carbon black (10%)
- *standards d1-d3* containing: SiO₂ and graphite in different concentrations, i.e. 4.7%, 1730 ppm and 3300 ppm, respectively.

The substances employed for the preparation of the standard samples are commercial products. Graphite powder was obtained grinding E441 Shaped Carbon Rods (Assing, Italy); carbon black was a powder of Monarch (Cabot Corporation, France); silica, sodium oxalate, palmitic acid, stearic acid and benzoic acid were supplied by Aldrich (Italy).

As for the mixtures preparation, the chosen materials were at first mixed in an agate mortar and then in a ball mill (Retsch model S1, operating with three balls 3 mm diameter) in order to obtain a homogeneous sample of powder with small grain dimensions to be deposited on the filter supports.

The carbon concentration in our standards has been verified by CHN (Carbon/Hydrogen/Nitrogen Analyzer, Perkin Elmer instrument model 2400). In particular, as for standards d1-d3 used in the instrument calibration, the actual carbon concentrations were verified by CHN for standard d1 and by TOC (Total Carbon Analyzer, Dohrmann Apollo 9000 instrument equipped with a NDIR-detector and a solid sampler allowing to analyze small sample quantities) for standards d2 and d3. The use of TOC was necessary as CHN was not suitable to analyze samples d2 and d3 because of their low carbon content. It has been found that the measured carbon concentrations (i.e. those used for the calibration curve; see Sect. 3.2) were slightly lower than those calculated on the base of the weighed quantities, probably because of some losses occurred during mixture preparation.

The NIST (National Institute of Standards and Technology) Standard Reference Material 1649a (urban dust) and the NIES (National Institute for Environmental Studies) Certified Reference Material No. 8 (vehicular exhaust particulate) have been analyzed to test the method reliability.

In order to realize measurement conditions quite similar to those typical of particulate matter samples, standard d1 has been deposited on quartz fiber filters and these filters were used for the TGA/FT-IR calibration (see further on in the text).

The deposition was done by means of a home-made re-suspension system composed of two differently sized chambers in order to get a homogeneous dispersion of the powder mixture in the chambers volume. At the inlet of the air flow there is a filter to prevent the entrance of ambient particulate matter in the re-suspension system.

The re-suspended powder was collected on the filter support (quartz fiber filters, Whatman QMA) after passing a size-selective inlet constituted by a cyclone, which allowed the sampling of particles with aerodynamic diameter smaller than 3.5 μm . The grains size was checked by scanning electron microscopy (SEM) using a Hitachi 2400 instrument equipped with a Quantum Kevex energy dispersive X-ray microanalyzer (EDX).

Before and after the depositions the quartz fiber filters were exposed for 24-48 hours on open but dust-protected sieve-trays in an air-conditioned weighing room ($T = 20 \pm 1$ °C and R.H. = 50 ± 3 %). The gravimetric determination of the mass was carried out using an analytical microbalance (precision 1 μg), which is

installed and operates in the weighing room. In order to remove static electricity from filters the balance was equipped with a special kit consisting in a Faraday shield.

3.3. Analytical techniques

EC and OC determination has been performed by a TGA/FT-IR (Thermo-gravimetric Analysis coupled with Fourier Transformed Infrared Spectroscopy) home-made instrument, assembled using a JASCO-FTIR spectrophotometer Model 360 and a Dupont Thermo-gravimetric analyzer model 951. A schematic diagram of the carbon analyzer apparatus is reported in Figure 3-1.

Basically, it is a thermal evolved method where carbon quantification is achieved by on-line continuous monitoring of CO₂ infrared absorption. At the moment, the facility of the thermo-gravimetric analysis (weight loss evaluation) is not used for carbon quantification.

The TGA/FT-IR system is also advantageous because it allows the continuous monitoring of CO₂ as well as of other species (e.g. water vapour, SO₂, NO_x and NH₃), which volatilize during the decomposition of sulphates and nitrates contained in the particulate matter. Indeed, from preliminary measurements on a few PM samples both SO₂ and NO_x have been detected from infrared spectra; nevertheless, the quantification of these species will require a suitable calibration and work is still in progress.

The system consists of a furnace (which is the core of the thermo-gravimetric analyzer) where the sample is heated under controlled conditions and the carbonaceous aerosol fraction is oxidized to CO₂ whose concentration is monitored by the FT-IR spectrophotometer. Two increasing temperature steps allow the separation of organic carbon from elemental carbon. CO₂ evolved during sample decomposition is transferred through a stainless steel tube heated at 110 °C to a 15 cm long multipass White cell equipped with KBr windows (thus, the optical path reaches a length of 120 cm), which is located inside the infrared spectrophotometer. In this way, during each thermo-gravimetric analysis, infrared spectra series are collected automatically by the FT-IR with a spectrum collected every 60 s.

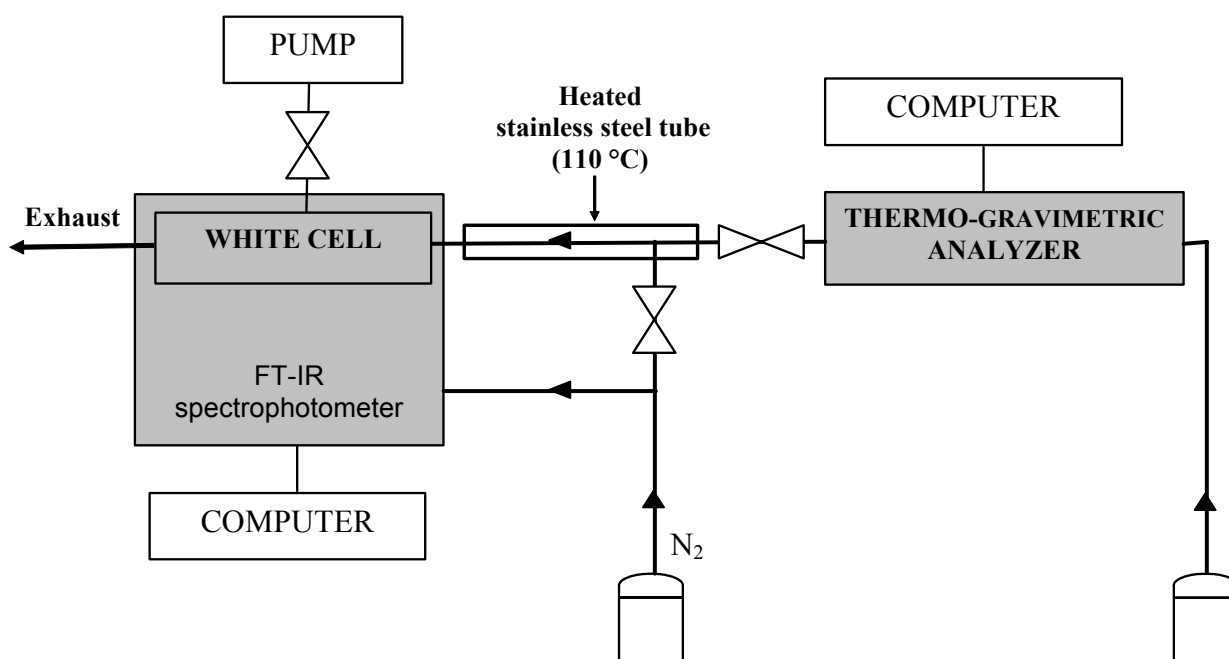


Figure 3-1: Diagram of the carbon analyzer obtained by coupling a thermo-gravimetric analyzer (TGA) with an infrared spectrophotometer (FT-IR).

By continuous monitoring of CO₂ absorbance at 2361 cm⁻¹ (which corresponds to the most intense signal in CO₂ infrared spectrum) vs. time, a CO₂ evolution curve (in the following called CEC) is obtained. The curve shows distinctive features and it is possible to distinguish, on the base of the different decomposition temperature, the two components OC and EC detectable as well separated peaks. CECs examples are shown in Figure 3-2 a-b. These curves were obtained analyzing both standards b and c, prepared as described in the experimental section (Figure 3-2a), and a couple of four-hour time resolution particulate matter samples collected in Milan as described further on in the paper (Figure 3-2b). Two fully separated peaks are detectable, the first one due to organic carbon and the second one due to elemental carbon. The area under each peak is proportional to the OC and EC content in the sample. It is worthy to note that the small peak corresponding to EC in the CEC of standard b has to be assigned to some organic carbon charring since this standard mixture doesn't contain any elemental carbon. Furthermore, the EC peak falls at higher time values in the real samples since the experimental conditions were slightly different. In fact, CECs corresponding to standards b and c were acquired by using the heating program reported for experiment No. 4 (Table 3-1) while the ambient samples were analyzed as described in experiment No.5 (Table 3-1).

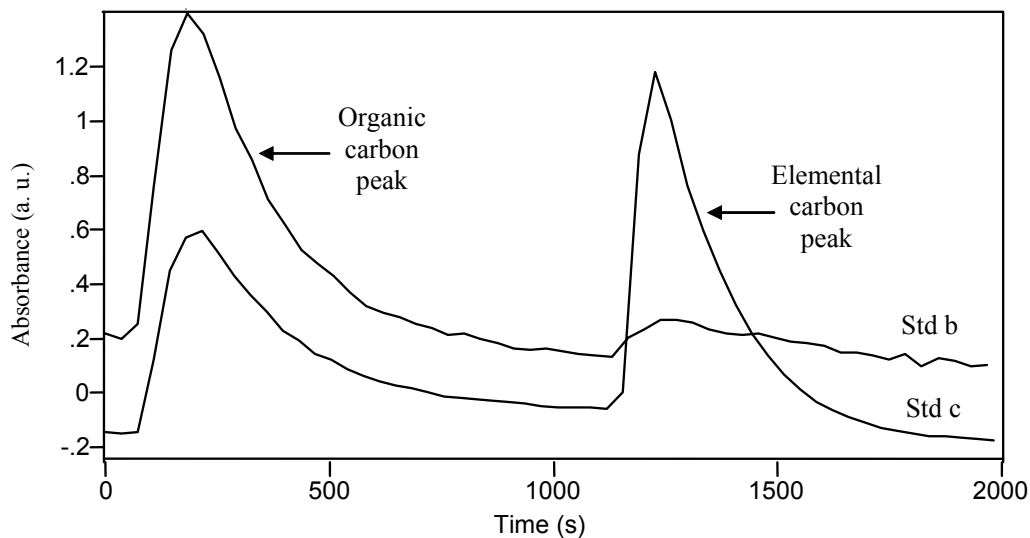


Figure 3-2a

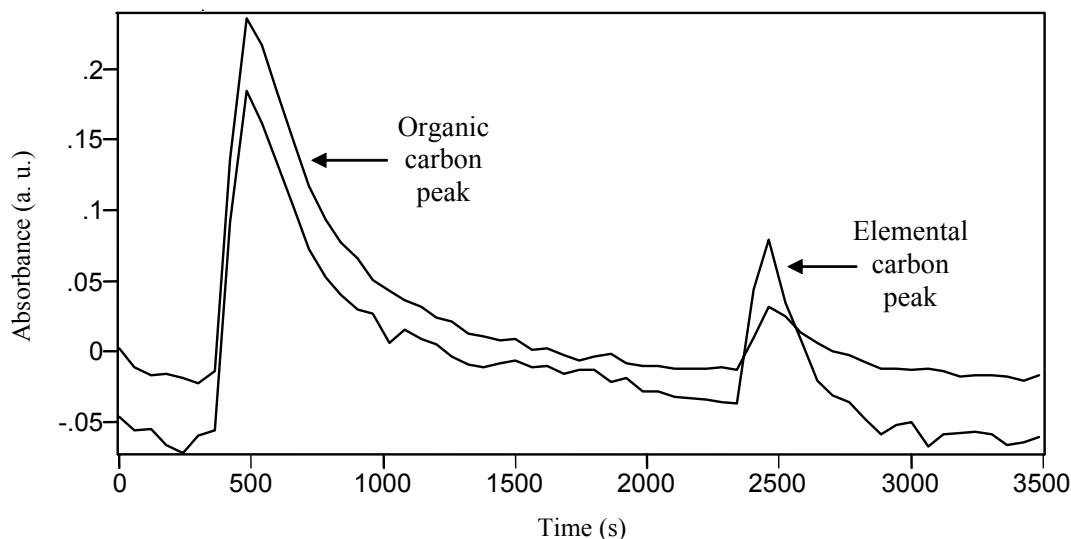


Figure 3-2b

Figure 3-2: CECs (CO_2 Evolution Curves) obtained by TGA/FT-IR analyzing standard b and c (2.a) and two particulate matter samples deposited on quartz fiber filters (2.b); the peaks due to organic carbon (OC) and elemental carbon (EC) are indicated with arrows.

All TGA/FT-IR analyses were carried out in O_2 atmosphere with a gas flow rate of 60 mL/min. Before each measurement the White cell was evacuated and purged by a nitrogen flux. Subsequently, oxygen was fluxed and the background spectrum

acquired. CO₂ is carried through the stainless steel tube and the White cell by means of O₂ flux (Figure 3-1)

Experiment No.	Sample	First step T (°C)	First isotherm duration (min)	Second step T (°C)	Second isotherm duration (min)	Carbon % recovered in the first step
1	Std a	350	120	700	10	72
2	Std a	425	10	700	10	84
3	Std b	350	10	700	10	60
4	Std b	425	10	700	10	90
5	ambient sample	435	25	700	10	
6	Std b	435	25	700	10	90

Table 3-1 Experimental conditions used for TGA/FT-IR analyses; standards composition is reported in Sect. 2.1.

A two-step heating procedure has been optimized in order to minimize both charring of organic carbon and pre-combustion of elemental carbon. The heating ramp, suitable to obtain the best separation between EC and OC, consists of a first jump at 435 °C, an isotherm for 25 min, a jump at 700 °C and an isotherm for 10 min. The heating program is displayed in Figure 3. Each jump takes about 2 minutes with a heating preset rate of 160 °C/min (corresponding to a rate of increase of about 200 °C/min as shown in Figure 3). The system takes about 5-10 minutes to equilibrate at the two desired temperatures of 435°C and 700°C. Each analysis takes altogether 55 minutes.

The analysis conditions, i.e. the two-step temperatures, the atmosphere and the isotherm duration, have been set-up analyzing standard samples (described in Sect. 3.2.1) and will be discussed later on in this paper.

In order to perform the TGA/FT-IR calibration, known quantities of standards d1-d3 were analyzed.

Thereafter, for each sample, the area of the peak due to elemental carbon was integrated and the obtained values plotted against the corresponding carbon concentrations. The instrument calibration has been carried out analyzing both powders of samples d1-d3 and standard d1 re-suspended on quartz fiber filter (Sect. 3.4.1). When analyzing real particulate matter samples (Figure 3-2a), the quantification is achieved by single-peak area integration (since the two peaks corresponding to OC and EC are fully separated) taking into account the point where the baseline regains its initial value.

It is worthy to note that suitable standard carbon concentrations have been selected according to the carbon concentrations expected both for ambient samples analyzed in this study (see Sect. 3.4.3) and for SRM1649a. In this way the concentrations determined in the samples fall exactly within the calibration ranges.

For TGA/FT-IR analysis one half of the quartz filter (corresponding to a deposit area of 6 cm²) was accurately cut from the exposed filter area or from the standard sample. The filter was then divided into small pieces, which were put into a circular shaped and flat platinum sample pan (inner diameter = 1 cm and height = 2 mm) placed in the TGA furnace oven.

3.4. Results and discussion

3.4.1. Operational conditions set-up

3.4.1.1. Heating rate and carrier gas

A number of procedures have been recently proposed for OC and EC quantification on filter samples of ambient particulate (Schmid et al., 2001; Chow et al., 2001; Chow et al., 2004; Chow et al., 1993; Birch and Cary, 1996; Cachier et al., 1989; Fermo et al., 2003). Nevertheless, a unique and validated method doesn't exist because of some problems encountered in assigning correctly the carbon content to the organic or to the elemental fraction.

Our methodology for OC and EC analysis is a thermal one based on TGA/FT-IR measurements. It allows OC/EC separation thanks to the different thermal behaviour of the two carbon components. OC and EC are oxidized to carbon dioxide whose quantification is accomplished by a FT-IR spectrophotometer, which acquires infrared spectra simultaneously with the thermo-gravimetric analysis. While non-dispersive infrared detection (NDIR) of evolved CO₂ has already been used (Cadle et al., 1980; Tanner et al., 1982; Novakov, 1997), as far as we know, a FT-IR spectrophotometer as a detector is here applied for the first time (see the Experimental section for details on the apparatus).

Our approach shows some analogies with the earlier thermal methods presented in the literature taking into account the specific problems previously described.

Evolved gas analysis procedures proposed in the literature differ in the temperature programs and in the atmosphere conditions (oxidation or pyrolysis). As concerns the sample heating, up to now three different systems have been employed: (1) direct insertion of the filter into the heated zone (Cadle et al., 1980), (2) flash heating (Tanner et al., 1982; Cachier et al., 1989), i.e. a very rapid heating which allows to reach the final desired temperature within a few minutes, and (3)

progressive heating (Chow et al., 1993; Birch and Cary, 1996; Novakov, 1997; Iwatsuki et al., 1998). As in our system the heating is realized by a thermogravimetric analyzer, we have tested both progressive and flash mode. In a previous work (Fermo et al., 2003) first attempts were made using a temperature rate of 5 °C/min in the range going from ambient temperature up to 650°C. The method accuracy in total carbon determination was verified analyzing SRM 1649a and the error was within 2 %. However, on examining particulate matter on filters, a good separation between OC and EC was not achievable. Therefore, in the present study the heating rate was increased at the maximum value allowed by the instrument (160 °C/min), which means to realize a flash heating.

When starting the analysis, at first the system is left to equilibrate for some minutes at 30°C (Figure 3-3) then a first jump at 425°C (at a rate of 160°C/min) takes place. At this point, after an isotherm step of 25 minutes, a second jump at 700 °C is performed maintaining the same heating rate (heating temperature values and isotherms duration are discussed in the next paragraph).

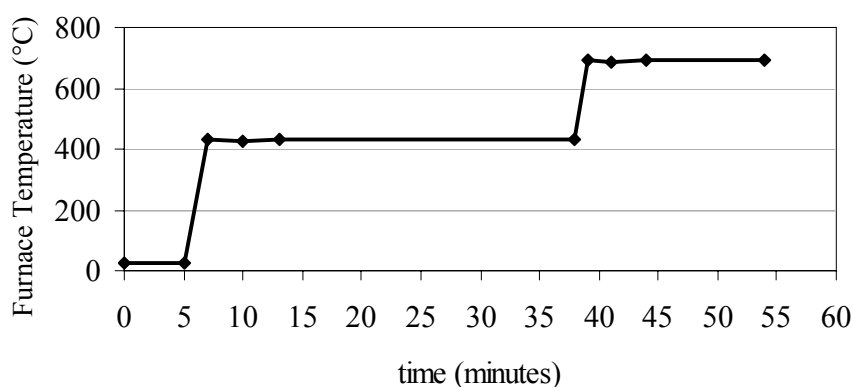


Figure 3-3: Heating program employed for the analysis of particulate matter samples by TGA/FT-IR

A very rapid heating allowed us to obtain two well distinguishable peaks in the CEC (CO₂ Evolution Curve). Furthermore, in these conditions the determination of low quantity of organic and elemental carbon is possible and the organic carbon volatilization is favoured against carbonization. In fact it is well known that, while heating, organic carbon could char, i.e. a pyrolytic organic-to-elemental carbon conversion takes place. Previous works (Cadle et al., 1980; Cachier et al., 1989) have also estimated the percentage of OC to EC conversion, which is about 10-20% in the worst case.

In the literature as carrier gas, He and a mixture of 10% O₂/He or 2% O₂/He are generally used for the OC and EC decomposition step, respectively (Chow et al., 1993; Birch and Cary 1996; Cadle et al., 1980; Tanner et al., 1982). When an inert atmosphere is used during the first step just the organic fraction decomposition takes place and EC decomposition is prevented. However, some authors observed that in order to minimize charring, oxygen has to be chosen instead of an inert atmosphere (Cachier et al., 1989; Ohta and Okita, 1984). In particular Cachier et al. (1989) found that using both flash heating and oxygen as carrier gas, pyrolysis would affect 10% or less of the initial organic carbon. On the base of some experiments previously carried out by TGA/FT-IR (Fermo et al., 2003), it has been concluded that also in our case charring was more pronounced in non-oxidizing media such as helium. For this reason we selected pure oxygen as carrier gas.

3.4.1.2. Heating temperature and isotherm duration

Once flash-heating mode has been selected, some experiments were carried out to optimize the two heating step temperatures in order to find a split point between OC and EC, which is not arbitrary. Nevertheless, it is important to stress that up to now the OC and EC definition is an operative one, depending on the analytical method used for their quantification and, as a consequence (see the introduction), this can produce different splitting between the two fractions.

Different temperatures have been proposed in the literature for the separation of organic carbon from elemental carbon such as 300°C-350°C (Cachier et al., 1989; Ohta and Okita, 1984; Ellis et al., 1884), 400 °C-430°C (Tanner et al., 1982; Iwatsuki et al., 1998) and 650°C (Cadle et al., 1980).

Isotherm duration is also quite variable and goes from a few minutes (Tanner et al., 1982) to longer periods such as 30 minutes (Novakov, 1997), 60 min (Iwatsuki et al., 1998) or 120 minutes (Cachier et al., 1989).

In setting the proper temperature it is mandatory taking into account some facts: temperature must be high enough to assure organic matter complete decomposition; charring must be minimized; elemental carbon pre-combustion must be avoided.

Some experiments were carried out on standard mixtures of known composition in order to establish the optimal temperature for the first step and the corresponding isothermal duration. We didn't check 650°C since the apparatus used in that case (Cadle et al., 1980) worked in an inert atmosphere, avoiding EC decomposition, while we had decided to work in oxygen (see Sect. 3.1.1).

The second temperature step has been in any case set at 700 °C since, working in oxidizing conditions, it is enough to decompose elemental carbon (Cadle et al.,

1980; Iwatsuki et al., 1998). This has been verified by our system analyzing both pure graphite and the standards d1-d3. No residual carbon was observed.

Results obtained in the optimization procedure are summarized in Table 3-1. Each experiment was replicated at least twice.

At first we reproduced the experimental conditions reported by Cachier et al. (1989), i.e. first step temperature of 350 °C and a heating duration of 120 min in order to decompose all the OC fraction (experiment No. 1, Table 3-1). The CEC corresponding to this experiment is reported in Figure 3-4, curve a. Only 72% of the total carbon, in the mixture as $\text{Na}_2\text{C}_2\text{O}_4$, is recovered in the first step (Table 3-1). From experimental results obtained in our laboratory by means of a standard thermo-gravimetric analysis, it has been noted that pure sodium oxalate shows two characteristic decomposition temperatures at about 500°C and 780°C respectively: at 500°C it decomposes and turns to carbonate which then decomposes at 780°C. This high temperature has been avoided in our analyses because of the possibility of carbonate decomposition during real PM samples measurements. The second peak present in the CEC is likely due to the initial carbonate decomposition. Oxalate is the most abundant of the dicarboxylic acids in the particulate matter and can potentially act as cloud condensation nuclei. Its atmospheric concentration is about $0.35 \mu\text{g}/\text{m}^3$ (Yao X. Et al., 2002) and together with malonate and succinate represent on average 5.5 % of sulphate concentration, one of the major PM component. It has also been demonstrated that mono and di-carboxylic acids represent one of the main classes in the so-called WSOC (water soluble organic carbon) fraction that accounts for about 50% of OC (Decesari et al., 2001). As a consequence, oxalate contribution to particulate matter mass is not negligible.

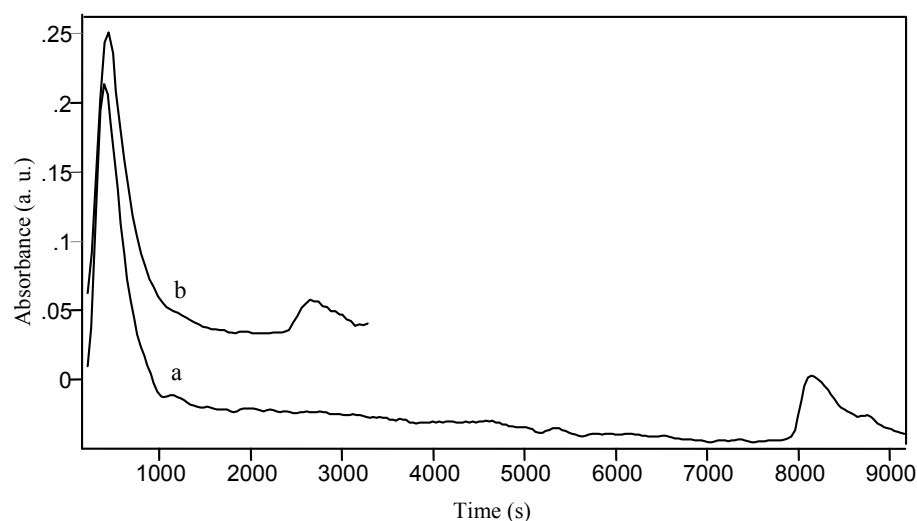


Figure 3-4: CECs obtained by TGA/FT-IR analyzing standard a during the experiment No.1-Table 3-1 (curve a) and experiment No.2-Table 3-1 (curve b).

It is also important observing that the OC fraction could include high molecular weight organic substances having a thermal behaviour quite similar to the soot one. For example a mixture of amid, starch and sucrose has been chosen as a model for this fraction and its thermal behaviour studied. It has been found that in order to have a complete combustion of this class of substances, it is necessary to reach a threshold temperature of 485 °C (Iwatsuki et al., 1998).

In our experiment, the first temperature step was then increased to 425 °C in order to test an intermediate value between 350 and 485 °C (experiment No. 2, Table 3-1). The duration step was drastically reduced to 10 minutes, which seems enough to regain the initial baseline signal and a recovery increase was observed (Figure 3-4, curve b). Nevertheless, when thermal analysis is performed at temperatures lower than 780°C - as in our case - OC may be slightly underestimated if oxalate is present, since it does not completely decompose.

A temperature of 350 °C is not enough to decompose standard b, a mixture containing organic acids (experiment No. 3, Table 3-1). Carbon recovery reaches 90% when heating at 425 °C (experiment No.4, Table 3-1). Taking into account the decomposition temperatures of the substances contained in standard b it is reasonable supposing that under these conditions a charring of 10% took place.

The temperature of 425 °C was then checked for the analysis of samples of ambient particulate matter. For this purpose a 24-hours filter was divided into two portions that were heated at 425°C with an isotherm duration of 25 minutes after which the baseline signal was regained (Figure 3-5, curves a and b). After cooling, one half of the filter was undergone to a 24-hour Soxhlet extraction in dichloromethane in order to dissolve the organic matter that was eventually still present. Soxhlet extraction is frequently used in the analysis of particulate matter organic compounds while dichloromethane has been chosen since it is one of the most widely used solvent (Pozzoli et al., 2004). The two halves were then submitted to the complete ramp program (heating at 425°C/isotherm/heating at 700°C/isotherm). A residual signal is detectable in both CECs in correspondence of the first step (Figure 3-5, curves c and d) suggesting that also by means of the extraction it was not possible to eliminate all the organic substances (the second peak in both curves c and d is due to EC). Afterwards, the experiment was carried out working at a 435 °C, which turned out to be high enough to decompose the whole OC fraction. As a consequence, we selected this value as the first step temperature and adopted the first isotherm duration of 25 min for ambient particulate samples analysis.

Some experiments were also performed in order to evaluate minimum EC combustion temperature. According to data reported by other authors (Iwatsuki et al., 1998) in oxidizing conditions the elemental carbon combustion starts beyond 485 °C and it is complete under 650-660 °C (Cadle et al., 1980; Iwatsuki et al.,

1998). Loss of elemental carbon can be reduced by a short pre-combustion step (Cachier et al., 1989). Samples of pure graphite were analyzed by TGA/FT-IR using the following first step temperatures: 425°C, 450°C, 470°C and 500°C. Starting from 470°C, CEC shows a signal in correspondence of the first step indicating that in our operational conditions some EC pre-combustion can take place.

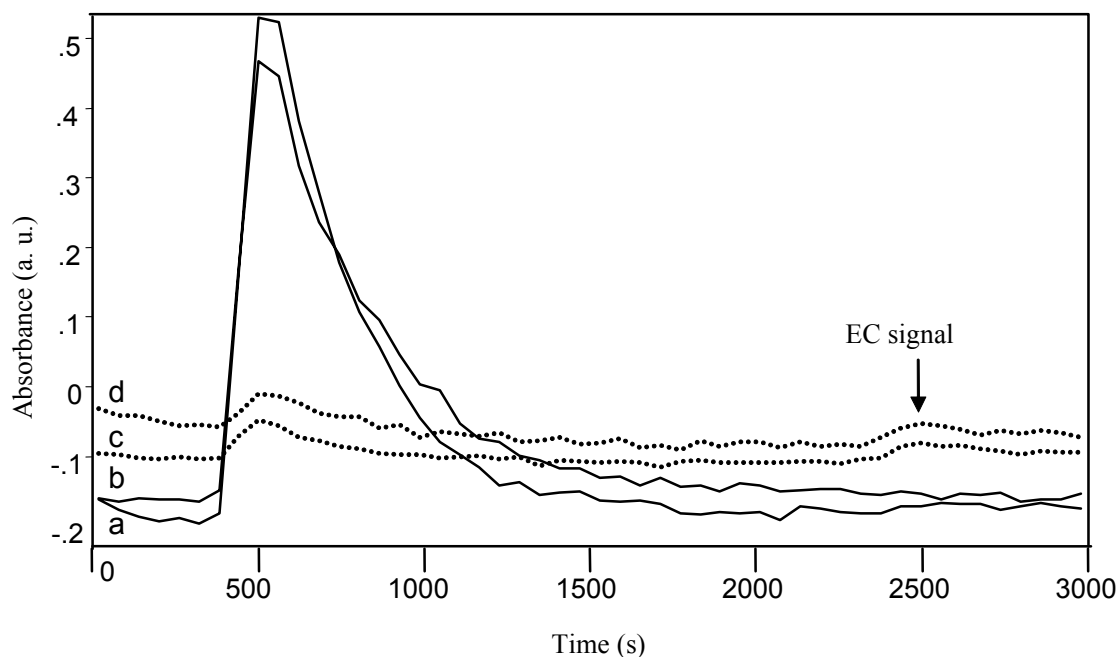


Figure 3-5: CECs obtained by TGA/FT-IR analyzing a 24-hour sample of particulate matter (on a filter). The filter was divided into two portions both heated at 425°C for 25 minutes (curves a and b). Curve c was obtained with the heating program reported in Fig. 3, on one half of the filter submitted to 24-hour Soxhlet extraction; curve d was obtained with the same heating program on the second half of the filter not extracted.

However, it is known that soot present in the atmospheric aerosol is not only composed by elemental carbon but contains a variety of highly condensed organic compounds (Cadle et al., 1980, Cachier et al., 1989). Standard reference material NIES No.8, being a vehicle exhaust particulate, contains about 80% of carbon so that it was used to check pre-combustion conditions in real particulate samples. Four standard samples, previously submitted to Soxhlet extraction in order to eliminate the soluble organic fraction, were analyzed by TGA/FT-IR testing the following first step temperatures: 425°C, 435°C, 450°C and 470°C. A signal attributed to pre-combustion already appeared at 450°C. We can therefore conclude that to avoid elemental carbon pre-combustion, in our operational condition the

maximum temperature for the first step must be 435°C. Even if it cannot be excluded that some quite refractory organic substances could be not still decomposed at this temperature, 435°C is a good compromise between the need to decompose OC and to avoid EC pre-combustion.

As carbon loss is associated with a change in the filter color, in order to verify if some variation occurred, a particulate matter filter was extracted from the furnace at the end of first isotherm step and no change in the filter color was evident.

The final selected operational conditions for ambient samples analysis are summarized in Table 3-1.

We would stress that also with our method OC charring cannot be excluded when analyzing particulate matter samples. However, for a standard mixture of known composition (standard b, experiment No.6, Table 3-1) where no elemental carbon was present, it was estimated to be 10% in accordance with literature data (Cachier et al., 1989). Pure substances with high molecular weights such as sucrose and starch have been analyzed and, from the ratio between areas of the first and the second peak, it was estimated a charring percentage of 10 and 14 %, respectively.

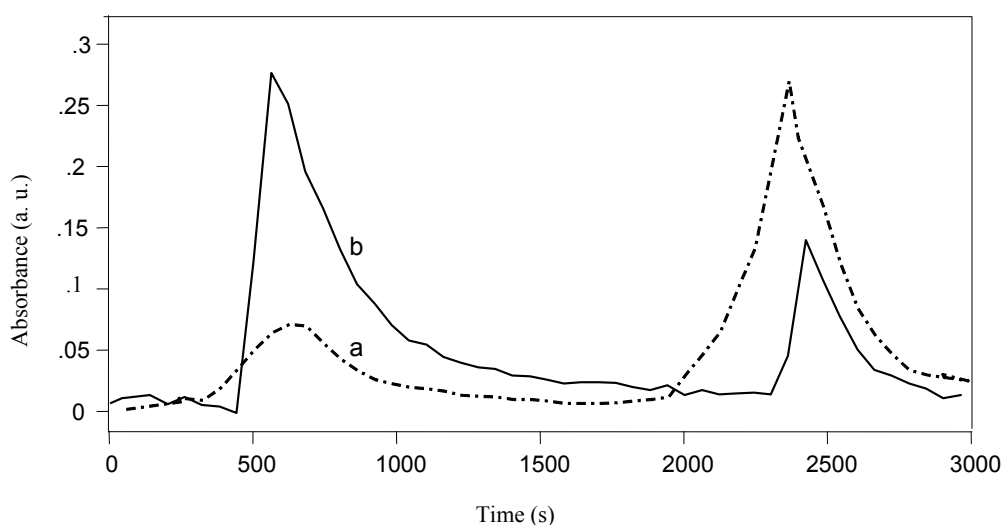


Figure 3-6: CECs obtained by TGA/FT-IR analyzing SRM1649a using a first temperature step of 350°C (curve a) and 435 °C (curve b), respectively

SRM1649a has been also analyzed using the final selected operational conditions. Figure 3-6 shows the CECs obtained with a first temperature step of 350°C (curve a) and 435°C (curve b). As expected, 350°C wasn't high enough to allow complete OC evolution. On the contrary, using a first temperature step of 435°C a good

agreement with literature values has been obtained (Currie et al., 2002). A total carbon content of 17.0% has been obtained against a certified value of 17.68 (± 0.19) % and OC and EC concentrations were 81.4% and 18.6% of TC, both values within the range of variation determined by the other methods (Currie et al., 2002).

3.4.2. Calibration and method validation

Some reference samples containing pure graphite and SiO₂ in known quantities have been prepared in order to perform instrument calibration (standards d1-d3 whose composition is described in Sect. 2.1).

It is important to stress that carbon concentration chosen for standards d1-d3 are found in ambient samples such those collected in this study, i.e. samples with four-hour time resolution. These filters are characterized by low carbon concentrations and the total carbon content on $\frac{1}{2}$ filter (that is the analyzed portion) is within the concentration range reported in Table 3-2 and Table 3-3.

The measurement conditions were the same employed for real samples analysis (experiment No. 5, Table 3-1) that allowed to obtain the best OC/EC separation. Two different calibration curves were constructed:

the first curve (Figure 3-7a) obtained analyzing different quantities of standard d1, d2 and d3 (Table 3-2) that can be used for OC/EC quantification when particulate matter powder samples have to be measured (e.g. SRM1649a);

the second curve (Figure 3-7.b) obtained analyzing one half filter loaded with standard d1 in different quantities (Table 3-3) varying between about 0.17 mg and 1.8 mg; this curve is used for OC/EC quantification in real particulate matter samples.

Std type	Mass of Std Carbon content		Peak area
	(mg)	(mg)	
No sample	0	0	11.4
d2	5.4	0.009	18.7
d2	5.8	0.010	24.0
d1	0.5	0.025	52.6
d2	44	0.074	114
d2	45	0.076	94.7
d3	23	0.077	109
d3	42	0.137	187
d3	43	0.142	167

Table 3-2 Standards used for the calibration curve shown in Fig. 7.a; together with the standard type the mass of the standard, the carbon content present in each standard and the peak area observed in the CEC are reported.

Std type	Mass of Std on ½ filter(mg)	Carbon content (mg)	Peak area
½ blank filter	0	0	17.3
d1	0.172	0.008	23.5
d1	0.277	0.013	30.0
d1	0.523	0.025	37.5
d1	0.702	0.033	44.5
d1	1.299	0.061	65.6
d1	1.480	0.070	91.6
d1	1.791	0.084	96.5

Table 3-3 Standards used for the calibration curve shown in Fig. 7.b; together with the standard type the mass of ½ filter (area 6 cm²), the carbon content present in each standard and the peak area observed in the CEC are reported.

The difference between the slopes of the two curves is about 20%.

As well known, TGA response depends on the physical status of the sample and this is the reason of our tests both on powder as is and on powder deposited on the filter. Working with two different matrices, slight different combustion efficiency can be hypothesized. However, the combustion efficiency at fixed analysis conditions shows a very good reproducibility.

In this work, all the carbon quantifications in PM samples have been made using the second curve (Figure 3-7b).

It has been estimated that our technique has a detection limit of 0.5 µgC/cm² and the precision of the method is 10%. In comparison to NIOSH-TOT and LSCE our methodology has a lower precision while the detection limit is comparable to LSCE one but lower than 1.5 µgC/cm² given by NIOSH-TOT.

An exhaustive comparison between two analytical techniques (TGA/FT-IR and TOT method) is reported in chapter 4. The TOT instrument was designed to specifically address some of the problems observed in other methods in assigning carbon either to the organic or elemental fraction. By the continuous monitoring of the optical absorbance of the sample during the analysis, this method is able to both prevent any undesired oxidation of original elemental carbon and make corrections for the possible generation of carbon char produced by the pyrolytic conversion of organics into elemental carbon.

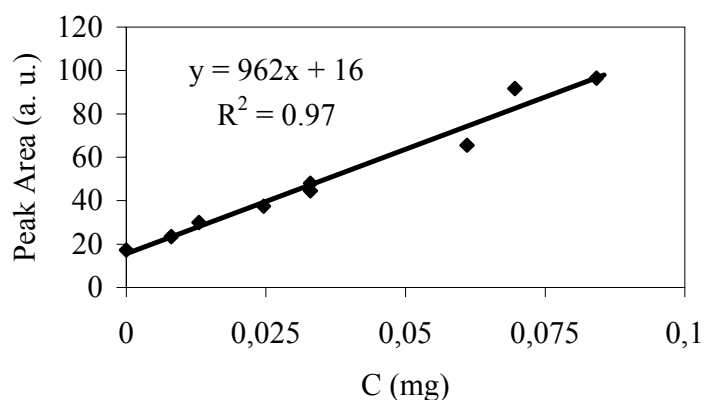


Figure 3-7a

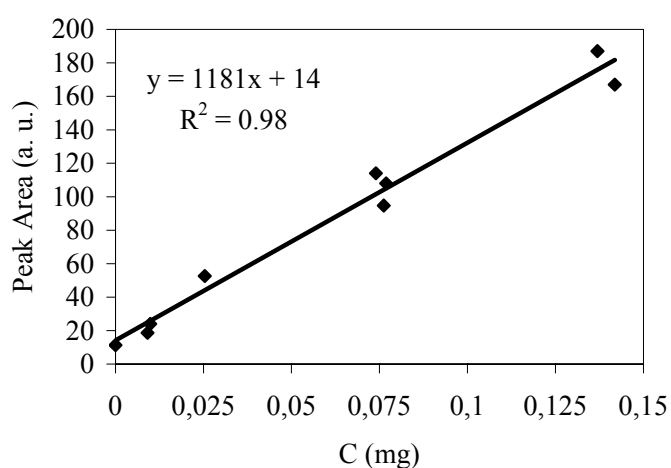


Figure 3-7b

Figure 3-7: Calibration curves obtained analyzing different quantities of standards d1, d2 and d3 (see Sect. 2.1 and Table 3-2) (7.a) and one half of the filter loaded with standard d1 in different quantities (see Table 3-3) (7.b)

3.4.3. Analysis of carbon content in PM samples

The analytical methodology above described was applied to PM₁₀ samples collected in the urban area of Milan to determine the EC/OC/TC content. Blank filters were also analyzed and no significant signals were observed.

The sampling site was a "background urban" location, according to the Italian Environmental Agency definitions, as it is not directly influenced by local emissions (i.e. traffic). The campaign was carried out in 2003, 27th January - 10th February, and the PM₁₀ was sampled daily with a four-hour time resolution. As a

consequence during each day six four-hour time resolution filters were collected with a total number of 90 (=6 x 15) ambient samples during the whole period.

During the second week of the campaign the PM threshold values were exceeded so that the local authorities decided to introduce the condition of an odd/even plate's traffic. However, this obligation was maintained only for a couple of days (starting from Monday, 3rd February) because of the occurrence of a strong Föhn episode, which cleaned up the atmosphere on the whole Po valley (see Figure 3-8). Thus, it was not possible to single out the effect of this action to prevent high pollution levels.

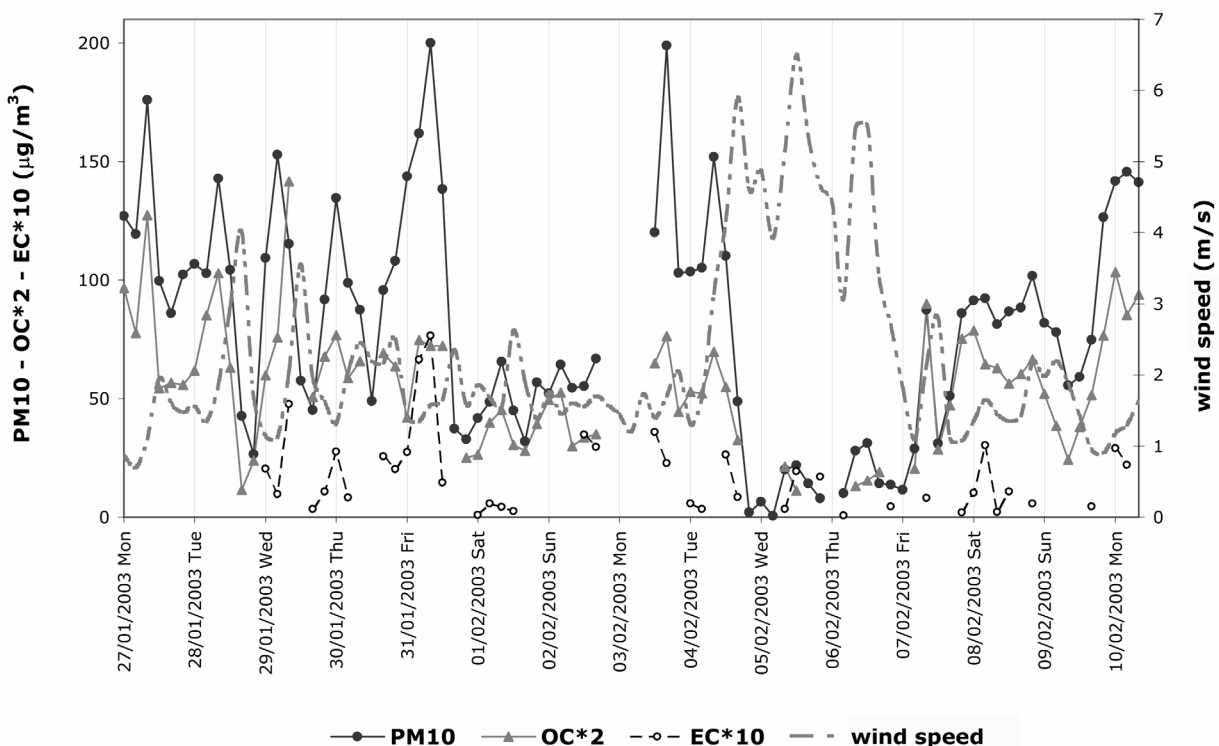


Figure 3-8: Temporal patterns of PM10, OC and EC concentrations together with wind speed (OC and EC values have been multiplied x2 and x10, respectively)

The samples were collected on quartz fiber filters (Whatman QMA) using low volume CEN-equivalent samplers (flow rate: 2.3 m³/h) equipped with PM10 (particulate matter with aerodynamic diameter smaller than 10 µm) inlets. The PM10 mass was gravimetrically determined using the same methodology described in Sect. 2.1.

In Figure 3-8 the temporal patterns of PM10, OC and EC concentrations are displayed together with the wind speed registered during the whole campaign. The

good correlation between the PM10 mass concentration and its carbonaceous component is a first qualitative evidence of TGA/FT-IR reliability. As the examined filters are characterized by a sampling time of 4 hours, the collected particulate matter amount is sometimes very low and EC is often below the detection limit (missing values in the figure).

During the campaign, PM mass concentration varied from $20.1 \mu\text{g}/\text{m}^3$ to $200 \mu\text{g}/\text{m}^3$ with an average value of $79 \mu\text{g}/\text{m}^3$ and a standard deviation of $48 \mu\text{g}/\text{m}^3$ (it is an expression of the observed variability in the data-set and not of the experimental error which is lower than 5%).

Ranges and average values were $12\text{-}70 \mu\text{g}/\text{m}^3$ and $20 \mu\text{g}/\text{m}^3$ for OC and $0.2\text{-}6 \mu\text{g}/\text{m}^3$ and $2 \mu\text{g}/\text{m}^3$ for EC. On average OC and EC made up $29.3 (\pm 12.8) \%$ and $2.5 (\pm 1.8) \%$ of PM10 mass, respectively.

Converting the organic carbon (OC) to organic matter (OM) concentrations using a mean molecular-to-carbon ratio of 1.6, as proposed by the recent literature (Salma et al., 2004; Turpin and Lim, 2001), an average contribution of about 53 % to the PM10 mass has been found.

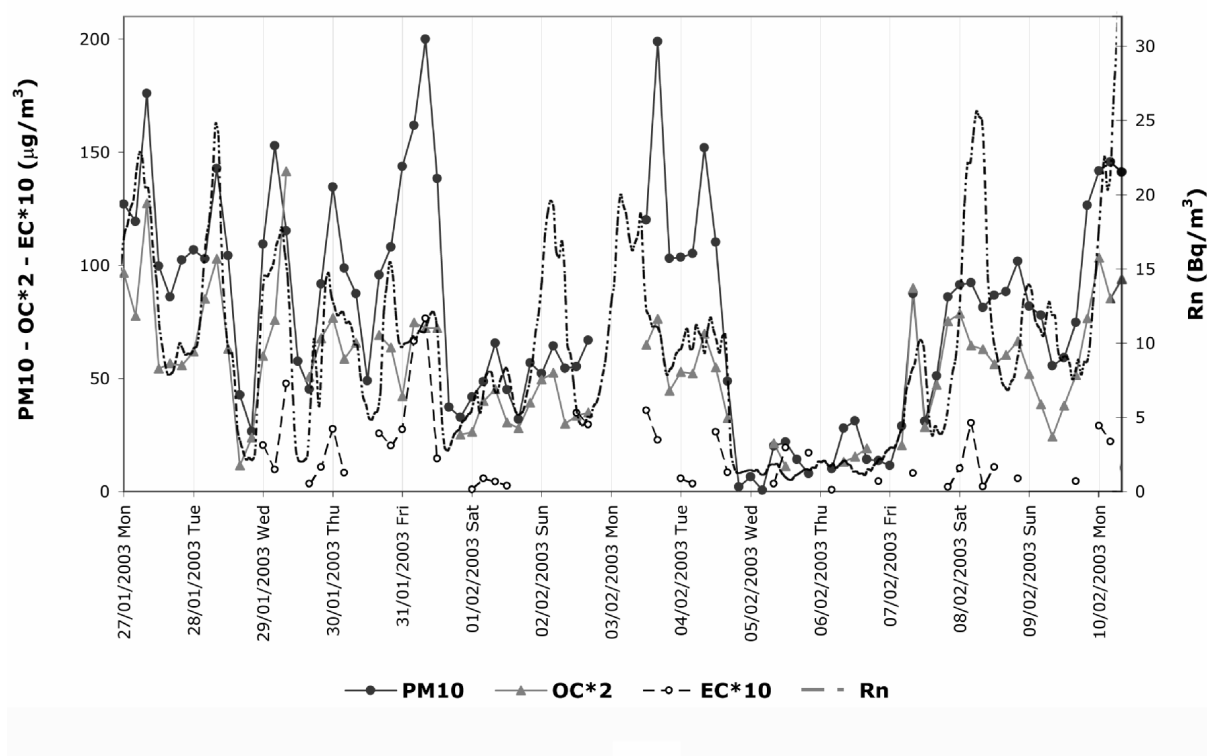


Figure 3-9: Temporal patterns of PM10, OC and EC concentrations together with Radon concentration (OC and EC values have been multiplied x2 and x10, respectively)

To study the observed temporal patterns the concentrations of the gaseous precursors of secondary aerosol as well as meteorological parameters (data available from the regional air quality network), have been also taken into account. Owing to the important role of the dispersion conditions of the atmosphere in determining PM₁₀ concentration levels in the urban area of Milan, and in general in the Po valley, also Radon measurements were carried out during the campaign (Figure 3-9). Radon can be considered a good natural tracer of vertical dispersion as it does not undergo chemical transformations in the air and it has a half-life of 3.8 days that is long enough to measure the atmospheric phenomena of interest here. It also has an approximately constant rate of exhalation from the ground over large, homogeneous areas and over time.

The Radon hourly concentration is routinely and continuously measured at ground level (6 meters asl) in Milan by the group of the Institute of Physics. Radon activity concentration outdoor is detected with hourly resolution through the collection of its short-lived decay products attached to aerosol particles and the spectroscopic evaluation of their alpha activity (estimated detection limit = 0.2 Bq m⁻³). Details on the experimental methodology to measure ²²²Rn concentration are reported in Sesana et al. (2003).

The temporal patterns of PM₁₀, OC and ²²²Rn show a fairly good correlation (Figure 3-9); and when radon concentration reaches the maximum value (during the night and the early morning) the atmospheric dilution power is poorer and the pollutants accumulate (Vecchi et al., 2004).

3.5. Conclusions

The method here presented appears suitable for the analysis of atmospheric aerosol carbonaceous fraction. It is based on evolved gas analysis and it consists of a simple home-made apparatus obtained by the coupling of a thermo-gravimetric analyzer and a FT-IR spectrophotometer. In the framework of our study particular attention has been devoted to the method set-up. In particular, it is well known that the choice of both heating program and carrier gas are tricky points in the analysis of the two components OC and EC. The adopted analytical conditions led to the minimization of both charring of OC and pre-combustion of EC.

The method reliability for carbon quantification is supported by the fairly good agreement with TOT technique, which is one of the most widely used systems for TC/OC/EC analysis. Nevertheless, a clear separation between OC and EC is not easy to achieve either using more sophisticated systems such as TOT or TOR.

TGA/FT-IR was applied to PM10 samples collected in the urban area of Milan to determine the EC/OC/TC content. The technique reliability was also qualitatively demonstrated by the good correlation between the particulate matter mass concentration and its carbonaceous component. As for the method sensitivity, EC values were often below the detection limit but this is mainly due to the fact that the filters were sampled with four-hour time resolution.

Acknowledgment

I'm grateful to G. Marcazzan (University of Milan) for the helpful suggestions

References

- Birch and Cary (1996) *Aerosol Sci. Tech.*, 25, 221-241
Cachier et al., (1989) *Tellus*, 41B, 379-390
Cadle et al. (1980) *Anal. Chem.*, 52, 2201-2206
Chow et al. (1993) *Atmos. Environ.*, 27A, 1185-1201
Chow et al., (2001) *Aerosol Sci. Tech.*, 34, 23-34
Chow et al. (2004) *Sci. Technol.*, 38, 4414-4422
Currie et al., (2002) *J. Res. Inst. Stand. Technol.*, 107, 279-298
Decesari et al., (2001) *Atmos. Environ.*, 35, 3691-3699
Delumyea et al., (1980) *Atmos. Environ.*, 14, 647-652
Duan et al., (2004) *Atmos. Environ.*, 38, 1275-1282
Ellis et al., (1984) *Sci. Total Environ.*, 36, 261-270
Fermo et al., (2003) *Ann. Chim. - Rome*, 93, 389-396
Iwatsuki et al., (1998) *Anal. Sci.*, 14, 321-326
Novakov et al. (1997) *J. Geophys. Res.*, 102, No. D25, 30,023-30
Oberdörster et al., (1990) *J. Aerosol Sci.*, 21, S397
Ohta et al., (1984) *Atmos. Environ.*, 18, 2439-2445
Pozzoli et al., (2004) *Ann. Chim.* 94, 17- 33
Ruellan et al., (2001) *Atmos. Environ.*, 35, 453-468
Salma et al., (2004) *Atmos. Environ.*, 38, 27-36

4. Intercomparison between two different analytical techniques for Organic and Elemental Carbon in Atmospheric Aerosol Samples

The comparability of two techniques, TGA/FT-IR and TOT, has been tested for measuring the concentration of organic carbon (OC) and elemental carbon (EC) in aerosol particulate matter (PM). TGA/FT-IR and TOT have been employed for carbonaceous fraction analysis in PM samples (41 samples) of different provenience and belonging to two different size fractions (PTS and PM1). Portions of the same filters have been analyzed in parallel by both methods.

While equivalence for total and organic carbon with the two methodologies is achieved, the equivalence for EC is much more critical because of difficulties in the optical evaluation of the splitting point. The average differences for TC and OC are respectively $6 \pm 5\%$ and $8 \pm 6\%$ and are within the measurement uncertainty while for EC the difference is higher ($25 \pm 19\%$). These results are in agreement with what observed in the literature when the comparison between different methods for OC/EC analysis is performed.

The techniques validation through the intercomparison between the two methods is needed to confirm the reliability of the analytical data collected during the research programs where this laboratory is involved.

4.1. Introduction

Airborne particulate matter is responsible of adverse effects on both human health and environment (e.g. climate change). The carbonaceous component of atmospheric aerosol, elemental carbon (EC), organic carbon (OC) and carbonate, makes up more than 50% of total mass and is considered one of the most relevant PM fractions with respect to observed adverse health outcomes. In spite of the numerous studies focused on OC/EC quantification, nowadays a universal methodology for their determination doesn't exist and, as a consequence, OC and EC are operationally defined by the method of analysis (Countess, 1990; Schmid, H. et al., 2001; Chow et al., 2004).

The different methods employed in literature studies give results in fairly good agreement just with respect to total carbon (TC) concentrations while difficulties have been encountered in the determination of the two fractions i.e. EC and OC, in

particular because of the pyrolytic conversion of organics into elemental carbon (charring) during the sample analysis. The methods most commonly applied are based on thermal evolution and reflectance/transmission measurements and, amongst them TOT (Thermal-Optical Transmission) is widely employed. An alternative system recently set up in our laboratory is represented by TGA/FT-IR, which consists of a thermo-gravimetric analyzer coupled with an infrared spectrophotometer (Fermo et al., 2006).

In this study TGA/FT-IR and TOT are compared with each other. For this purpose, PTS and PM1 samples collected at different locations have been analysed in parallel by the two systems. Comparability between methods used for OC/EC quantification should be achieved in order to guarantee the reliability of the results obtained by means of different techniques.

4.2. Experimental procedures

4.2.1. Instrumentation

Aerosol carbon content (OC and EC) has been determined by means of a Thermal-Optical Transmission (TOT) instrument and by a TGA/FT-IR (Thermo-gravimetric Analysis coupled with Fourier Transformed Infrared Spectroscopy) system. These two techniques are based on the analysis of thermal evolved gas analyses carried out on a portion of the filter sample placed into a chamber and heated in the presence of one or more gases (O_2 for TGA/FT-IR and He or a mixture of O_2/He for TOT).

TGA/FT-IR consists of a simple home-made apparatus obtained by the coupling of a thermo-gravimetric analyzer and a FT-IR spectrophotometer. More information dealing with system set-up are given in chapter 3 and Fermo et al., 2006. By monitoring CO_2 infrared absorbance at 2361 cm^{-1} it is possible to obtain CO_2 evolution curves where the two components OC and EC are detectable as well separated peaks. EC and OC determination has been performed by a TGA/FT-IR home-made instrument, assembled using a JASCO-FTIR spectrophotometer Model 360 and a Dupont Thermo-gravimetric analyzer model 951. The technique detection limit is $0.5\text{ }\mu\text{gC}/\text{cm}^2$ and the precision is 10%.

The TOT instrument is a carbon analyzer by Sunset Laboratory Inc.. More detail on the methodology can be found in Birch and Cary, 1996. The technique detection limit is $0.15\text{ }\mu\text{gC}/\text{cm}^2$ and the precision is 5%.

Thanks to the monitoring of the optical sample transmittance during the analysis, TOT corrects for carbon char produced by the pyrolytic conversion of organics into

elemental carbon (charring). On the contrary, TGA/FT-IR minimizes the pyrolytic conversion using suitable analysis conditions (Fermo et al., 2006).

Altogether 41 filters were analysed in parallel by means of both techniques.

4.2.2. Samples collection

The samples used for our intercomparison study were PTS and PM1 collected at different locations during previous monitoring campaigns.

Pre-heated (heated at 700°C for 1h) quartz fiber filters were employed for PM collection.

24-hour PM1 samples were collected during a campaign carried out in Milan, Genoa and Florence in 2004 (Vecchi et al., 2005) using low volume CEN-equivalent samplers (flow rate: 2.3 m³/h) equipped with PM1 (particulate matter with aerodynamic diameter lower than 1 µm) inlet. PTS samples have been collected during a campaign carried out in Milan during 2005 (Fermo et al., 2006, in press).

4.3. Results and discussion

In order to test the comparability of TGA/FT-IR and TOT in a wide range of concentrations typical of different kind of sites, the PM1 filters chosen ranged from 7 to 30 µg/m³ for Genoa and Florence and from 30 to 85 µg/m³ for Milan while for PTS (collected in Milan) the concentrations were higher and ranged from 40 to 140 µg/m³. Concentration ranges (minimum and maximum) for TC, OC and EC determined, for all the data set (41 samples), by means of TGA/FT-IR and TOT are reported in Table 4-1. Percentage values are within 9-47% for OC and 2-14% for EC, for TGA/FT-IR, while those obtained by TOT are within 12-40% for OC and 2-19% for EC.

In order to compare the analytical data obtained by the two methods, TC, OC and EC concentrations have been plotted, for each technique, versus the values obtained for each single filter as averages between the TGA/FT-IR and TOT (Figure 4-1) as reported in Ten Brink et al., 2004.

A good correlation is evident for both TC and OC while for EC significant differences are found. Indeed, on one hand it cannot be excluded that TGA might be affected by some OC char or EC pre-combustion during sample heating (even if the experimental set-up adopted minimizes this problem as described in chapter 3 and Fermo et al., 2006). On the other hand, TOT results are affected by

uncertainties in case of heavy loaded PM samples because of difficulties in the optical evaluation of the OC/EC splitting point.

Looking at the correlations reported in Figure 4-1 it is also observable that TGA/FT-IR underestimates EC (or TOT overestimates) while OC is overestimated (or underestimated by TOT). This result suggests that using TGA/FT-IR technique OC char formation is minimized since, in this case, because of the pyrolytic conversion of OC into EC, higher EC values would be found.

It should be taken into account that, as already observed by other authors, problems can arise in the choice of the splitting point for TOT (i.e. difficulties in reading laser transmittance which is very low) in particular for heavy loaded filters. Such a behaviour has been detected in our case for some PTS filters. In fact, looking at Figure 4-1, the difference between the methods increases for the higher concentrations.

	min value ($\mu\text{g}/\text{m}^3$)		max value ($\mu\text{g}/\text{m}^3$)	
	TGA/FT-IR	TOT	TGA/FT-IR	TOT
OC	1.3	1.9	45.5	34.7
EC	0.2	0.2	7.0	16.3
TC (OC+EC)	1.5	2.4	50.6	45.3

Table 4-1: Comparison between TGA/FT-IR and TOT methodologies: minimum and maximum values for OC, EC and TC concentrations ($\mu\text{g}/\text{m}^3$)

Nevertheless, some studies (Chow et al., 2004) have demonstrated how the position of the splitting point is heavily influenced also by PM composition since the presence of catalysts, such as NaCl, Fe_2O_3 , SiO_2 , Al_2O_3 , MnO_2 , may increase oxidation and cause an early evolution of EC. This important aspect can be studied with a greater detail performing the comparison between filters characterized by a different chemical composition, i.e. belonging to different size fractions and/or coming from different site (urban, back-ground, remote). This work is in progress in our laboratory.

It is worthy to note that among the methods used for OC/EC analysis also the most widely used such as TOR (Thermal-Optical Reflectance) and TOT do not yield to the same results as concerns EC (with TOT concentrations lower) mainly because of differences in analysis protocols and instrumentation (Chow et al., 2004). In fact the EC values determined by TOT are up to 30% lower than those obtained by TOR if the same analytical protocol is employed. In case different protocols are employed, the differences can be 70-80% (Chow et al., 2004). Testing the

comparability of numerous methods of analysis sometimes EC concentration differ significantly (Ten Brink et al., 2004).

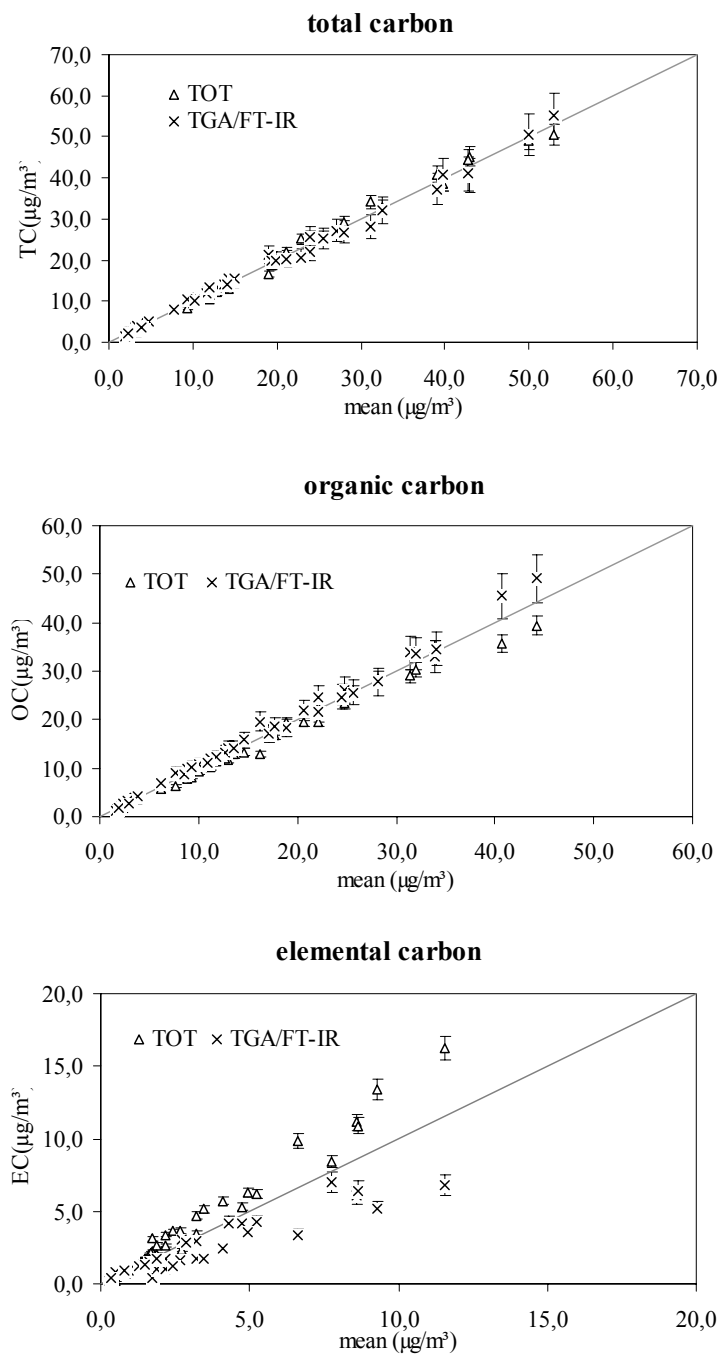


Figure 4-1 Comparison between TGA/FT-IR and TOT methodologies for the analysis of TC, OC and EC in particulate matter samples; the values have been plotted versus the

The average differences observed between the two methods considered in the present work, for TC and OC are $6 \pm 5\%$ and $8 \pm 6\%$ respectively, and are within the measurement uncertainty. These values are comparable with data literature where TC concentrations are typically equivalent within $\pm 5\%$.

For EC the difference is higher ($25 \pm 19\%$) because of the difficulty in the splitting point determination. Taking into account that, for example, an error of 30% is obtained in the literature when the same method is applied but using different protocols, TGA versus FT-IR/TOT agreement seems quite good taking into account that these two methodologies are based on different working procedures (TOT corrects for OC charring and TGA not).

It is also worth to notice that a suitable choice of the splitting point yields a correct evaluation of both OC and EC (due to different sources) and the OC/EC ratio from which it is possible to estimate SOA (secondary organic aerosol) contribution.

If we compare directly TGA/FT-IR with TOT good correlation coefficients are obtained (Table 4-2). The correlation is worst for EC. The regression slopes, with their standard deviations, are also shown in Table 4-2.

Furthermore in Table 4-2 are reported average y/x values (TGA/FT-IR/TOT), standard deviations of the ratios and the distributions of the data pairs with difference ($y - x$) less than 1σ , between 1 and 2σ , between 2 and 3σ and greater than 3σ (Watson and Chow, 2002). It is worthy noting that most of the samples are within 1σ for all the three components OC, EC and TC.

	y	x	regression slope \pm standard error			intercept \pm standard error			r^2	number of pairs
OC	TGA/FT-IR	TOT	1,103	\pm	0,034	0,085	\pm	0,630	0,965	41
EC	TGA/FT-IR	TOT	0,456	\pm	0,037	0,471	\pm	0,212	0,798	41
TC (OC+EC)	TGA/FT-IR	TOT	0,957	\pm	0,026	0,675	\pm	0,614	0,973	41

	average ratio of $y/x \pm$ standard		distribution		
			dev<1s	1s-2s	2s-3s
OC	1,096	0,190	35	2	1
EC	0,728	0,487	34	3	2
TC (OC+EC)	1,007	0,166	32	7	1

Table 4-2 averages y/x ratio (where $y = \text{TGA/FT-IR}$ and $x = \text{TOT}$), standard deviation of the average ratios and distribution of the data pairs whose differences ($y - x$) are less than 1σ , between 1 and 2σ , between 2 and 3σ and greater than 3σ .

4.4. Conclusions

An intercomparison between the two methodologies TGA/FT-IR and TOT have been carried out analysing a statistically significant number of aerosol samples. A good comparability is achieved for TC and OC while the agreement is poorer for EC, in accordance with what previously observed by other authors.

Thanks to the validation procedure performed through the intercomparison, the data reliability is assured. Both techniques have been applied for the analysis of PM samples from different monitoring sites (urban, back-ground and remote sites) collected in the frame of the PARFIL (Particolato Fine in Lombardia) Project carried out in the Lombardy region (Italy).

References

- Birch and Cary (1996) *Aerosol Sci. Tech.* 25, 221
Chow et al. (2004) *Environ. Sci. Technol.* 38, 4414
Countess (1990) *Aerosol Sci Technol.* 12, 114
Fermo (2006) *Atmos. Chem. Phys.* 6, 255
Schmid (2001) *Atmos. Environ.* 35, 2111
Ten Brink (2004) *Atmos. Environ.* 38, 6507
Vecchi (2001) *Abstracts of the European Aerosol Conference, Ghent, Belgium*
Watson (2002) *J. Geophys. Res.* 107, 8341

5. Development of a novel technique for WSOC (Water Soluble Organic Carbon) quantification by Sunset Instrument and discussion about an hypothetical error in EC quantification

5.1. Introduction

Studies encompassing both urban and rural locations have shown that a significant fraction of the particulate organic carbon (OC) in the atmosphere is water-soluble organic Carbon (WSOC) (Sempere and Kawamura, 1994; Zappoli et al., 1999). Due to its affinity with water, WSOC plays an important role in aerosol-cloud interactions, wet scavenging of atmospheric particles, and formation of haze (Facchini et al., 2000; Watson, 2002). Measurement of WSOC concentrations is necessary for quantifying the relative contribution of individual water-soluble organic compounds to the total WSOC mass and for assessing the need for identifying additional water soluble compounds (Yang et al., 2002).

Several study have reported that a significant portion of smoke particles (from 11% to as high as 99%) is water-soluble organic material (Novakov and Carrigan, 1996; Narukaawa et al., 1999; Ruellan et al., 1999). According to other authors in addition to primary emission a main source of WSOC is secondary oxidation of organic precursor (Saxena and Hildeman, 1996; Feng et al. 2006). This fraction of carbon is also used to evaluate the particulate matter ageing (Feng et al. 2006).

5.2. WSOC quantification with TOT instrument

We have been estimated that in Lombardy Region (northern Italy) the influence of wood burning during the winter season is relevant, on average 30% of OC is due to this source (see chapter 8), and also the impact of OC secondary formation is significant, more than 30% of organic matter is due to secondary process (see chapter 8 *and* 12). So we have used PM samples collected in different sites of Lombardy Region to apply a new approach for WSOC quantification.

The WSOC are generally isolated by extraction of aerosol samples with water and measuring their total carbon concentration by liquid total carbon (TOC) analysis (Graham et al., 2002; Mayol-Bracero et al., 2002; Yang et al., 2003; Jaffrezo et al., 2005; Feng et al., 2006)

The aims of this work are (1) to estimate the WSOC concentration in some particulate matter samples (2) to evaluate the feasibility of using TOT (Thermal Optical Transmittance method) analyzer by Sunset for WSOC measures and evaluated a possibly error on the separation between OC and EC during this analysis.

We have determined Water Soluble Organic Carbon (WSOC) with Thermal Optical Transmittance Method (Sunset Instrument) (chapter 4, Birch and Carry 1996,).

With this technique the main problem is that during analysis, some organic compounds pyrolyze before they thermally evolve under the He/O₂ step of the analysis.

The pyrolysis that is formed in the analysis process, if not properly accounted for, would be incorrectly reported as EC present in the original sample, thermal-optical methods are commonly used techniques in which a laser transmittance procedure is used to correct for pyrolysis (Schauer et al., 2003). The pyrolysis of OC and the uncertainties to separate PyC (Pyrolyzed OC) fraction from EC fraction should be cause of an error in quantifying the two carbon fractions (OC and EC).

This analytical method is based on the NIOSH 5040 protocol and the OC is separated into four thermal fractions by the following temperature steps, OC1 at 310°C, OC2 at 475°C, OC3 at 615°C and OC4 at 870°C in a helium environment. PyC is considered the fraction evolved in a mixture of 2% oxygen and 98% helium environment until the laser transmittance returns to its original value. EC fraction is defined as that which evolves in a subsequent heating step in the presence of a gas mixture containing oxygen after PyC, when the transmittance value is higher than the original value.

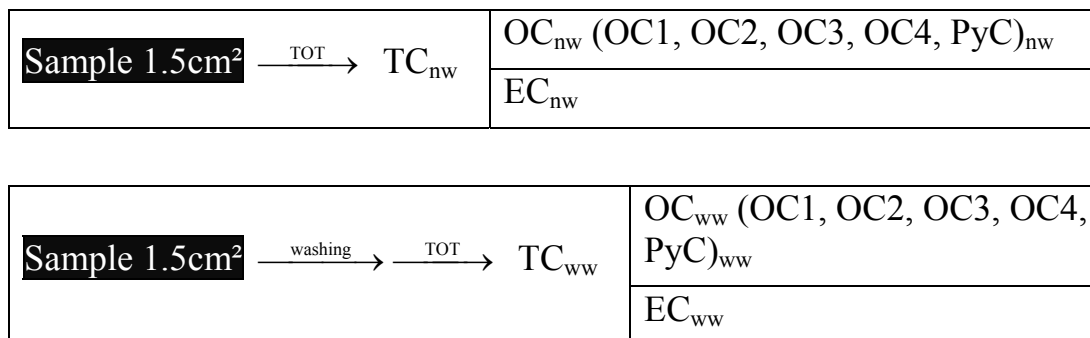
In this study we have analyzed 20 urban particulate matter samples. PM concentration is between 10µg/m³ and 180µg/m³, the OC concentration between 3 and 60µg/m³ (equivalent to a concentration between 7 and 150µg/cm² on the filter) and the EC concentration between 0.5 and 9µg/m³ (equivalent to a concentration between 1 and 20 µg/cm² on the filter).

The quartz filter portion (1.5cm²) analyzed has been washed with MQ water, the sample has been put in a small bunker filter and few milliliters of water have been leached through it.

After the washing, the samples have been dried in a cleaning atmosphere.

Two portions of the same filter have been analyzed, one without washing it, in the following called nw (not washed) and the other washing it, ww (with washing).

The schematic representation of the analytical procedure to quantify WSOC and other carbon fractions are reported in Figure 5-1.



$$WSOC = TC_{nw} - TC_{ww}$$

$$EC = EC_{ww}$$

$$OC = TC_{nw} - EC_{ww}$$

$$WINSOC = OC - WSOC = OC_{ww}$$

$$PyC = EC_{nw} + PyC_{nw} - EC_{ww}$$

Figure 5-1: schematic representation of the analytical procedure in order to quantify WSOC concentration.

WSOC concentration average in these samples is 25% (±10%) of total carbon, in Figure 5-2 we show the carbonaceous fraction composition in the samples.

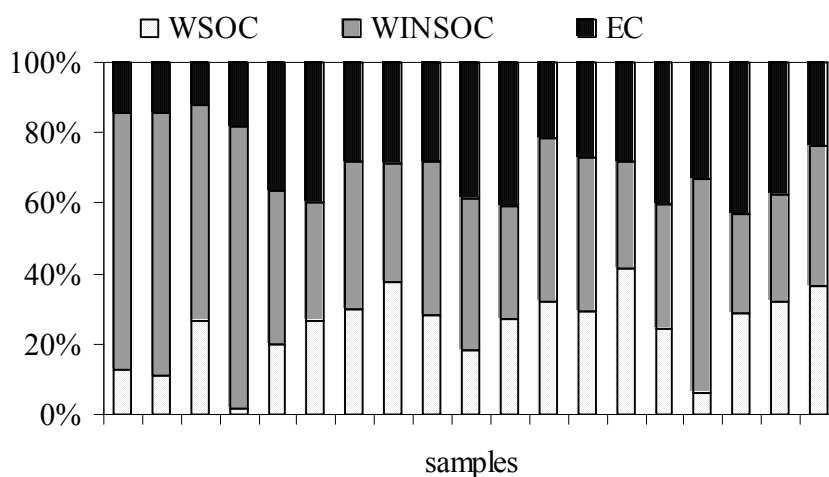


Figure 5-2: percentage of WSOC, WINSOC and EC in the samples

5.3. An hypothetical error in EC quantification

The WSOC concentration, calculated as the difference $TC_{nw} - TC_{ww}$, does not match the difference between the Organic Carbon before and after washing, because this procedure modifies the EC values.

As a matter of fact, the presence of WSOC compounds increases the PyC formation during thermal analysis, in fact after the washing the PyC percentage decreases from 36% to 10% of the OC, the values of these ratios are reported in Table 5-1..

	$(PyC/TC)_{nw}$	$(PyC/OC)_{nw}$	$(PyC/TC)_{ww}$	$(PyC/OC)_{ww}$	PyC_{ww}/TC_{nw}
average	28%	35%	6%	9%	4%
standard deviation	10%	12%	6%	10%	5%
min	9%	11%	0%	0%	0%
max	46%	52%	20%	32%	14%

Table 5-1: PyC percentage in the nw and ww samples

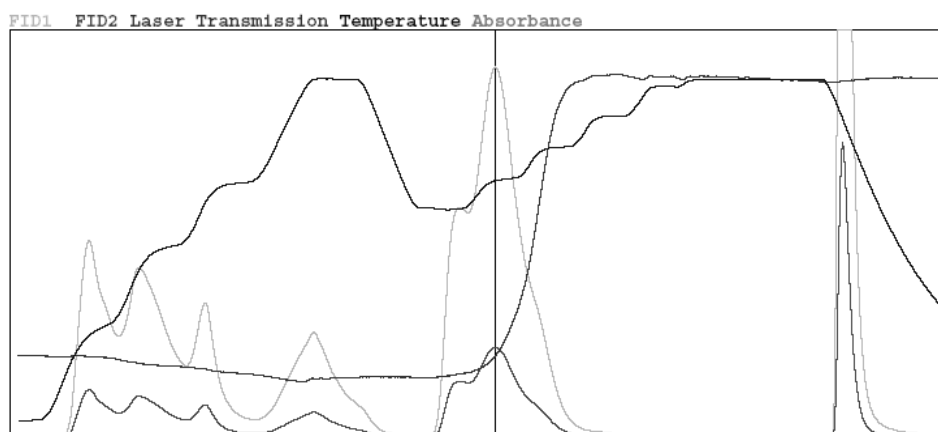
The lower abundance of PyC in the washed samples improves the quantification of EC. As shown before, the key point of this analytical method is the separation between PyC and EC. In Figure 5-3 the analysis signal of the same sample before and after washing is shown. Before washing, the PyC and EC evolve in the same peak: a small change of the position in the *time split* produces a large difference in the EC quantification; instead, after washing, the PyC peak is smaller: the EC peak is well defined and consequently the separation of two peaks is improved.

The “true” values of PyC (in no washed samples) is calculated as reported in Figure 5-1, and the TC average percentage is 19% ($\pm 7\%$), this value is lower than the one directly measured in nw samples and reported in Table 5-1.

In the washed samples the smaller PyC contribution produces a variation in the EC analytical quantification and, consequently, in the OC values: according to our experiment, the EC concentration after washing increases up to average value of 46%. In Figure 5-4 and Figure 5-5 the correlation between EC after and before washing is shown; the difference between the two EC values can be significative (from -33% to +129%).

The high quantity of pyrolytic carbon in the original samples also influences the quantification of OC, the organic carbon concentration calculated as shown in figure 1 is on average the 20% lower than the OC in original samples (OC_{nw}) (Figure 5-6).

No washed sample



Washed sample

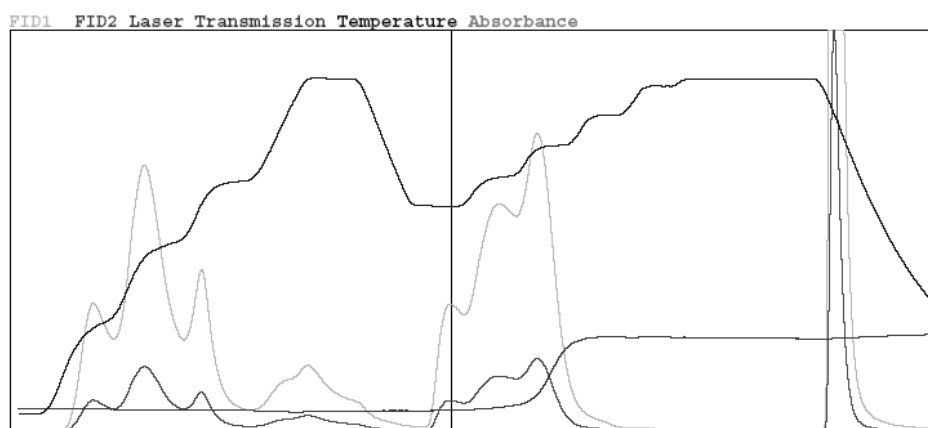


Figure 5-3: analytical signals from the same sample, before washing (up figure) and after washing (down figure)

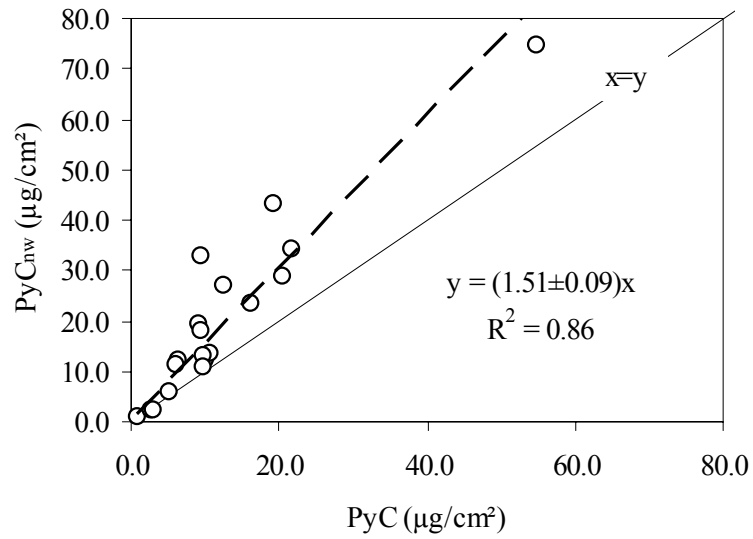


Figure 5-4: comparison between PyC calculated as shown in Figure 5-1 and PyC in nw samples (PyC_{nw})

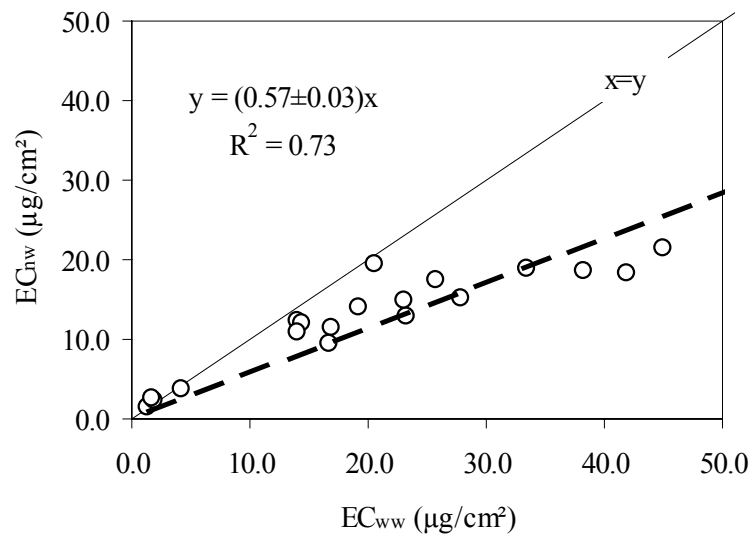


Figure 5-5: comparison between EC in the ww samples (EC_{ww}) EC in nw samples (EC_{nw})

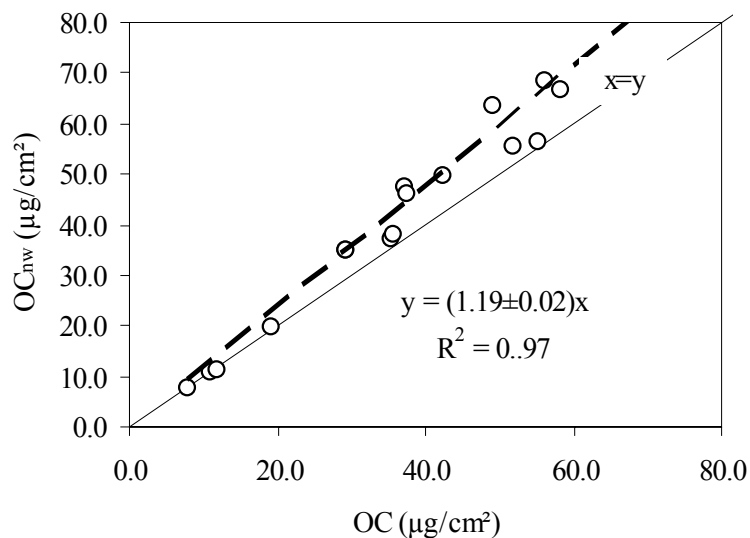


Figure 5-6: comparison between OC calculated as shown in Figure 5-1 and OC in nw samples (OC_{nw})

The error on OC, EC and PyC reported in Table 5-2, is calculated as the difference between the original values and the new values (calculated as shown in Figure 5-1) versus the new values.

	OC error	EC error	PyC error
average	15%	32%	62%
standard deviation	12%	16%	59%
minimun	1%	5%	9%
maximun	39%	56%	249%

Table 5-2: error on OC, EC and PyC between original values and the “true” values calculated as shown in Figure 5-1

The error in the PyC quantification is very high and influences the OC and EC quantification.

	OC	EC	OC1	OC2	OC3	OC4	PyC	WSOC	OC err.	EC err.	PyC err
OC		0.79	0.84	0.96	0.90	0.77	0.92	0.92	0.41	0.48	0.25
EC	0.79		0.91	0.82	0.77	0.60	0.59	0.75	0.84	0.65	0.73
OC1	0.84	0.91		0.76	0.66	0.47	0.76	0.71	0.72	0.66	0.54
OC2	0.96	0.82	0.76		0.96	0.86	0.79	0.93	0.44	0.41	0.33
OC3	0.90	0.77	0.66	0.96		0.90	0.70	0.93	0.39	0.34	0.33
OC4	0.77	0.60	0.47	0.86	0.90		0.51	0.75	0.20	0.16	0.22
PyC	0.92	0.59	0.76	0.79	0.70	0.51		0.82	0.24	0.47	0.01
WSOC	0.92	0.75	0.71	0.93	0.93	0.75	0.82		0.38	0.44	0.28
OC err.	0.41	0.84	0.72	0.44	0.39	0.20	0.24	0.38		0.79	0.91
EC err.	0.48	0.65	0.66	0.41	0.34	0.16	0.47	0.44	0.79		0.62
PyC err	0.25	0.73	0.54	0.33	0.33	0.22	0.01	0.28	0.91	0.62	

Table 5-3: correlation matrix between results and errors obtained with this new approach

If we correlate

Table 5-1) the new values calculated we can note that PyC is higher correlated with the two OC fraction that evolve at lower temperatures, while the WSOC concentration in our samples are higher correlated with OC2 and OC3 fractions.

The error on OC shows a good correlation (0.84) with EC concentration, indeed high EC produces lower transmittance at the beginning analysis and as a consequence the laser variation reading is more difficult.

5.4. Conclusions

The WSOC fraction is a consistent portion of OC and its quantification can provide important information on the particulate matter sources and on the chemistry and physics atmospheric processes.

The TOT instrument by Sunset can be used for WSOC quantification, the intercomparison with TOC analyses is still in progress on our laboratory.

There is a not constant ratio between the error and OC concentration, so it is difficult to define a factor which enables to due correction of the results. Probably, in order to obtain a more correct EC quantification, it would be necessary to analyze washed sample during routine TOT analyses.

Acknowledgment

I'm grateful to A. D'Alessandro (University of Milan) for the helpful suggestions and C.Abate for WSOC analyses.

References:

- Birch and Cary (1996) *Aerosol Sci. Tech.* 25, 221
Facchini et al., (2000) *Atmospheric Environmental* 34, 4853-4857
Feng et al., (2006) *Atmospheric Environmental* 40, 3983-3994
Graham et al., (2002;) *J.Geophysical Research-Atmospheres* 107 (D20): Art. No. 8047
Jaffrezo et al., (2005) *Atmospheric chemistry and Physic* 5, 2809-2821
Mayol-Bracero et al., (2002) *J.Geophysical Research-Atmospheres* 107 (D20): Art. No. 8091
Narukawa et al., (1999) *Geophysical Research Letters* 26 (20): 3101-3104
Ruellan et al., (1999) *J.Geophysical Research-Atmospheres* 104 (D23): 30673-30690
Saxena and Hildeman, (1996) *J. Atmospheric Chemistry* 24, 57-109
Schauer et al (2003) *Environmental Science and Technology* 37, 993-1001.
Sempere and Kawamura, (1994) *Atmospheric Environmental* 28, 449-459
Watson (2002) *J. Air waste management ass.* 36 (4), 228 - 713
Yang et al., (2002) *Atmospheric Environmental* 40, 3983-3994
Yang et al., (2003) *Atmospheric Environmental* 37, 865 – 870
Zappoli et al. (1999) *Atmospheric Environmental* 33, 2733-2743

6. Identification and estimation of atmospheric aerosol main components: hit the target by means of a single analytical method

6.1. Introduction

Atmospheric aerosol main components are represented by some principal ions (sulphate, nitrate and ammonium) and by the carbonaceous fraction, i.e. total carbon (TC) which is mainly formed by organic carbon (OC) and elemental carbon (EC). These two components (main ions and TC) account for about 40 and 50% of the particulate matter mass.

Ions determination in aerosol is commonly achieved by means of ion chromatography (IC) (chapter 2) after extraction of the filter. The methods most commonly applied for OC and EC quantification are based on thermal evolution and reflectance/transmission measurements (Birch and Cary, 1996), i.e. TOT and TOR. In a recent study (Fermo *et al.*, 2006) a new method consisting of a TGA/FT-IR (thermo-gravimetric analyzer combined with an infrared spectrophotometer) (chapter 3) has been proposed and validated through the comparison with TOT.

We have investigate the possibility to monitor simultaneously CO₂, deriving from OC and EC decomposition, with other species (SO₂, NO, NO₂, N₂O, NO₃⁻ and NH₄⁺) which volatilize during the decomposition of sulphates and nitrates contained in the particulate matter. While the system turned out to be reliable for OC and EC quantification, the assessment of ammonium, sulphate and nitrate concentrations by means of TGA/FT-IR is still in progress and here we present some preliminary results.

6.2. Methods

TGA/FT-IR system is based on the continuous acquisition of IR spectra for the gaseous species of interest while the filter is thermally decomposed following a thermal program consisting of two heating steps and previously set-up (Fermo *et al.*, 2006).

This allows, for each examined sample, to obtain 64 IR spectra in the region 4000-600 cm⁻¹.

By monitoring the single species infrared absorbance at its typical frequency an evolution curve is obtained. The evolution curve peak areas are proportional to the compounds concentration.

In Table 6-1 are reported the compounds of interest in the aerosol characterization, the gaseous or ionic species deriving from their thermal decomposition and the corresponding IR frequencies.

Compound	Analyzed species	Frequency (cm⁻¹)
OC	CO ₂	2361
EC	CO ₂	2361
SO ₄ ⁻	SO ₂	1360
	NO ₂	1628
	NO	1896
NO ₃ ⁻	N ₂ O	2236
	NO ₃ ⁻	1360, 830
	NH ₄ ⁺	3200, 1420

Table 6-1: analyzed compounds and their typical IR frequencies

Sometimes, the species observed in the IR spectrum are in ionic form, because of a condensation process probably occurring in the White cell for gas analysis, placed inside the spectrophotometer.

The measurements have been carried out on both standard materials (NH₄NO₃, (NH₄)₂SO₄ and mixtures of these two salts) and about 150 real urban PM1 samples, collected during a campaign carried out in Milan, Genoa and Florence in 2004 (see chapter 11) using low volume CEN-equivalent samplers (flow rate: 2.3 m³/h) equipped with PM1 inlet.

Standard analysis allowed to identify the peaks of interest.

In order to verify the method reliability in the assessment of ions concentrations, different portions of the same filter have been analyzed by both TGA/FT-IR (chapter 3) and IC (after sample ultrasonic extraction with MQ water) (chapter 2).

6.3. Result and discussion

The aim of the present work is the simultaneous analysis of OC and EC with the major ions by TGA/FT-IR system.

The evolution curves obtained for the different species on a real PM sample are shown in Figure 6-1 together with an IR spectrum belonging to the collected series.

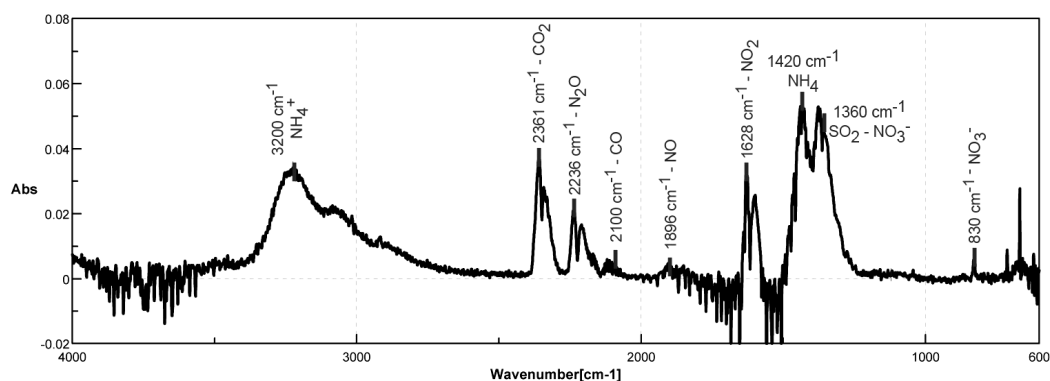


Figure 6-1a

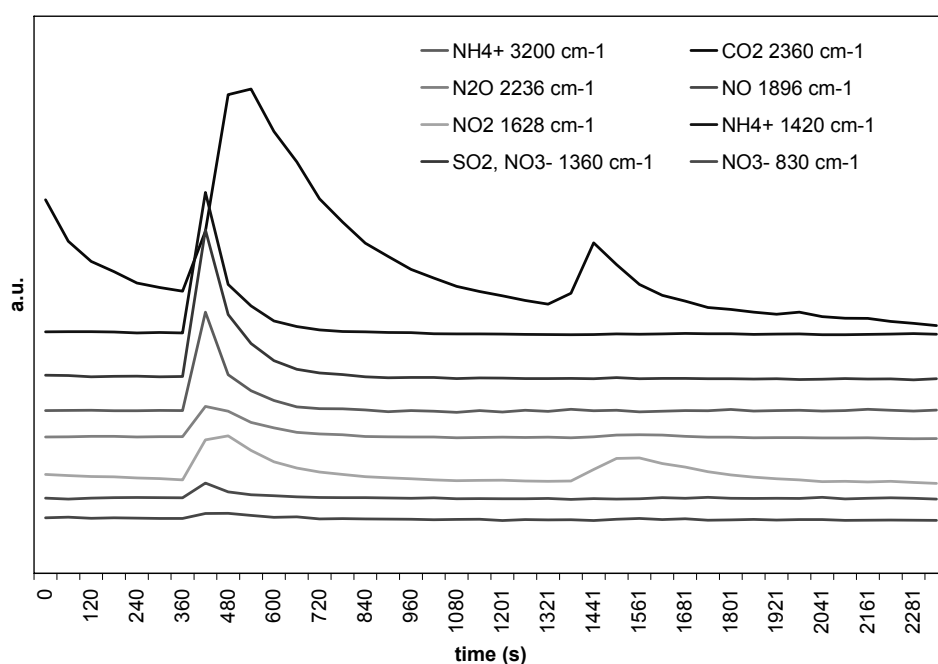


Figure 6-1b

Figure 6-1 Evolution curves (b) for the different species and the corresponding IR spectrum (a)

It is worthy to note that each species has a different response factor in the IR spectrum; as a consequence comparing different compounds, the peaks intensities are not proportional to real concentrations. The evolution curves in Figure 6-1 are reported in the real intensities.

In the following pictures (Figure 6-2) the more significant temporal trends of the major compounds obtained by the two methods (IC and TGA/FT-IR) are compared.

It has to be pointed out that the validation of OC/EC concentrations determined by TGA/FT-IR has been performed by an inter comparison with another technique, i.e. TOT, and this is the subject of another poster presentation (4G12).

At present, compounds concentration determined by TGA/FT-IR are not reported in $\mu\text{g}/\text{m}^3$ since the optimization of calibration procedure is still in progress. Values obtained are reported as evolution curves peaks areas, expressed in a.u..

Generally good agreements between TGA/FT-IR and IC data on PM samples are observable. For nitrates the best accordance has been observed in Milan and Florence during wintertime (figure 2b and 2c) when ammonium nitrate concentration is higher (since the signal at 830 cm^{-1} is less intense than that at 1628 cm^{-1} , the trend of the first one is shown only for Milan, where NH_4NO_3 is present in a higher quantity than in Florence).

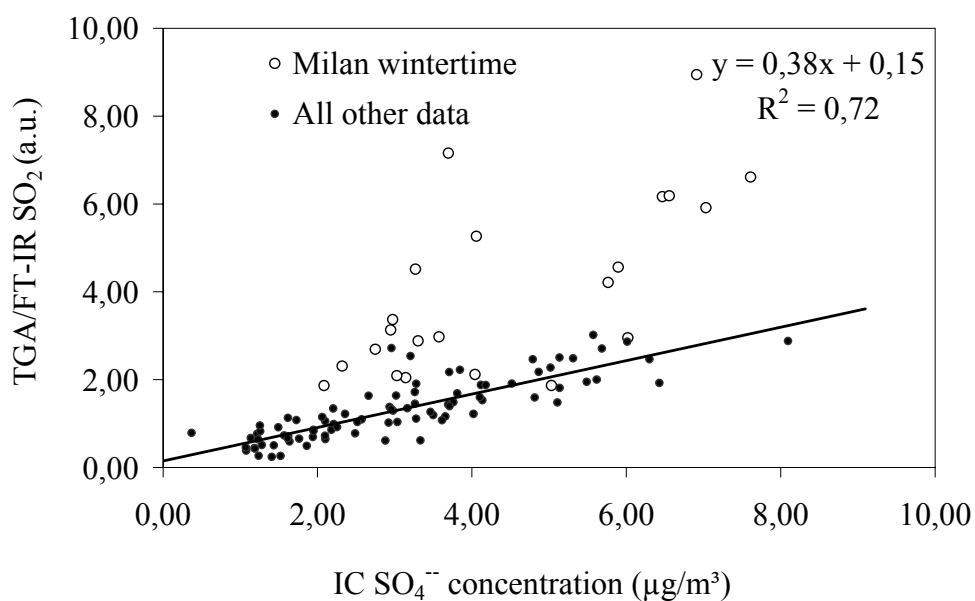


Figure 6-2: 3a: SO_4^{2-} (IC) and SO_2 (TGA/FT-IR) correlation

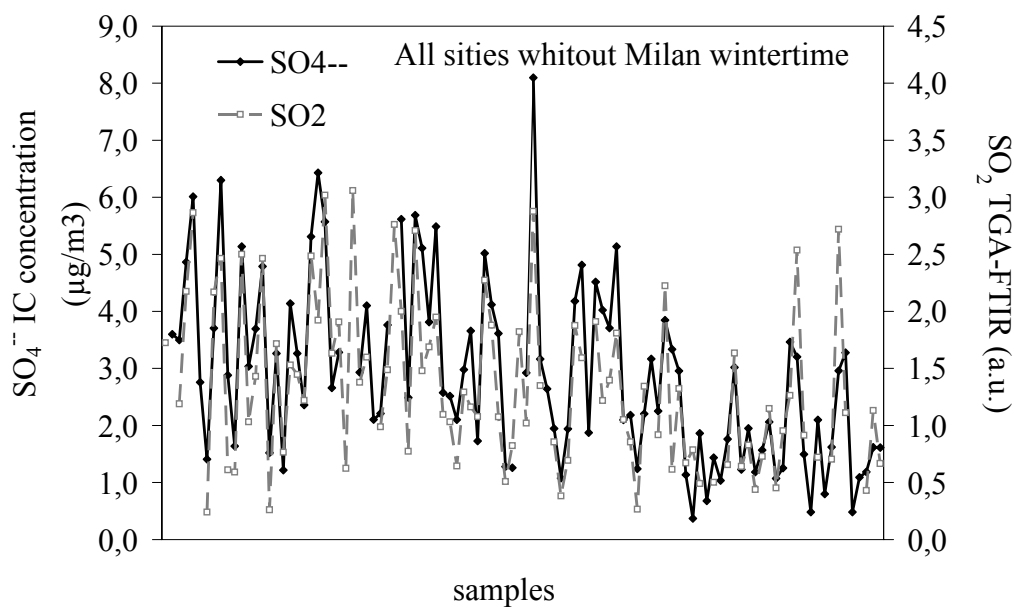


Figure 6-3: SO_4^{2-} (IC) and SO_2 (TGA/FT-IR) patterns

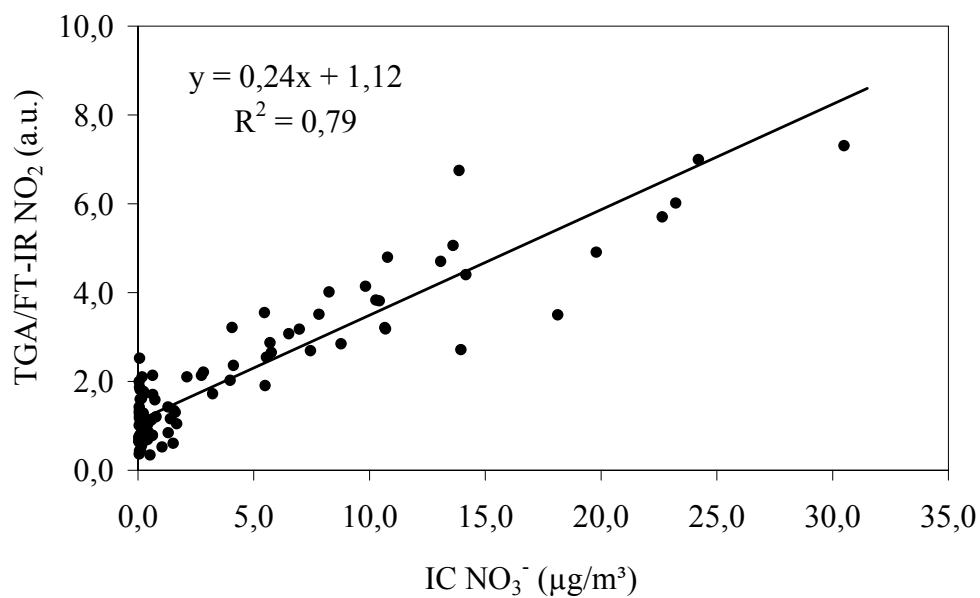


Figure 6-4: NO_3^- (IC) and NO_2 (TGA/FT-IR) correlation

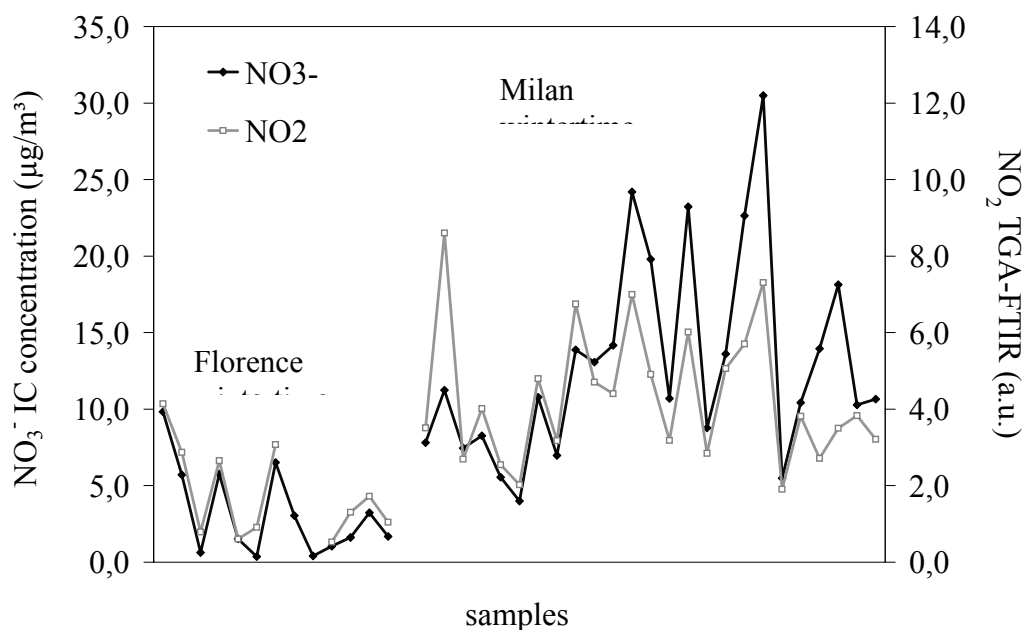


Figure 6-5: NO_3^- (IC) and NO_2 (TGA/FT-IR) patterns

For sulphates the accordance is good in all the cases (Figure 6-3) but in Milan during wintertime. As shown in table 1 the 1360 cm^{-1} signal is due to both SO_2 , coming from sulphate decomposition, and NO_3^- but it has to be observed that the signal intensity due to nitrate is not comparable with those of the other to signals previously used, i.e. 830 cm^{-1} and 1628 cm^{-1} . When nitrates concentration are not particularly high, the contribution of this species to the band at 1360 cm^{-1} is negligible, and sulphates determined by IC are in accordance with TGA/FT-IR data.

In Figure 6-2 and Figure 6-4, the correlations between data turned out by the two methods are shown.

Likewise what observed for the trends, the correlations are good with the exception of Milan-wintertime. This poor correlation is due, as previously mentioned, to the spectral interference between SO_2 and NO_3^- at 1360 cm^{-1} .

Nitrate low concentration points (Figure 6-5) are spread because of the interference of the water signal.

At the moment, by means of reference materials analysis and calculation of the sensitivity factors, we are trying to separate the different interfering contributions, in order to go back to sulphates and nitrates concentrations.

6.4. Conclusion

It is worthy to note that the hyphenated method TGA/FT-IR is here proposed for the first time to our knowledge for the simultaneous quantification of particulate matter main components, by means of a single analytical method.

A first advantage is represented by the direct measurement of the filters without any pre treatment, generally a tricky step which could introduce further sample contamination.

Furthermore, TGA/FT-IR is a cheaper technique (no chemical reagents and expensive spare parts are required).

Moreover, analyses required a lower time consumption: no sample treatment and simultaneous assessment of both ionic and carbonaceous components.

Finally, the quantification of all the components is performed on the same sample portion, saving the remaining filter for further analyses.

Since the sensitivity is lower than that one achievable by means of IC, a drawback is that concentrations lower than about $1\mu\text{g}/\text{m}^3$ are at the moment not valuable, because of the IR signal to noise ratio.

On the other hand, a drawback of IC is represented by the complex and time consuming extraction procedure in order to obtain good recoveries.

It is also worthy to note that while IC allows the measurement of only the soluble fraction of ions, by means of TGA/FT-IR total species (soluble and insoluble) are quantified.

Acknowledgment

I'm grateful to A. D'Alessandro (University of Milan) for the helpful suggestions

References

- Birch and Cary (1996) *Aerosol Sci. Tech.*, 25, 221-241
- Chow and Watson (1999) Ion chromatography in elemental analysis of air borne particles in elemental analysis of airborne particles, vol. 1, edited by S. Landsberger and M. Gretchman, pp. 97-137, Gordon and Breach Science Publishers.
- Fermo et al. (2006) *Atmos. Chem. Phys.*, 6, 255-266

7. New analytical technique for levoglucosan quantification

7.1. Introduction

Nowadays, very few data on the possible contribution of particles emitted by residential wood combustion in Italy are available.

To achieve more informations on this source of particulate matter, our group has began a study on wood smoke contribution by means of the chemical characterization of aerosol samples. In the literature potassium, oxalate and levoglucosan are regarded as good signatures of biomass/wood combustion in the atmosphere (Simoneit et al., 1999; Duan et al., 2004).

It's known that wood smoke contains high concentrations of levoglucosan (1,6-anhydro- β D-glucopyranose) as well as other monosaccharide anhydrides.

Levoglucosan arises from the pyrolysis of cellulose, the main building material of wood, at temperatures higher than 300°C and it is coupled by minor quantities of its isomers, galactosan and mannosan.

In contrast to other molecular markers of biomass burning (i.e. diterpenoids, triterpenones, etc.) levoglucosan is emitted in large amounts, sufficiently stable, specific to cellulose-containing substances and meets all important criteria to serve as an ideal molecular marker of biomass burning (Pashynska et al., 2002).

Detection of levoglucosan and its isomers in atmospheric aerosol samples is typically performed in literature by gas chromatography - mass spectrometry (GC-MS), the first (GC) for the separation and the second (MS) for the detection and identification of the compound (Pashynska et al., 2002). However, these compounds are particularly difficult to analyze by GC-MS, due to their polar nature, requiring labor-intensive and expensive sample preparation. Typical preparation on filter-collected aerosol samples for GC-MS analysis of anhydrosugars involves extractions with one or more organic solvents, evaporation of the majority of the solvent, and generally chemical derivatization. This step represents the tricky point of the whole procedure since it is time consuming and quite expensive because of the reagents involved.

Consequently, some recent efforts have been directed towards alternative analytical methods that are simpler and faster, yet sensitive, precise and accurate.

7.2. Analytical techniques

7.2.1. Instrument

Though HPAEC-PAD (also referred to as ion chromatography (IC) coupled with PAD) has been utilized for carbohydrate analysis in various matrices, its application to aerosol chemistry is limited to only a few recent efforts (Gao et al. 2003; Puxbaum, 2004, in press; Engling et al. 2006).

With regard to the studies already reported in literature, we have introduced some modifications to the analytical setting. In particular, instead of a in gradient mode, the analysis is carried out in isocratic way using an ion chromatograph already available in the laboratory for ions quantification.

The HPAEC-PAD method requires minimal samples preparation. Aqueous extracts of filter sample, (the same employed for ion analysis (chapter 2) are separated on an anion exchange column without prior chemical derivatization.

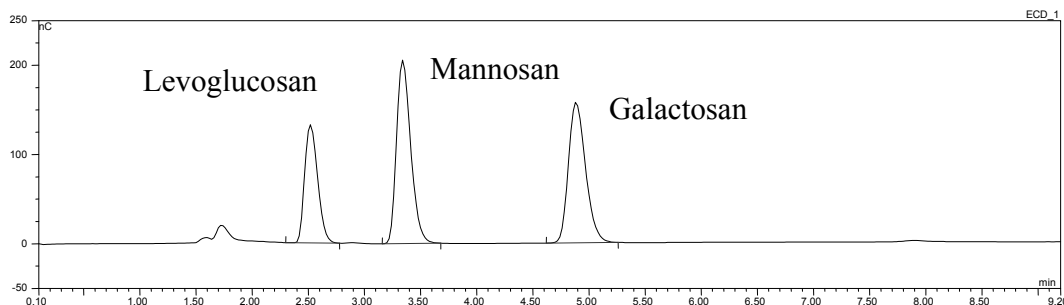


Figure 7-1: chromatogram of levoglucosan, mannosan and galactosan

Chromatographic conditions have been optimized for the separation of levoglucosan, mannosan and galactosan. With PA10 column by Dionex with NaOH 18mM, all three anhydrosugar elute during the first 10 minutes (see figure Figure 7-1).

In the next 20 minutes additional carbohydrates, including glucose, mannose, sucrose and selected sugars are separated under the same conditions. Some of these compounds have been recently detected in ambient aerosol samples (Decesari et al. 2006).

After each analysis the column is cleaned with NaOH 200mM. Since our instrument (Dionex ICS1000) works in isocratic way, the cleaning procedure is

difficult because it would require the replacement of the eluent. In order to simplify this step the original two way valve has been replaced with a three way valve, in order to control directly the cleaning procedure through the software (box *a* in Figure 7-2).

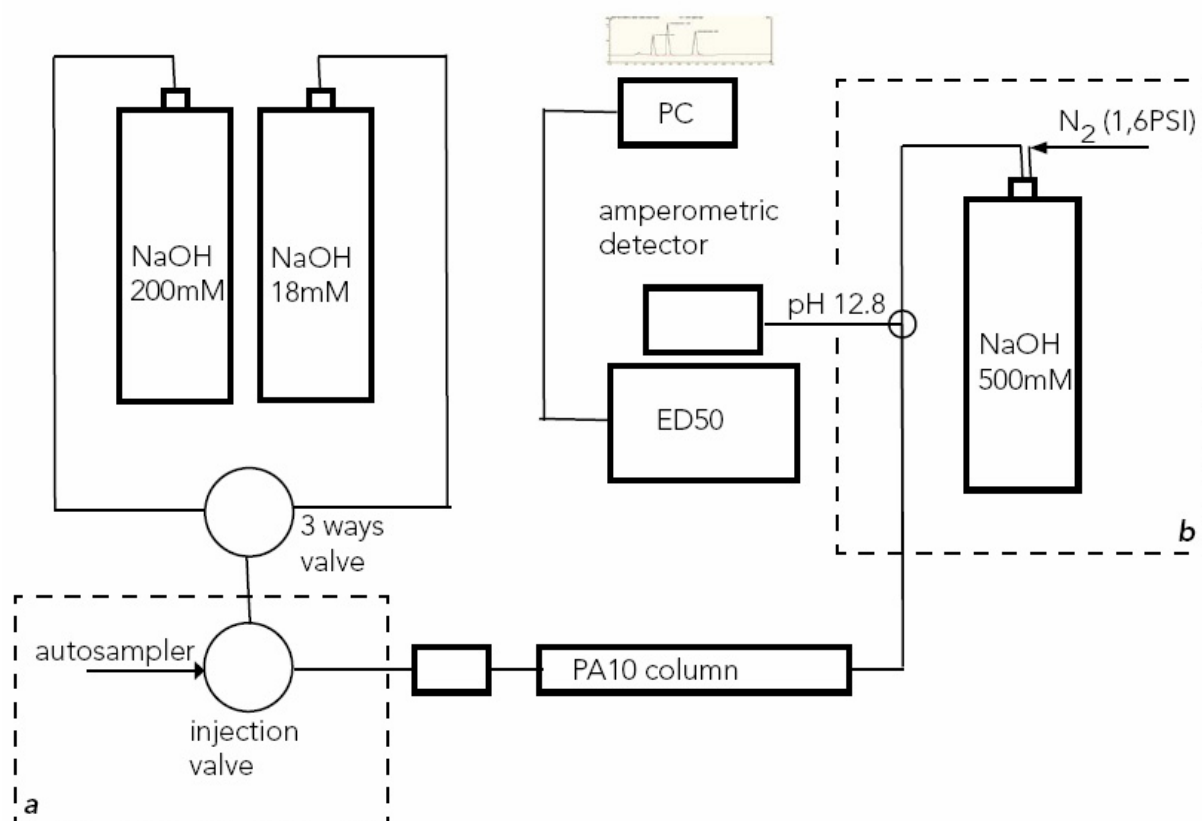


Figure 7-2: analytical set-up, upgrade of ICS 1000 – Dionex instrument

The instrument is equipped with an electrochemical detector (Dionex, ED50). The detection mode is pulsed amperometry with a gold working electrode. The response of the amperometric detector to the pH of our eluent (NaOH 18mM, pH=12.2) is quite low.

Nevertheless it is known that the response grows when the pH is higher. Therefore we add more concentrate NaOH (500mM) after the column and before the detector, in order to increase the signal and consequently the signal to noise ratio. The addition of this eluent is performed by means of a pressured bottle and it is connected by a three way connector (box *b* in Figure 7-2).

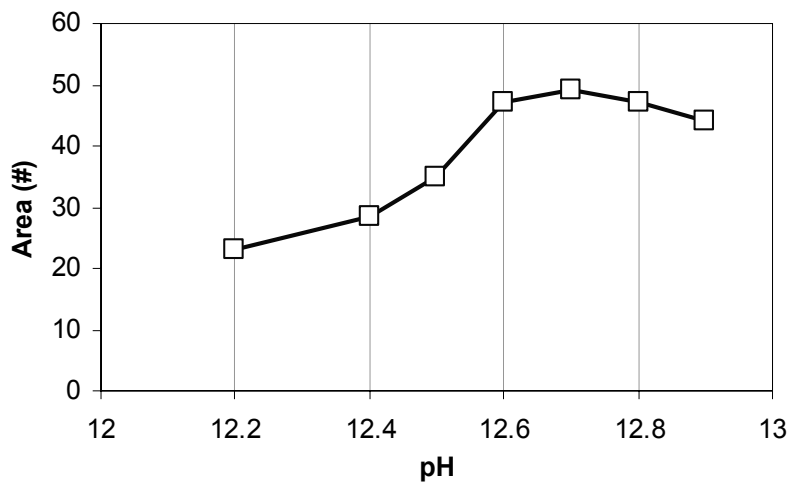


Figure 7-3: trend of the signal when the pH increases

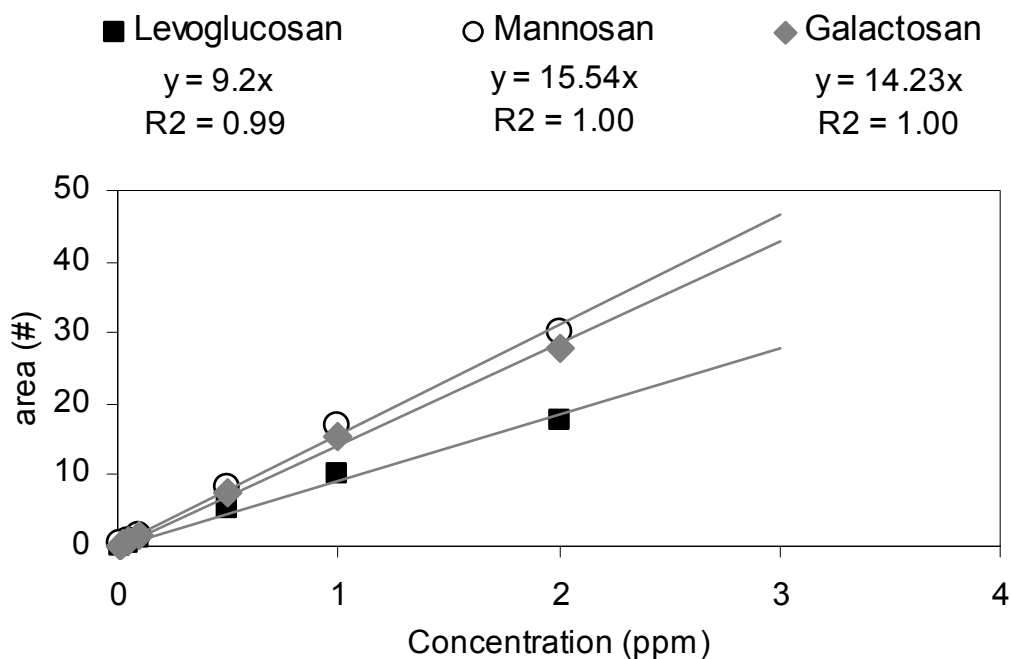


Figure 7-4: calibration curves for Levoglucosan, Mannosan and Galactosan

In Figure 7-3 it is shown the signal growth corresponding to an increase of pH.

Calibration curves for levoglucosan, mannosan and galactosan typically show a correlation coefficient (R^2) > 0.99 for quadratic regression, as illustrated in Figure 7-4.

7.2.2. Analytical performance of HPAEC-PAD technique and intercomparison with GC-MS

Anydrosugar mass concentration obtained by HPAEC-PAD were compared to data generated by an independent GC-MS method. It is worth noting that the two methods differ significantly in separation and detection principles, and they use different sample preparation procedures (Pasynska at all., 2002). A good agreement in levoglucosan mass concentrations determined independently by the two methods has been achieved, as demonstrated in Figure 7-5 ($R^2=0.97$).

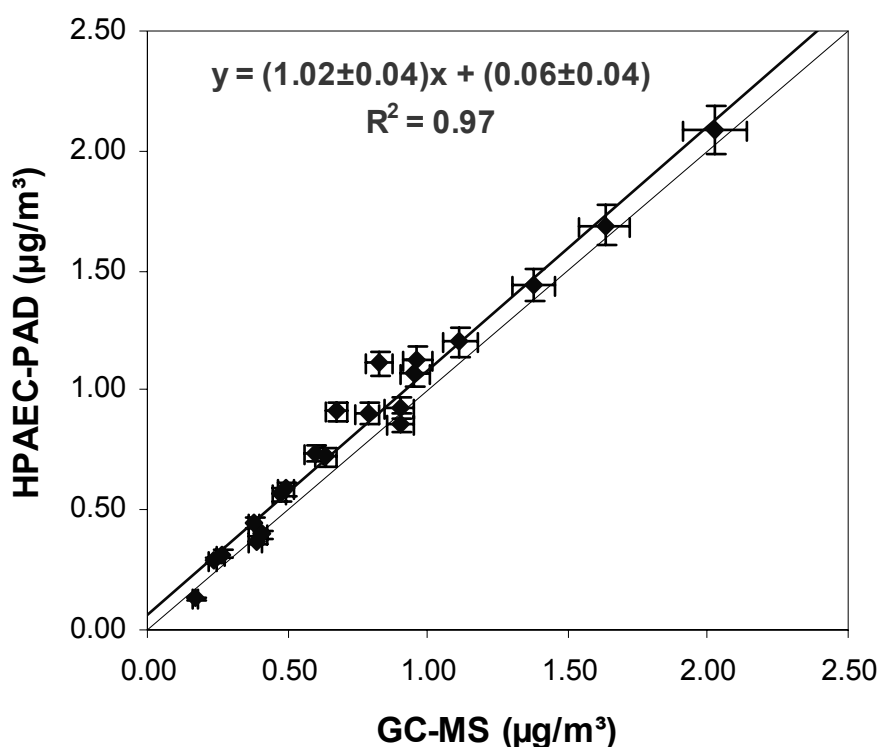


Figure 7-5: figure 5: comparison between GC-MS and HPAEC-PAD

Precision measurements for levoglucosan by the two methods based on replicated analyses of standard solution for three different concentrations are reported in Table 7-1.

The percentage of recovery is calculated on extraction experiments spiking a levoglucosan solution of known concentration on the filter submitted to the same procedure followed for the samples. The recovery has been calculated by filter spike with a solution of levoglucosan in two different concentrations. Both techniques show a good recovery.

	HPAEC-PAD		GC-MS	
Percentage of recovery	98.7% ± 7.0% (n=6)		101.7% ± 5.1% (n=6)	
Precision	10 ng	3.6% (n=5)	2.5ng	6% (n=9)
	100 ng	6.1% (n=5)	10ng	5% (n=9)
	200ng	4.8% (n=5)	20ng	6% (n=9)
		4.8%		5.5%

Table 7-1: comparison between GC-MS and HPAEC-PAD performance

The analytical limit of detection has been estimated to be good for both techniques and it is based on the signal to noise ratio. The LOD value (ng/m³) is reported in Table 7-2; the LOD value in ng/m³ is calculated referring to our sampling and analytical conditions as reported in the same table.

The simpler extraction, sample preparation procedures and a shorter time of analysis represent advantages of HPAEC-PAD method against GC-MS analysis. Moreover HPAEC-PAD shows great potential for detecting other carbohydrates in aerosol extract.

filter low volume (Ø 47mm) quartz prefired
sampling time: 24h, air volume: 24m³

	HPAEC-PAD	GC-MS
Portion of filter analyzed	1,5cm ² (~1/7)	1,5cm ² (~1/7)
V_{extraction} (µL)	6000	200
V_{extraction} (µL)	100	1
Calibration range (ppm)	0.01 - 2	0.01 – 20
Calibration range (ng/m³)	17.5 - 3500	0.6 - 1200
LOD		
	ppm	0.005
	ng/m³	8.7
		0.088
		5

Table 7-2: LOD value of HPAEC-PAD and GC-MS techniques

The HPAEC-PAD was used to determine concentration of anydrosugars in fresh smoke samples; the result is reported in chapter 8.

7.3. Conclusions

The HPAEC-PAD method, a relatively new analytical approach for aerosol samples, was shown to be a high sensitive, yet relatively simple analytical

technique for separation and quantification of anhydrosugars in aqueous extract of aerosol particle from biomass combustion.

Unlike traditional methods, there is not need for prior chemical derivatization or other complex sample preparation, the extraction procedure for ions quantification is suitable also for this method.

Simple adjustment to the chromatography fitted up with isocratic pump improves the sensitivity and the reproducibility.

Due to high sensitivity of the method, HPAEC-PAD may also be suitable for semi-continuous measurements of fine-particles levoglucosan, or for high time resolution samples.

The sensitivity and simplicity of the method also offer promise for those interested in routine analysis of biomass combustion tracers in samples collected in large aerosol monitoring network.

The intercomparison between HPAEC-PAD method and GC-MS method, the analytical technique more used in the literature work, shows fairly good agreement.

Acknowledgment

I'm grateful to C. Reschioto for the helpful suggestions and to G. Ferracin (Dionex Italia) for her availability

References

- Decesari et al. (2006)
<http://apps.isiknowledge.com/WoS/CIW.cgi?SID=T2LK7AgfeiC7gGAJ6he&Func=Abstract&doc=9/5> *Atmo Chem Phys* 6: 375-402
- Duan (2004) *Atmos Environ* 38 (9): 1275-1282
- Fermo et al. (2006) *Chemical Engineering Transactions* 10, 203-208.
- Engling et al. (2006) *Atmos Environ* 40: S299-S311 Suppl. 2
- Gao et al. (2003) *J. Geophys Res* 108 (D13): Art. No. 8491
- Pashynska V, et al. (2002) *J. Mass Spec* 37 (12): 1249-1257
- Punxbaum et al. (in press) *J. Geophys Res* 112
- Simoneit (1999) *Environmental Science and Pollution Research* 6 (3): 159-169

Part 2

Field campaigns

8. Carbonaceous particles in Lombardy region: the results of a two years campaign

Human health hazard associated with exposure to airborne particulate matter (PM) include increased mortality (Schwartz et al., 1996; Dockery and Pope, 1996; Kunzli et al., 2000; Pope, 2000; Samet et al., 2000; Pope et al., 2002) and morbidity from respiratory and cardiopulmonary disease (Ackermann-Liebrich et al., 1997; Zemp et al., 1999; Sunyer, 2001). Based on this epidemiological evidence, the European Commission has established limit values for PM₁₀ in the air quality directive 1999/30/EC (European Union, 1999), also prescribing the assessment of PM_{2.5}. Clean Air For Europe (CAFE) Working Group recommended the use of PM_{2.5} as the metric for the assessment of the exposure to particulate matter (CAFE, 2004). However, several European cities still have great problems in complying with the current limit values set for PM₁₀ concentrations: according to the results of the AutoOil-II programme (<http://europa.eu.int/comm/environment/autooil/>), by 2010 the tighter stage-two air quality standards for PM₁₀ are expected to be exceeded in half of the European cities. In particular in Lombardy, Italy's most industrialised region, atmospheric pollution due to airborne fine particles is an environmental issue of great concern: air quality standards for PM₁₀ are frequently exceeded, especially in Milan, the greatest city of the region, and in its metropolitan area, where about 4 million inhabitants live. Implementation of strategies for the compliance with the long-term (annual average) standard, as well as traffic restrictions to control the acute pollution events, largely exceeding the short-term (24 h average) standard, are currently enforced. PM emission inventory data and the source apportionment by chemical speciation of the fine particulate are basic tools supporting the control policy.

The atmospheric circulation of the Po valley is characterized by the strong modification of synoptic flow due to the high mountains (Alps and Apennines) that surround the valley on three sides. Calm atmospheric conditions (defined as conditions in which the hourly-averaged wind speed at a height of 10m is lower than 1.0 m/s) and light winds occur frequently. The most severe winter episodes are commonly associated with strong temperature inversions.

The concentration of particulate matter is the biggest ambient problem in Lombardy Region (Po valley, Northern Italy). Although in the last years the PM concentrations has decreased, the pollution level continues to be high and characterized by frequently exceedances of limits values, in particular in the urban

areas, especially in winter, when relatively prolonged periods of anticyclonic stability provide the formation of both radiative and subsidence inversions decreasing the dispersion of atmospheric pollutants. In Figure 8-1 we have reported the particulate matter concentration temporal trend (during the last 30 years) in Milan.

The standards for PM10 established by the European Union Directive are the long-term limit, $40 \mu\text{g}/\text{m}^3$ as annual average concentration, and short-term one, no more than 35 exceedances per year of $50 \mu\text{g}/\text{m}^3$ for the daily average (EU, 1999)

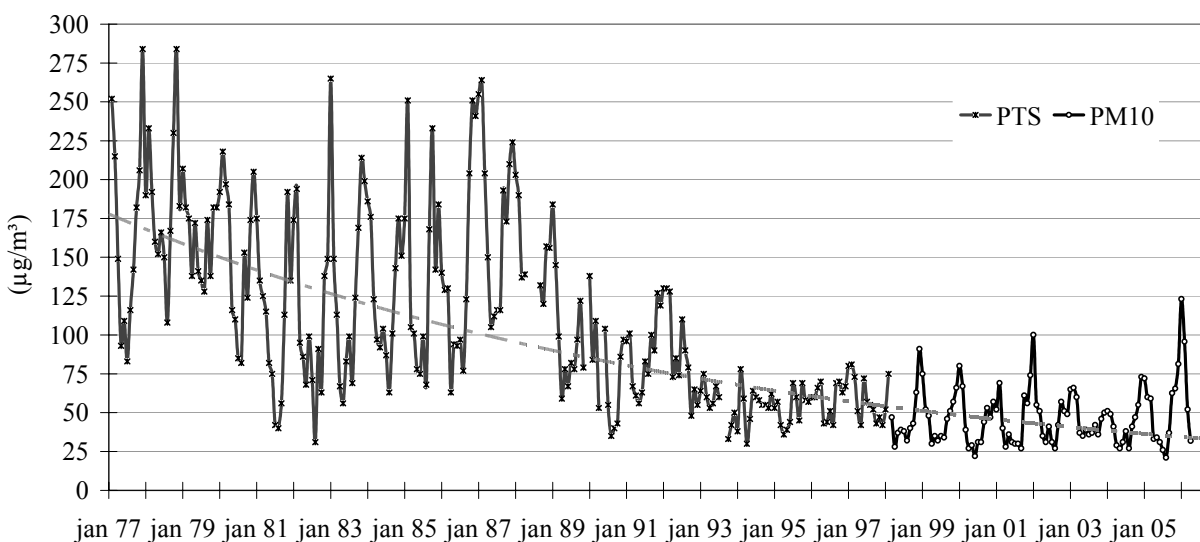


Figure 8-1: average month concentration of PTS (from 1977 to 1998) and PM10 (from 1999 to 2005) in Milan (source: ARPA Lombardia)

Carbonaceous species – elemental carbon (EC) and organic carbon (OC) – are known to contribute significantly to the atmospheric particulate matter (PM) all around the world with occasionally dominant relative contribution to the fine PM mass (Van Dingenen et al. 2004). EC is a product of incomplete combustion of carbon-based materials and fuels and it has solely primary nature, whereas OC can be directly released into the atmosphere or produced via secondary gas-to-particle conversion processes.

Besides adverse health effects associated to fine PM mass exposure (WHO, 2006), carbonaceous species cause serious health effects: though EC is generally considered inert, the combustion process results in the EC being coated by organic matter such as PAHs, which are known to have carcinogenic and mutagenic

properties (Na et al., 2004) and to pose significant human health risks (Lin and Tai, 2001).

Carbonaceous aerosols also have significant impacts on the global radiation balance and on global climate change through direct and indirect radiation forcing. OC aerosols play a key role in the formation of cloud condensation nuclei that lead to a higher albedo of cloud and finally to the global climate change (Hitzenberger et al., 1999; Dan et al., 2004) and it are an efficient scatter for solar light. In contrast, whereas EC is one of the dominant species that result in the global warming (O'Brien and Mitchel, 2003; Dan et al., 2004) and visibility reduction (Liousse et al., 1996; Na et al., 2004) by absorbing and scattering solar radiation.

Besides toxicological implications, information on carbonaceous fractions in fine PM, and particularly on their partitioning between primary and secondary origin, can usefully address air quality management plans.

The main goal of this work is to provide a better understanding of the concentration and the speciation of PM carbonaceous fraction in the Lombardy region area.

8.1. Material and methods

8.1.1. Monitoring site

In the ParFiL (Particolato Fine in Lombardia) project (by Regione Lombardia) we have analysed samples of particulate matter coming from ten sites of Lombardy Region (Figure 8-2). The sites are different for typology (urban, rural, remote), geographic features, and for the presence of various main sources of particulate matter.

For each site we have analyzed 1 week in a month for two years 2005-2006.

In Table 8-1 we report the metric, the typology of site and the period of sampling. We have considered summer from April to September and winter from October to March.

With urban background we mean that the sampler has been placed not directly exposed to particulate sources (i.e. traffic emission) and so the sampled aerosol is representative for the average air pollution in the city.

Milan is a large town with about 1500000 inhabitants and considering the whole area of the Milan province the population rises up to about 4 millions inhabitants. Milan is heavily industrialized, trafficked and populated and it is considered one of the largest pollution hot spots in Europe. The other urban background sites are located in cities smaller than Milan, and they represent different areas of the region for geographic features and economic activity.

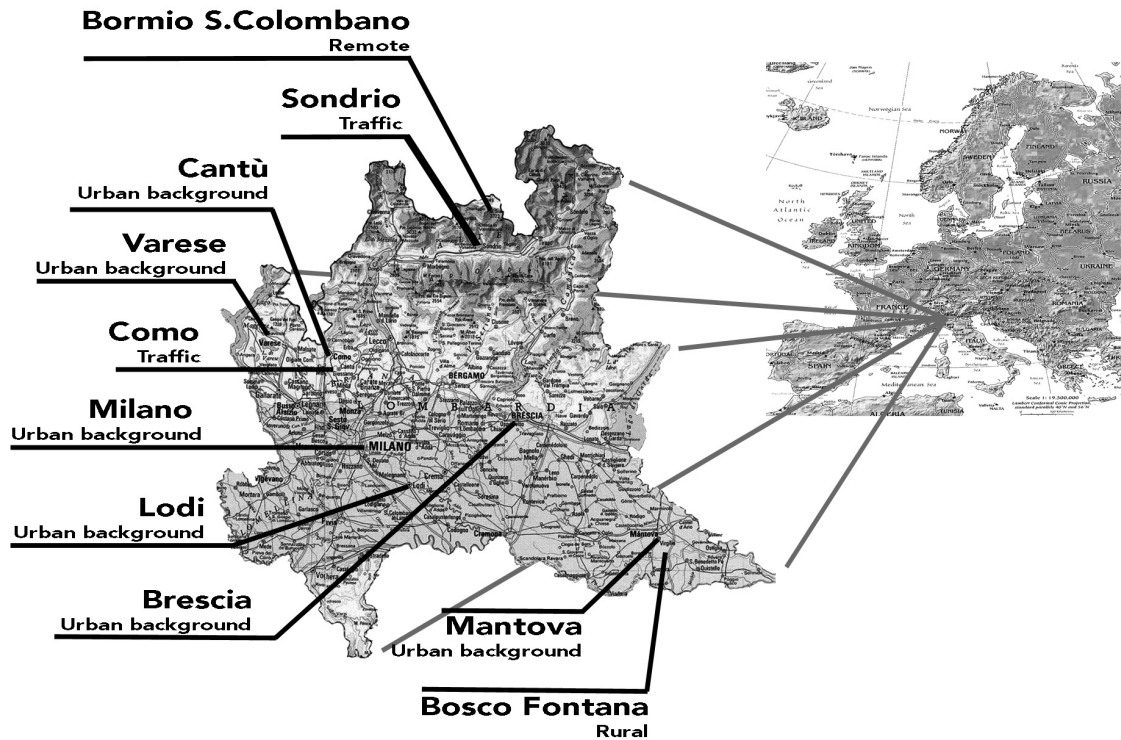


Figure 8-2: sampling site and typology of site

In the traffic sites the samplers were placed near the road.

Boscofontana is a rural site located in the centre of the Po valley, about 130 km far from Milan in the south-east direction; agriculture and breeding are the main activities so that BF can be considered representative of the regional background of the valley itself.

Bormio San Colombano (2.200 m a.s.l.), the alpine remote site, is located in the middle of Southern alps. It is characterized by a continental climate with short summers and harsh winters.

8.1.2. Instruments and techniques

PM₁₀ and PM_{2.5} fractions were sampled using LVS automatic samplers in compliance with EN 12341 (it should be noted that there was not an official method for PM_{2.5}). 24 hour samples were collected on pre-fired quartz fibre filters. In order to limit losses of volatile compounds in the warm season, samplers were equipped with air conditioning systems.

PM mass concentrations were determined using an analytical microbalance (sensitivity 1 μ g) after 48 hours conditioning at about 30% RH. The uncertainty of gravimetric measurements was $\pm 2 \mu\text{g}/\text{m}^3$ and the limit of detection was 2 $\mu\text{g}/\text{m}^3$.

	Type of site	Time of sampling	
		From	To
PM₁₀			
Milan	Urban Background	21-Feb-05	31-Dec-06
Varese	Urban Background	24-Feb-05	25-Sep-05
Cantù	Urban Background	21-Feb-05	8-Oct-06
Como	Traffic	18-May-05	8-Oct-06
Sondrio	Traffic	21-Feb-05	31-Dec-06
Bormio	Remote	21-Feb-05	31-Dec-06
Mantova	Background	21-Feb-05	14-Aug-05
Lodi	Urban Background	17-May-05	23-Apr-06
Brescia	Urban Background	31-Oct-05	16-Jul-06
PM_{2.5}			
Milan	Urban background	21-Feb-05	30-Dec-06
Cantù	Traffic	21-Feb-05	8-Oct-06
Bormio	Remote	21-Feb-05	30-Dec-06
Mantova	Urban Background	21-Feb-05	14-Aug-05

Table 8-1: ParFiL project: sampling site, typology and sampling period

Organic and elemental carbon (hereon OC and EC, respectively) were determined using a Thermal-Optical Transmission (TOT) instrument (Sunset Laboratory Inc., USA). More details on this methodology can be found in chapter 4 (Fermo et al., 2006, Birch and Cary, 1996).

A portion of quartz filters (1.5cm²) was water extracted following the same procedure for the ions analyses (chapter 2) and the levoglucosan concentrations were determined by HPAEC-PAD (chapter 7).

8.2. PM and carbonaceous particles concentration

8.2.1. PM mass concentration

PM10 and PM2.5 concentrations are reported in Table 8-2 and Table 8-3.

During the summer the concentrations are lower than during winter (winter/summer =2.3), for both fractions in all sites (except Bormio). In fact, additional sources and lower MLH (Mixing Layer Height) contribute to the growth of PM concentration during the cold season.

All sites show an annual average value higher than $40\mu\text{g}/\text{m}^3$, the standard for PM10 established by the European Union Directive. In Milan this value is exceeded by the PM2.5 fraction too.

During the summer Mantova and Mantova BF (rural site) show average values of PM10 higher than the other sites, while PM2.5 concentrations of are lower. The higher contribution of *coarse fraction* is probably due to resuspension processes. Mantova shows the highest absolute value during the hot season ($115\mu\text{g}/\text{m}^3$) too. Milan shows the highest average value and the highest absolute value ($191\mu\text{g}/\text{m}^3$) during winter.

In Table 8-4, Table 8-5 and Table 8-6 we report the concentration of OC and EC in the two fractions (PM10 and PM2.5).

8.2.2. Carbonaceous particles concentration

Highest annual OC concentration is registered in Milan (Table 8-4), while the lowest values are registered in Brescia and Varese, where the concentrations are approximately one half than in Milan. EC concentrations confirm this trend: in fact Milan and Como show the highest value, while Brescia and Varese are the lowest.

The standard deviation to average ratio of EC shows the same value (62%) in both seasons

PM10 ($\mu\text{g}/\text{m}^3$)	Lombardia	Milano	Varese	Cantù	Como	Sondrio	Mantova	Lodi	Brescia	Mantova BF	Bormio
years 2005-2006											
average	50.2	66.9		43.6	41.2	41.6	65.1	45.9	42.3	46.9	9.0
standard deviation	36.4	41.7		28.1	30.5	28.9	31.1	31.2	33.2	32.3	7.2
median	38.1	65.7		36.2	30.6	32.2	62.6	36.6	32.6	40.0	6.9
min	5.0	9.2		10.0	5.0	6.9	12.9	12.0	7.0	10.4	1.4
max	191.4	191.4		131.4	157.5	151.0	130.5	171.9	178.7	154.2	31.7
n	438	78		70	45	118	35	51	38	42	66
summer											
average	32.3	32.6	29.1	32.6	27.9	24.6	56.3	32.5	23.8	39.1	12.4
standard deviation	20.6	18.1	17.0	21.7	17.1	16.1	24.4	16.7	13.1	27.7	8.4
median	26.0	25.9	23.8	25.0	25.9	21.3	58.1	27.5	19.2	35.8	8.4
min	5.0	9.2	5.2	10.0	5.0	6.9	12.9	12.0	7.0	10.4	3.9
max	115.0	77.0	64.7	102.4	77.8	87.0	115.0	83.2	51.7	154.2	31.7
n	248	25	27	46	32	54	28	34	20	35	25
winter											
average	73.7	83.1		64.5	73.9	61.2	72.8		62.9		8.5
standard deviation	39.0	39.9		27.4	31.9	31.0	36.2		36.9		7.3
median	71.8	80.6		67.3	72.2	53.7	73.3		58.9		5.5
min	13.0	13.7		26.0	26.0	15.0	18.6		16.8		1.4
max	191.4	191.4		131.4	157.5	151.0	171.9		178.7		31.0
n	190	53		24	13	49	17		18		28
winter/summer	2.3	2.5		2.0	2.6	2.5	2.2		2.6		0.7

Table 8-2: concentration ($\mu\text{g}/\text{m}^3$) of PM10 in Lombardia (average of eight urban sites) and in ten sites

PM2.5 ($\mu\text{g}/\text{m}^3$)	Lombardia	Milano	Cantù	Mantova	Bormio
years 2005-2006					
mean	36.0	42.3	29.4	28.3	8.1
standard deviation	22.9	26.7	14.7	20.2	6.2
median	32.5	39.7	29.9	20.3	5.9
min	7.1	7.9	7.9	7.1	2.7
max	125.4	125.4	64.8	67.0	30.2
n	147	56	61	16	70
summer					
mean	20.8	21.7	25.1	15.4	9.1
standard deviation	11.5	13.8	13.5	7.5	7.3
median	17.3	16.3	22.9	13.6	6.0
min	7.1	9.0	7.9	7.1	3.0
max	53.1	59.4	61.2	31.3	30.2
n	63	18	36	10	44
winter					
mean	47.5	39.6	35.7	49.7	7.0
standard deviation	22.6	28.3	14.6	15.6	3.9
median	45.0	32.3	33.6	51.2	5.9
min	7.4	7.9	12.4	21.4	2.7
max	125.4	125.4	64.8	67.0	15.0
n	84	44	24	6	26
winter/summer	2.3	1.8	1.4	3.2	0.8

Table 8-3: concentration ($\mu\text{g}/\text{m}^3$) of PM2.5 in Lombardia (average of three urban sites) and in four sites

OC ($\mu\text{g}/\text{m}^3$) PM10	Lombardia	Milano	Varese	Cantù	Como	Sondrio	Mantova	Lodi	Brescia	Mantova (BF)	Bormio
years 2005-2006											
average	10.3	13.4	6.8	9.3	10.9	10.8	9.9	7.4			1.8
standard deviation	6.6	8.2	2.7	4.5	6.6	7.6	6.2	4.5			0.9
median	8.3	11.2	5.8	8.1	9.0	8.3	7.4	6.4			1.5
min	2.7	3.9	2.8	4.2	3.0	2.7	3.8	2.9			0.5
max	42.0	39.9	12.6	28.4	40.4	42.0	37.0	25.6			4.4
n	534	79	36	80	56	112	50	30			71
summer											
average	7.4	6.8	6.4	7.5	8.3	7.3	8.6	7.1	5.5	6.2	2.0
standard deviation	2.7	2.4	2.5	2.3	2.6	2.6	2.6	1.7	1.3	1.9	1.0
median	6.8	6.0	5.7	7.4	8.6	6.5	7.9	6.8	5.7	5.5	1.8
min	2.7	3.9	2.8	4.2	3.0	4.1	4.5	3.8	2.9	3.5	0.5
max	17.6	12.2	12.6	13.1	15.8	17.6	14.4	11.2	7.5	10.6	4.4
n	334	25	32	52	37	55	28	32	20	33	32
winter											
average	15.3	16.4		12.7	15.9	15.5	14.8	11.0			1.2
standard deviation	8.0	8.2		5.6	8.9	9.2	8.2	6.3			0.5
median	13.5	15.1		11.4	13.3	12.9	14.4	8.3			1.0
min	2.8	4.4		5.3	5.5	2.8	3.8	5.3			0.5
max	42.0	39.9		28.4	40.4	42.0	37.0	25.6			2.8
n	200	54		28	19	49	18	10			26
winter/summer	2.1	2.4		1.7	1.9	2.1	2.1	2.0			0.6

Table 8-4: concentration ($\mu\text{g}/\text{m}^3$) of OC in Lombardia (average of eight urban sites) and in ten sites .

EC ($\mu\text{g}/\text{m}^3$) - PM10	Lombardia	Milano	Varese	Cantù	Como	Sondrio	Mantova	Lodi	Brescia	Mantova (BF)	Bormio
years 2005-2006											
average	2.8	4.2	1.5	2.1	4.6	2.8	2.2	1.7			0.2
standard deviation	2.2	3.0	0.7	1.1	1.9	2.4	1.3	1.1			0.1
median	2.1	3.3	1.3	1.8	4.4	1.8	2.1	1.4			0.1
min	0.1	0.8	0.3	0.3	1.4	0.1	0.8	0.4			0.0
max	13.7	13.7	3.6	5.0	9.4	11.4	5.8	5.0			0.7
n	535	79	36	80	56	111	50	31			69
summer											
average	1.9	2.3	1.5	1.7	3.9	1.7	2.1	1.6	1.3	1.1	0.2
standard deviation	1.2	1.3	0.7	0.9	1.4	0.9	0.7	0.8	0.6	0.4	0.2
median	1.5	2.1	1.3	1.5	4.1	1.6	2.0	1.4	1.2	1.0	0.2
min	0.1	0.8	0.3	0.3	1.4	0.5	0.8	0.8	0.4	0.5	0.0
max	7.0	6.1	3.6	4.2	7.0	6.2	3.6	3.6	2.6	1.8	0.7
n	336	25	32	52	37	55	28	32	21	34	30
winter											
average	4.2	5.0		2.7	5.9	4.2	3.3	2.5			0.1
standard deviation	2.6	3.1		1.0	2.2	2.9	1.3	1.5			0.1
median	3.5	3.9		2.8	6.0	3.7	3.4	2.0			0.1
min	0.1	1.4		0.9	2.5	0.1	1.0	0.5			0.0
max	13.7	13.7		5.0	9.4	11.4	5.8	5.0			0.4
n	199	54		28	19	48	18	10			26
winter/summer	2.2	2.1		1.6	1.5	2.5	2.1	1.9			0.6

Table 8-5: concentration ($\mu\text{g}/\text{m}^3$) of EC in Lombardia (average of eight urban sites) and in ten sites, PM10 fraction

	OC ($\mu\text{g}/\text{m}^3$) - PM2.5					EC ($\mu\text{g}/\text{m}^3$) - PM2.5				
	Lombardia	Milano	Cantù	Mantova	Bormio	Lombardia	Milano	Cantù	Mantova	Bormio
years 2005-2006										
average	7.9	9.7	6.6	5.8	1.9	2.3	3.4	1.5	1.5	0.2
standard deviation	4.5	5.5	3.4	2.8	0.9	1.8	2.1	1.0	0.6	0.1
median	6.6	8.8	5.5	4.3	1.6	1.7	2.7	1.3	1.5	0.1
min	2.6	3.1	2.6	2.6	0.6	0.2	1.1	0.2	0.4	0.0
max	32.8	32.8	18.1	11.9	4.6	10.2	10.2	6.3	2.8	0.5
n	215	60	84	17	99	215	60	84	17	97
summer										
average	5.1	5.5	4.9	4.1	2.2	1.4	2.2	1.3	1.3	0.2
standard deviation	1.5	1.8	1.5	1.1	1.0	0.8	0.9	0.6	0.7	0.1
median	4.7	4.9	4.6	3.9	2.0	1.2	1.8	1.2	1.1	0.2
min	2.6	3.1	2.6	2.6	1.0	0.2	1.2	0.2	0.4	0.0
max	9.9	9.9	8.9	7.0	4.6	4.1	4.1	2.7	2.8	0.4
n	99	19	50	11	58	99	19	50	11	56
winter										
average	10.4	9.1	9.1	8.9	1.3	3.0	3.4	1.9	1.8	0.1
standard deviation	4.7	5.9	3.9	2.3	0.5	2.1	2.2	1.4	0.4	0.1
median	9.4	7.2	8.5	8.8	1.2	2.4	2.7	1.8	1.9	0.1
min	3.7	3.1	3.9	6.0	0.6	0.3	1.2	0.3	1.2	0.0
max	32.8	32.8	18.1	11.9	2.8	10.2	10.2	6.3	2.2	0.5
n	116	47	33	6	41	116	47	33	6	41
winter/summer	2.1	1.7	1.8	2.2	0.6	2.1	1.5	1.5	1.4	0.6

Table 8-6: concentration ($\mu\text{g}/\text{m}^3$) of OC and EC in Lombardia (average of three urban sites) and in four sites, PM2.5 fraction

The temporal trend at the three sites Milan, Mantova and Mantova BF (rural site) is shown in Figure 8-3. Milan shows the lowest value of PM10 in both seasons. Mantova BF can be considered representative of the regional background and PM concentrations show the same behaviour of the urban sites: in fact the correlation of PM concentration is very high (Table 8-7). During the summer the Mantova BF OC concentration is highly correlated with OC values in Mantova: the secondary formation and the biogenic source influence these values.

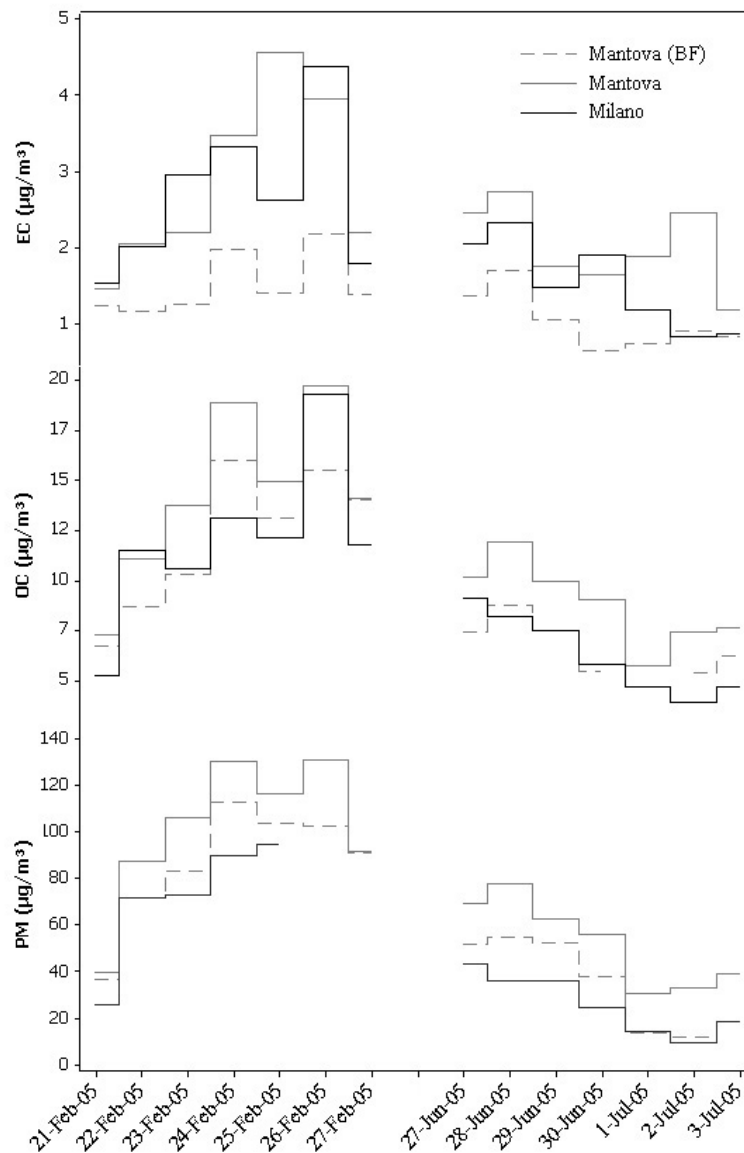


Figure 8-3: temporal trend of PM, OC and EC concentrations in three sites Mantova BF (rural site), Mantova and Milan

The concentration of EC in Mantova BF, during the winter, is lower than in the other two sites and it is highly correlated with the OC in Mantova (0.87) and with both OC and EC in Milan (0.79, 0.85). On the contrary the EC concentration in the rural site during the summer is weakly correlated with the concentrations of carbonaceous particles in the other two sites.

During the winter the concentrations of PM and carbonaceous particles in Mantova are highly correlated with the concentration in Milan. During the summer only PM and OC concentrations are correlated, while the correlation with EC concentrations is lower.

		Mantova BF			Mantova			Milano		
		PM	OC	EC	PM	OC	EC	PM	OC	EC
Mantova BF	PM		0.93	0.66	0.96	0.93	0.81	0.96	0.78	0.69
	OC	0.93		0.81	0.86	0.95	0.74	0.83	0.79	0.69
	EC	0.66	0.81		0.71	0.87	0.64	0.49	0.79	0.85
Mantova	PM	0.96	0.86	0.71		0.95	0.80	0.94	0.85	0.83
	OC	0.93	0.95	0.87	0.95		0.77	0.88	0.89	0.87
	EC	0.81	0.74	0.64	0.80	0.77		0.77	0.69	0.69
Milano	PM	0.96	0.83	0.49	0.94	0.88	0.77		0.97	0.65
	OC	0.78	0.79	0.79	0.85	0.89	0.69	0.97		0.85
	EC	0.69	0.69	0.85	0.83	0.87	0.69	0.65	0.85	

		Mantova BF			Mantova			Milano		
		PM	OC	EC	PM	OC	EC	PM	OC	EC
Mantova BF	PM		0.80	0.71	0.98	0.93	0.35	0.96	0.95	0.86
	OC	0.80		0.92	0.85	0.89	0.47	0.79	0.82	0.66
	EC	0.71	0.92		0.79	0.81	0.73	0.72	0.78	0.67
Mantova	PM	0.98	0.85	0.79		0.97	0.44	0.94	0.93	0.91
	OC	0.93	0.89	0.81	0.97		0.47	0.86	0.85	0.83
	EC	0.35	0.47	0.73	0.44	0.47		0.32	0.45	0.50
Milano	PM	0.96	0.79	0.72	0.94	0.86	0.32		0.99	0.82
	OC	0.95	0.82	0.78	0.93	0.85	0.45	0.99		0.85
	EC	0.86	0.66	0.67	0.91	0.83	0.50	0.82	0.85	

Table 8-7: correlation between PM, OC and EC in three sites Mantova, Mantova BF (rural site) and Milan in the two season.

Comparing temporal trends Milan and in the alpine site (Figure 8-4:) we note that during the summer the PM and carbonaceous particles concentrations are similar in the two sites confirming the homogeneity of particulate diffusion during the hot season. During the winter the importance of local sources and the lower mixing layer height produce some differences. The remote site shows a lower

concentration, during the summer the EC concentration shows a good correlation with the PM concentration in Milan (Table 8-8) (0.73), while during the winter the EC concentrations in the remote site are more correlated with the PM concentrations in Bormio. This fact suggests that during summertime the mixing layer is high enough to allow particles advection and mixing from the Po Valley to Alpine sites. On the contrary, during wintertime the two systems are separated and the lower impact of local sources at Bormio justifies the differences between Milan and the Alpine site.

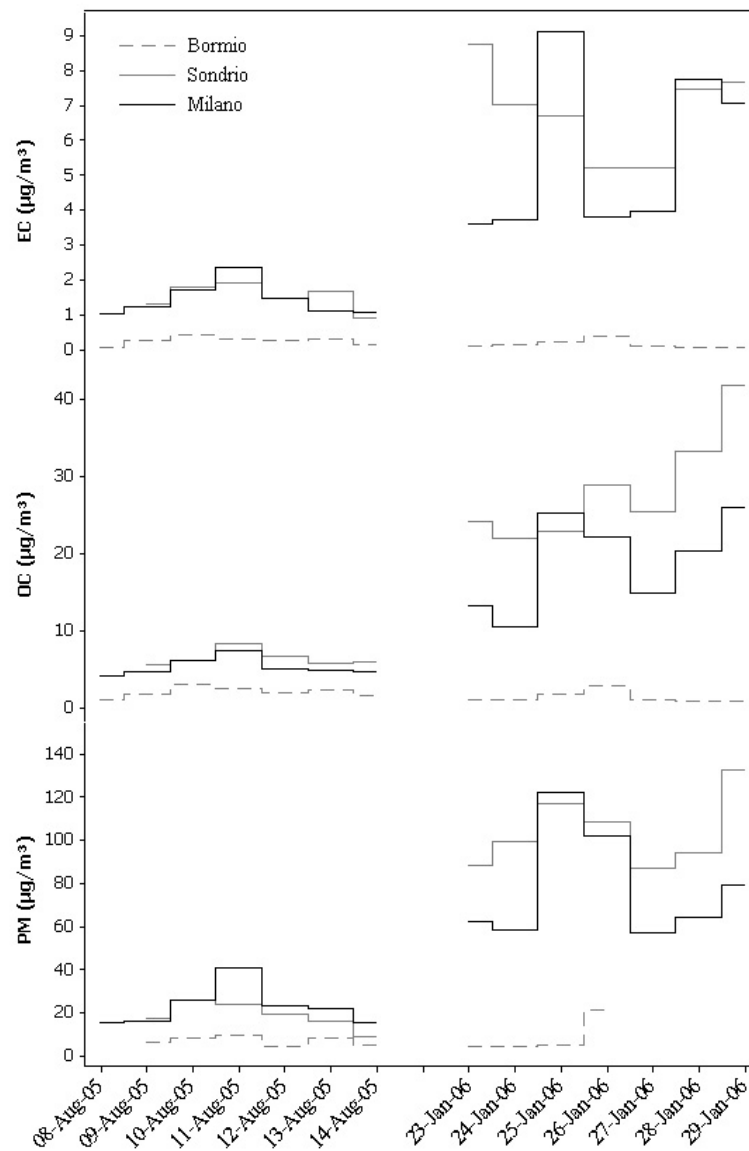


Figure 8-4: temporal trend of PM, OC and EC concentrations in three sites Bormio SC (remote site), Sondrio and Milan

During the winter there is a good correlation between carbonaceous concentration in Sondrio and in Milan, while during the summer this correlation gets worse.

		Bormio			Sondrio			Milano		
		PM	OC	EC	PM	OC	EC	PM	OC	EC
Bormio	PM		0.77	0.70	0.60	0.40	0.79	0.70	0.73	0.61
	OC	0.77		0.97	0.85	0.30	0.85	0.66	0.75	0.67
	EC	0.70	0.97		0.90	0.16	0.86	0.58	0.65	0.61
Sondrio	PM	0.60	0.85	0.90		0.48	0.88	0.71	0.72	0.78
	OC	0.40	0.30	0.16	0.48		0.53	0.92	0.87	0.90
	EC	0.79	0.85	0.86	0.88	0.53		0.80	0.75	0.73
Milano	PM	0.70	0.66	0.58	0.71	0.92	0.80		0.97	0.96
	OC	0.73	0.75	0.65	0.72	0.87	0.75	0.97		0.97
	EC	0.61	0.67	0.61	0.78	0.90	0.73	0.96	0.97	

		Bormio			Sondrio			Milano		
		PM	OC	EC	PM	OC	EC	PM	OC	EC
Bormio	PM		0.85	0.81	0.18	0.29	-0.78	0.37	0.37	-0.26
	OC	0.85		0.99	0.17	-0.23	-0.63	0.67	0.28	-0.18
	EC	0.81	0.99		0.26	-0.25	-0.58	0.73	0.31	-0.13
Sondrio	PM	0.18	0.17	0.26		0.58	0.04	0.62	0.79	0.54
	OC	0.29	-0.23	-0.25	0.58		0.17	-0.02	0.62	0.36
	EC	-0.78	-0.63	-0.58	0.04	0.17		-0.27	-0.11	0.19
Milano	PM	0.37	0.67	0.73	0.62	-0.02	-0.27		0.75	0.54
	OC	0.37	0.28	0.31	0.79	0.62	-0.11	0.75		0.75
	EC	-0.26	-0.18	-0.13	0.54	0.36	0.19	0.54	0.75	

Table 8-8: correlation between PM, OC and EC in three sites Bormio SC (remote site), Sondrio and Milan in the two season.

8.2.3. OC and EC percentage

During the summer the percentage of OC (Figure 8-5) is higher than during winter, probably due to the secondary photochemical formation. On the contrary, the percentage of EC (Figure 8-6) is similar in the two seasons. Como, the traffic site, shows the highest value of EC percentage, confirming that EC is a good marker for traffic.

Mantova and Mantova BF, the sites in the valley, during the summer show high absolute OC concentration (Table 8-4, Figure 8-3), but low relative OC concentration (Figure 8-5), and this might be due to high contribution of resuspended dust to PM mass.

In both seasons, OC is a major contributor to PM mass. The organic carbon concentrations can be converted in organic matter (OM) concentrations using an average mean molecular-to-carbon ratio of 1.6 as proposed by Turpin and Lim (2001) for urban aerosol. In Lombardy region, the average percentage of OC in summer and in winter are 23% and 20% respectively, so we obtain OM relative concentration of 37% and 33% in the two seasons.

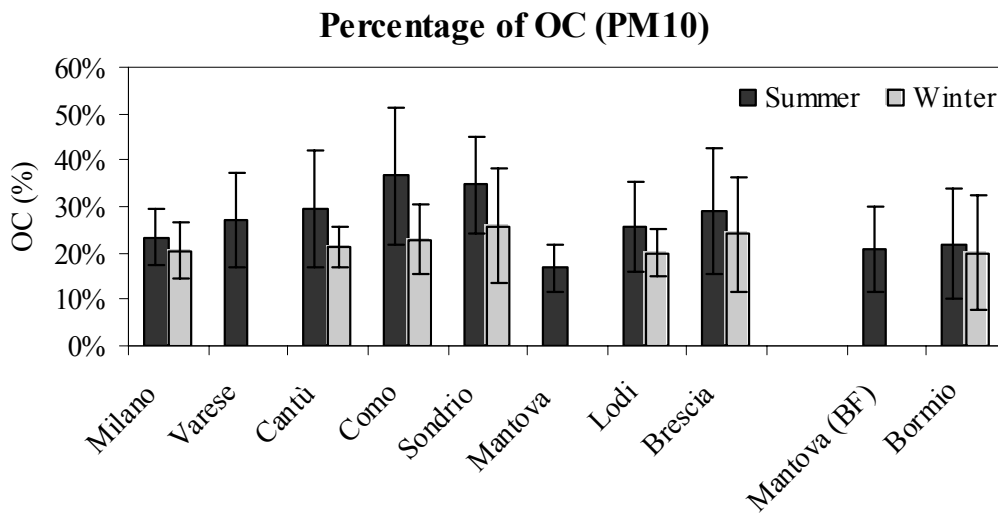


Figure 8-5: average percentage of OC (error bar is 1 standard deviation)

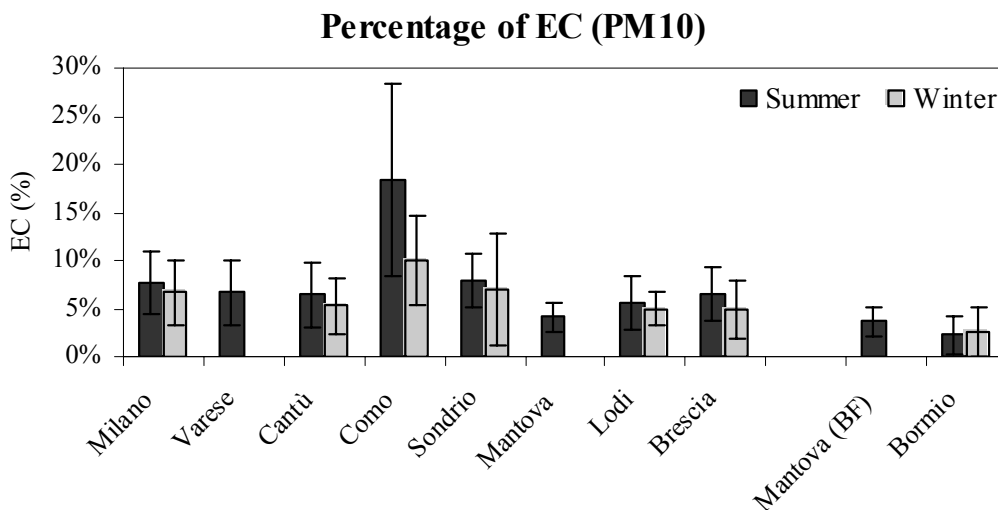


Figure 8-6: average percentage of EC (error bar is 1 standard deviation)

8.2.4. OC and EC ratio

During the summer (Figure 8-7), the OC /EC ratio is more homogeneous than the winter (Figure 8-8). In both seasons Como shows the lowest value; in summer this value is constant, the ratio between standard deviation and average (yaken as a parameter to represent data relative dispersion) is 34% in the summer and 67% during the winter, to confirm that in the hot season only the traffic source and the secondary formation influence this ratio, while in the cold season there are additional sources of carbonaceous particles which can give origin to higher variability in OC/EC ratio.

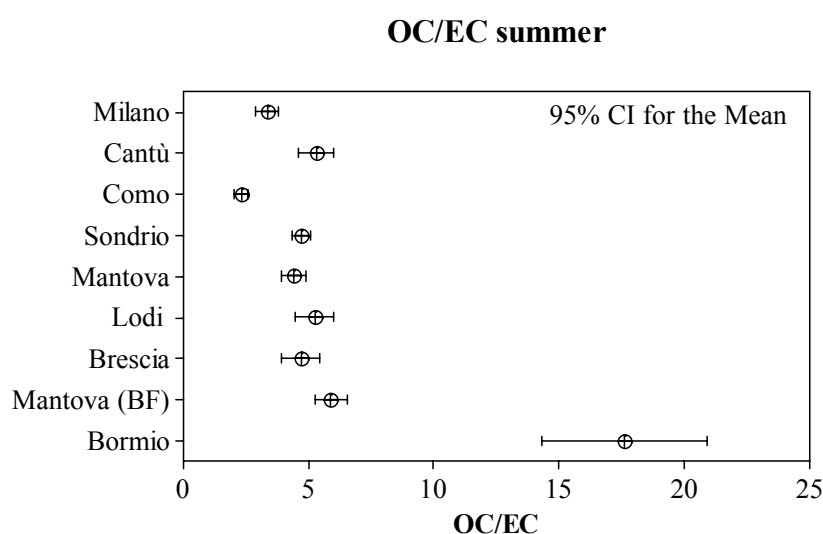


Figure 8-7: OC/EC ratio in summer

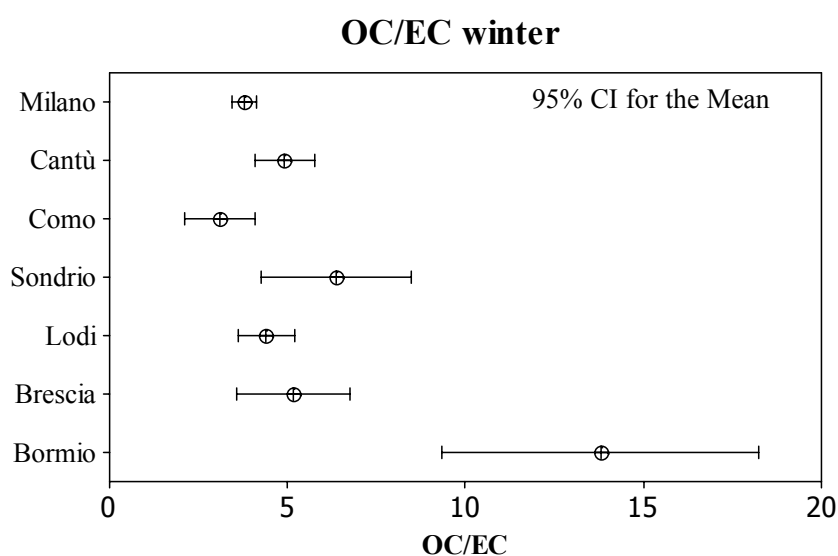


Figure 8-8: OC/EC ratio in winter

In both seasons Milan shows a low and constant value of OC/EC ratio, this means that the major source of carbonaceous particles is the road traffic. A high value of OC/EC ratio means there are additional sources of OC, during the summer these sources can be biogenic carbon or secondary formation, while during the winter the concentration of biogenic carbon is very low (Castro et al., 1999) but there are additional sources as domestic heating and condensation processes.

8.2.5. Thermal fractions of OC

The thermograms, i.e. the output from TOT analysis (chapter 4, Birch and Cary, 1996), are comparable in all cities but show a seasonal variability.

In Figure 8-9 as example we report the percentage composition of OC for Milan, Cantù and Sondrio.

The average mass apportionment of the five OC thermal fractions – labelled OC1, OC2, OC3, OC4, PyC, - in the two seasons is reported in Table 8-9.

	OC1	OC2	OC3	OC4	PyC
summer	30%	20%	10%	19%	22%
winter	25%	15%	8%	16%	36%

Table 8-9: average mass portion of the OC thermal fraction

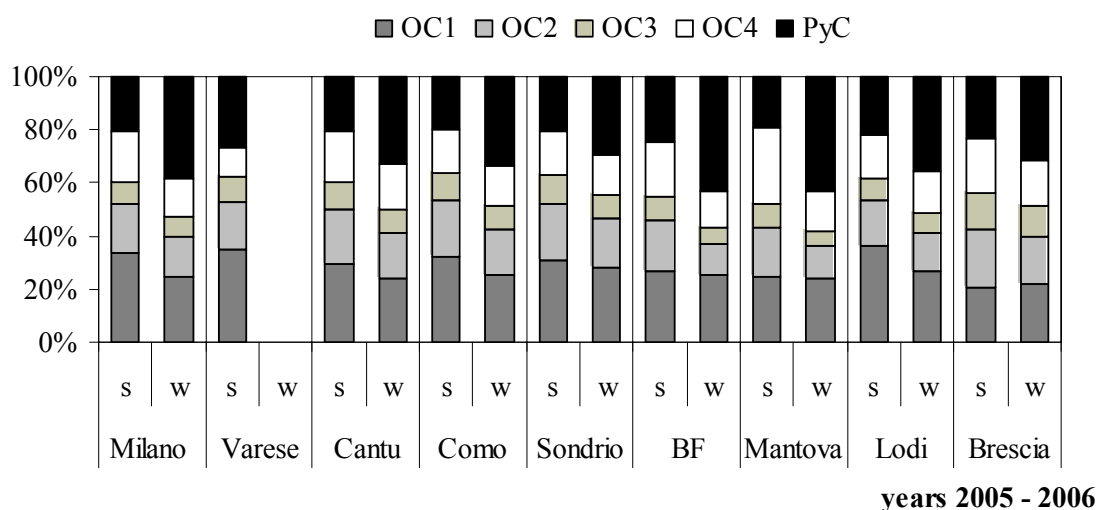


Figure 8-9: the relative contribution (%) of the four OC thermal fractions (OC1-OC4) and pyrolyzed OC (PyC) to the total OC in PM10 of the three urban site (s=summer, w=winter, BF=Mantova BF)

During the winter, in all sites, the percentages of OC1, OC2 and OC4 decrease, while PyC increases and varies in the range 30-38% (Figure 8-9). We have demonstrated (chapter 5) that the PyC is due to the presence of WSOC (Water Soluble Organic Carbon). According to many authors (Facchini et al., 2000) a significant portion of smoke particles is water soluble, then the increase the PyC fraction during the winter is probably due to the use of the wood combustion in the domestic heating. In the next section we will discuss the estimation of the contribution of these sources in Lombardia.

8.3. The contribution of wood combustion to particulate matter concentration

Levoglucosan can be used as a specific indicator for the presence of emission from biomass burning in atmospheric samples of particulate matter (Simoneit et al. 1999). Levoglucosan is emitted in large amounts, it is sufficiently stable and it is specific of the burning of cellulose-containing substances (Simoneit et al. 1999).

In Europe, wood fire emissions are considered around 60% of the primary OC from combustion (Bond et al., 2004). Major sources are wood combustion, agricultural and garden waste burning in the winter season and forest fire in summer, in particular in the Mediterranean countries.

In Lombardy region the inventory of the emission by Regione Lombardia (www.ambiente.regione.lombardia.it/inemar/) estimates that about 28% of PM10 and 31% of PM2.5 are due to wood combustion.

In Europe, limited data on the contribution of wood combustion to the OC using levoglucosan as a tracer are available. At the moment the only available values are the ones referred to Ghent in Belgium (Pashynska et al., 2005) and Oslo in Norway (Yttri et al., 2005). In Ghent, this contribution has been estimated about 35%, while in Oslo the data indicate that about 24% of OC comes from wood burning. Using ¹⁴C measurements Szidat et al., (2006) wood combustion is estimated to give a contribution up to 41% of the OC during winter in Zurich, Switzerland.

A recent work (Puxbaum et al., in press) reports the impact of biomass combustion in the European background aerosol. In this study five sites in central Europe have been investigated; the results indicate that in the winter season the contribution of biomass smoke to OC is in a range between 21.2% and 68.4%.

For the first time in Italy we have studied the concentration of levoglucosan in five sites in Lombardy region during winter and summer time. The investigated sites are characterized by different features: industrial activity, geographical features (i.e. alpine, plain,) and estimated use of wood for heating.

8.3.1. Determination of levoglucosan

The quantification of levoglucosan in PM samples was carried out by HPAEC-PAD (see chapter 7).

Table 8-10 summarizes the average, minimum and maximum values, as well as summer and winter average (with their standard deviation) for levoglucosan in all the five sites studied. These values vary considerably in relation to the sampling sites and the two seasons

Levoglucosan ng/m³	Mantova BF	Sondrio	Cantù	Milan	Mantova
average	148.4	426.3	416.6	169.7	293.8
minimum	27.4	50.7	64.8	13.0	25.0
maximum	470.4	884.8	884.8	634.8	807.4
summer ^a	52.0 (30.4)	95.9 (46.0)	96.0 (28.4)	15.7 (2.6)	58.1 (26.6)
winter ^a	405.4 (65.7)	701.7 (114.2)	691.5 (232.2)	385.4 (180.0)	568.7 (195.8)
winter/summer	7.8	7.3	7.2	24.5	9.8

Table 8-10: average, minimum and maximum values, as well as summer and winter average for levoglucosan in five sites in Lombardy region. ^a first number is the average, second (between brackets) the standard deviation.

Mantova BF, a background site near Mantova, shows the lowest values. Milan and Mantova show lower values than Sondrio and Cantù.

In the hot season Mantova shows values comparable to Mantova BF and higher than Milan; this is probably due to the burning of residual of agriculture waste or to a potential analytical interference (Puxbaum et al., in press) of the levoglucosan signal from arabitol, a constituent of fungal spores (Lewis and Smith, 1967).

Cantù is a smaller city in the central area of the region where the main industrial activity is joinery and furniture production and Sondrio is an alpine town where consumption of wood for residential combustion per head is estimated to be the highest in Lombardy.

The average contribution of levoglucosan to OC is shown in Figure 8-10, the highest contribution is found in Sondrio and Cantù.

During summertime Bosco Fontana shows lower PM values than Mantova ($24.7\mu\text{g}/\text{m}^3$ $58.3\mu\text{g}/\text{m}^3$ on average), but similar values of levoglucosan: as a consequence the ratio between levoglucosan to OC increases (Figure 8-10), indicating a higher contribution from biomass burning at the rural site.

We have also investigated the concentration of Levoglucosan during the Christmas period in Milan 2005 and 2006, since it is expected that, during this period, people spend much more time at home and wood consumption increases for this reason. The daily trend for this period during 2006 is shown in Figure 8-11: it can be observed an increase of the concentration on Christmas' Eve.

For both years in Milan the average contribution of Levoglucosan to OC, and consequently to PM, increases during the Christmas period (Figure 8-12).

The estimation of the contribution of residential wood combustion to ambient particulate OC is made by averaging available residential wood combustion profiles, calculating a ratio of levoglucosan concentration to emitted OC or PM₁₀ $(\text{lev}/\text{OC})_{\text{ER,bb}}$, and applying this ratio to measured levoglucosan concentrations (equation 1).

$$\text{OC}_{\text{bb,lev}} = \frac{\text{lev}}{(\text{lev}/\text{OC})_{\text{ER,bb}}} \quad (1)$$

According to some authors (Engling et al., 2006, Fine et al., 2002), the ratio between levoglucosan and OC $(\text{lev}/\text{OC})_{\text{ER,bb}}$ varies with different kinds of biomass burned and combustion conditions. It is very difficult to obtain the representative value of this ratio taking into account these variables. At the moment, in order to estimate the contribution of biomass burning to OC, we prefer using a literature value. Puxbaum et al. (2007) estimates this contribution in five background sites in Europe using 0.14 as value, while Szidat et al. (2006) in Zurich, Switzerland uses 0.15. The experimental determination of emission ratio is still in progress.

In Figure 8-13 it is shown the contribution of biomass burning to OC (using 0.15 as emission factor). In the winter season Sondrio shows the highest value of OC due to biomass burning (45%), while Milan and Mantova show percentages lower than 30%.

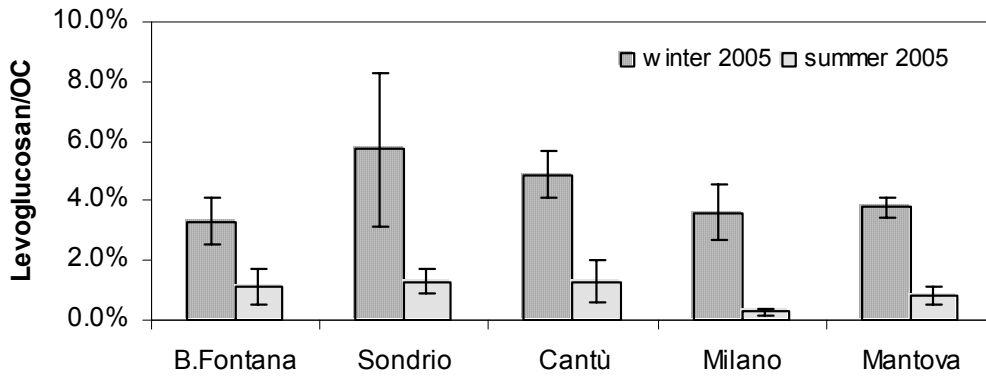


Figure 8-10: average (error bars represent \pm standard deviation) contribution of levoglucosan to OC in five sites in Lombardy region

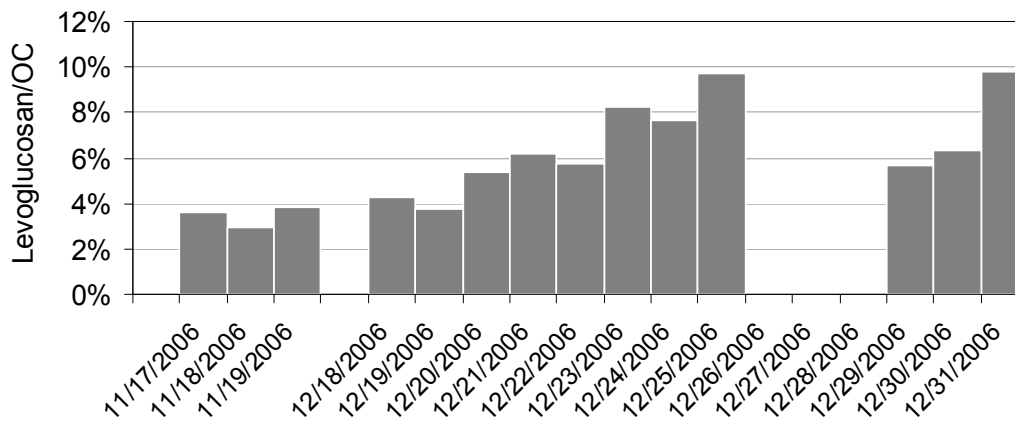


Figure 8-11: trend of levoglucosan concentration in Milan during Christmas period (year 2006)

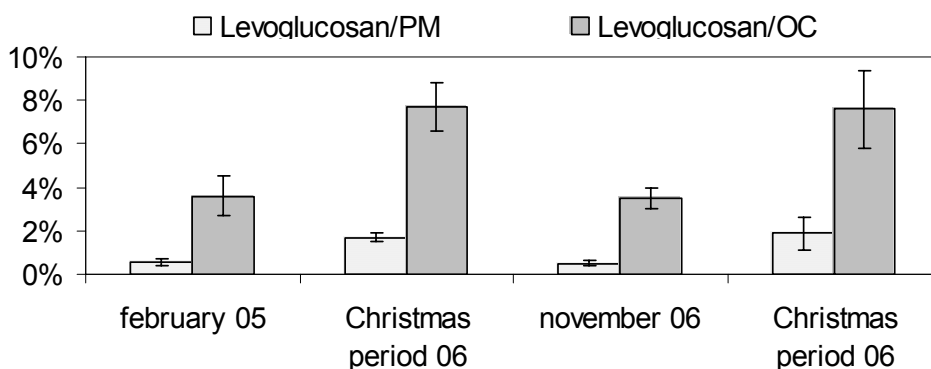


Figure 8-12: average (error bars represent \pm standard deviation) of levoglucosan contribution to OC and PM during two Christmas periods (2005 and 2006) in comparison to two other periods of the same years

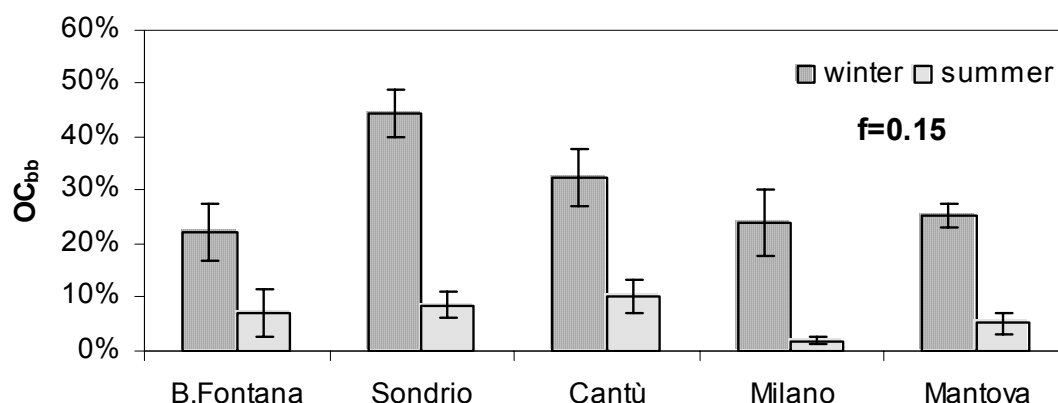


Figure 8-13: average (error bars represent \pm standard deviation) values of the contribution of biomass burning in both seasons, obtained using an emission factor of 0.15 (Szidat et al., 2006)

In Table 8-11 we report the percentage of OC_{bb} in Milan during winter time for two years (2005 and 2006) compared to the Christmas period of same years. It can be observed that biomass burning is an important source of PM₁₀, also in the urban site, and its contribution increases during Christmas period.

	% OC _{bb}	Standard deviation
Winter time 2005	24% \pm	6%
Christmas period 2005	51% \pm	7%
Winter time 2006	23% \pm	3%
Christmas period 2006	44% \pm	13%

Table 8-11: percentage of OC due to biomass burning

We have sampled simultaneously PM₁₀ and PM_{2.5} for ten days.

The ratio between PM_{2.5} and PM₁₀ for levoglucosan is 0.85 ± 0.16 , while for OC is 0.78 ± 0.16 , therefore the biomass combustion emits mainly fine particles.

8.4. Estimation of secondary OC and preliminary apportionment of primary OC

OC is composed of a primary (OC_{pri}) and secondary (OC_{sec}) fraction, well known as secondary organic aerosol (SOA). Using the EC tracer method (Turpin and Huntzicker, 1995; Cabada and Pandis, 2002, chapter 13) we can estimate the magnitude of OC_{sec}.

The key point of this method is the identification of the $(OC/EC)_{pri}$ representative of the sources: a discussion on this topic and the comparison between different criteria is reported in chapter 13.

During the summer we can use 2.1, which is the OC/EC ratio measured in Como during the working days (Sundays are not included in the average). In Como, the sampler was placed near a high traffic road. This value, during the summer, is fairly constant: the ratio between the standard deviation and the average is 24% and it agrees with another estimate from Turpin and Huntzicker (1995).

During the winter it is more complicated to estimate this ratio because we have a larger number of sources and the condensation processes influenced the OC measured. At Como the OC/EC ratio, during the winter, is 3.4 but if we do not consider weekends and festivity the ratio becomes 2.6 ± 1.3 , so we have used this value in order to estimate the percentage of primary OC during the cold season.

These ratios are probably influenced by secondary processes (condensation), so our OC_{pri} values can be overestimated.

In Figure 8-14 we report the average percentage of OC_{pri} for all samples, Milan and Como show values higher than the other sites. The percentage of OC_{pri} in the urban background sites (except Milan) are more similar and according to our estimation one half of organic carbon is of secondary origin.

The rural site (Mantova BF) shows the lowest value of OC_{pri} .

The urban background sites show the same behaviour in the two seasons, with primary OC relative contribution increasing during wintertime (Figure 8-15).

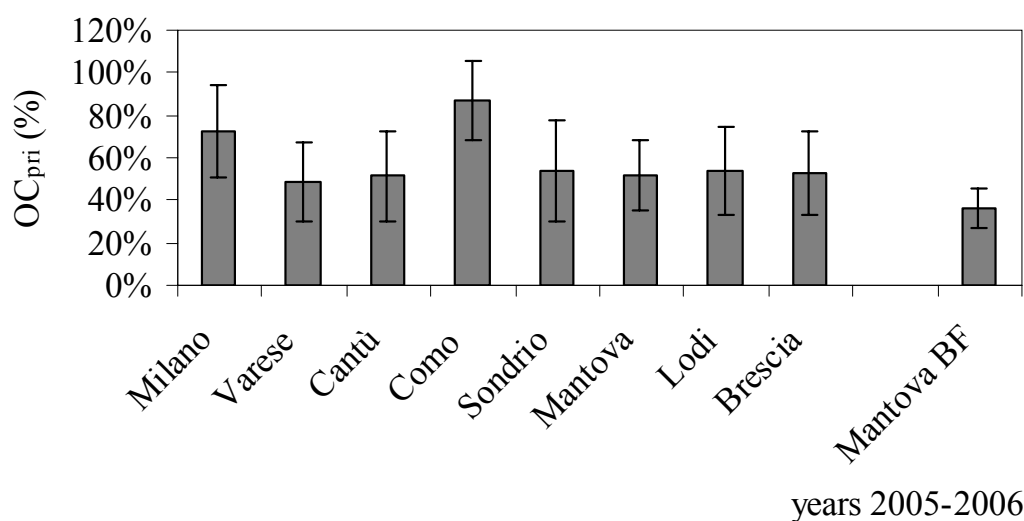


Figure 8-14: average percentage of primary OC, the error bar is one standard deviation

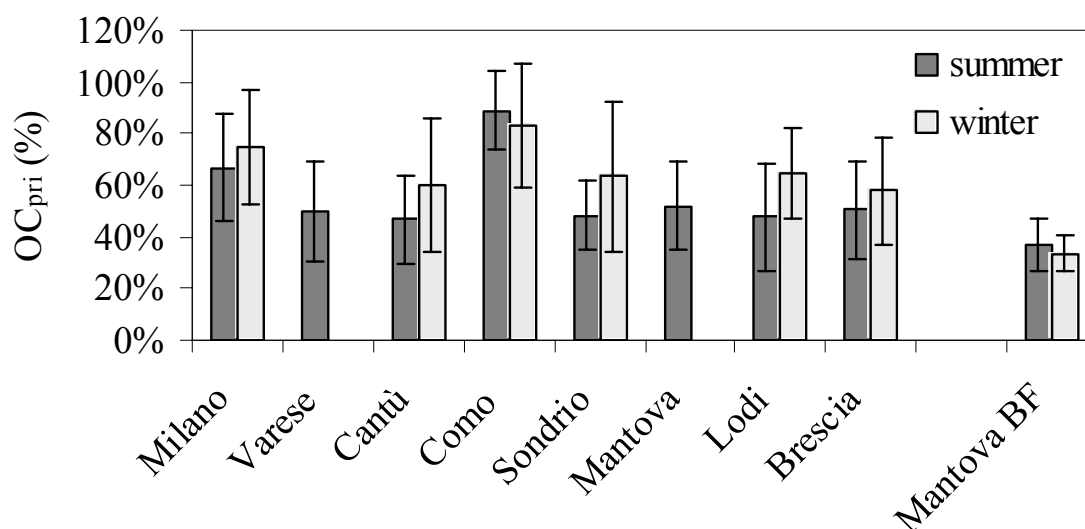


Figure 8-15: average percentage of primary OC in the two seasons, the error bar is one standard deviation

In order to apportion the OC_{pri} to different sources, in the selected site we compare the data obtained by levoglucosan analysis (paragraph 8.3) and the results of OC_{pri} estimation.

According to our data a percentage of 40% - 80% of primary OC, during the winter season, is due to biomass burning. We obtained the highest values in the rural site (Mantova BF) where the contribution from other primary sources (i.e. traffic, industry) is limited. Cantù shows the highest value of the biomass burning contribution to OC_{pri} , in this city the principal industrial activity is joinery, the high values of OC_{bb} probably is not due only to domestic heating but to the industrial activity too.

Mantova BF	Sondrio	Cantù	Milan	Mantova
78% ± 13%	39% ± 18%	76% ± 11%	42% ± 16%	44% ± 23%

Table 8-12: ratio between OC_{bb} (see paragraph 8.3) and OC_{pri} , (February 2005)

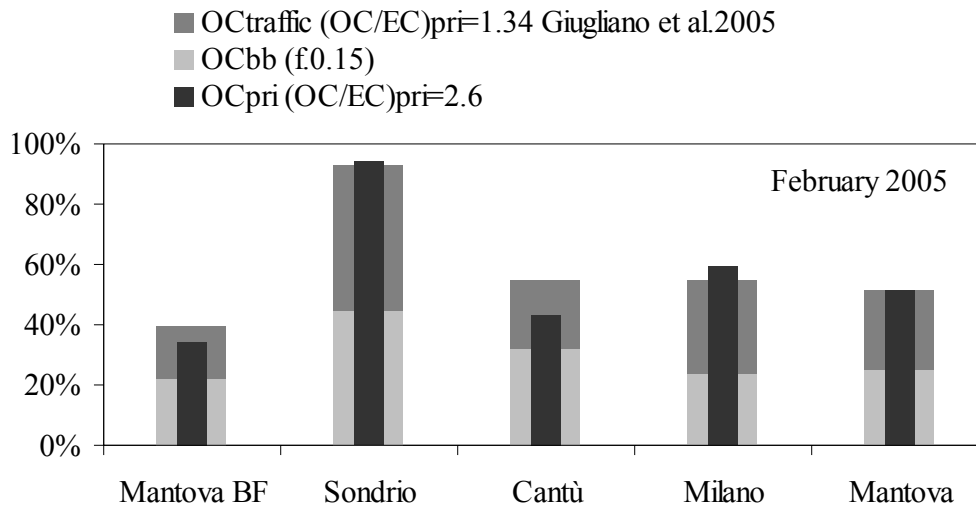


Figure 8-16: OC_{pri} percentage of the total OC and sum of OC due to traffic ($OC_{traffic}$) (Giugliano et al. 2005) and OC_{bb} (paragraph 8.3)

Using the $(OC/EC)_{pri}$ 1.34 estimated by Giugliano et al. (2005) in a traffic tunnel in Milan and supposing it to be representative only for the traffic source we can estimate the primary OC due to this source ($OC_{traffic}$), in Figure 8-16 we report the comparison between the sum of $OC_{traffic}$ and OC_{bb} and the primary OC estimate using 2.6 as primary ratio.

The comparison shows a good agreement and confirms that the road traffic and wood combustion are the main sources of primary carbonaceous particle during the winter time.

8.5. Conclusions

The high concentration of PM measured in Lombardy region confirms that it is one of the largest pollution hot spots area in Europe, and that it is very difficult to respect the limits imposed by European commission due both to high PM loading from emission and to adverse meteorological conditions.

The carbonaceous particles are major constituents of particulate matter and they represent an important portion of PM mass: the carbonaceous particles can explain up to 50% of the mass.

During the summer season all the sites show a similar concentration of OC and, in the selected period taken as example, the three sites (Milan, Mantova, Mantova BF) placed in the plain show the same temporal behaviour. The rural site (Mantova BF)

shows the same concentration of PM and OC as the urban sites. The PM concentration in the Lombardy region is more homogeneous during the hot season when meteorological conditions make easier secondary photochemical production and diffusion of pollutants, also in the alpine region.

In contrast, the EC concentrations are more related to local sources: Milan and Como (traffic site) show the highest percentage of elemental carbon.

The thermal fractions of OC show the difference between summer and winter samples: the winter samples show an increase of PyC percentage, probably due to the growth of the WSOC concentration, which are strongly emitted by biomass burning.

Levoglucosan is a good tracer to quantify the contribution of wood combustion in atmospheric particles. A preliminary evaluation indicates that wood combustion is a significant source of particulate matter in Lombardy region and also in urban sites.

According to EC tracer method, using OC/EC primary ratio estimated in Como, a percentage between 20% - 50% of OC is due to secondary processes. During the winter season about one half of primary OC is due wood burning: this source and road traffic are the main sources of carbonaceous particulate matter.

The high number of data (600 samples) allowed, for the first time, on extensive knowledge of carbonaceous composition of the particulate matter in many sites in the Lombardy region.

These data may be use to study abatement strategies to improve the air quality.

Acknowledgments

I would like to acknowledge V. Bernardoni (General Applied Physics Institute, University of Milan) for the helpful suggestions and ParFiL project for the financial support

References

- Ackermann-Liebrich et al. (1997) *American J. of Respiratory and Critical Care Medicine*, 155, Issue: 1, 122-129
- Birch and Cary (1996) *Aerosol Sci. Tech.* 25, 221
- Bond TC, et al. (2004) *J. Geophys Res* 109 (D14): Art. No. D14203
- CAFE, (2004) Working Group on Particulate Matter, 2004 CAFE Working Group on Particulate Matter, 2004. Second Position Paper on Particulate Matter.
http://europa.eu.int/comm/environment/air/cafe/pdf/working_groups/2nd_position_paper_pm.pdf.
- Castro (1999) *Atmos. Environ.*, 33, 2771-2781
- Dan et al. (2004) *Atmos. Environ.* 38, 3443-3452 http://sdosnew.cilea.it/cgi-bin/sciserv.pl?collection=journals&journal=13522310&issue=v38i0021&article=3443_tccocsatsipib
- Dan et al. (2004) *Atmos. Environ.* 38, 3443-3452
- Dockery and Pope (1996) *Particles in Our Air: Concentration and Health Effects*, Harvard University Press, Cambridge, MA, USA., 123-147
- Engling, et al. (2006) *Atmos Environ* 40: S299-S311 Suppl. 2
- European Union, (1999) *Council Directive* 1999/30/EC of 22 April 1999 relating to limit values for sulphur dioxide, nitrogen dioxide and oxides of nitrogen, particulate matter and lead in ambient air.
- Fermo, et al. (2006) *Chemical Engineering Transactions* 10, 83-88.
- Fine et al. (2002) *Environ. Sci. Technol.*, 36 : 1442-1451
- Giugliano et al. (2005) *Atmos Environ* 39: 2421-2431
- Hitzenberger et al. (1999) *Atmos. Environ.* 33, 2647-2659
- Kunzli et al. (2000) *The Lancet*, 356, 795-801
- Lewis and Smith (1967) *New Phytol.*, 66, 143-184
- Lin and Tai, (2001) *Atmos. Environ.* 35, 2627-2636
- Lioussse et al. (1996) *J. Geoph. Res. D*, 101, 19411-19432
- Na et al. (2004) *Atmos. Environ.* 38, 1345-1355
- Na et al. (2004) *Atmos. Environ.* 38, 1345-1355
- O'Brien and Mitchel, (2003) *Atmos. Environ.* 66, 21-41
- Pashynska, et al. (2002) *J. Mass Spec* 37 (12): 1249-1257
- Pope et al. (2002) *J. of the American Medical Association*, 287, 1132-1141
- Pope, (2000) *Environmental Health Perspectives*, 108, Suppl 4, 713-723
- Punxbaum, et al. (in press) *J. Geophys Res* 112
- Puxbaum et al. (2004) *Atmos Environ* 38 (24): 3949-3958
- Samet et al. (2000) *New England Journal of Medicine*, 343, 1742-1749
- Schwartz et al. (1996) *J. Air and Waste Management Association*, 46, 927-939
- Simoneit, (1999) *Environmental Science and Pollution Research* 6 (3): 159-169
- Sunyer, (2001) *European Respiratory J.* 17, 1024-1033
- Szidat, et al. (2006) *J. Geophys Res* 111 (D7): Art. No. D07206
- Turpin, and Lim, (2001) *Aerosol Science and Technology* 35 (1), 602-610.
- Van Dingenen et al. (2004) *Atmos. Environ.*, 38, 2561-2577
- World Health Organization (2006) *Global update 2005*. WHO/SDE/PHE/OEH/06.02.

9. PM mass concentration and chemical composition in the alpine remote site Bormio – San Colombano (N. Italy; 2,200 m a.s.l.)

A study on PM mass and composition was carried out between April 2004 and March 2006 in the remote site Bormio - San Colombano (2,200 m a.s.l. - 46°27'N; 10°18'E).

Annual means of PM_{2,5} and PM₁₀ were 6 and 7 µg/m³ respectively and the ratio PM_{2.5}/PM₁₀ was 0.9. Both PM_{2,5} and PM₁₀ mass concentrations presented mean spring-summer values higher than those observed in autumn-winter. From April to October, when the site was included in the mixed layer, PM concentrations in the remote site were correlated to those registered in the sites of the valley floor. Concentrations of sulphate, nitrate, chloride and ammonia were similar in PM_{2.5} and PM₁₀. In the warm season concentrations of sulphate reached their maximum levels while those of nitrate felt to minimum levels. The percentages of these anions with respect to particulate mass were similar in both size fractions. Sulphates were higher in Bormio S.C. with respect to the values observed in PM₁₀ in the urban site of Sondrio. On the contrary, nitrate and ammonia mean percentages in Sondrio were higher than those observed in Bormio S.C. As concerns organic carbon (OC) and elemental carbon (EC), average concentrations in the PM₁₀ fraction were lower in Bormio S.C. than in Sondrio. During spring-summer, OC average values were 2.8 µg/m³ and 2.9 µg/m³ in PM_{2.5} and PM₁₀, respectively, with a ratio PM_{2.5}/PM₁₀ of 0.9. In both sites organic matter was the most abundant component of PM.

9.1. Introduction

The aims of the present study, which is part of the regional project PARFIL, are to establish regional background levels of PM mass and chemical composition and to identify the influence of medium to long range transport processes in this site.

Continuous particulate matter (PM) sampling and chemical analysis started in 2004 in two alpine sites: the remote site Bormio - San Colombano (2.200 m a.s.l.; 46°27'N; 10°18'E) (hereon Bormio S.C.) and the urban site Sondrio (298 m a.s.l.; 46°11'N; 9°53'E).

Bormio S.C. is located in the middle of southern alps. It presents a continental climate with short summers and harsh winters. Precipitations (both liquid and solid) reach 1,600 mm/y and prevalent winds blow from S and W quadrants. Mean annual temperature is 2°C while summer and winter means are 6°C and -2°C respectively (CNMB, 2002).

9.2. Experimental settings

PM₁₀ and PM_{2.5} fractions were sampled from April 2004 to March 2006 using LVS automatic samplers in compliance with EN 12341 (in the absence of an official method for PM_{2.5} was used an inlet analogous to that of PM₁₀). 24 hour samples were collected on three different kind of membranes according to the chemical analysis to be performed: coated borosilicate (PAH's and ICP not reported in this paper), PTFE (XRF) and pre-fired quartz fiber (TOT). In order to limit losses of volatile compounds in the warm season, samplers were equipped with air conditioning systems.

PM mass concentrations were determined using a precision scale (sensitivity 1µg) after 48 hours conditioning at circa 30% RH. The uncertainty of gravimetric measurements was $\pm 2 \mu\text{g}/\text{m}^3$ equivalent and the limit of detection was $2 \mu\text{g}/\text{m}^3$.

Ammonia was determined by the indophenol colorimetric method using a UV-VIS spectrophotometer.

The present study includes preliminary results of 11 trace elements sampled in 2004 (As, Cd, Ni, Al, Mn, Pb, Zn, Cu, Cr, Fe Va) measured by spectrometry using optic ICP.

Analytical methods are described elsewhere (Belis et al., 2006)

Organic and elementary carbon (hereon OC and EC respectively) were determined by means of a Thermal-Optical Transmission (TOT) instrument (Sunset Laboratory Inc., USA). More details on this methodology can be found in Birch and Cary (1996).

Organic matter was computed assuming an OM/OC ratio of 1.6 in the urban site (Turpin and Lim, 2001) and 1.9 in the remote site (El-Zanan et al., 2005).

Data below LD were computed using a conventional value equal to LD/2 (Menichini and Viviano, 2004).

9.3. The mass of PM

From 1/4/04 to 31/3/06 PM_{2.5} and PM₁₀ means (\pm std. dev.) were $6 \pm 5 \mu\text{g}/\text{m}^3$ and $7 \pm 7 \mu\text{g}/\text{m}^3$ respectively while the ratio PM_{2.5}/PM₁₀ was 0.9 ± 0.3 . Both fractions presented a seasonal pattern opposite to that observed in urban sites (Figure 9-1). Spring-summer median ($6 \mu\text{g}/\text{m}^3$ in PM_{2.5} and $8 \mu\text{g}/\text{m}^3$ in PM₁₀) were higher than those observed in autumn-winter ($3 \mu\text{g}/\text{m}^3$ in both PM_{2.5} and PM₁₀). During the cold season, in coincidence with thermic inversion between the study site and the nearby town of Bormio (1,250 m a.s.l.), background mass concentrations were below $4 \mu\text{g}/\text{m}^3$ and there was a poor correlation with permanent sites in the valley floor. On the contrary, during the warm season background levels were often interrupted by short episodes (3-5 days) with concentrations up to five times higher. During this period, the site was included in the mixed layer and PM trends were correlated with those observed in Valtellina's valley floor and to a lesser extent with those in the rest of Lombardy Region.

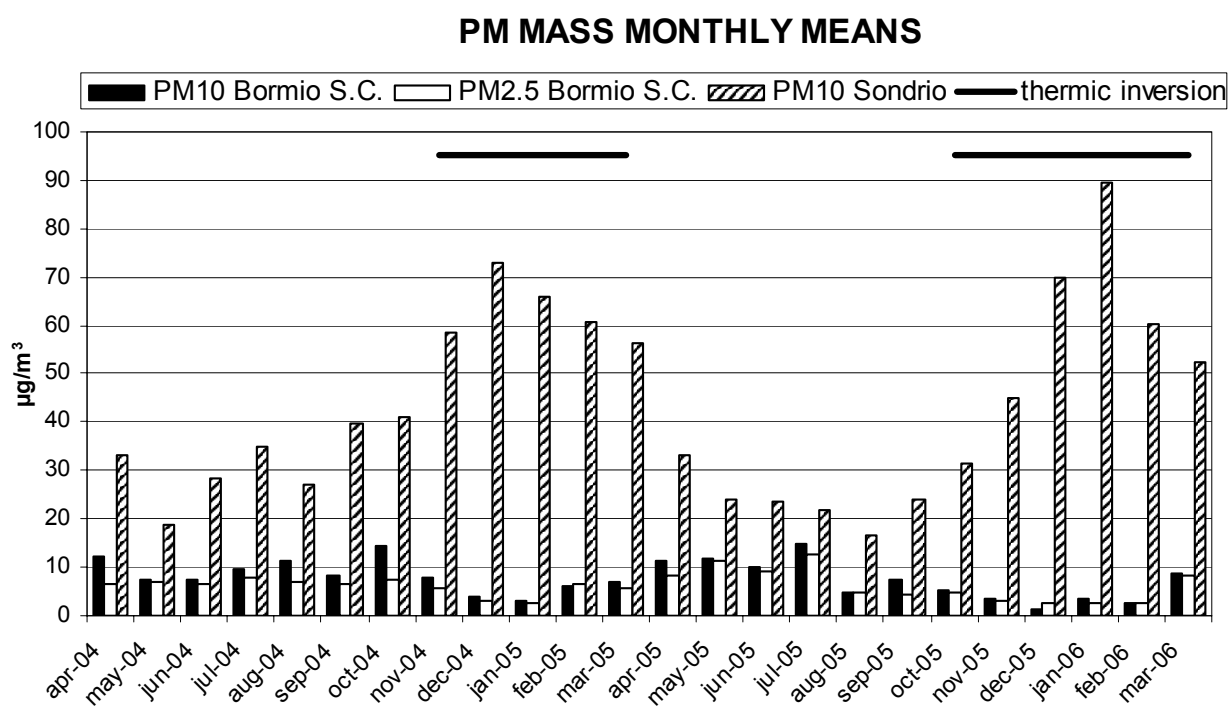


Figure 9-1 Comparison of PM trends between the remote site Bormio S. C. and Sondrio, the main urban site in the valley floor. At the top are indicated the periods with thermic inversion.

9.4. The chemical composition of PM

9.4.1. The trends in the concentration of major chemical components.

In Bormio S.C., mean concentrations of sulphate, ammonia and chloride were similar in PM_{2.5} and PM₁₀: 0.9 $\mu\text{g}/\text{m}^3$, 0.5 $\mu\text{g}/\text{m}^3$ and 0.8 $\mu\text{g}/\text{m}^3$ respectively. Nitrate mean concentration was, on the other hand, higher in PM₁₀ than in PM_{2.5}: 0.4 $\mu\text{g}/\text{m}^3$ and 0.7 $\mu\text{g}/\text{m}^3$ respectively (Figure 9-2).

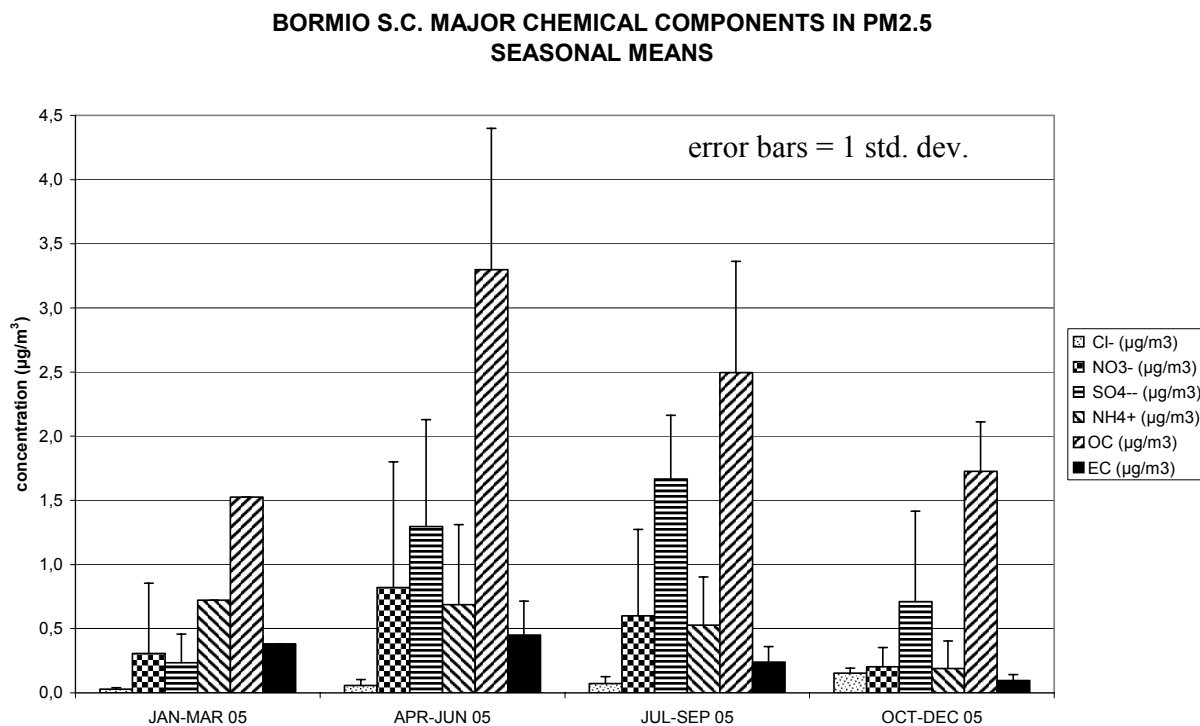


Figure 9-2 Seasonal means of some chemical components in PM_{2.5} in the remote site Bormio S.C. in 2005

As for PM mass, sulphate in Bormio S.C. presented a clear seasonal trend, both in PM_{2.5} and PM₁₀, with maximum concentrations during the warm season. Instead, no clear trend in sulphate concentrations was observed in Sondrio. Nitrate minimum concentrations were observed in summer and autumn in Bormio S.C. and in summer in Sondrio. Similar seasonal variations in nitrate concentrations in rural and remote sites have been related to a greater gas/solid partitioning during colder periods (Putaud *et al.*, 2004). Moreover, the lower affinity of nitrate in the competition with sulfate for ammonia may contribute to explain the seasonality of nitrate considering the role that ammonia plays in bounding nitrates to the fine particulate (Hueglin *et al.*, 2005).

Ammonia presented relatively constant concentrations throughout the year with a minimum in autumn in Bormio S.C. and in summer in Sondrio.

Due to the low concentrations, it is difficult to identify any trend in chloride levels.

In Bormio S.C. during spring-summer OC average values were $2.8 \pm 1 \mu\text{g}/\text{m}^3$ and $2.9 \pm 1 \mu\text{g}/\text{m}^3$ in PM_{2.5} and PM₁₀, respectively, while EC was $0.3 \pm 0.2 \mu\text{g}/\text{m}^3$ in both size fractions. In winter mean OC and EC concentrations in PM_{2.5} were $1.7 \pm 0.4 \mu\text{g}/\text{m}^3$ and $0.1 \pm 0.01 \mu\text{g}/\text{m}^3$ respectively. In this site, OC(PM_{2.5})/ OC(PM₁₀) ratio was 0.9 matching the PM_{2.5}/PM₁₀ mass ratio. Sondrio presented higher values of both OC and EC during winter while Bormio S.C. showed the opposite situation, probably due to its position above the mixing layer in this season.

OC/EC ratio in Sondrio (4.4 ± 1.0) was typical for urban sites and indicated the presence of some SOA (Secondary Organic Aerosol) (Turpin and Huntzicker, 1995). In Bormio S.C., the higher OC/EC ratio (9.1 ± 3.4) was probably related to both, the higher contribution of the biogenic OC component (Turpin and Lim, 2001), and the relatively low EC values in this site.

The seasonal trend of OC/EC in Sondrio, with higher values during the warmer period, was likely caused by an increased photo-oxidation of organic aerosols during this season (El-Zanan et al., 2005).

Aluminium, zinc, copper and iron were the most abundant trace elements in PM_{2.5} and in PM₁₀ in both sites. Arsenic, cadmium and nickel were below the air quality standards of the directive 2004/107/CE ($6 \text{ ng}/\text{m}^3$, $5 \text{ ng}/\text{m}^3$ and $20 \text{ ng}/\text{m}^3$ respectively).

9.4.2. Mass Closure

In Bormio S.C. the percentage of OM was more abundant in PM_{2.5} than in PM₁₀ and both of them were higher with respect to the percentage of OM in PM₁₀ in Sondrio (Figure 9-3). Sulfate was the second most abundant compound in Bormio S.C. followed by nitrate and ammonia. In this site EC was only a minor component. On the contrary, nitrate sulphate and EC were all comparable in PM₁₀ in Sondrio. Chloride was always below 2% and considering the distance to the sea it can be excluded a marine source.

Excepting OM, the chemical compositions of PM_{2.5} and PM₁₀ in Bormio S.C. were quite similar. Such resemblance may be related to the high PM_{2.5}/PM₁₀ ratio, which reflects the small contribution of the coarse fraction (PM₁₀-PM_{2.5}) in this site. This fraction, that in average represents 10 % of the PM₁₀, is poor in EC and OC with respect to PM_{2.5}. The relatively high unaccounted fraction in PM₁₀-

PM_{2.5} probably include components of mineral dust (e.g. Si, Ca.) whose determination is in progress.

The percentages of OM and sulfate in Bormio S.C. were higher than those observed in Sondrio. On the other hand, the urban site showed higher percentages of nitrate and EC than the remote site. The higher content of sulfate, a secondary pollutant, may indicate the ageing of the PM present in Bormio S.C. (Raes *et al.*, 2000) while the reduced amounts of nitrate and EC may result from the considerable distance from anthropogenic sources (i.e. combustion processes).

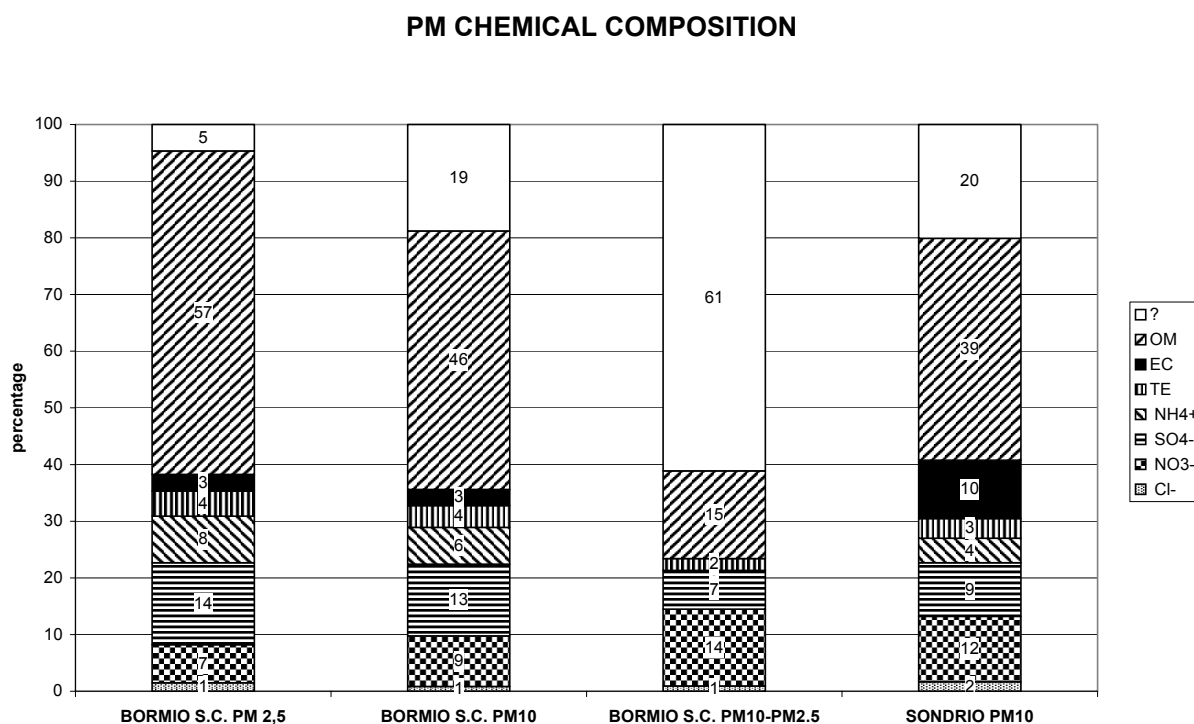


Figure 9-3 Estimated mean composition of PM in Bormio S.C. and Sondrio. (?) unaccounted, (OM) organic matter, (EC) elementary carbon; (TE) trace elements.

9.5. Conclusions

As a whole, the dynamics of PM in Bormio S.C. is influenced by meteorological factors that control the transport of air masses from polluted areas towards remote areas. A detailed analysis of single episodes (Belis *et al.*, 2006) revealed that in spring and autumn the increase in PM concentrations coincide with air masses blowing from SW or S quadrants while in summer, when wind system is dominant, there is no correlation between wind direction and PM mass.

In Bormio S.C. annual levels of nitrate, chloride, ammonia and EC are similar to those observed in the elevated Swiss site of Chaumont (1000 m a.s.l.; Hueglin *et al.* 2005). Nevertheless, in the Italian site levels of sulphate are halved and levels of OM are twice as much of those observed in the Swiss site.

Acknowledgment

I would like to acknowledge ParFiL Project for financial support, C.Balis (ARPA Sondrio) for the PM and ions data and for the contribution in drawing up of this paper

References

- Birch M. E., R. A. Cary, 1996. *Aerosol Sci. Tech.* 25, 221
- Belis et al. (in press) Centro Nivometeorologico di Bormio , 2002 *Annale Nivometeorologico delle montagne Lombarde 2000*. Regione Lombardia.
- El-Zanan et al. (2005) *Chemosphere*. 60, 485
- Facchini et al., (2000) *Atmospheric Environmental* 34, 4853-4857
- Hueglin et al. (2005) *Atmospheric Environment*. 39, 637
- Menichini and Viviano (2004) *Rapporti ISTISAN 04/15*. I.S.S., Roma.
- Putaud et al. (2004) *Atmos. Chem. Phys.* 4, 889
- Raes et al.(2000) *Atmos. Environ.* 34, 4215.
- Seinfeld and Pandis (1998) *Atmospheric Chemistry and Physics. From air pollution to climate change*. John Wiley & Sons, New York
- Turpin and Lim (2001) *Aerosol Sci. Tech.* 35, 602
- Turpin and Huntzicker (1995) *Atmos. Environ.* 29, 3527

10. Characterization of atmospheric aerosols at Monte Cimone, Italy, during summer 2004

Atmospheric aerosols in the PM₁₀ and PM₁ fractions have been sampled at the Global Atmospheric Watch station Mount Cimone, Italy (2165 m above mean sea level) for 3 months during summer 2004, and simultaneous size distributions have been derived by means of an optical particle counter. Samples have been analyzed by X-ray fluorescence, ion chromatography, and thermal-optical methodology in order to quantify their elemental, ionic, and carbonaceous constituents. The concentration of PM₁₀ was $16.1 \pm 9.8 \mu\text{g}/\text{m}^3$ (average and standard deviation). Source apportionment allowed us to identify, quantify and characterize the following aerosol classes: anthropogenic pollution ($10 \mu\text{g}/\text{m}^3$), mineral dust ($4 \mu\text{g}/\text{m}^3$), and sea salt ($0.2 \mu\text{g}/\text{m}^3$). Pollution has been further split into ammonium sulfate (44%), organic matter (42%), and other compounds (14%). The nitrate/sulfate ratio in the polluted aerosol was 0.1. Fine particles have been completely related to the polluted aerosol component, and they represented 70% in weight of pollution. Coarse particles characterized the dust and salt components, and crustal oxides have been found to be the largest responsible for the aerosol concentration variations that occurred during the campaign. Nitrate has also been found in the coarse particles, representing ~10% of mineral dust.

10.1. Introduction

Atmospheric aerosols are a major unknown to climate research since they present a large day-to-day variability in terms of origin, composition, size distribution and global distribution. A major issue concerns the magnitude of the natural and anthropogenic components of the aerosol population (Intergovernmental Panel on Climate Change, 2001). Besides being important for the evaluation of climatic impacts, the same issue is relevant to the application of environmental limits on aerosol concentration. In fact, local and regional sources are not the only factor affecting the aerosol contribution at a measurement site, since longrange transport can occur. The Sahara desert, for instance, is a major source of particulate matter, usually considered of natural origin (although a relevant part of mineral aerosols is attributed to desertification and land misuse, and thus to human activities (Tegen and Fung, 1995). Saharan dust can travel over distances of several thousands kilometers (Morales, 1986; Chiapello et al., 1999; Borbely-Kiss et al., 2004),

reaching altitudes going almost up to the tropopause (Gobbi et al., 2000). In southern European environments Saharan sources may cause a number of PM₁₀ exceedances with respect to air quality standards (Rodri'guez et al., 2001).

Aerosol samples are usually collected at urban sites. However, as local sources dominate in cities, it can be difficult to isolate features proper of long-range transport and of background conditions. Instead, sampling at remote sites is mostly useful for characterizing the regional background and for identifying air mass transport effects (see, e.g., Braga Marcazzan et al., 1993; Schwikowski et al., 1995). Aerosol sources can be revealed through the evaluation of the composition. More insight is given by source apportionment and the correlation with relevant meteorological parameters.

In this work, results of aerosol samplings in the PM₁₀ and PM₁ fractions carried out in 2004 at the Mount Cimone Global Atmospheric Watch (GAW) station during a 3-month summertime campaign are presented. Mount Cimone (44°11'N, 10°42'E, 2165 m above mean sea level (amsl)), the highest peak of the Italian northern Apennines, is considered representative of southern European continental background conditions (Bonasoni et al., 2000b; Fischer et al., 2003). Located in the free troposphere most of the time, it has, however, been verified that during the warm season boundary layer air masses may reach this site, because of vertical mixing and mountain wind regime (Fischer et al., 2003; Van Dingenen et al., 2005).

The aerosol sampling campaign started on 30 June (Julian day (JD) 182) and ended on 6 October 2004 (JD 280), with the aim of improving the description of the background aerosols in southern Europe, with emphasis on fine particles, and on evaluating the contribution of remote and regional sources. A significant subset of aerosol properties (size-fractionated concentration, detailed composition and size distribution) have been continuously monitored. In the past, the compositional characterization of aerosol samples collected at this mountain site has been examined for ionic, carbonaceous and refractory components (Putaud et al., 2004; Van Dingenen et al., 2005). Within this research, elemental analysis has allowed us to identify the major aerosol components, in order to obtain a more complete picture.

For the size fraction PM₁, only few previous elemental characterizations at mountain sites have been reported before (Streit et al., 2000). The study of this fraction is of importance since accumulation mode particles (0.1–1 μ m diameter) dominate radiative effects in the visible range, due to the fact that they are preponderant in number and, having a size comparable to visible wavelength, they have a large scattering efficiency. Moreover, it is in the fine aerosol fraction that

the anthropogenic influence is preponderant, including emissions of strongly absorbing aerosols such as black carbon.

Aerosol composition and air mass origin are intimately correlated and can be used to distinguish between aerosol types and thus quantify the natural and anthropogenic components.

In this paper, source apportionment techniques are used for the characterization of the aerosols.

10.2. Sampling and Methods

10.2.1. Field Campaign

Aerosols have been sampled on 47 mm diameter filters, using CEN-equivalent sequential samplers from TCR-Tecora equipped with PM10 and PM1 sampling heads. PM10 was sampled on polytetrafluoroethylene (PTFE) substrate, at the rate of one filter every 24 hours. PM1 was sampled in parallel on both PTFE and pre-fired quartz fiber filters, at the rate of one every 48 hours. Sampling was performed at a constant air flux of 2.3 m³/h (actual flux) through each filter, and filter changes were programmed to take place at midnight local time.

Additional daily PM10 samples on PTFE filters have been collected in Modena, Italy, by the Regional Agency for Prevention and Environment, Emilia-Romagna (D'Alessandro et al., 2006). Modena is a midsized town located in the Po Valley (60 km north of Mount Cimone, 30 m amsl). These samples are used here as a term of comparison with the Mount Cimone results, in order to give a hint on the correlation between the two sites.

In addition to PM samplers, a Grimm 1.108 optical particle counter (OPC) placed at Mount Cimone provided the aerosol number size distribution for diameters (D_p) between 0.3 and 20 μm in 15 size channels, with a 1-min time resolution (not reported here)

10.2.2. Laboratory Analyses

Samples have been analyzed gravimetrically after being conditioned for 48 hours at constant temperature (20 ± 1°C) and relative humidity (50 ± 5%). To determine the particulate matter concentration, filters have been weighed both before and after sampling with an analytical balance (sensitivity 1 mg). All concentrations given in this paper, gravimetric and compositional, refer to normalized air volumes, i.e., to 1 atm and 0°C.

Information on the aerosol composition has been gathered through the use of energy dispersive X-ray fluorescence (ED-XRF). This technique has sensibility for elements with atomic number $Z > 11$, and thus the carbonaceous part and nitrates remain undetected (Van Grieken and Markowicz, 1993). The technique is efficient in distinguishing several important aerosol types, such as for instance mineral dust, sulfur-containing particles and sea salt. Elemental concentrations on the PTFE filters were determined at the laboratories of the Universities of Genova and Milano, using two ED2000 spectrometers by Oxford Instruments, following a methodology already adopted in previous works (Marcazzan et al., 2001). The following elements have been identified: Na, Mg, Al, Si, P, S, Cl, K, Ca, Ti, V, Cr, Mn, Fe, Ni, Cu, Zn, Se, Br, Sr, Pb. Detection limits were 2–100 ng/cm² on the filter deposit (depending on element); in terms of airborne concentration, 0.6–30 ng/m³ for 24-hour samples and 0.3–15 ng/m³ for 48-hour samples.

The water-soluble inorganic portion of the Mount Cimone PTFE samples has been determined by standard ion chromatography, IC (see chapter 2), using an ICS-1000 Ion Chromatography System (Dionex). The concentration of the following species has been retained: ammonium (NH₄⁺), sulfate (SO₄²⁻) and nitrate (NO₃⁻).

The carbonaceous content of samples deposited on Mount Cimone PM1 quartz fiber filters has been quantified for both organic (OC) and elemental carbon (EC). A rectangular portion (area 1.5 cm²) of each filter has been analyzed by a thermal-optical transmission method (TOT) by means of an OC/EC carbon analyzer (Sunset Laboratory Inc., USA) using the NIOSH 5040 protocol (Chow et al., 2001). Filters were pre-fired prior to sampling, by heating them at 700°C for 1 hour. Details on the methodology are given by Birch and Cary (1996) and is described in chapter 4. The estimated uncertainty on derived concentrations is 5–10%.

10.2.3. Source Apportionment Methodologies

10.2.3.1. Aerosol Composition

Estimate of mineral dust concentration has been made by combining the concentrations for crustal elements, multiplied by the respective molar correction factors, according to Eldred et al. (1987) and Malm et al. (1994). The factors have been derived assuming that the elements are present in the form of oxides, according to the composition of the Earth's crust given by Lide (1992); the two iron oxides have been assumed equally abundant; and the concentration of K has been extrapolated from Fe so that non soil K (from smoke) is not accounted (based on our correlation line between the two elements, $[K]_{\text{soil}} = 0.47 [Fe]$). Finally, molar correction factors have been proportionally increased by 12% to account other compounds present in the average sediment. The relationship used is the following:

[crustal oxides]

$$= 1.12 \times \{1.658[\text{Mg}] + 1.889[\text{Al}] + 2.139[\text{Si}] \\ + 1.399[\text{Ca}] + 1.668[\text{Ti}] + 1.582[\text{Mn}] \\ + (0.5 \times 1.286 + 0.5 \times 1.429 + 0.47 \times 1.204)[\text{Fe}]\}.$$

The above formula yields correct results for all types of soil listed by Lide (1992), except for limestone where a large fraction of the mass, given by carbonate, is missed.

A first estimate of sea salt could be given by $[\text{Na}] + [\text{Cl}]$; however, actual sea salt resembles more a mixture of NaCl (82% by weight), MgCl_2 (8%) and MgSO_4 (10%). A full characterization is given by Lide (1992), and based on the composition of seawater given therein the following relationship has been adopted:

$$[\text{sea salt}] = 1.46[\text{Na}] + [\text{Cl}]$$

which is similar to the approach by Virkkula et al. (1999). The 1.46 factor in front of Na stands for other ionic constituents (representing 14% of sea salt), and Cl is added separately.

Concerning sulfur compounds, a few preliminary considerations based on our IC results must be made, based on the observation that daily S, SO_4^{2-} and NH_4^+ concentrations have been found to be strongly correlated. The correlation coefficient between S and SO_4^{2-} , obtained by linear regression, is 0.98 for the PM10 data and 0.995 for PM1; the correlation coefficient between NH_4^+ and SO_4^{2-} is 0.97 for PM10 (after the removal of three outliers) and 0.98 for PM1. The overall average $\text{SO}_4^{2-}/\text{S}$ ratio (PM10 and PM1 samples together) is 3.4 ± 0.4 , which is compatible with the hypothesis that all S is present as sulfate ion (the value expected for sulfate is 3.00). The overall average $\text{SO}_4^{2-}/\text{NH}_4^+$ ratio (PM10 and PM1 samples together) is 2.4 ± 0.3 , and is compatible with the assumption that all sulfate is neutralized by ammonium, in the form of ammonium sulfate, $(\text{NH}_4)_2\text{SO}_4$ (the expected ratio for pure ammonium sulfate is 2.66). The data are therefore compatible with associating S to secondary sulfates, originating from sulfur dioxide due to fossil fuel burning, and transported from polluted areas (as also assumed by Malm et al. 1994). Ammonium sulfate has been quantified in two ways, multiplying the concentration of elemental S by 4.125 and multiplying the concentration of sulfate ion by 1.375; in the following, we have considered the average between these two determinations.

Their difference is compatible within the experimental uncertainties (± 5 –10% on XRF concentrations, ± 10 –15% on determinations by IC). It has to be mentioned that the second concentration exceeds the first one by 10–12% (systematic): This may be explained by the fact that the techniques were independently calibrated.

Nitrate deserves similar observations as those made for sulfate. One must, however, be aware of the fact that NO_3^- measurements are affected by sampling artifacts, since losses may take place in the form of gaseous HNO_3 , and moreover NH_4^+ associated with nitrate may evaporate during sampling (Henning et al., 2003). In this paper, ammonium nitrate has been evaluated by adding together the excess NH_4^+ , determined after subtraction of the quantity needed to neutralize SO_4^{2-} , and the corresponding equivalents of NO_3^- . The remaining part of NO_3^- has been separately accounted as unbalanced nitrate: In the sample the ionic balance might have been provided by H^+ (acidic aerosols), or the metals observed by ED-XRF (and already accounted as crustal oxides). It is known, for instance, that mineral dust particles containing calcium carbonates (calcite and dolomite) may react with gaseous nitric acid in the atmosphere to form nitrate salts, and that this reaction is not surface-limited and affects the bulk of the particle (Krueger et al., 2004). Considering NH_4^+ , SO_4^{2-} and NO_3^- , in our data set the balance between anions and cations is verified in the PM1 fraction, but not for PM10 where an excess anions is found, denoting the presence of unbalanced NO_3^- .

Organic matter (OM) can be deduced from OC with a conversion coefficient of 2, appropriate for rural sites as documented by Turpin and Lim (2001) and El-Zanan et al. (2005). The use of a “large” OM/OC ratio for rural sites is explained by the fact that, on one side the contribution of biogenic aerosols is expected larger than in urban areas, and on the other side anthropogenic particles tend to be aged and therefore more oxygenated (El-Zanan et al., 2005). It must be remembered, however, that using an a priori ratio is not a robust approach, as the mix of organic compounds in aerosols varies (Turpin and Lim, 2001).

10.2.3.2. Principal Components

The statistical interpretation of data was also carried out.

The correlation of multiple variables can be studied by means of multivariate statistical techniques (Mather, 1976; Hansson et al., 1984; Swietlicki et al., 1987; Marcazzan et al., 2003). Here principal component analysis (PCA) has been applied to the aerosol data set: the resulting factor loadings table is used to group measured variables into different components, each representing a set exhibiting a correlated behavior. The fluctuation of elemental concentrations within each component can therefore be assumed to be associated to a common cause, e.g., a same production or advection mechanism. Moreover, absolute principal component analysis (APCA) permits to quantify the portion of the measured aerosol concentration, determined gravimetrically, that is associated to each identified component (Thurston and Spengler, 1985; Keiding et al., 1986; Swietlicki et al., 1996). On the basis of a statistical approach, the method is thus capable of

quantifying the overall portion of the aerosol concentration associated to each component, including the part that is not directly observed by our analytical techniques: For instance, the ED-XRF data set does not include light elements such as H, C, N and O; however, the APCA may reconstruct the overall concentration in each component.

PCA has been applied to the PM10 data set only, since the number of PM1 samples has been judged statistically insufficient; moreover, as will be shown, source apportionment for PM1 appears quite simple so as to be interpreted directly.

10.3. Campaign Results

10.3.1. General Features of Mount Cimone Aerosols

In Figure 10-1a and Figure 10-1b, the graphs of the PM10 and PM1 aerosol concentration (determined gravimetrically) are displayed. The following average quantities have been determined: PM10 $16.1\mu\text{g}/\text{m}^3$ (standard deviation $9.8\mu\text{g}/\text{m}^3$); PM1 $7.1\mu\text{g}/\text{m}^3$ (standard deviation $3.4\mu\text{g}/\text{m}^3$); where the standard deviation is a measure of the variability of the observed variable.

These quantities show large variations. As far as PM10 is concerned, for instance, the minimum and maximum concentrations amount to 5.4 and $69.9\mu\text{g}/\text{m}^3$, respectively. The most striking feature is the aerosol peak on days 222–224; by removing those three days from the data set, the PM10 average reduces to $14.5\mu\text{g}/\text{m}^3$ (standard deviation: $6.0\mu\text{g}/\text{m}^3$). The PM1 concentration seems unaffected by the large PM10 variations that occur on JD 222–224 (Figure 10-1a): This indicates that the observed feature has to be ascribed to coarse particles.

Table 10-1 and Table 10-2 display the average concentrations of individual constituents, together with the standard deviations over the campaign period, medians, low and high percentiles. Among detected elements, the most abundant one is S, with a concentration of $1.0\mu\text{g}/\text{m}^3$ in PM10 and $0.7\mu\text{g}/\text{m}^3$ in PM1; its largest part (70%) is thus in the fine fraction. Other elements abundant in the PM10 fraction (but not in PM1) are Si, Ca, Al, Fe, Na, K, Mg, Cl and Ti. Traces of P, V, Mn, Ni, Cu, Zn, Br, Sr and Pb have also been found (average values in PM10 $\leq 10\text{ ng}/\text{m}^3$ for each of them).

Noteworthy are also the concentrations of SO_4^{2-} ($3.5\mu\text{g}/\text{m}^3$ in PM10 and $2.4\mu\text{g}/\text{m}^3$ in PM1) and NH_4^+ ($1.4\mu\text{g}/\text{m}^3$ in PM10 and $1\mu\text{g}/\text{m}^3$ in PM1): Their distribution among PM1 and PM10 reflects that of S (70–72% in PM1), confirming the ammonium sulfate assumption. Relevant are also the amounts of OC in PM1, $1.5\mu\text{g}/\text{m}^3$, and NO_3^- in PM10, $0.8\mu\text{g}/\text{m}^3$.

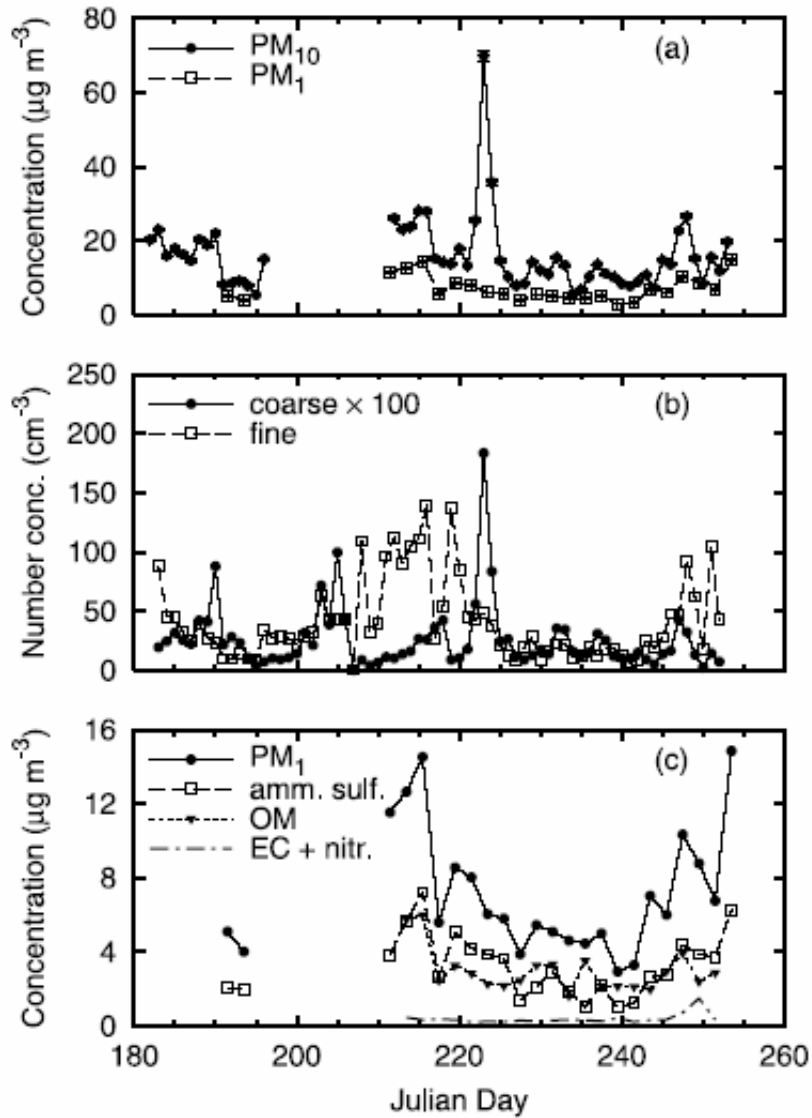


Figure 10-1: (a) Aerosol concentration versus time at Mount Cimone during summer 2004, based on 24-hour PM_{10} samples (solid circles, solid line) and 48-hour PM_1 samples (open squares, dashed line). (b) Particle number concentration, daily averages for coarse (solid circles, solid line) and fine (open squares, dashed line) particles. Data for the coarse mode are multiplied by 100 for graphical purposes. (c) PM_1 concentration (solid circles, solid line) at Mount Cimone during summer 2004, decomposed into ammonium sulfate (open squares, dashed line), organic matter (solid triangles, dotted line), and EC plus nitrate (dashed-dotted line).

Element	Samples	Mean	SD	Median	10th Percentile	90th Percentile
Na	57	210	150	180	42	420
Mg	57	81	82	65	25	110
Al	57	300	460	140	40	670
Si	57	700	1100	400	120	1600
P	31	10.3	6.5	8.8	3.3	15.4
S	57	1040	570	1000	340	1780
Cl	26	82	98	45	19	175
K	57	160	210	120	53	250
Ca	57	360	550	240	73	630
Ti	53	30	50	16	5	58
V	35	3.1	1.5	2.8	1.8	4.6
Mn	49	6.2	7.0	4.5	2.2	10.3
Fe	57	260	440	140	37	400
Ni	26	1.4	0.5	1.3	0.9	2.1
Cu	50	2.9	3.1	1.8	1.2	5.3
Zn	57	9.9	6.0	8.4	3.6	19.6
Br	56	3.0	1.1	3.0	1.7	4.3
Sr	40	2.7	2.8	2.1	1.1	3.7
Pb	48	3.9	2.4	3.4	1.5	7.5
NH ₄ ⁺	47	1430	800	1240	440	2560
SO ₄ ²⁻	47	3500	2000	3500	1100	6200
NO ₃ ⁻	47	840	670	700	280	1310
PM ₁₀	57	16100	9800	14200	7900	25800

^aConcentrations are given in ng m⁻³. The "Sample" column indicates number of valid samples for which there is a detectable quantity of the given element (i.e., above the minimum detection limit). SD is standard deviation. Data are omitted for elements for which the number of valid samples is less than 40% of the total number of samples.

Table 10-1: Summary of Elemental and Ionic Concentrations in PM₁₀ During the Mount Cimone Campaign^a

Element	Samples	Mean	SD	Median	10th Percentile	90th Percentile	PM ₁ /PM ₁₀
Al	11	10.6	6.3	9.4	4.0	16.8	0.04
Si	23	25	17	21	8	47	0.06
P	10	2.6	1.4	2.2	1.3	4.7	0.27
S	24	700	360	610	300	1230	0.70
K	24	36	25	32	10	60	0.25
Ca	23	9.0	5.5	7.0	4.2	16.7	0.04
Fe	24	8.5	8.3	5.0	1.8	17.9	0.05
Zn	24	5.9	5.0	4.2	1.5	9.7	0.54
Br	23	2.1	0.7	2.1	1.3	3.1	0.69
Pb	19	2.1	1.3	1.6	1.0	3.7	0.50
NH ₄ ⁺	24	970	460	880	480	1570	0.73
SO ₄ ²⁻	24	2400	1200	2100	1000	4000	0.71
NO ₃ ⁻	24	260	350	130	90	640	0.19
OC	21	1490	560	1340	1070	1970	NA
EC	21	171	61	159	102	249	NA
PM ₁	24	7100	3400	5900	3900	12300	0.47

^aConcentrations are given in ng m⁻³. The last column displays the average PM₁/PM₁₀ ratio for each displayed element or ion. Total PM₁ and elemental and ionic concentrations have been determined from PTFE filters, while OC and EC have been determined from quartz fiber filters. NA indicates not available.

Table 10-2: Summary of Elemental, Ionic, and Carbonaceous Compound Concentrations in PM₁ During the Mount Cimone Campaign (Similar to Table 10-1)a

10.3.2. Characterization of PM1 at Mount Cimone

From Table 10-2 and the above considerations, we deduce that one of the principal constituents of PM1 is ammonium sulfate, with an average concentration of $3.1\mu\text{g}/\text{m}^3$. OC is also significant, with $1.5\mu\text{g}/\text{m}^3$ on average, corresponding to $3.0\mu\text{g}/\text{m}^3$ organic matter. The reconstruction of the PM1 aerosol is detailed in

Table 10-3 and Figure 10-1c. Besides the two major components mentioned above, minor constituents have been identified as ammonium nitrate, EC and crustal oxides ($0.6\mu\text{g}/\text{m}^3$ globally). Finally, one ends up with a reconstructed mass of $6.7\mu\text{g}/\text{m}^3$, representing 94% of the gravimetric datum ($7.1\mu\text{g}/\text{m}^3$). The two major contributors, ammonium sulfate and organic matter, are found in a nearly 1:1 proportion. Both are individually very well correlated to PM1 (linear regression correlation coefficients of 0.94 and 0.81, respectively): We can thus reasonably assume that during the campaign PM1 is the result of a relatively constant mix of these two aerosol types. The same cannot be said for ammonium nitrate and EC, which besides being observed in a relatively small amount, are poorly correlated to the overall PM1 concentration.

Aerosol Class	Average Concentration	
	Micrograms per Cubic Meter	Percentage
Ammonium sulfate	3.1	44
Organic matter	3.0	42
Ammonium nitrate	0.3	4
Elemental carbon	0.2	3
Crustal oxides	0.1	1
Reconstructed	6.7	94
Average PM ₁	7.1	100

Table 10-3: Mass Reconstruction for the PM1 Aerosol at Mount Cimone

10.3.3. Characterization of PM10 at Mount Cimone

PCA has been applied to the gravimetric and elemental PM10 data set, where the daily size-resolved number concentrations determined by OPC have been included in the analysis: Table 10-4 lists the resulting factor loadings. Ionic concentrations have been omitted because ten samples could not be submitted to IC, which is destructive, since they have been kept aside for additional analyses (but in the end the latter analyses were not possible). The ten samples were selected in correspondence to significant dust episodes (see below) and thus removing them from the data set would have been a restriction that could have significantly altered the picture given by the statistical approach. We have thus preferred removing the

ionic concentrations from the data set rather than excluding these particularly significant samples.

Variable	Factor 1 Mineral Dust	Factor 2 Pollution	Factor 3 Sea Salt
PM ₁₀ , gravimetric	0.84	0.51	0.02
PM ₁₀ elemental concentrations			
Na	-0.01	-0.31	0.87
Mg	0.97	0.00	0.18
Al	0.99	0.05	-0.02
Si	0.99	0.07	-0.02
S	0.11	0.87	0.15
Cl	0.23	-0.17	0.68
K	0.98	0.14	0.00
Ca	0.95	0.14	-0.01
Ti	0.99	0.08	-0.03
V	0.66	0.27	0.30
Mn	0.95	0.16	-0.08
Fe	0.99	0.09	-0.03
Cu	-0.04	0.28	-0.10
Zn	0.07	0.88	-0.14
Br	0.18	0.63	0.43
Sr	0.96	0.11	0.04
Pb	0.27	0.76	-0.09
Particle number concentrations			
0.3–0.4 μm	0.01	0.95	-0.15
0.4–0.5 μm	0.01	0.94	-0.16
0.5–0.65 μm	0.11	0.95	-0.07
0.65–0.8 μm	0.76	0.57	0.23
0.8–1 μm	0.94	0.15	0.25
1–1.6 μm	0.94	0.05	0.28
1.6–2 μm	0.87	0.07	0.43
2–3 μm	0.98	0.03	0.11
3–4 μm	0.99	0.01	0.05
4–5 μm	0.94	0.00	0.11
5–7.5 μm	0.77	-0.06	0.18
Explained variance, %	56	21	7

^aFactor loadings larger than 0.6 are in boldface.

Table 10-4: Factor Loadings From Principal Component Analysis on the Mount Cimone Data Set Performed on PM₁₀ Gravimetric Concentration, PM₁₀ Elemental Concentrations, and Particle Number Concentrations in the OPC Size Classes^a

Three components have been identified. Factor 1 represents 56% of the PM₁₀ variability, and is correlated to Mg, Al, Si, K, Ca, Ti, V, Mn, Fe and Sr: This sequence of elements is a clear signature of mineral dust. Factor 2, correlated to S, Zn, Br and Pb, has been associated to anthropogenic pollution, where Zn, Br and Pb are quantitatively present in traces (Table 10-1). Factor 3, correlated to Na and Cl, has been associated to sea salt. APCA permitted to quantify the contribution of each component, as listed in Table 10-5. It is also interesting to note how the number concentrations in size bins, determined by OPC, fit into this picture (Table

10-4): Fine particles are correlated with pollution and coarse particles with mineral dust. The separation between the two components appears to be around a diameter of 0.7 μm . No significant correlation has been found for particles above 7.5 μm .

The reconstruction of the PM₁₀ composition has been done also with compositional (rather than statistical) considerations, as summarized in Table 10-5. When they are added together, elements ascribed to the Earth's crust amount to 1.9 $\mu\text{g}/\text{m}^3$ in PM₁₀ (campaign average); computed oxides, instead, amount to 3.7 $\mu\text{g}/\text{m}^3$. The average S concentration amounts to 1.0 $\mu\text{g}/\text{m}^3$; the average SO_4^{2-} concentration amounts to 3.5 $\mu\text{g}/\text{m}^3$, and the resulting concentration for ammonium sulfate is 4.6 $\mu\text{g}/\text{m}^3$. Sea salt has been quantified in 0.3 $\mu\text{g}/\text{m}^3$ average concentration.

Aerosol Class	Approach		
	Stoichiometric, $\mu\text{g m}^{-3}$	Multivariate, $\mu\text{g m}^{-3}$	Multivariate, %
Mineral dust			
Crustal oxides	3.7		
Unbalanced nitrate	0.4		
Total	4.1	4.3	27
Pollution			
Ammonium sulfate	4.6		
Ammonium nitrate	0.5		
OM plus EC	NA		
Total	≥ 5.1	9.7	60
Sea salt	0.3	0.2	1
Reconstructed		14.2	88
Average PM ₁₀		16.1	100

^aSee text. NA indicates not available.

Table 10-5: Source Apportionment of the PM₁₀ Aerosol at Mount Cimone Obtained With the Stoichiometric and Multivariate (APCA) Approaches^a

Nitrate is found both in the fine and coarse aerosol fractions, and mostly in the latter, since its average concentration in PM₁ represents about one third of its average concentration in PM₁₀. This observation is in line with the observations made by Henning et al. (2003) at the Jungfraujoch and by Putaud et al. (2004) at Mount Cimone, which have found nitrate internally mixed with mineral dust, because of adsorption of HNO_3 . In our data set, 45% NO_3^- is balanced with 110 ng/m^3 NH_4^+ , yielding 0.5 $\mu\text{g}/\text{m}^3$ ammonium nitrate; the additional NO_3^- , 0.4 $\mu\text{g}/\text{m}^3$, is accounted as unbalanced nitrate. We have placed ammonium nitrate with the pollution component, and unbalanced NO_3^- with mineral dust: we thus assume that the ionic balance is provided by crustal elements, such as Ca [see, e.g., Krueger et al., 2004]. We tend to believe that the unbalanced nitrate may be underestimated from our data set, due to the fact that ten samples, associated to significant dust advection episodes, were omitted in the IC analysis. If we could

assume, for a crude evaluation, that unbalanced nitrate is proportional to Ca, we would increase its average concentration by 50% in order to account for the missing samples. A final observation on nitrate: In the polluted air mass, we have found a $\text{NO}_3^-/\text{SO}_4^{2-}$ ratio of 0.1 (ratio of balanced NO_3^- to total SO_4^{2-} in both PM10 and PM1 fractions). This is in line with the conclusions by Henning et al. (2003), i.e., that low values are found at remote sampling sites.

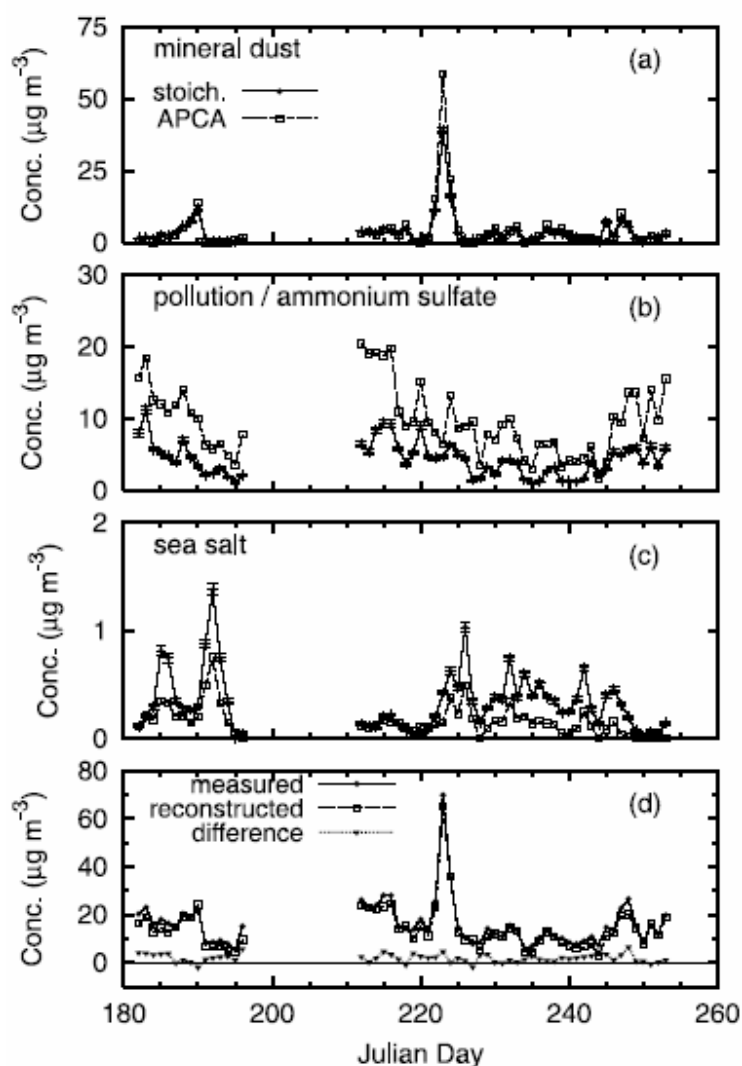


Figure 10-2: Concentration for the PM10 aerosol types identified during the Mount Cimone campaign, quantified by stoichiometric approach (solid circles, solid line) and by absolute principal component analysis (APCA) (open squares, dashed line): (a) mineral dust, (b) pollution (APCA) and ammonium sulfate (stoichiometric), and (c) sea salt. (d) Comparison of gravimetric results (solid circles, solid line) and PM10 aerosols reconstructed by adding the three APCA components displayed in Figure 10-2a and Figure 10-2c (open squares, dashed line). Also shown is the difference between the two (solid triangles, dotted line).

The average aerosol concentration reconstructed by APCA amounts to $14.2\mu\text{g}/\text{m}^3$, 88% of the gravimetric determination. The reconstructed evolution with time of the three components is shown in Figure 10-2: as expected, the different aerosol types exhibit a quite different behavior, but the independent reconstructions by APCA and stoichiometric considerations are similar. In Figure 2b, only ammonium sulfate (deduced from elemental S) is displayed with the stoichiometric curve, since OM data are unavailable for PM10. This is the reason for the strong quantitative difference between the two curves in Figure 10-2b. The PM10 pollution component is strongly correlated to gravimetric PM1 (linear regression correlation coefficient 0.89, after reduction of the data set to a 48-hour resolution): This fact, in combination with the results for the compositional reconstruction of PM1 in section 10.3.2 and to the factor loadings for aerosol sizes in Table 10-4 leads to the conclusion that PM1 is mostly associated to the pollution component, and represents $\sim 70\%$ of it ($7.1\mu\text{g}/\text{m}^3$ out of 9.7).

Figure 10-2d compares the aerosol reconstruction by APCA to the gravimetric determination, and displays the missing part ($\sim 2\mu\text{g}/\text{m}^3$ on average). Results obtained with both approaches (multivariate and compositional) are in agreement (Table 10-5), taken into account that the methodologies are quite different. A reasonable quantitative estimate of the different contributors to the Mount Cimone PM10 (to the first significant digit) can be summarized as follows: $10\mu\text{g}/\text{m}^3$ pollution, $4\mu\text{g}/\text{m}^3$ mineral dust, and $0.2\mu\text{g}/\text{m}^3$ sea salt. The proportions of ammonium sulfate and ammonium nitrate to the pollution component reflect those in total PM1, and thus we can roughly estimate that this peculiarity may be extended to organic matter, for which we have no data in the PM10 fraction. With this assumption, OM could almost fill the gap between the APCA and stoichiometric approaches

10.4. Discussion

Knowing that our measurements were taken at a site isolated from direct anthropogenic emissions, the concentrations obtained can be considered significant when compared to concentrations taken for reference at urban sites. In the European Union, for instance, a limit on average PM10 concentrations of $20\mu\text{g}/\text{m}^3$ has been proposed for 2010, and it has been proposed that concentrations larger than $50\mu\text{g}/\text{m}^3$ should not be tolerated for more than 7 days per year (indicative limit values for stage II, as in directive 1999/30/EC). We note, however, that our average of $16.1\mu\text{g}/\text{m}^3$ cannot be assumed representative of the annual average at Mount Cimone, as our measurements refer to a relatively short period of time and to the summer season only. It must also not be assumed as representative of boundary layer PM concentration, since our measurements have been taken at an altitude of

2km above sea level, and thus above the boundary layer for a significant fraction of observation time. It is anyways noteworthy that a single mineral dust episode was associated to a concentration of as much as $69.9\mu\text{g}/\text{m}^3$, and that episodes with even larger concentrations have been found frequent in the Mediterranean basin.

10.5. Conclusions

Daily aerosol properties have been measured at Mount Cimone during a 3-month period in summer 2004. On average, $16.1\mu\text{g}/\text{m}^3$ have been observed (PM10), but a large variability of all measured parameters dominated the campaign, as is usual with aerosol measurements. A combination of source apportionment approaches using stoichiometric considerations and multivariate statistics allowed us to separate the signal due to three different aerosol classes, each being driven by an independent variability pattern: mineral dust, anthropogenic pollution, and sea salt.

The most abundant component of the aerosol has been associated to anthropogenic pollution ($10\mu\text{g}/\text{m}^3$, mostly in the fine fraction); this component has also been found to yield a relatively small contribution (21%) to the overall aerosol variability. Regarding the composition of pollution, the representation is more complete with the PM1 fraction, for which carbonaceous concentrations are available. The most of it is represented by ammonium sulfate and organic matter, in a nearly 1:1 proportion, which together represent the 86% of the total and show a significant correlation with each other. Small concentrations of ammonium nitrate, elemental carbon, and crustal oxides were also identified. A small nitrate/sulfate ratio has been found, as already observed by Henning et al. (2003) at the Jungfrauoch. Simultaneous observations in Modena and the mixed layer depth suggested that for a large part this component could be ascribed to regional pollution, transported at Mount Cimone under a boundary layer convection regime.

Mineral dust reconstruction by APCA was found quantitatively compatible with a composition based on the metallic oxides that are found in the Earth's crust, amounting to $4\mu\text{g}/\text{m}^3$. Besides crustal oxides, $\sim 10\%$ of the mineral dust concentration has been attributed to nitrate ions. The presence of nitrate in advected mineral dust particles confirms the conclusions of Henning et al. (2003), Putaud et al. (2004) and Krueger et al. (2004).

Mineral dust contributed mostly to the concentration of coarse particles. Despite representing on average only one fourth of the aerosol concentration, it has been the cause for most (56%) of the observed aerosol variability.

The observed concentration of sea salt at Mount Cimone was quite low (average $0.2\mu\text{g}/\text{m}^3$, maximum $1-1.5\mu\text{g}/\text{m}^3$). Roughly speaking, the concentration of sea salt has been associated to low aerosol periods and to the "cleaning" of the atmosphere after African dust events.

The three aerosol classes explain 88% of the observed aerosol concentration and 84% of its variability. We have therefore provided an estimate, at this site and for the period of time under study, of the relative contribution of anthropogenic (pollution) and natural aerosol components (mineral dust and sea salt).

Acknowledgment

I would like to acknowledge all the colleagues who collaborated to this work:

F. Marengo, F. Mazzei, P. Prati

Physics Department, University of Genoa and Istituto Nazionale di Fisica Nucleare-Genova, Genoa, Italy.

P. Bonasoni, F. Calzolari, P. Cristofanelli

Institute of Atmospheric Sciences and Climate, National Research Council, Bologna, Italy.

M. Ceriani, A. D'Alessandro, G. Valli, R. Vecchi

General Applied Physics Institute, University of Milan and Istituto Nazionale di Fisica Nucleare-Milano, Milan, Italy.

M. Chiari, F. Lucarelli, S. Nava

Physics Department, University of Florence and Istituto Nazionale di Fisica Nucleare-Firenze, Florence, Italy.

P. Fermo

Inorganic, Metallorganic and Analytical Chemistry Department, University of Milan, Milan, Italy.

References

- Birch and Cary (1996) *Aerosol Sci. Technol.*, 25, 221–241.
Bonasoni et al. (2000) *Atmos. Environ.*, 34, 5183–5189
Borbély-Kiss et al. (2004) *J. Aerosol Sci.*, 35, 1205–1224.
Braga Marcazzan et al. (1993) *Nucl. Instrum. Methods Phys. Res.*, Sect. B, 75, 312–316.
Chiapello et al. (1999) *J. Geophys. Res.*, 102, 13,701–13,709
D'Alessandro et al. (2006) Rep. INFN/TC-06/01, *Ist. Naz. Di Fis. Nucl., Frascati, Italy*.
Eldred et al. (1987) *Nucl. Instrum. Methods Phys. Res.*, Sect. B, 22, 289–295
El-Zanan et al. (2005) *Chemosphere*, 60, 485–496
Fischer et al. (2003) *Atmos. Chem. Phys.*, 3, 725–738.
Gobbi et al. (2000) *Atmos. Environ.*, 34, 5119–5127
Hansson et al. (1984) *Nucl. Instrum. Methods Phys. Res.*, Sect. B, 3, 483–488

- Henning et al. (2003) *J. Geophys. Res.*, 108(D1), 4030, doi:10.1029/2002JD002439
- Keiding et al. (1986) *Anal. Chim. Acta*, 181, 79–85.
- Krueger et al. (2004) *Atmos. Environ.*, 38, 6253–6261
- Lide (ed. 1992) *CRC Handbook of Chemistry and Physics 1991–1992*, CRC Press, Boca Raton, Fla.
- Malm et al. (1994) *J. Geophys. Res.*, 99, 1347–1370
- Marcazzan et al. (2003) *Sci. Total Environ.*, 317, 137–147.
- Mather (1976) *Computational Methods of Multivariate Analysis in Physical Geography*, John Wiley, Hoboken, N. J.
- Morales (1986) *Clim. Change*, 9, 219–241.
- Putaud et al. (2004) *Atmos. Chem. Phys.*, 4, 889–902
- Rodríguez et al. (2001) *Atmos. Environ.*, 35, 2433–2447
- Schwikowski et al. (1995) *Atmos. Environ.*, 29, 1829–1842
- Streit et al. (2000) *Int. J. Environ. Anal. Chem.*, 76, 1–16
- Swietlicki et al. (1987) *Nucl. Instrum. Methods Phys. Res., Sect. B*, 22, 264–269.
- Swietlicki et al. (1996) *Atmos. Environ.*, 30, 2795–2809
- Tegen and Fung (1995) *J. Geophys. Res.*, 100, 18,707–18,726.
- Thurston and Spengler (1985) *Atmos. Environ.*, 19, 9–25
- Turpin and Lim (2001) *Aerosol Sci. Technol.*, 35, 602–610
- Van Dingenen et al. (2005) *Atmos. Chem. Phys. Discuss.*, 5, 1067–1114.
- Virkkula et al. (1999) *J. Geophys. Res.*, 104, 23,681–23,696

11. A mass closure on the sub-micron sized aerosol fraction at urban sites in Italy

Sub-micron sized particles are of increasing concern owing to their effects on human health and on the environment. Up to now there are still very few studies on PM₁ chemical characterisation; the sub-micron sized fraction is not under regulations although of interest because almost exclusively associated to anthropogenic sources.

To perform the first large scale assessment of sub-micron sized aerosol concentrations, composition and sources two monitoring campaigns at three urban sites in Italy with different characteristics were performed during wintertime and summertime 2004.

Chemical characterisation (elements, soluble ionic fraction, elemental and organic carbon) was carried out on PM₁ samples: major contributions are due to organic matter (about 30% in summer and 50 % in winter) and ammonium sulphate (about 10 % in winter and 40 % in summer). During the cold season nitrates also contribute up to 30 % in Milan (lower contributions were registered at the other two urban sites). Chemical mass closure was achieved with an unaccounted mass in the range 14 - 22 %.

11.1. Introduction

During the last years, an increasing interest for aerosol fine particles has grown in the research community. Literature studies suggest that atmospheric particles of small sizes ($< 2.5\mu\text{m}$) are responsible for health effects in urban polluted areas because they act as carriers for toxicants and mutagenic components (Arden Pope and Dockery, 2006 and reference therein).

Elevated PM concentrations in urban areas result not only from direct particulate emissions but also from gas-to-particle conversion in the atmosphere and secondary aerosols are found mainly in the accumulation mode, i.e. between 0.1 and $1\mu\text{m}$ (EPA, 2004). Moreover, sub-micron sized particles are those with the highest atmospheric number concentration at urban locations, typically up to 10^4 - 10^5 particles cm^{-3} . The control of the fine fraction of particulate matter is a challenging problem in urban areas and to be effective it is necessary to determine fine particles

physical-chemical properties and to identify and quantify emission sources especially in cities where large populations are exposed to high concentrations. Up to now many papers in the literature dealt with PM₁₀ and/or PM_{2.5} chemical composition; even at the same sites investigated in this paper (Prati et al., 2000; Marcazzan et al., 2001; Lucarelli et al., 2004). Nevertheless, there is still a little number of investigations on PM₁, i.e. particles with aerodynamic diameter smaller than 1 µm, in spite of the consideration that these particles are almost exclusively associated to anthropogenic sources and awareness is growing for their adverse effects. Moreover, available data on PM₁ mass concentration and composition are often limited to short measurement campaigns and/or to a single site (Putaud et al., 2002; Pakkanen et al., 2003; Vecchi et al., 2004; Spindler et al., 2004; Ariola et al., 2006). Preliminary results show that PM₁ can be a consistent part of PM₁₀ and PM_{2.5}; this observation increases concern for the possibility of attaining the EU limit (EU Directive 99/62) in force for PM₁₀ and the provisional limit for PM_{2.5}.

To have a wide outlook of mass concentration and chemical composition of sub-micron sized aerosol, we performed two measurement campaigns (winter/summer period) at three Italian towns with different characteristics. As far as we know, this was the first large-scale investigation on PM₁ in Italy and likely in Europe. As a part of this national research project, the source apportionment method Positive Matrix Factorization (PMF) was applied to aerosol elemental composition data aiming at the identification of PM₁ sources and at the estimation of their contributions to mass concentrations.

11.2. Materials and methods

11.2.1. Site description

The monitoring campaigns have been performed at three major Italian towns (Milan, Genoa, and Florence) with differences in their orography, extension, population and emission sources. In the following a brief description of their main characteristics is reported.

Milan (45° 28'N; 9° 13'E) is the second largest town in Italy, after Rome, with about 1 500 000 inhabitants and considering the whole area of the Milan province the population rises up to about 4 millions inhabitants. Milan is situated in the Po valley (Northern Italy), it is heavily industrialised, trafficked and populated and is considered one of the largest pollution hot spots in Europe. It is characterised by a typical continental climate and during wintertime very frequent stagnant atmospheric conditions leading to high pollution levels occur.

Boscofontana (BF, 45° 12'N; 10° 44'E) is a rural site located in the centre of the Po valley, about 130 km far from Milan in the south-east direction; agriculture and breeding are the main activities so that BF can be considered representative of the regional background of the valley itself.

Genoa (44° 24'N; 8° 55'E) is the most populated coastal town in the North-West of Italy (about 600 000 inhabitants), grown during the centuries around the biggest harbour in Italy, also with large steel factories and power plants nearby. It has a Mediterranean climate, and during summertime it experiences stable atmospheric conditions.

Florence (43° 47'N; 11° 17'E) is located in central Italy and with its 400 000 inhabitants is the smallest among the investigated towns. Commercial and tertiary activities are the most important, due to the huge number of tourist visiting of the town. Its location in a closed basin and its continental climate favour atmospheric stability conditions during wintertime.

11.2.2. PM sampling and mass measurement

Samplings were carried out in parallel at the three towns, and the same experimental methodology for sampling and mass determination has been adopted. All the sampling sites were background urban locations, not directly influenced by traffic emissions. Measurements were performed daily during wintertime (December 2003 - March 2004) and summertime (June - September 2004) using sequential CEN-equivalent samplers (flow rate: 2.3m³/h) equipped with PM1 inlets. A daily sampling campaign was also carried out during February and July 2004 in parallel in BF for a preliminary assessment of the sub-micron sized aerosol concentration and composition at a rural site. Due to the limited number of samples, in this paper BF data will be not used for the mass closure and source apportionment study.

24-hours samplings were carried out daily alternating PTFE and pre-fired quartz fibre filters; the use of different filter types was necessary to achieve the full chemical characterization of the sample (see the next paragraph).

PM1 mass was gravimetrically determined by the three laboratories involved in the research (University of Florence, Genoa and Milan), using microbalances (sensitivity 1µg) located in air controlled weighing rooms (T=20±1°C and R.H.=50±5%) where the filters were conditioned for 48 hours before weighing. Routine calibration procedures checked the microbalance performance. According to our weighing laboratory protocol both before and after sampling each filter was weighed three times to obtain one mass measurement result.

11.2.3. Analytical techniques

Energy Dispersive X-ray Fluorescence analysis was performed on all aerosol samples collected on PTFE filters. The concentrations of 16 elements (Al, Si, S, Cl, K, Ca, Ti, V, Cr, Mn, Fe, Ni, Cu, Zn, Br, Pb) were measured by laboratories of the University of Milan and the University of Genoa, using two identical XRF spectrometers (Oxford Analytical, mod. ED2000) and the same analytical procedure (Marcazzan et al., 2004). An inter-comparison between the two laboratories was carried out before the campaign with results in agreement within 10%. The minimum detection limit was in the range 1-10ng/m³ for different elements. Micromatter standard reference samples were used for the quantitative calibration of the system. A check of the calibration was periodically performed analysing the NIST standard SRM2783. A programme on a personal computer supervised the data acquisition, storage and reduction; the analysis of X-ray spectra was performed using the Axil code (Van Espen et al., 1977). Experimental overall uncertainties were in the range 10-15 %.

The water-soluble inorganic fraction was determined by standard ion chromatography (IC). A quarter of each quartz fibre filter was extracted in MilliQ ultrapure water (three successive extractions of 20 minutes in an ultrasonic bath, with the renewal of the water at each step, were needed for a complete recovery) (chapter 2, Fermo et al., 2006a), and the extracts were analysed by IC for major ionic species, i.e. NO₃⁻, SO₄²⁻, NH₄⁺. The overall uncertainty for ionic concentrations was estimated to be 10 %.

The PM1 carbon content (elemental and organic carbon, in the following indicated as EC and OC, respectively) was determined on all pre-fired quartz fibre filters by means of a thermal-evolved method using TGA-FTIR (Thermo-Gravimetric Analysis/Fourier Transformed Infrared Spectroscopy). The TGA/FT-IR analyser consists of a homemade apparatus obtained by the coupling of a thermo-gravimetric analyser and a FT-IR spectrophotometer. By monitoring CO₂ infrared absorbance at 2361cm⁻¹ it was possible to obtain CO₂ evolution curves where the two components OC and EC were detectable as well separated peaks. The technique detection limit was 0.5µgC/cm² and the uncertainty was 10%. More information dealing with system set-up and the experimental methodology are given in chapter 3 and in Fermo et al. (2006b), where a comparison between data obtained by TGA/FT-IR and by Thermal Optical Transmission analyser (Sunset inc.) using NIOSH5040 protocol is also reported (chapter 4).

Meteorological parameters (temperature, pressure, relative humidity, solar radiation, rainfall, wind speed and direction) and criteria gaseous pollutants as well as PM10 and PM2.5 data were available from the regional air quality monitoring networks. In addition, 222Rn hourly measurements were performed in Milan to

account for the atmospheric stability/dispersion conditions. The calculation of the “Radon index”, basically defined by the ratio R between wintertime and summertime average minimum Radon concentrations (Vecchi et al., 2004), allowed the normalisation of PM1 mass and compositional data to account for the seasonal effect due to differences in atmospheric dispersion conditions. The Radon hourly concentration is routinely and continuously measured at ground level (6 meters asl) by the University of Milan group through the collection of its short-lived decay products attached to aerosol particles and the spectroscopic evaluation of their alpha activity (detection limit is 0.2 Bq/m^3). Details on this experimental methodology are reported in Sesana et al. (2003).

11.3. Results and discussion

11.3.1. PM1 mass concentration

Sub-micron sized aerosol mass concentrations (in $\mu\text{g/m}^3$, standardised at 273K and 101.3kPa) are reported in Table 11-1 for the whole monitoring campaign.

	Samples #	Median	Average	Standard deviation	10 th percentile	90 th percentile
Milan_winter	90	44.5	48.8	22.9	21.9	78.1
Florence_winter	44	21.5	25.3	17.9	5.6	53.2
Genoa_winter	73	11.0	11.5	5.4	5.3	18.0
BF_winter	33	32.1	31.4	14.5	12.6	50.6
Milan_summer	93	19.1	19.4	7.5	9.9	29.8
Florence_summer	84	11.7	11.8	4.2	6.9	18.3
Genoa_summer	89	15.6	17.4	8.1	9.0	30.1
BF_summer	29	10.7	10.4	4.3	4.8	15.6

Table 11-1: PM1 mass concentration at the three urban sites and at the rural location (BF). The values in $\mu\text{g m}^{-3}$ are given as median, mean, 10th and 90th percentile. The standard deviation (in $\mu\text{g m}^{-3}$) here represents the variability in the data set.

During wintertime a very high PM1 concentration (median value: $44.5\mu\text{g/m}^3$) was registered in Milan, due to the high loading of pollutants and the atmospheric stability typical of the Po valley. This peculiar meteorological condition, together

with the heavy emission of pollutants from different sources, makes the Po valley one of the most critical areas in Europe as for limit values exceedances.

Also in Florence during the winter the poor atmospheric dilution influences PM1 values, ranging from 5.6 up to 53. $\mu\text{g}/\text{m}^3$ (as 10th and 90th percentile, respectively). A completely different situation is observed in Genoa, where lower PM1 concentration levels (median: 11.0 $\mu\text{g}/\text{m}^3$) were detected as a consequence of the wintertime wind regime, which favours pollutants dispersion.

During summertime the concentrations are significantly lower both in Milan (19.1 $\mu\text{g}/\text{m}^3$, as median value) and in Florence (11.7 $\mu\text{g}/\text{m}^3$, as median value) thanks to the higher mixing layer heights and the higher average wind speeds registered during this period. On the contrary, in Genoa the PM1 median value for the summer period was 15.6 $\mu\text{g}/\text{m}^3$ (higher than the wintertime value); indeed, in this site during summertime the atmosphere is often stable and the dilution is poor so that pollutants concentration builds-up. Considering only data referring to August, and in particular those measured during the central part of the month which is the traditional vacation period for Italians, there is a reduction of about 25-35% in mass concentrations at all the monitored sites.

High wintertime PM1 levels (median value: 32.1 $\mu\text{g}/\text{m}^3$) were also measured at the rural site BF; this might be an indication of the pollution major emission sources (cities, industries and highways) influence on sub-micron sized aerosol over the whole valley although local sources, mainly ascribed to agricultural activities (see paragraph 11.3.2), can impact on the measured levels. Furthermore, the good linear correlation ($R=0.86$) between Milan and BF mass data series and the similarity in elemental composition (see paragraph 11.3.2) suggest the role of regional meteorology in the Po valley, which acts as a single basin. During the summer a PM1 concentration value of 10.7 $\mu\text{g}/\text{m}^3$ was measured in BF, to be compared with 16.7 $\mu\text{g}/\text{m}^3$, as median value registered in Milan in the same days. An interesting observation is that the PM1 median concentration monitored by our group (Marenco et al., 2006) during summertime 2004 at a remote high-altitude site (Mt. Cimone, 44° 11'N; 10° 42'E; 2 165 metres asl) located at the Southern border of the Po valley was 7.1 $\mu\text{g}/\text{m}^3$; this value should be considered representative of the summertime background tropospheric PM1 level over the investigated area.

The concern for possible adverse health effects and problems in attaining PM10 and PM2.5 limits is enhanced by the observed ratios between PM1 and the other fractions, which are $\text{PM1}/\text{PM2.5} = 0.6\text{-}0.9$ (winter) and $0.5\text{-}0.8$ (summer) and $\text{PM1}/\text{PM10} = 0.4\text{-}0.6$ (winter) and $0.4\text{-}0.5$ (summer) at the three urban sites.

11.3.2. Chemical composition and mass closure

Average elemental (in ng/m^3), EC, OC and ionic concentrations (in $\mu\text{g}/\text{m}^3$) are reported in Table 11-2 for the urban sites.

	MILAN		FLORENCE		GENOA	
	Winter	Summer	Winter	Summer	Winter	Summer
Al	16	11	12	19	14	16
Si	37	40	24	32	27	45
S	1 200	1 500	560	1 100	550	1 000
Cl	440	<15	190	<15	31	24
K	300	98	270	94	91	59
Ca	27	22	28	34	18	56
Ti	4	4	4	4	4	4
V	4	4	3	4	4	15
Cr	3	2	1	1	1	1
Mn	9	5	2	2	1	3
Fe	86	42	41	26	24	37
Ni	6	2	6	2	3	5
Cu	7	4	4	4	2	7
Zn	59	34	20	9	13	9
Br	9	5	4	2	3	2
Pb	31	11	12	4	6	4
EC	1.8 (0.5-4.3)	1.1 (0.4-2.4)	0.9 (0.4-1.9)	0.6 (0.3-1.4)	0.9 (0.3-1.8)	0.9 (0.2-1.6)
OC	14.8 (2.2-33.0)	4.8 (1.8-12.7)	12.0 (3.1-29.6)	2.7 (1.3-5.3)	5.0 (2.4-9.8)	3.4 (1.3-7.3)
SO ₄ ²⁻	4.7 (2.1-7.6)	3.9 (1.2-8.5)	1.7 (0.5-3.3)	3.2 (0.4-8.8)	1.7 (0.7-3.5)	3.8 (1.3-13.1)
NO ₃ ⁻	13.6 (4.0-30.5)	0.9 (0.1-5.5)	3.2 (0.4-9.8)	0.1 (0.04-0.2)	1.1 (0.4-2.8)	0.2 (0.1-0.7)
NH ₄ ⁺	4.2 (2.1-6.9)	1.8 (0.6-3.2)	1.6 (0.2-3.6)	1.3 (0.1-3.0)	1.0 (0.5-1.8)	1.4 (0.5-4.4)

Table 11-2: Average elemental values (in ng m^{-3}). Ions, elemental carbon and organic carbon are given in $\mu\text{g}/\text{m}^3$ and minima and maxima values are also reported in brackets

At all locations, S and K give the highest contributions. During wintertime also chlorine concentration is not negligible, but due to its volatile nature, in summer it has been detected only at the coastal town suggesting that the sea can also be a contributor for fine particles.

Contrarily to the results found for the PM1 mass, elemental relative concentrations are generally lower in Milan than at the other urban sites (with some exceptions, like Pb, Zn and Mn). In particular, the emissions due to power plants and to harbour activities are evident in Genoa, where high S, Ni and V concentrations are measured during wintertime as well as during summertime. In Florence the most remarkable feature is the high K concentration during both seasons. To investigate on the possibility that biomass/wood burning being the K source, we optimised a methodology for levoglucosan measurements in PM samples (following Ion et al., 2005) and, although not planned in our original research program, we carried out measurements on very few PM1 samples still available after the chemical analyses. In fact, in the literature potassium and levoglucosan are regarded as good signatures of biomass/wood combustion in the atmosphere (Simoneit et al., 1999). Nevertheless, potassium can also be derived from soil or from solid waste incineration while levoglucosan is produced during cellulose pyrolysis and emitted in fine smoke particulate matter, so that it could be a more specific tracer for biomass/wood burning. Preliminary results show that levoglucosan relative contribution is higher in wintertime samples and especially in Florence (0.69%) with respect to Milan (0.46%) and Genoa (0.20%). Another feature is that only in Milan there is a good correlation ($R=0.94$) between levoglucosan and potassium concentrations. Taking the levoglucosan as the specific marker of biomass/wood burning we can infer that the high K concentration values in Florence must be ascribed to additional sources not yet identified (e.g. industrial plants such as paper-mills); these indications on biomass/wood source contribution in sub-micron sized samples will need further investigations in the next future.

Most of the elemental concentrations (Figure 11-1a,b; in ng/m^3) measured at the rural site are, as expected, lower than in Milan but K and Ca. K concentration in BF is comparable to the one measured in Milan, suggesting the presence of a local source, i.e. wood/biomass burning used for domestic heating and for agricultural purposes (levoglucosan analyses are not available at this site for confirming this hypothesis) and Ca is more abundant in BF the summer month, very likely due to agricultural activities performed in the nearby fields.

To compare elemental data series from different locations, the coefficient of divergence (CD) – a parameter which accounts for similarities in temporal series from different sites (a value near 0/1 indicates maximum/minimum similarity) - was evaluated following the approach described by Zhang and Friedlander (2000). The CD calculated between the Milan and BF elemental data series is 0.29 for

wintertime and 0.20 for summertime; both CD values indicate a fairly good similarity between the two elemental series suggesting a regional character of aerosol pollution in the Po valley.

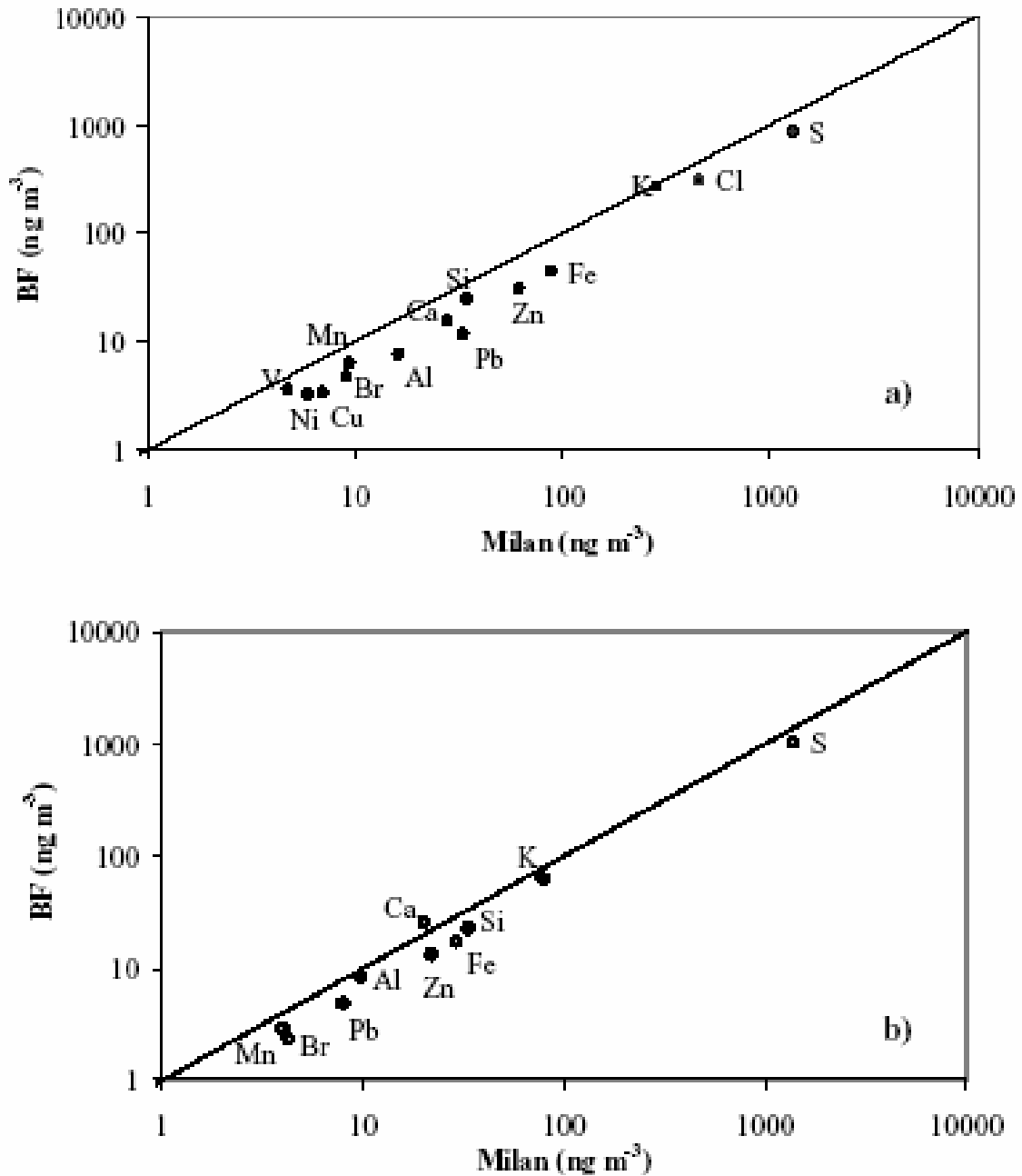


Figure 11-1: Elemental concentrations (in ng/m³) for contemporary samplings performed in Milan and in the rural site (BF) in February (a) and July (b) 2004.

As regards the water-soluble ions results (see Table 11-2), during wintertime in Milan and Florence the major contributor to PM1 mass is nitrate while in Genoa sulphate has concentrations slightly higher than nitrate ones. During the summer at all sites the sulphate level is the highest in the water-soluble fraction, accounting for about 3-4 $\mu\text{g}/\text{m}^3$. At the rural site BF average concentrations of 3.1-2.8 $\mu\text{g}/\text{m}^3$ for sulphate, 9.4-0.2 $\mu\text{g}/\text{m}^3$ for nitrate and 9.9-1.2 $\mu\text{g}/\text{m}^3$ for ammonium during February and July, respectively, were measured. The strong reduction in nitrate concentration can be explained by summertime temperatures (on average 25°C) which favour the gas phase in respect to the particulate one; moreover, possible negative sampling artefacts cannot be completely excluded.

The ionic balance is substantially in equilibrium at all sites in both seasons (only in Milan acidic species slightly prevail during wintertime). This means that ammonium neutralizes almost all nitrate and sulphate and, as a consequence, they are mainly in the form of $(\text{NH}_4)_2\text{SO}_4$ and NH_4NO_3 .

As reported in Table 11-2, the organic carbon is the most abundant species at the three sites accounting, on average, for 4.8-14.8 $\mu\text{g}/\text{m}^3$ of the PM1 mass in Milan, 3.4-5.0 $\mu\text{g}/\text{m}^3$ in Genoa, and 2.7-12.0 $\mu\text{g}/\text{m}^3$ in Florence during summertime and wintertime, respectively. At the rural location OC is also an important contributor as it explains a considerable part of the sub-micron sized aerosol mass: 3.8 $\mu\text{g}/\text{m}^3$ in July and 14.8 $\mu\text{g}/\text{m}^3$ in February. The elemental carbon contribution was 1.1-1.8 $\mu\text{g}/\text{m}^3$ in Milan, 0.9-0.9 $\mu\text{g}/\text{m}^3$ in Genoa, 0.6-0.9 $\mu\text{g}/\text{m}^3$ in Florence and 0.6-2.5 $\mu\text{g}/\text{m}^3$ at BF during summer-winter, respectively.

Literature data (Turpin and Huntzinger, 1995) report that OC/EC ratios higher than 2-2.5 are indicators for secondary organic aerosol formation. Indeed, at the monitored sites high OC/EC ratios were observed in Milan (4.5-8.2), Genoa (4.0-5.6) and Florence (4.3-13.4) with higher values typically measured in winter. The abundance of organic carbon during the winter is likely due to the lower temperatures which favour the aerosol particle phase of organic compounds and to the low mixing layer heights which allow the accumulation of gaseous precursors and the acceleration of secondary organic aerosol formation (Strader et al., 1999). To assess the contribution of secondary organic aerosol (SOA), the primary OC/EC ratio approach (Turpin and Huntzinger, 1995) was applied using the experimental ratio $(\text{OC}/\text{EC})_{\text{primary}} = 1.34$ reported for PM2.5 measured in a traffic tunnel in Milan by Giugliano et al. (2005). The SOA contribution was higher during wintertime contributing for $81 \pm 12\%$, $73 \pm 14\%$ and $83 \pm 12\%$ to organic carbon measured in sub-micron sized aerosol in Milan, Genoa and Florence, respectively. Summertime SOA percentages to OC were $69 \pm 16\%$, $64 \pm 13\%$ and $68 \pm 13\%$ at the same locations.

The chemical mass closure obtained at the three urban locations is shown in Figure 11-2. Mineral and heavy metals oxides have been calculated from XRF data using the sum of oxides algorithm (Marcazzan et al., 2001). These two components explain a little part of the sub-micron sized aerosol mass: a percentage of 0.3-0.6% is due to heavy metals oxides and 0.7-2.3% to mineral oxides at all locations. Ammonium sulphate and nitrate were obtained by IC analyses as previously described. At all sites, $(\text{NH}_4)_2\text{SO}_4$ accounted for high percentages: 10-12% in winter and 34-45% in summer; NH_4NO_3 percentages were in the range 0.5-5 % in summer and 9-29% in winter. The organic carbon concentrations have been converted in organic matter (OM) concentrations using an average mean molecular-to-carbon ratio of 1.6 as proposed by Turpin and Lim (2001) for urban aerosol. Nevertheless, this ratio varies significantly with location, season, time of the day and aerosol ageing as the mix of organic compounds in the aerosol changes and generally it is higher where a large fraction of the aerosol is organic (as in our monitoring locations). Organic matter was the major contributor during both season explaining a large part of the sub-micron sized aerosol mass (on average about 40%); elemental carbon percentages were comparable at all site during both seasons (about 4%). The unaccounted mass fraction (14-22%) given by the chemical mass balance resulted from aerosol-bound water, minor components and measurement errors evaluated in 10% following Rees et al., 2004. It is worth noting that the mass balance is sensitive to the choice of average organic molecular weight per carbon weight and, if an average ratio of 1.8 is taken instead of 1.6, the unaccounted mass fraction is about 7-17%; however, both estimates are in the range that can be mainly attributed to aerosol water (Andrews et al., 2000).

Applying the method of the 'Radon index' (see paragraph 11.2.3), a normalization of PM mass and compositional data can be done for the Milan dataset with the aim of accounting for the seasonal effect due to differences in atmospheric dispersion conditions. This approach allows the evaluation of differences in the contribution from emission sources for aerosol of primary origin and reveals variations in the strength of production mechanisms for PM of secondary origin during the two seasons. Results show that the sub-micron sized normalised aerosol mass concentration is 1.5 times higher in winter than in summer evidencing the presence of additional sources during the cold season (e.g. domestic heating) and the influence of low temperatures typical of the cold season on particle-phase compounds. The winter/summer ratios of OM and ammonium nitrate normalised components are 2.4 and 4, respectively, because wintertime low temperatures favour the aerosol particle phase instead of the gaseous one in the formation of secondary aerosol and the stability of particulate NH_4NO_3 in the atmosphere (Strader et al., 1999). During the summer period the ammonium sulphate component normalised to the Radon index evidences a strong increase (by a factor

2) showing the importance of atmospheric photochemical production. These results are in good agreement with those found by Vecchi et al. (2004) for PM1 in Milan during the year 2002.

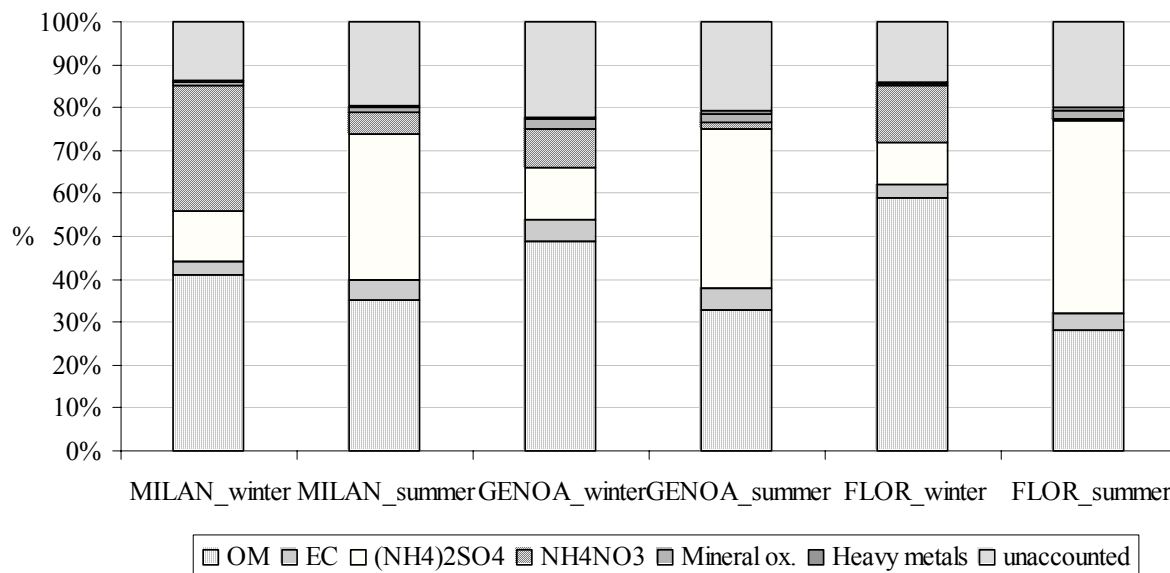


Figure 11-2: Chemical mass closure for summer and winter at Milan, Florence and Genoa.

11.4. Conclusions

In this work mass concentrations and composition are given for sub-micron sized particulate matter at three urban sites in Italy. Experimental results show that PM1 has some common features at the three investigated urban sites; nevertheless, significant differences are evident in mass concentrations, elemental composition and seasonal patterns as each site is also characterized by local emissions and peculiarities in topographical and meteorological conditions.

An interesting result obtained in this study is the sub-micron sized aerosol mass closure obtained at different urban sites in winter and summer; it shows that compounds mainly of secondary origin like ammonium sulphates and organics account for the largest part of its mass. The assessment of SOA at the three urban sites allowed a preliminary estimation of the relevance of secondary aerosol (secondary organic matter, ammonium sulphate and ammonium nitrate) in the sub-micron fraction, which contributed for 64-75% in Milan, 61-58% in Genoa and 66-69% in Florence during summer-winter periods, respectively.

The data presented in this study enhance the concern for possible health effects because of the high PM1 concentration measured. Moreover, PM1 is about 40-60% of PM10 at the investigated urban sites during both seasons, this result highlights

difficulties in attaining the EU-PM₁₀ and the proposed EU-PM_{2.5} limit. Future PM control strategies should take into account these indications and, in particular, the fact that aerosol of secondary origin dominates the sub-micron sized aerosol mass contributing for 60-70%. The high PM₁ levels measured at the rural location are also of interest, because they evidence the presence of a background concentration in the Po valley and the role of PM diffusion in the basin from emission areas.

Acknowledgment

I would like to acknowledge all the colleagues who collaborated to this work:

F. Mazzei, P. Prati

Physics Department, University of Genoa and Istituto Nazionale di Fisica Nucleare-Genova, Genoa, Italy.

A. D'Alessandro, G. Valli, R. Vecchi

General Applied Physics Institute, University of Milan and Istituto Nazionale di Fisica Nucleare-Milano, Milan, Italy.

M. Chiari, F. Lucarelli, S. Nava

Physics Department, University of Florence and Istituto Nazionale di Fisica Nucleare-Firenze, Florence, Italy.

P. Fermo

Inorganic, Metallorganic and Analytical Chemistry Department, University of Milan, Milan, Italy.

References

- Annegarn et al. (1992) *Atmospheric Environment* 26A, 333-343.
Andrews et al. (2000) *J. Air & Waste Management Association* 50, 648-664.
Arden Pope and Dockery (2006) *J. Air and Waste Management Association* 56, 709-742.
Ariola, et al. (2006) *Chemosphere* 62/2, 226-232
D'Alessandro (2003) *J. Aerosol Science* 34, 243-259.
EPA, 2004. *Air Quality criteria for Particulate Matter*, EPA/600/P-99/002aF
Fermo et al. (2006) *Chemical Engineering Transactions* 10, E. Ranzi ed., 203-208.
Fermo et al. (2006b) *Chemistry and Physics* 6, 255-266.
Giugliano et al. (2005) *Atmospheric Environment* 39, 2421-2431.
Han et al. (2006) *Atmospheric Chemistry and Physics* 6, 211-223.
Ion et al (2005) *Atmospheric Chemistry and Physics* 5, 1805-1814.

- Kim and Hopke et al. (2007) *Atmospheric Environment* 41, 567-575.
- Lucarelli et al. (2004) *J. Air & Waste Management Association* 54, 1372-1382.
- Marcazzan et al. (2001) *Atmospheric Environment* 35, 4639-4650.
- Marcazzan et al. (2004) *X-Ray Spectrometry* 33, 267-272.
- Marengo et al. (2006) *J. Geophysical Research*, 111, D24202.
- Pakkanen et al. (2003) *Atmospheric Environment* 37, 1673-1690.
- Polissar et al. (1998) *J. Geophysical Research* 103, 19045-19057.
- Prati et al. (2000) *Atmospheric Environment* 34, 3149-3157.
- Putaud et al. (2002) *J. Geophysical Research* 107, D22, 8198-8209.
- Rees et al. (2004) *Atmospheric Environment* 38, 3305-3318.
- Salvador et al. (2007) *Atmospheric Environment* 41, 1-17.
- Sesana et al. (2003) *J. Environmental Radioactivity* 65, 147-160.
- Simoneit et al. (1999) *Atmospheric Environment* 33, 173-182.
- Spindler et al. (2004) *Atmospheric Environment* 38, 5333-5347.
- Strader et al (1999) *Atmospheric Environment* 33, 4849-4863.
- Turpin and Huntzicker (1995) *Atmospheric Environment* 29, 23, 3527-3544.
- Turpin, and Lim (2001) *Aerosol Science and Technology* 35 (1), 602-610.
- Van Espen et al (1977) *Nuclear Instruments and Methods* 142, 243 - 250.
- Vecchi et al. (2004) *Atmospheric Environment* 38, 4437-4446.
- Vecchi et al. (2007) *Atmospheric Environment* 41, 2136-2144.
- Zhang and Friedlander (2000) *Environmental Science and Technology* 34, 4687-4694

12. PM₁₀ physical and chemical characterisation using high-time resolved samplings in an air pollution “hot-spot” area in Europe

12.1. Introduction

In urban areas, besides the determination of PM levels for regulatory and health protection purposes, a topic of great concern is the identification and the quantification of source contributions to PM mass and chemical composition.

Many studies (for example in Europe: Borbély-Kiss et al., 1999; Artiñano et al., 2001; Marcazzan et al., 2001; Hoek et al., 2002; Putaud et al., 2004; Vecchi et al., 2004, among others) have been devoted to PM characterisation used 24-h averaged data. However, it should be noted that within a 24-h time interval, PM concentration and composition at a given location could vary significantly. Generally, the average contribution of different sources active in an urban area is also available but these mean estimates, although valuable, cannot single out temporal patterns and profiles of the sources as well as the contributions of episodic sources. The interest for a detailed, size-resolved and high-time resolution PM characterisation is due to the fact that source emissions exist which can heavily impact on air quality with very high emission loading of toxic (or potentially toxic) elements during a few hours in a day, and the knowledge about the timing and intensity of specific episodes may be important for assessing human exposure. Their identification is also useful for a complete emission inventory of the monitored area when emission control strategies must be adopted. Moreover, high time-resolved and size-segregated samplings give insights to physical-chemical processes involving aerosols (production, transformation, transport, removal) and allow a direct comparison with gaseous pollutants and meteorological parameters, which are generally monitored on an hourly basis.

In this work a detailed physical-chemical characterisation of PM₁₀ with high temporal resolution has been performed. The aim was to gather a deeper knowledge on processes and sources influencing PM₁₀ levels and patterns in Milan, the largest town in the Po valley that is a “hot-spot” area in Europe, as concerns particulate matter pollution.

12.2. Experimental

12.2.1. Site and sampling

Milan (45° 28'N; 9° 13'E) is the second largest town in Italy, after Rome, with about 1500000 inhabitants and considering the whole area of the Milan province the population rises up to about 4 millions inhabitants. Milan is situated in the Po valley (Northern Italy), it is heavily industrialized, trafficked and populated and is considered one of the largest pollution “hot spots” in Europe.

The samplings were carried out on the roof of the Institute of Physics, at a height of about 10m a.g.l., at the University campus in Milan. The sampling site is considered an urban background site: it is quite representative of the average air pollution in the city as, generally, it is not directly influenced by local source emissions. However, many construction works were carried out both in the garden of the institute and in the whole university campus area during the sampling periods.

PM10 was sampled with 4-hours resolution in 2006 during two field studies, starting at 12 a.m., local time, from June 27th to July 11th during summertime and from November 21st to December 6th (except between 04 a.m. and 04 p.m. on 30th November, due to technical problems) during wintertime; every day six samples have been collected. Samplings were carried out in parallel on PTFE filters (PALL R2PJ047, diameter: 47 mm, pore size: 2 μ m) and quartz fibre filters (PALL 2500QAO_UP, diameter: 47 mm, pre-fired at 700°C for 1 hour) using CEN-equivalent samplers operating at a flow rate of 2.3 m³ h⁻¹. A total of 180 quartz fibre filter and 174 PTFE filters were collected.

12.2.2. Laboratory analyses

Before and after the samplings, all the filters were exposed for 48 hours on open but dust-protected sieve-trays in an air-conditioned weighing room (T=20±1°C and R.H.=50±5%) and then weighed using an analytical microbalance (precision 1 μ g), which is installed and operates in the weighing room (the weighing protocol is described in Vecchi et al., 2004). Calibration procedures check the microbalance performance.

Analysis by Energy-Dispersive X-Ray Fluorescence (ED-XRF) technique (details on the technique set up are in Marcazzan et al., 2004), carried out on PTFE filters, allowed the determination of concentration values for Mg, Al, Si, S, Cl, K, Ca, Ti, Cr, Mn, Fe, Ni, Cu, Zn, Br, Sr, Ba, Pb. Other elements, like V, As, Se, Zr, and Mo, were in principle detectable, but they resulted often below the minimum detection limit (MDL), which was in the range 2–20 ng/m³ for most elements. When PTFE

filters were not available because of problems occurred during the sampling, ED-XRF analysis was performed on quartz fibre filters. For this kind of filters the analysis of elements with $Z < 15$ was impossible and only concentration for elements heavier than P are available. Experimental overall uncertainties were in the range 10-15 %.

One half of the quartz fibre filters was analysed for water-soluble major components (i.e. SO_4^{2-} , NO_3^- , and NH_4^+) by ion chromatography (IC). A particular care should be used in IC analyses of particulate matter collected on quartz fibre substrates due to high blank levels (minimum detection limits: 167, 359 e 46 ng/m^3 for SO_4^{2-} , NO_3^- , and NH_4^+ , respectively); information about extraction procedures and blanks correction can be found in chapter 2. The overall uncertainty for ionic concentrations was estimated to be 10 %.

One punch (area: 1.5cm^2) cut from the quartz fibre filter was analysed by TOT (Thermal-Optical Transmittance) method (Birch and Cary, 1996) to quantify elemental and organic carbon fractions (chapter 4). Organic fraction was divided in 5 fractions: OC1, OC2, OC3, OC4 and PyC (pyrolytic carbon). OC1-4 fractions were evaluated as the organic carbon evolved at 4 different (increasing) temperatures, while PyC was determined by optical correction. The technique detection limit is $0.15\mu\text{g/cm}^2$ and the precision is 5%.

12.2.3. Additional measurements

To evaluate atmospheric dispersion conditions, that influence pollutants concentration at different time scales, ^{222}Rn short-lived decay products measurements were performed using the experimental methodology reported in Marcazzan et al., 2003a. The evaluation of mixing layer heights (MLH) with hourly resolution was also carried out by means of a box model suitably set up by the group of the Institute of Physics; it uses ^{222}Rn concentration measurements as input data (Pacifico F., 2005; Casadei et al., 2006).

Meteorological parameters (wind speed and direction, temperature, relative humidity, pressure, solar radiation and precipitation) were also measured at the Institute of Physics monitoring station.

Gaseous pollutants (NO_2 , NO , CO , O_3) hourly data recorded at monitoring stations located near the University campus as well as information on hourly traffic volumes in the city centre were available by the Regional Environmental Protection Agency of Lombardy (ARPA Lombardia).

12.3. Results and discussion

12.3.1. Meteorological conditions and mass concentration

In Table 12-1, some statistical values about hourly-averaged meteorological parameters in both seasons are shown.

		Temp. (°C)	Wind speed (m/s)	Pressure (hPa)	U.r. (%)	Precipitation (mm/h)	²²² Rn (Bq/m ³)	Mixing layer (m)
Summertime	Average	26,54	1,36	1001,28	49,25		10,49	224,29
	Standard deviation	3,78	0,62	2,16	12,54		4,98	249,44
	Minimum	17,90	0,31	997,20	25,65		3,70	11,24
	Maximum	33,67	5,17	1006,47	84,42	25,00	26,41	1201,73
	Median	26,70	1,43	1001,02	48,47		9,83	127,89
	10° percentile	21,71	0,51	998,58	34,33		4,75	36,17
	90° percentile	31,67	2,07	1004,42	66,07		17,74	571,06
Wintertime	Average	10,53	0,89	1004,18	78,35		13,56	117,08
	Standard deviation	1,99	0,41	9,12	11,58		4,41	74,79
	Minimum	4,42	0,20	980,26	20,58		2,86	8,48
	Maximum	17,86	2,29	1018,34	93,38	1,20	27,63	378,73
	Median	10,46	0,80	1005,07	80,41		12,78	105,12
	10° percentile	8,38	0,45	991,11	64,45		8,99	31,25
	90° percentile	12,88	1,49	1014,91	89,16		20,19	226,78

Table 12-1: statistical values about hourly-averaged meteorological parameters in summer and in winter season

During summer campaign, there were mainly good weather conditions, with high temperature (about 30°C during day-time and above 20°C during night-time), pressure almost constant (growing during the period from about 997hPa to 1006hPa) and maximum solar radiation at about 800W/m². Some events must be highlighted: rainfalls were registered during 29th June morning, between 04 a.m. and 07 a.m. and between 09 a.m. and 12 p.m. (this second episode was a thunderstorm, and wind speed reached 2.9 m/s, averaged on 10 minutes), as well as during 6th July evening, when during a strong thunderstorm 34 mm of rainfall in 4 hours (25 mm between 7 p.m. and 8 p.m.) were registered and wind speed, averaged on 10 minutes, reached 7.5 m/s. Moreover, opposite to typical summer wind condition in Milan - generally characterized by a breeze regime with winds coming from northeast-northwest during the night (wind speed generally about 0.5 m/s) and from southeast-southwest during the day (wind speed rarely above 2.0 m/s) - during the period 2nd-6th July a wind about 1.8 m s⁻¹ coming from east both during daytime and night-time occurred. ²²²Rn concentrations and mixing layer

heights indicated stability conditions during 1st-2nd July and during 7th (afternoon)-10th July (morning).

During the winter campaign, the weather was generally cloudy or rainy, except on five days (22nd, 23rd, 26th, 30th November and 1st December). The temperature during cloudy/rainy days was about 10-12°C, with slight differences between daytime and nighttime. During sunny days, temperatures up to 18°C during daytime and lower than 8°C during nighttime occurred and the solar radiation reached 400 W/m². Rainfalls were registered on 21st, 24th, 25th, 28th November and 3rd, 5th, 6th December, but their intensity was at most 1mm/h.

In Figure 12-1, PM10 mass and ²²²Rn concentration during both field campaigns are shown. PM10 concentrations were generally higher during wintertime (median value: 49.4µg m⁻³ during summertime and 102.4µg/m³ during wintertime; maxima concentrations with 4-hour resolution: 109.3µg/m³ during summertime and 203.7µg/m³ during wintertime), and this is due both to additional sources (i.e. domestic heating) and to stability conditions, as evidenced by the analysis of ²²²Rn temporal patterns.

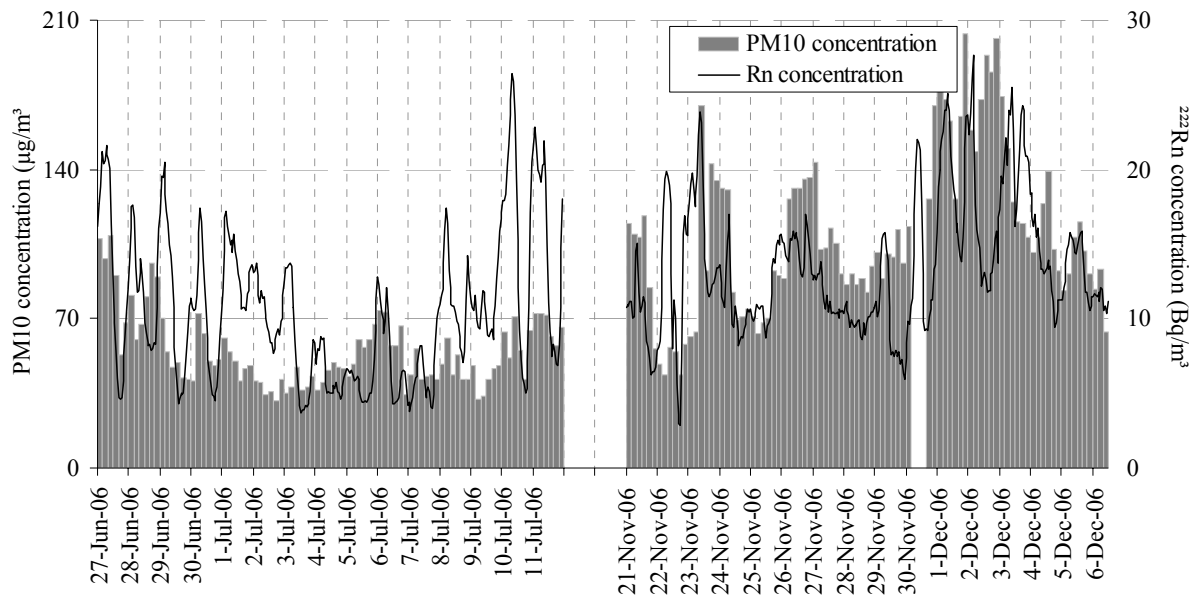


Figure 12-1: PM10 mass concentration (µg/m³) and ²²²Rn concentration (Bq/m³) during summer and winter campaign

Indeed, if the average PM10 concentrations in the two seasons are compared, it can be noticed that winter values are on average 2 times summer ones. Taking ²²²Rn daily minimum concentration as indication of the dispersion conditions of the atmosphere and averaging these values in the two seasons (Vecchi et al., 2004), it

can be observed that winter values are 1.6 times the summer ones. Therefore, it can be concluded that about 80% of the registered increase in concentrations during wintertime was due to atmospheric stability conditions and that additional sources can contribute for about 20% to the winter PM10 mass growth.

12.3.2. Mass balance

The complete chemical characterisation (elements, ions and carbon fractions) of the PM10 sampled allowed the evaluation of the mass balance.

From elemental concentration, an estimation of crustal matter was made considering Al, Si, Ca, Ti, K, and Fe as oxides (Eldred et al. 1987; Marcazzan et al., 2001 and 2004) with an adaptation due to relatively high enrichment factors (often higher than 4 in both seasons) presented by Ca during our campaigns. Crustal matter was estimated as $1.15 (1.89 \text{ Al} + 2.14 \text{ Si} + 1.2 \text{ K}^* + 1.4 \text{ Ca}^* + 1.67 \text{ Ti} + 1.36 \text{ Fe}^*)$, where K^* , Ca^* and Fe^* are natural fractions of K, Ca and Fe, which were calculated as their concentration divided by their enrichment factors (evaluated using Si as reference element and the crustal composition given by Mason, 1966). The factor 1.15 accounts for contribution of Na e Mg oxides, which were not detected. In addition, metal oxides were evaluated from Cu, Zn, Br, Pb and the anthropogenic component of Fe (that is $1 - \text{Fe}^*$) (Marcazzan et al., 2001).

Organic matter was evaluated from OC as $\text{OM} = 1.8 \text{ OC}$, considering that in Milan area air masses are usually aged due to stability conditions (Turpin and Lim, 2001).

From Figure 12-2 it can be seen that the principal contribution to PM10 mass came from organic matter in both seasons and its value did not change significantly between summertime and wintertime (34% and 33%, respectively).

An important contribution to total PM10 mass in both seasons came also from other secondary compounds such as sulphate, nitrate and ammonium, which, summed up, accounted for 16% and 24% during summer and winter, respectively.

During summertime, another important contribution was due to crustal matter (14%), while during wintertime this contribution was 6%. The higher contribution during summertime can be justified considering the drier condition of the ground (that fosters dust resuspension) and higher atmospheric turbulence, which slows the deposition process of suspended particles; moreover, the contribution of local construction works must be considered during some episodes. Particularly strong construction works contribution was identified during 3rd July morning and during 23rd and 27th November, using both information on Al, Si and Ca concentration and sudden and short-lasting increases in coarse-fraction particle number concentration (not shown).

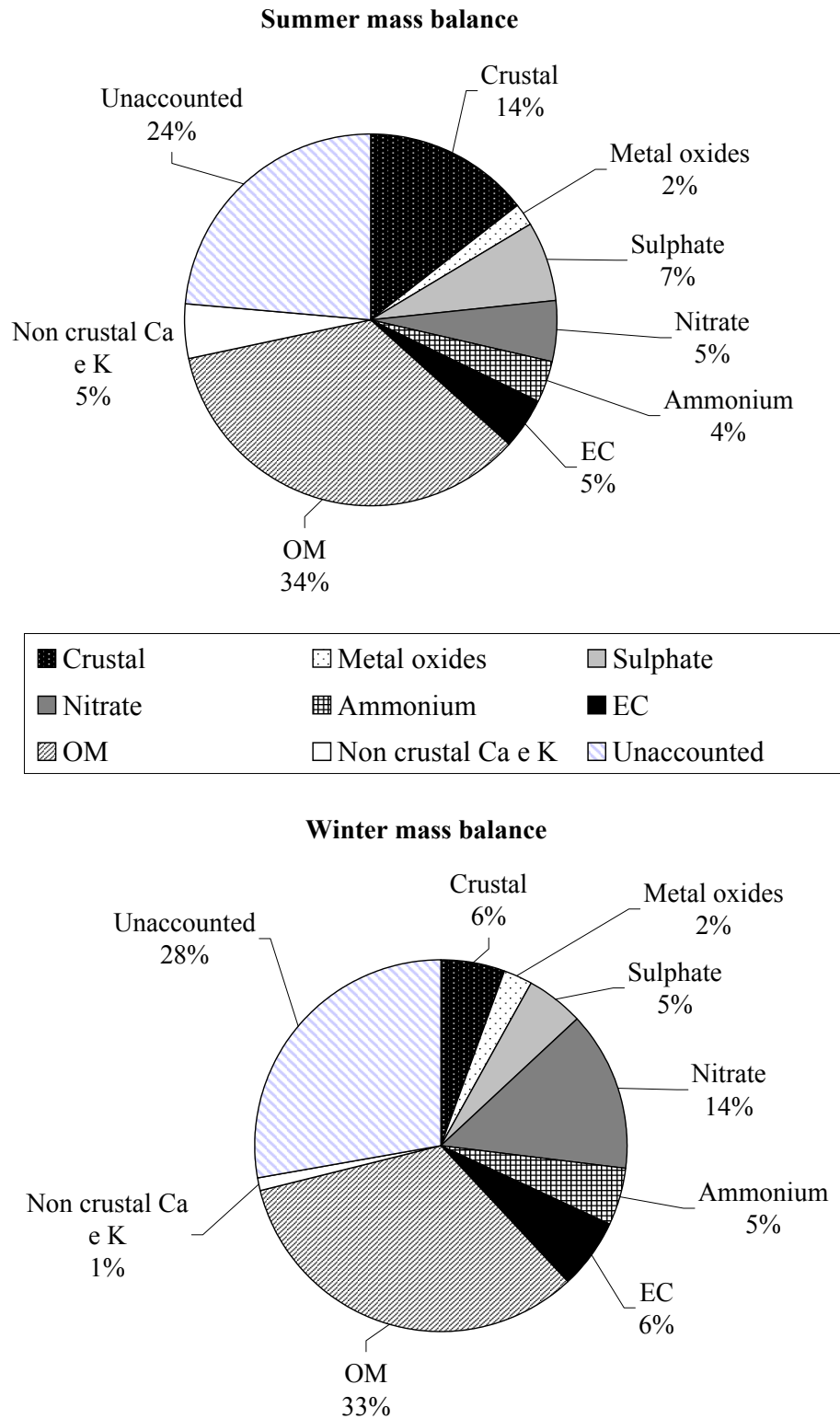


Figure 12-2: chemical mass balance

High temporal-resolution allowed the evaluation of the mass balance during the different time-intervals. From Table 12-2 it can be seen that crustal matter presented higher contributions during daytime in both seasons, when resuspension due to traffic and construction works is higher. Summer sulphates began to rise from 12 p.m., reached a maximum between 04-08 p.m. and then lowered during nighttime. Indeed, the mixing layer reaches its maximum evolution during afternoon, and can include in the ML sulphates produced by photochemical processes at higher altitudes (Raes et al., 2000). During the evening, mixing layer height diminishes and the entrainment of sulphates from upper atmospheric layers is inhibited. Nevertheless, as secondary sulphates usually lay in smaller size ranges (Querol et al, 1998; Alastuey et al., 2004; and therein literature), their residence time is quite long and during the night, when larger particles deposit rapidly, their relative contribution to the mass did not change significantly. The minimum daily concentration was reached on average between 08 a.m. and 12 p.m. when other sources (resuspended dust, traffic, construction work) re-activate, while ML is not yet high enough to reach sulphates eventually present at higher altitudes.

		Metal		Sulphate	Nitrate	Ammonium	EC	OM	OM	Non crustal	
		Crustal	oxides					primary	seconday	Ca e K	Unaccounted
Summer	12 - 04 a.m.	12%	3%	7%	7%	4%	5%	12%	24%	5%	21%
	04 - 08 a.m.	12%	3%	6%	8%	4%	5%	12%	22%	5%	23%
	08 a.m. - 12 p.m.	17%	2%	5%	4%	3%	5%	13%	22%	5%	24%
	12 - 04 p.m.	15%	1%	7%	4%	4%	3%	8%	28%	5%	26%
	04 - 08 p.m.	16%	1%	8%	4%	4%	4%	8%	27%	5%	24%
	08 p.m. - 12 a.m.	13%	3%	7%	4%	4%	5%	11%	25%	5%	24%
Winter	12 - 04 a.m.	4%	2%	5%	14%	5%	6%	13%	21%	1%	28%
	04 - 08 a.m.	4%	2%	5%	15%	6%	6%	13%	22%	1%	26%
	08 a.m. - 12 p.m.	7%	2%	5%	14%	5%	7%	16%	16%	1%	28%
	12 - 04 p.m.	7%	2%	5%	15%	5%	6%	12%	17%	1%	30%
	04 - 08 p.m.	7%	3%	5%	13%	5%	6%	16%	17%	1%	27%
	08 p.m. - 12 a.m.	5%	3%	6%	12%	5%	6%	14%	21%	1%	28%

Table 12-2: chemical mass balance during the different time-interval

It should be also noticed that, during summertime, nitrates contribution was higher during nighttime, when lower temperatures both limited losses due to volatilization and favoured condensation processes.

Errors on mass balance were calculated following Andrews et al. (2000): 50% was given to crustal matter and metal oxides, as their evaluation comes from assumptions on principal oxides, while analytical error (10%) was given to sulphate, nitrate, ammonium EC and OM. In this way, the total error on mass balance was estimated to be about 10%. This was not enough to justify the PM10 unexplained mass, which was about 25% in both seasons. Nevertheless, it should be considered that there are components, i.e. carbonates and water, which were not measured with our analytical techniques. Carbonates (CC) are in general a minor

fraction of total carbon (Chow et al., 2002). However, even if only 5% of carbon considered as OC were CC, considering $CC=5.0OC$ due to the molecular carbonate weight (instead of the 1.8 factor used for the conversion OC-OM), CC would contribute at 5% to total PM10 mass. Moreover, water contents at 50% R.H. can give a contribution of about 10% (Mc Murry, 2000). In particular, K (Andrews et al, 2000), sulphates and nitrates (Hueglin et al., 2005) can be responsible for water contents in particulate matter. The larger discrepancies in mass balance observed during wintertime may be explained considering that higher nitrate concentration and R.H. registered in this season may have increased water content in PM10. Therefore, if we consider about 15%-20% of contribution coming from H2O and CC, our mass balance approaches to 100% within the evaluated errors. Mass closure between 70% and 90% are commonly reported in literature (Turpin et al., 1997; Chan et al., 1997; Andrews et al, 2000; Putaud et al., 2004; Rees et al., 2004; Hueglin et al., 2005; Viana et al., 2007).

PMF applied on the complete data set (carried out by D.Cricchio, General applied Physics Institute, University of Milan; the detailed discussion on the PMF results will be not given here) resolved six sources: secondary nitrate, secondary sulphate and OM, resuspended dust, construction works, traffic primary emissions and industry). Seasonal apportionment and PMF-evaluated errors for each source are shown in Table 12-3.

	Secondary nitrate	Secondary sulphate	Resuspended dust	Construction works	Traffic	Industry
Summertime	9±3%	20±4%	24±4%	15±3%	12±2%	11±2%
Wintertime	38±6%	21±4%	7±2%	6±1%	18±2%	8±2%

Table 12-3: Seasonal apportionment and PMF-evaluated errors

From PMF analysis it was noticed that some sources presented a strong seasonal variation (i.e. nitrate, resuspended dust, construction work and traffic), while no significant seasonal trend was noticed in industry and secondary sulphate and OM sources. From the analyses of time-slot segregated winter data for traffic source, it was noticed that rush-hours could be detected in 8.00a.m.-12.00p.m. and 4.00p.m.-8.00p.m. periods.

12.3.3. Episodes

The high-time resolution of the samplings allowed a detailed study of production/formation, transport, removal and settling of the particles in atmosphere and

allowed the detection of different sources acting contemporaneously. As examples, in the following paragraphs some episodes are described and analysed in detail.

12.3.3.1. Local production

A remarkable increase in Cl, Cr, Mn, Fe, Ni, Cu, Zn, Pb, EC concentrations and in primary gaseous pollutants CO and NO, was registered during the nights 30th November - 1st December and 1st-2nd December (see Figure 12-3 as an example). The average values for all these components during the two periods were 3 times higher than the values registered during 28th-29th November (the two days before the episode) and 3rd-4th December (the days after this episode; the 2nd December was excluded because of another episode analysed in the following paragraph). It is noteworthy that all the listed components are of primary origin and secondary components did not show any significant increase during the episode. ^{222}Rn analysis showed a strong stability condition (see Figure 12-1) with both daily minima and maxima concentration constantly growing from 29th November to 2nd December morning. The strong daytime (low concentration)-nighttime (high concentration) modulation of the analysed components was mainly ascribed to mixing layer evolution.

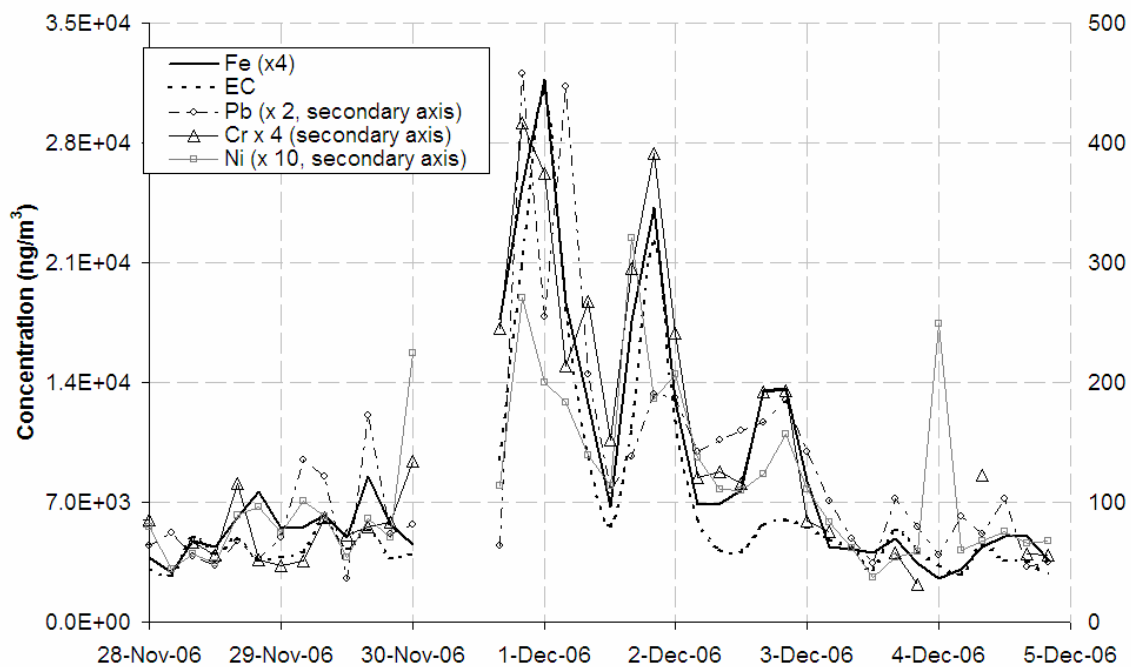


Figure 12-3: local production episodes

EC is the tracer for traffic emission (Querol et al., 2004), as well as Fe, Cu and Cr (Marcazzan et al., 2003b; Vecchi et al., 2007b). Mn and Zn were associated to industrial emissions in this area (Marcazzan et al., 2003b). CO and NO are typically emitted during combustion processes and Cl, Ni, Pb may be emitted by incinerators or by oils combustion (Artaxo et al., 1999; Song et al., 2001; Thomaidis et al., 2003; Qin and Oduyemi, 2003; Graney et al., 2004). The origin of all these components is likely due to local emissions (in the urban or suburban area) and the increase and modulation in concentration is well described by local emissions from different sources and atmospheric stability. In fact, from Figure 12-3, it's noteworthy that maxima concentrations in different components were registered during different time-slot, indicating that the components came from different sources.

12.3.3.2. Long range transports.

Looking at S concentration temporal pattern with 4 hours resolution, two peculiar behaviours were noticed on 5th-6th July and 2nd-3rd December. During both episodes, there was a good correlation ($R^2=0.85$ between 12.00 a.m. on 5th July and 12.00 a.m. on 7th July; $R^2=0.78$ between 12.00 p.m. on 2nd December and 4 p.m. on 3rd December) between S and pyrolytic carbon (PyC) concentration temporal trend.

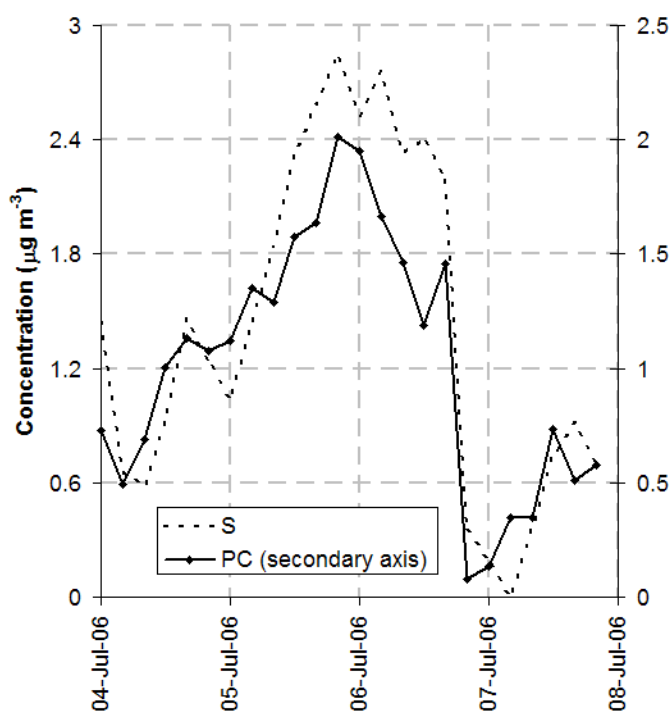


Figure 12-4: sulphur and pyrolytic carbon concentration during long range transport episode

Literature studies report the possibility of PyC formation as result of acid-catalysed reactions between acidic sulphate and volatile organic compounds to give secondary organic formation (Jang et al., 2003); moreover, volatile organic compounds can condense on sulphate particle surface (Kim and Hopke, 2006; Zhao e Hopke 2006). Sources of OP-rich secondary sulphates were also detected by PMF analysis in different sites (Kim and Hopke 2004 and 2006; Begum et al., 2005).

During the summer episode (5th-6th July), both S and PyC (see Figure 12-4) concentrations more or less doubled (1.9) if compared to the average levels registered during the rest of the period. In addition, their relative contribution to the total mass increased, indicating that the growth was not due to stability condition, but to additional sources. During 5th-6th July, the contribution of sulphates and PyC to the mass summed up to 13%, which is higher than the average value of 8% registered during the rest of the summer campaign. During the episode it is also noteworthy the absence of daytime-nighttime modulation; on the contrary, no anomalous trends were registered for other PM10 components or gaseous pollutants. As Ox ($\text{NO}_2 + \text{O}_3$, taken as photochemical indicator) did not show an anomalous behaviour if compared to previous days, the hypothesis of photochemical production was rejected and the possibility of a long-range transport was considered.

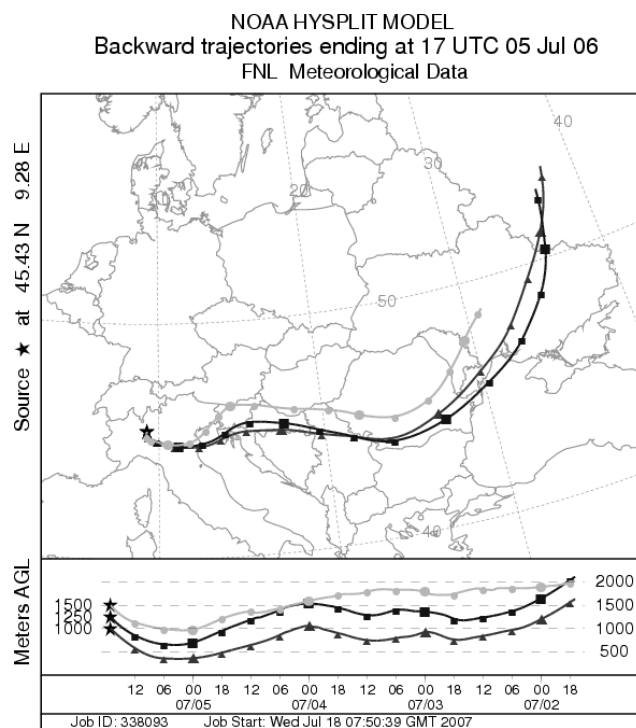


Figure 12-5: Back trajectories during the day classified as influenced by long range transport (NOAA-Hysplit model)

Looking at back trajectories (Figure 12-5) calculated using NOAA-Hysplit model (Draxler and Rolph, 2003; Rolph, 2003) it can be seen that the air mass on Milan on 5th July had travelled through east-Europe countries during the previous days. As fuels containing high quantities of S are still largely used in those countries, sulphates and/or their precursors may have been produced there and then transported to Milan area. Therefore, a long-range transport was the most reasonable explanation to this phenomenon.

The importance of high-time-resolved samplings is remarkable in the detection of these episodes, which would not have been noticed with traditional 24-hours samplings, as the maxima in concentration values were similar to the ones registered during other days in the same period. On the contrary, 4-hours resolution samplings allowed the detection of the long-range transport and 1-hour resolved samplings revealed the contribution of construction works.

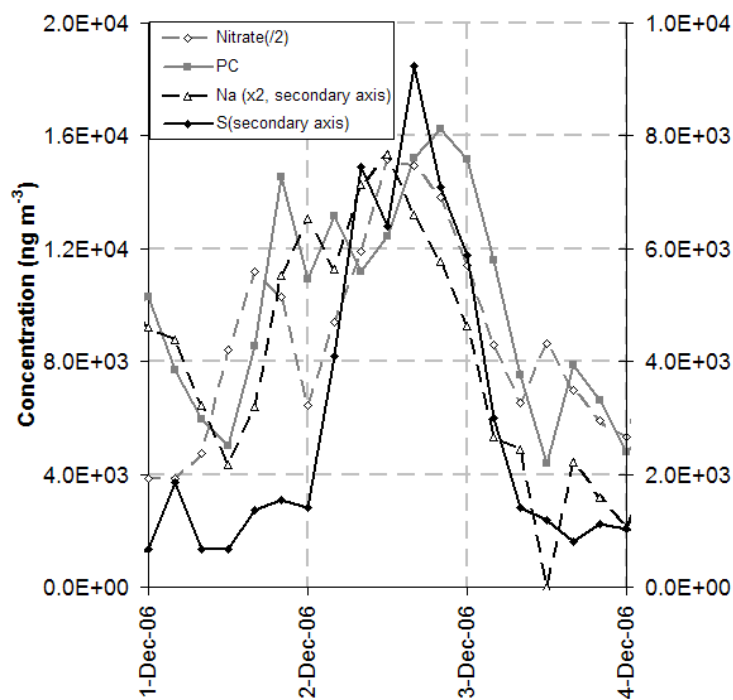


Figure 12-6: nitrate, sodium, pirolitic carbon and sulphur concentration during the transport phenomenon

During the winter episode (2nd-3rd December) a significant sudden growth in S concentration was noticed (see Figure 12-6) both in absolute values (that reached almost $10\mu\text{g}/\text{m}^3$ as S average concentration on 4 hours) and in relative values: sulphate concentration increased from 4% (on average during the rest of the period) to 12% for sulphate during the episode. Increases were also detected in absolute

concentrations of ammonium, nitrate, PyC and Na (2% for nitrate and ammonium, 3% for PyC and 0.6% for Na). Back trajectories showed that the air mass on Milan on 2nd December had travelled in the previous 5 days through the Po Valley (48 hours), where all the pollutants detected could be included and still before over the Adriatic sea, where Na particles could have been added to the air mass.

12.4. Conclusions

The complete chemical characterization allowed the evaluation of the mass balance for the two seasons. The main component during both seasons was OM (about 35%); during the summer, the other main components were crustal matter (14%) and sulphates (7%), followed by nitrate and EC (5%) and ammonium (4%). During wintertime, nitrates gave an important contribution to PM10 mass (14%), followed by EC and crustal (6%), sulphate and ammonium (5%).

PMF analysis resolved six main sources: secondary nitrates, secondary sulphates and OM, resuspended dust, construction works, traffic primary emissions and industry.

High temporal-resolution allowed the mass balance evaluation during the different time-intervals. Fast variations in PM10 composition during contiguous time-slots and general trends during the day were identified. In both seasons, the crustal component gives higher contributions (higher than 15% during summertime and 7% during wintertime) during the daytime, when resuspension due to traffic and construction works is higher. During summertime, sulphate contribution is higher during the afternoons, due to secondary photochemical formation. During summertime, nitrate concentration is higher during nighttime, when the temperatures are lower, favouring condensation processes.

Moreover, high time-resolved samplings allowed the detection of episodes such as long range transports or local production; they also allowed the identification of periods with low secondary production. The importance of high-time-resolved samplings is remarkable in the detection of these episodes, which would not have been noticed with traditional 24-hours samplings.

Acknowledgment

I would like to acknowledge V. Bernardoni (General Applied Physics Institute, University of Milan) for the helpful suggestions and D. Cricchio (General Applied Physics Institute, University of Milan) for PMF analysis.

References

- Alastuey et al. (2004) *Atmos Environ* 38, 4979-4992
- Allen et al. (2001) *Environ Sci Tech* 35, 4189-4197
- Andrews et al. (1995) *J Air Waste Manage* 50, 648-664
- Artaxo et al. (1999) *Nucl Instrum Meth B* 150, 409-416
- Artiñano et al. (2001) *Atmos Environ* 35, suppl.1, S43-S53.
- Begum et al. (2005) *Environ Sci Technol* 39, 1129-1137
- Birch and Cary (1996) *Aerosol Sci Tech* 25, 221-241.
- Cabada et al. (2004) *Aerosol Sci Tech* 38(S1), 140-155
- Calzolari et al. (2006) *Nucl Instrum Meth B* 249, 1-2, 928-931.
- Casadei et al. (2006) *Ingegneria Ambientale*, XXXV, 4, 155-168 (in Italian)
- Chan et al. (1997) *Atmos Environ* 31, 3773-3785
- Chate (2005) *Atmos Environ* 39, 6608-6619
- Chow and Watson (2002) *J Geophys Res* 107, D21, 8344, doi:10.1029/2001JD000574
- Draxler and Rolph (2003) HYSPLIT (HYbrid Single-Particle Lagrangian Integrated Trajectory), NOAA Air Resources Laboratory, Silver Spring, MD. Model access via NOAA ARL READY Website <http://www.arl.noaa.gov/ready/hysplit4.html>
- Eldred et al. (1987) *Nucl Instrum Meth B* 22, 289-295
- Fermo et al. (2006a) *Chemical Engineering Transactions* 10, 203-208.
- Fermo et al. (2006b) *Chemical Engineering Transactions* 10, 83-88.
- Giugliano et al. (2005) *Atmos Environ* 39, 2421-2431.
- Graney et al. (2004) *Atmos Environ* 38, 1725-1726
- Greenfield (1957) *J Meteorology* 14, 115-125
- Hoek et al. (2002) *Atmos Environ* 25, 4077-4088.
- Hueglin et al. (2005) *Atmos Environ* 39, 637-651
- Jang et al. (2003) *Atmos Environ* 37, 2125-2138
- Kim and Hopke (2004) *J Air Waste Manage* 54, 773-785
- Kim and Hopke (2006) *Sci Total Environ* 368, 781-794
- Marcazzan et al. (2001) *Atmos Environ* 35, 4639-4650
- Marcazzan et al. (2003a) *J Environ Radioactiv* 65, 77-90
- Marcazzan et al. (2003b) *Sci Total Environ* 317, 137-147
- Marcazzan et al. (2004) *X-Ray Spectrom* 33, 267-272
- Mason (1966) *Principles of Geochemistry*, New York: Wiley and Sons
- Mazzei et al. (2007) *Atmos Environ*, doi:10.1016/j.atmosenv.2007.04.012
- McMurry (2000) *Atmos Environ* 43, 1959-1999
- Pacifico (2005) Degree Thesis in Physics, University of Milan, Italy (in Italian)
- Polissar et al. (1998) *J Geophys Res* 103, 19045-19057
- Prati et al. (1998) *Nucl Instrum Meth B* 136-138, 986-989
- Putaud et al. (2004) *Atmos Environ* 38, 2579-2595
- Qin and Odoyemi (2003) *Atmos Environ* 37 (2003), 1799-2809
- Querol et al. (1998) *Atmos Environ* 32, 719-731
- Querol et al. (2004) *Atmos Environ* 38, 6547-6555
- Plaza et al. (2006) *Atmos Environ* 40, 1134-1147
- Raes et al. (2000) *Atmos Environ* 34, 4215-4240
- Rees et al. (2004) *Atmos Environ* 38, 3305-3318

- Rolph (2003) Real-time Environmental Applications and Display System (READY) Website (<http://www.arl.noaa.gov/ready/hysplit4.html>). NOAA Air Resources Laboratory, Silver Spring, MD.
- Salma et al. (2004) *Atmos Environ* 38, 27-36
- Seinfeld and Pandis (1998) *Atmospheric Chemistry and Physics*. John Wiley and Sons, Inc
- Song et al. (2001) *Atmos Environ* 35, 5277-5286
- Thomaidis et al. (2003) *Chemosphere* 52, 959-966
- Turpin and Huntzicker (1995) *Atmos Environ* 29, 3527-3544
- Turpin et al. (1997) *J Air Waste Manage* 47, 344-356
- Turpin and Lim (2001) *Aerosol Sci Tech* 35, 602-610
- Vecchi et al. (2004) *Atmos Environ* 38, 4437-4446
- Vecchi (2007a) *Geophys Res Abstr* 9, 04380.
- Vecchi (2007b) *Atmos Environ* 41, 2136-2144
- Viana et al. (2007) *Atmos Environ* 41, 315-326
- Yuan et al. (2006) *Atmos Chem Phys* 6, 25-34
- Zhao and Hopke (2004) *Atmos Environ* 38, 5901-5910
- Zhao and Hopke (2006) *Atmos Res* 80, 309-322

13. Identification of secondary inorganic and organic aerosol components in urban particulate matter samples

Elevated particulate matter concentrations in urban areas result not only from direct particulate emission but also from gas-to-particle conversion in the atmosphere. Gas to particle conversion of sulphur and nitrogen species has been observed in the atmosphere, and these secondary processes are often responsible for high particulate mass concentrations. For what concerns carbonaceous species in particulate matter, it must be considered that they can be both of primary and secondary origin. Although carbonaceous species account for a large fraction of aerosol mass, the relative contribution of primary and secondary organic components is still under discussion.

Atmospheric carbonaceous aerosols are mainly composed of elemental carbon (EC) and organic carbon (OC). While EC is emitted only by combustion processes, being a by-product of OC incomplete combustion, organic carbon is produced by both primary and secondary sources (Castro et al. 1999; Yu et al 2004).

A subject of great concern in aerosol science is the identification of primary and secondary contribution. The biggest problem in the identification of these components consists in the separation of the contributions from organic carbon.

A variety of approaches have been used to estimate the magnitude of secondary organic aerosol formation in the atmosphere; this evaluation is difficult and not straightforward because of the large number of organic compounds involved.

In this study 4-hours time resolution PM₁₀ samples (180 in total) collected in Milan during two field campaigns have been chemically characterised. The data have been used to evaluate Secondary Organic Carbon (SOC) with two different approaches:

1. the SOC estimation is based on the $(OC/EC)_{pri}$ ratio; the key point is the accuracy and significance of this ratio in relation to the mixture of local primary PM sources (EC tracer method).
2. the SOC estimation is performed using an advanced receptor model (PMF, Positive Matrix Factorization). PMF modelling of speciated PM₁₀ concentration data is carried out to identify sources categories by collectively considering component abundance in the derived source profiles and the corresponding temporal variation in the source contributions. SOC is subsequently taken to be the

sum of the OC contained in secondary sources identified by PMF and quantified using Multilinear Regression

13.1. EC tracer method

Secondary organic carbon can be estimated by subtracting the expected primary OC from the total observed ambient OC.

$$OC_{\text{sec}} = OC - OC_{\text{pri}} \quad (1)$$

Primary OC can be assessed as follows (Turpin et al., 1995; Plaza et al., 2006; Salma et al., 2004; Strader et al., 1999):

$$OC_{\text{pri}} = (OC/EC)_{\text{pri}} EC \quad (2)$$

or:

$$OC_{\text{pri}} = a + bEC \quad (3)$$

where a and b are the intercept and the slope, respectively, of the best fit line. The intercept a is considered to be the primary OC background (OC_{back}) concentration originating from non-combustion sources. It is supposed that primary OC and EC have the same sources, and therefore there is a representative OC/EC ratio for the primary aerosol. Since $(OC/EC)_{\text{pri}}$ emission rates vary by source (vehicles, fireplaces, heating, etc.) and are influenced by meteorological conditions, it is mandatory to estimate a local and seasonal value for this ratio. The ratio can be calculated when Secondary Organic Aerosol (SOA) is expected to be low (e.g. reduced local photochemical activity with both low O_3 concentration and NO_2/NO_x ratio).

Giugliano et al., (2005) suggest to investigate the role of a single source sampling in a site which is supposed to be influenced only by that source. To estimate the role of the traffic source under typical driving conditions Giugliano and coworkers have sampled in a tunnel in the city center of Milan.

In our study many different criteria, some of which already used in the literature, have been employed to estimate $(OC/EC)_{\text{pri}}$: (1) selecting the ratio in the interval time 4-8 a.m. (low photochemical activity and, during summer, traffic as the only active source); (2) low values for NO_2/NO_x ratio; (3) low SO_4^{2-} concentrations; (4)

low values for OC/EC; (5) low values of both SO_4^{2-} and OC/EC; (6) low SO_4^{2-} and $\text{C}_2\text{O}_4^{2-}$ concentrations. It is worth noting that both sulphate and oxalate are typically secondary components originating by SO_2 and VOCs oxidations, respectively.

Depending on the criteria used, OC_{sec} and OC_{back} resulted highly variable (Table 13-1).

Summer season

	N	Intercept (OC_{back})	Slope (OC/EC) _{pri}	R ²	OC primary		OC secondary		OC background		Negative values (%)
					%OC	%PM	%OC	%PM	%OC	%PM	
4-8	15	7,08	1,11	0,50	25%	5%	16%	3%	71%	14%	42%
NO_2/NO_x minimum values	12	-4.1	3,80	0,82	75%	15%	40%	8%			37%
$\text{SO}_4^{2-} < 2\mu\text{g}/\text{m}^3$	13	5,40	1,30	0,68	30%	6%	21%	4%	54%	11%	16%
$\text{C}_2\text{O}_4^{2-} < 0,2\mu\text{g}/\text{m}^3$	15	5,37	1,11	0,65	25%	5%	25%	5%	54%	11%	12%
$\text{OC}/\text{EC} < 3$	14	2,66	1,95	0,70	45%	9%	33%	7%	27%	5%	11%
$\text{OC}/\text{EC} + \text{SO}_4^{2-}$	6		2,70	0,93	62%	12%	44%	9%			10%

Winter season

	N	Intercept (OC_{back})	Slope (OC/EC) _{pri}	R ²	OC primary		OC secondary		OC background		Negative values (%)
					% OC	%PM	% OC	%PM	% OC	%PM	
4-8	15	11,89	1,45	0,60	45%	8%	20%	4%	67%	12%	68%
NO_2/NO_x minimum values	10	13,44	0,89	0,69	27%	5%	20%	4%	76%	14%	54%
$\text{SO}_4^{2-} < 3\mu\text{g}/\text{m}^3$	13	4,90	1,82	0,86	56%	10%	28%	5%	27%	5%	23%
$\text{C}_2\text{O}_4^{2-} < \text{lod}$		9,46	1,36	0,66	42%	8%	21%	4%	53%	10%	40%
$\text{OC}/\text{EC} < 2,4$	14	8,73	1,12	0,78	34%	6%	26%	5%	54%	10%	26%
$\text{OC}/\text{EC} + \text{SO}_4^{2-}$	6		2,24	0,98	69%	12%	42%	8%			18%

Table 13-1: OC_{pri} , OC_{sec} and OC_{back} obtained applying different criteria. N represents the number of data matching the criteria and for which the OC/EC has been calculated. Negative values percentages represent the number of data for which OC_{pri} is higher than $\text{OC}_{\text{measured}}$; when they are higher than 25%, the criterium is considered not to be valid.

For more accurate analysis of OC secondary process formation it is necessary take into account the meteorological conditions.

During summer OC/EC measured ratios show the same temporal behavior wind velocity (Figure 1) and the ratio increase may be due to the particulate ageing and to the presence of biogenic carbon too; thus when we observe high OC/EC in coincidence with high wind velocity, we suppose that this high ratio is not only due to local secondary production also do air maxies advection.

In this study we applied the EC-tracer method for the summer season using two different $(OC/EC)_{pri}$ values: first of all we used 1.34, as reported in Giugliano et al. (2005) for tunnel measurement in Milan.

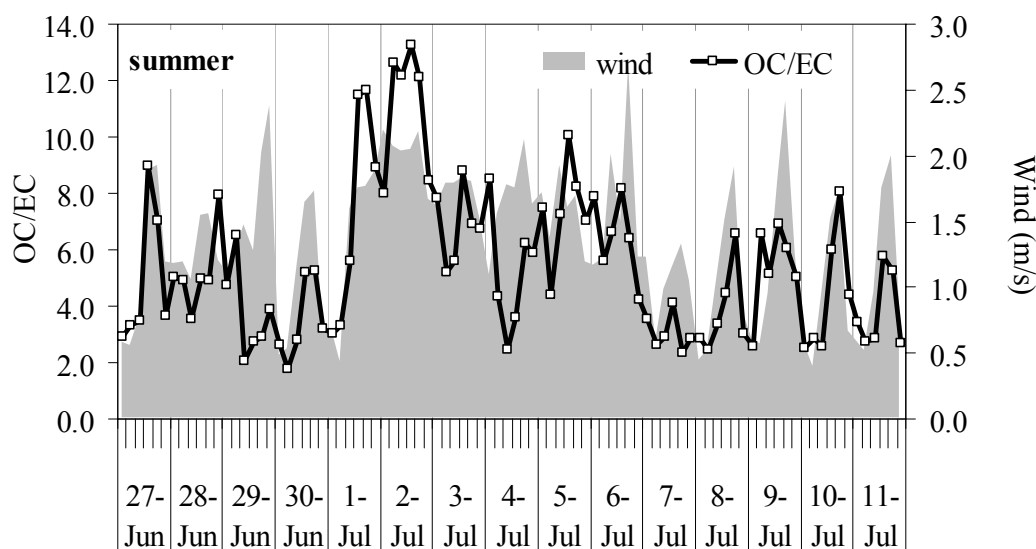


Figure 13-1: temporal behaviour of OC/EC and wind velocity during summer season

In order perform a comparison we estimated primary OC/EC ratio in selected samples characterized by a low wind velocity. In particular we selected data with: low OC/EC ratio ($OC/EC < 3$), high NO and low Ox, low percentages of sulphate and oxalate (Figure 13-3). In the second step we estimate the percentage of OC_{pri} , OC_{sec} , and OC_{tra} (transported OC) using EC concentration and wind velocity data.

With this second approach, the high-time resolution data allowed:

- the identification of samples without SOC, which is difficult to single out with 24-hour time resolved samplings because inside the same day there may be periods with high primary influence as well as periods with high secondary production (in our case samples selected to calculate $(OC/EC)_{pri}$ are not consecutive);
- to obtain a robust value for $(OC/EC)_{pri}$;

In this way we obtained a data-set characterized by components of primary origin; in Figure 13-2 the linear regression obtained by the selected OC and EC values is shown.

$(OC/EC)_{pri}$ used in this second method for the summer season was 2.77.

The difference between the two $(OC/EC)_{pri}$ can be ascribed to analytical problems in the determination of the two fractions: as we show in chapter 4 and 5, with standard TOT analyses the EC might underestimated an average about 32% and consequently OC might overestimated on average about 15%. Moreover tunnel measurements are probably more representative of the ratio near the source, while $(OC/EC)_{pri}$ estimated using sample selected during our field campaign might be more influenced by gas to particle conversion and it should represent the lowest $(OC/EC)_{pri}$ value for the urban area during the campaign. Consequently, we suppose that 1.34 and 2.77 can represent minimum and maximum OC/EC primary ratio in Milan area during summertime.

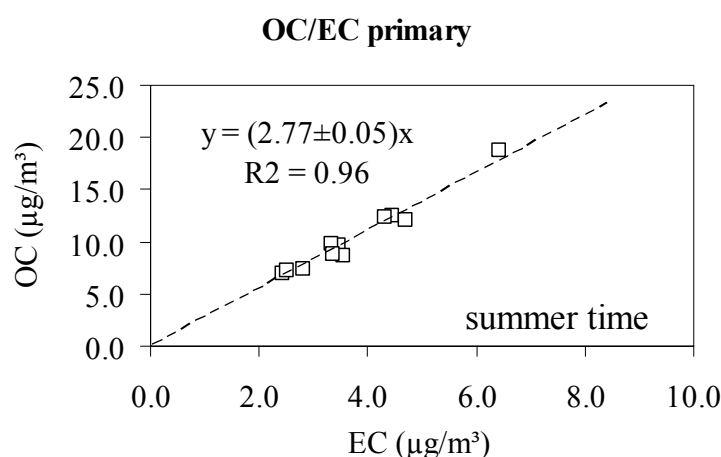


Figure 13-2: scatter plot of OC and EC selected in samples characterised by components of only primary origin

It should be noticed that no intercept appears in the scatterplot and it seems to indicate a low (or absent) contribution from biogenic emission in the city during days when the low wind speed limits air masses advection from regional rural areas.

According to Turpin et al. (1995) the $(OC/EC)_{pri}$ can be estimated in the samples after rainfall episodes, because should be observed the rain cleans of the air and only the primary pollution. In Figure 13-4 we report OC/EC in the days during a rainfall episode the ratio after it is quite similar to 2.77 value, that we have estimated for the summer season.

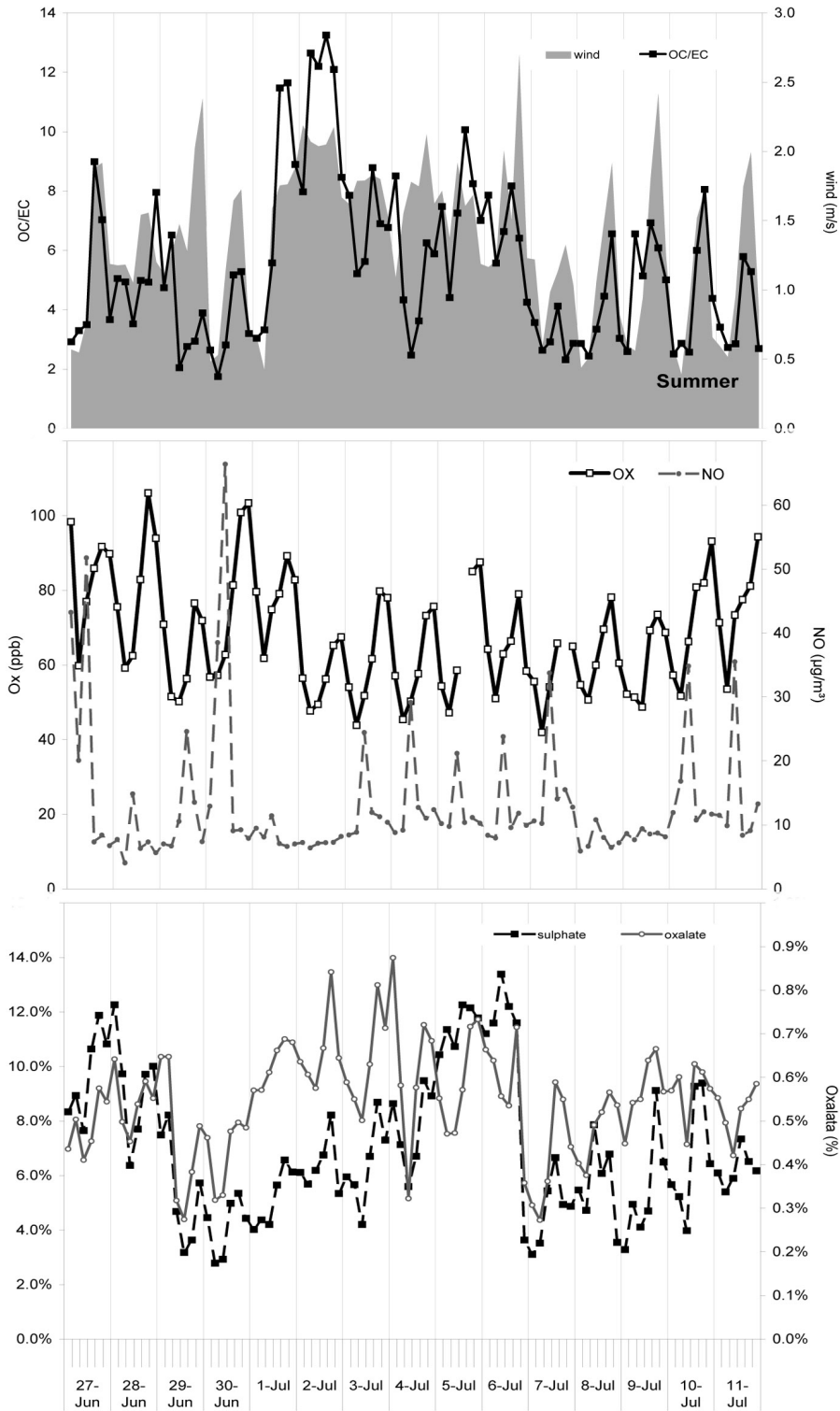


Figure 13-3: temporal trend of OC/EC, wind velocity, NO and O_x concentration, sulphate and oxalate percentage, in the summer campaign.

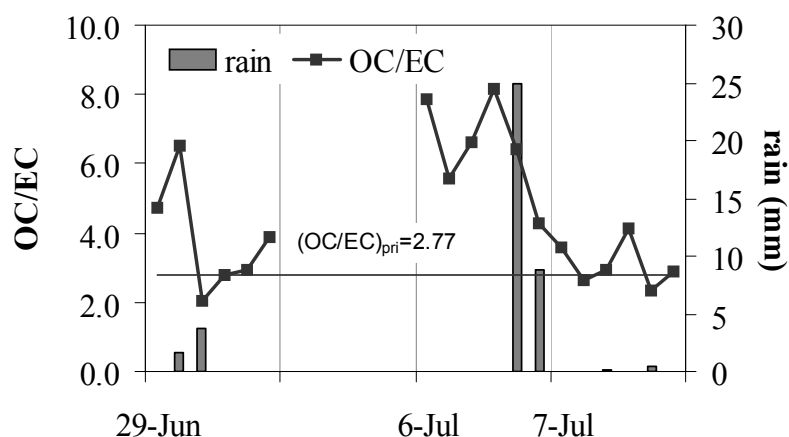


Figure 13-4: figure 4: OC/EC during rainfall episode, in comparison to $(OC/EC)_{pri}$ estimated

Considering all the above listed criteria, it is possible to separate our summer data-set in three categories characterized by different values of the OC/EC ratio as represented in Figure 13-5. The $(OC/EC)_{pri}$ has been previously defined, $(OC/EC)_{tra}$ is the ratio observed when the wind velocity is higher than 1.7m/s, and $(OC/EC)_{sec}$ is the ratio observed in the remainder samples (characterized by wind velocity lower than 1.7m/s and OC/EC ratio larger than 3).

To calculate primary OC we have used the following equation:

According to Giugliano et al. (2005)

$$OC_{pri} = 1.34 \times EC \quad (4a)$$

Using selected samples with low OC_{sec} and OC_{tra} contribution

$$OC_{pri} = 2.77 \times EC \quad (4b)$$

In both cases, to calculate OC_{tra} we used 5.45 as a multiplicative factor for EC. This value is the 75° percentile of secondary origin OC/EC (wind velocity < 1.7m/s, OC/EC > 3) data distribution:

$$OC_{tran} = 5.45 \times EC \quad (5)$$

OC_{sec} is calculated as follows (OC_{total} is the measured OC):

$$OC_{sec} = OC_{tot} - (OC_{pri} + OC_{tran}) \tag{6}$$

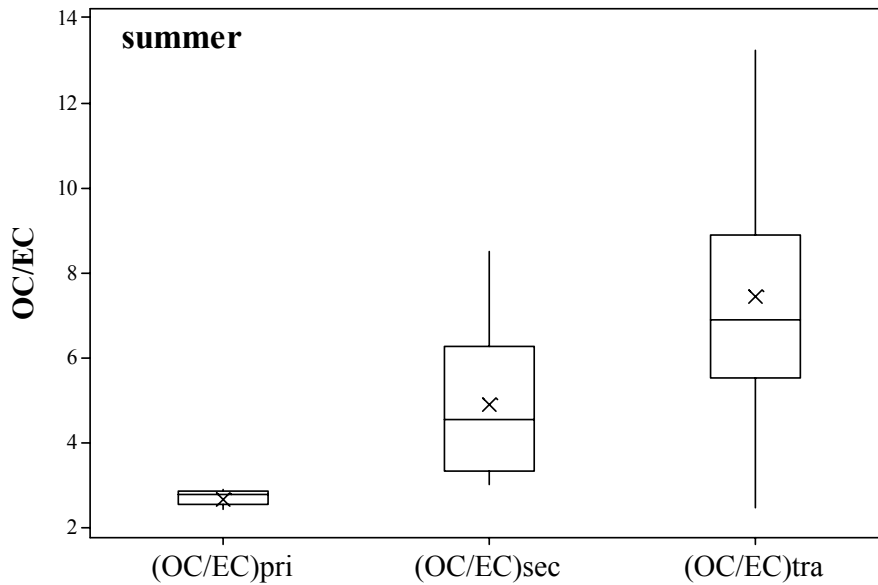


Figure 13-5: Distribution of OC/EC ratio separating in three different categories: minimum and maximum values, mean value (X), range of 25° and 75° percentile around the median.

The comparison between the two methods opposed in this work to estimate the contribution of primary sources to OC concentration is reported in Table 13-2. The percentage of OC_{pri} vary considerably in two methods applied.

Summer season					
	Selected method (equation 4b)	samples	Giugliano method (equation 4a)	et.	all
OC_{pri}	64%		31%		
OC_{sec}	31%		57%		
OC_{tra}	34%		34%		

Table 13-2: percentage of three OC origins, calculated by two different method. The percentages of OC_{sec} and OC_{tra} are calculated only when present

The percentage of OC due to advection is very high: when the wind velocity is high the percentage of OC_{tra} is one third of the OC.

In Figure 13-6 we report the temporal trend of three OC categories compared to the measured OC. In the figure the white area (OC_{pri} or OC_{sec} in the legend) is OC_{pri} when we use equation 4b, whereas is OC_{sec} when we use equation 4a.

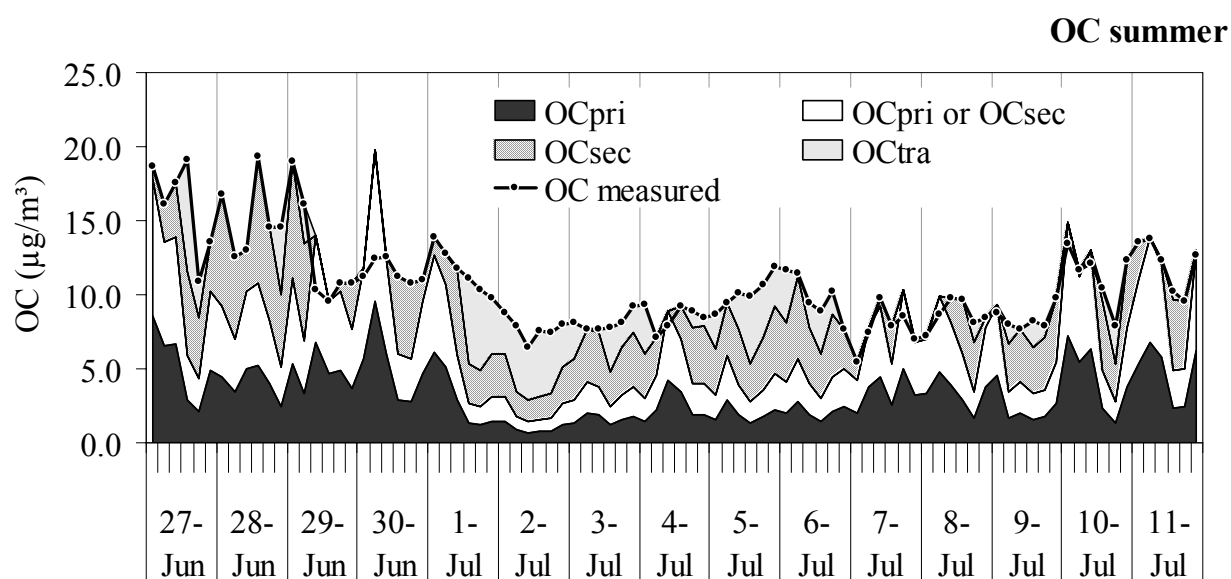


Figure 13-6: temporal trend of OC_{pri} , OC_{sec} and OC_{tra} , in comparison to OC measured. The white area is OC_{pri} or OC_{sec} according to the used method.

Looking at back trajectories (Figure 13-7a,b) calculated using NOAA-Hysplit model (Draxler and Rolph, 2003; Rolph, 2003) it can be seen that the air masses on Milan on 2nd July had travelled through Po Valley during the previous hours and we suppose that they transported the OC biogenic or aged particulate matter. In comparison the 7th July, the percentage of OC_{pri} is very high and the wind velocity is low, so we suppose that all the particulate matter is locally produced during the previous hours the air mass was stationary on the city (Figure 13-7b)

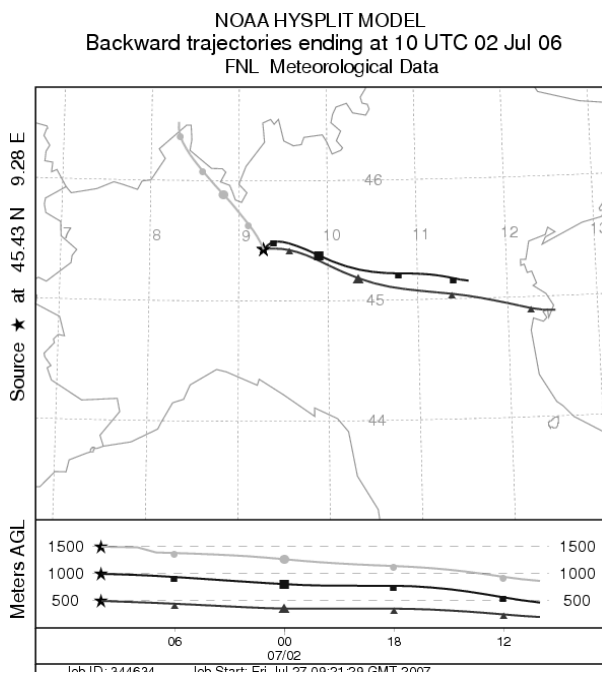


Figure 13-7a: back trajectories during OC_{tra} episode

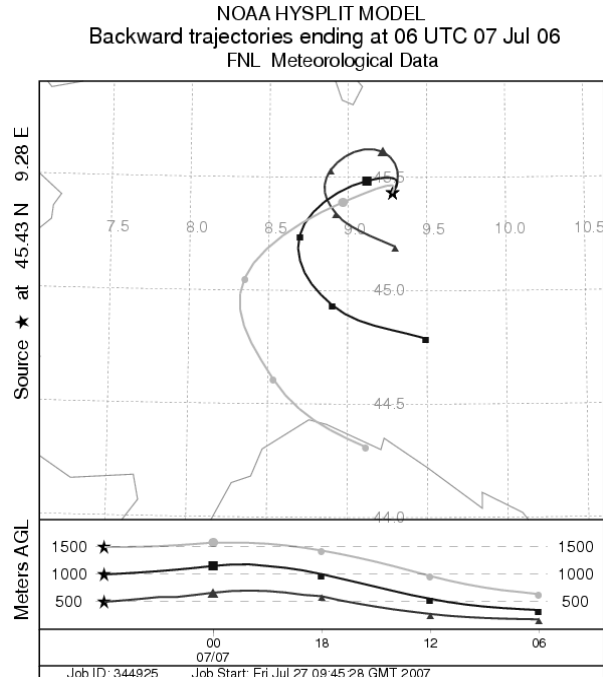


Figure 13-7b: back trajectories during local produced episode

The oxidation processes play an important role in secondary formation, during hot season, in Figure 13-8 we have compared the temporal trend of OC_{sec} concentration, calculated by equation 4b, and O_x concentration, calculated as the sum of NO₂ and O₃, the data show a good agreement suggesting that.

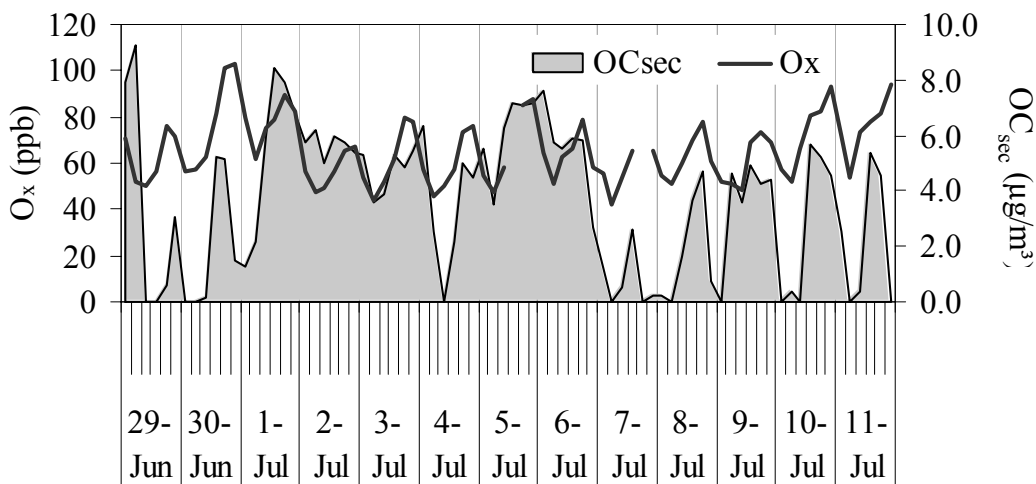


Figure 13-9: comparison between OC_{sec} concentration, calculated by equation 4b, and O_x concentration during summer season

During the winter season there was no similarity between wind velocity and OC/EC ratio temporal patterns as more stable meteorological conditions were generally observed in this period.

In the cold period we can not apply the primary ratio estimated in the tunnel, because during this season the road traffic is not the only source of OC and EC: indeed domestic heating plays a important role. In the chapter 0 we showed that a preliminary study estimated that in Milan the 30% of OC, during winter time, was due to wood burning.

Also during wintertime, we have applied two methods to estimate the $(OC/EC)_{pri}$. At first, we estimated primary OC/EC ratio in selected samples characterized by high percentage of EC ($EC > 10\%$) and high concentration of NO ($> 300 \mu g/m^3$). Elemental analysis showed strong accumulation of elements such as Fe, Cu, Cr, Mn, Zn, indicating a strong influence of primary sources in those samples. The selected samples are reported in Table 13-3; in these samples the percentage of secondary compounds (nitrate and sulphate) is low. The average of OC/EC in these samples is 1.58. Table 13-3 shows that the primary ratio is different in the 3 samples. The variability in this data is likely due to the mixture of the sources active during the cold season.

As a comparison we have singled out a period characterized by a low and constant OC/EC ratio. In the selected period (black box in Figure 13-10) secondary compounds (i.e. ammonium and sulphate) percentages are low ($< 4\%$). In this period the correlation between OC and EC is very good as shown in Figure 13-11, the $(OC/EC)_{pri}$ results 2.31. Also for the winter season data-set, the regression line intercept is zero. This result suggests that the OC_{back} or OC not-combustion, if present, are not produced in the urban area, according to Castro et al. (1999) in the winter season the OC biogenic is likely very low and may be ignored. This ratio is higher than the first one, but it can be influenced by condensation processes, indeed in this period the percentage of nitrate is high and this may mean that condensation processes play an important role.

Also for winter campaign we applied equation 5, and the OC/EC ratio higher than 5.45 is again an indication of the presence of OC_{tra} . Primary, secondary and transported OC wintertime concentrations are reported in Figure 13-12, the white area is OC_{pri} if we use $(OC/EC)_{pri}=2.31$, while it is OC_{sec} when 1.58 ratio is used.

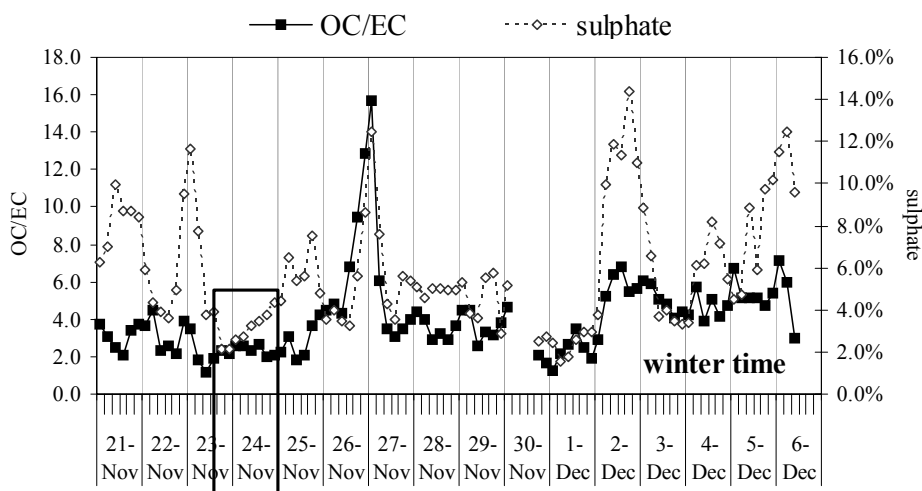


Figure 13-10: OC/EC and percentage of sulphate during winter campaign. Samples selected to estimate $(OC/EC)_{pri}$ (black box)

Data	time	OC	EC	OC/EC
30/11	20-24	34.1	20.8	1.64
12-Jan	0-4	37.5	31	1.21
12-Jan	20-24	41.8	22.2	1.89
average				1.58
standard deviation				0.34

Table 13-3: OC, EC, OC/EC values of three selected samples characterized by low secondary compounds (winter campaign)

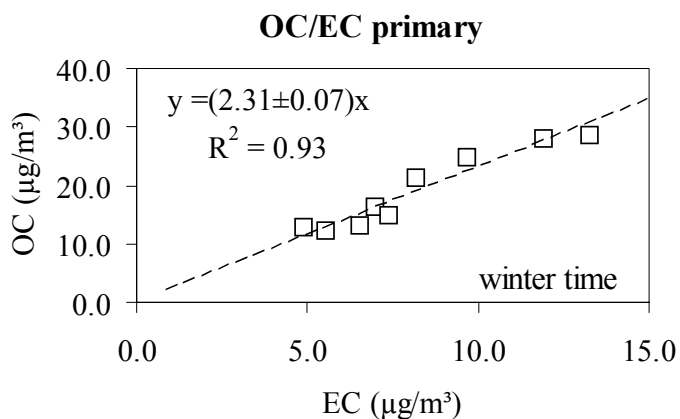


Figure 13-11: scatter plot of OC and EC selected in samples characterized by components of only primary origin (winter campaign)

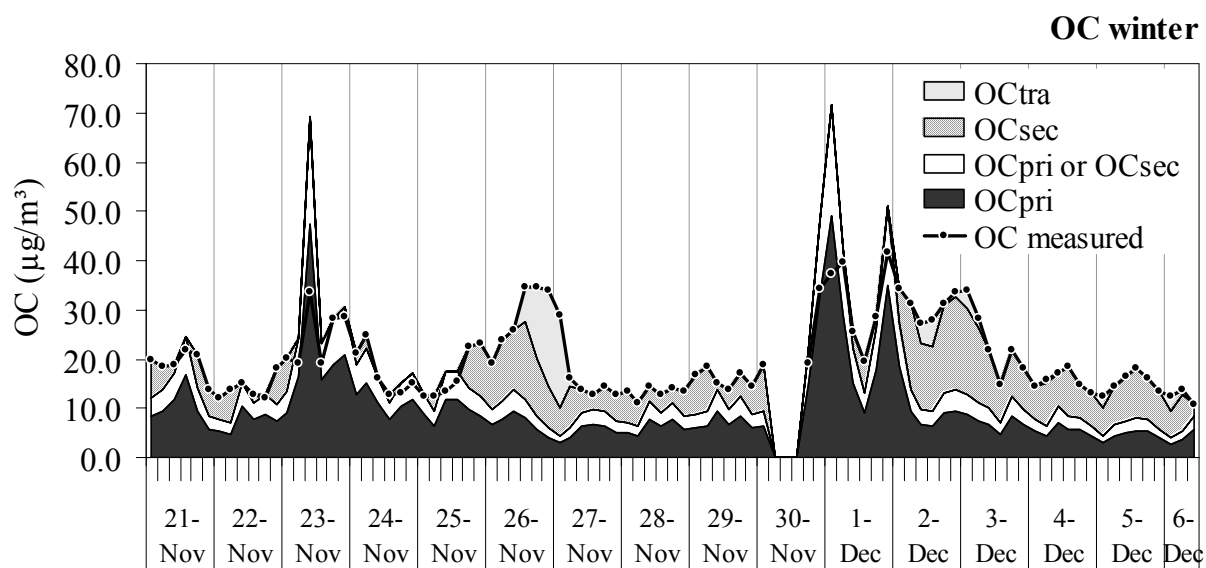


Figure 13-12: temporal trend of OCpri, OCsec and OCtra, in comparison to OC measured. The white area is OCpri or OCsec according to the used method.

The comparison between the two methods used to estimate the contribution of primary sources to OC concentration is reported in Table 13-4. The percentage of OC_{pri} vary considerably in two methods apply.

Winter season		
	(OC/EC) _{pri} =2.31	(OC/EC) _{pri} =1.58
OC _{pri}	66%	49%
OC _{sec}	38%	50%
OC _{tra}	20%	20%

Table 13-4: percentage of three sources of OC, calculated by two different primary ratio. The percentage of OCsec and OCtra is calculated only when present

Using a primary ratio 2.31 we overestimate OC_{pri}, in fact in 16 samples OC_{pri} is higher than measured OC. Probably for winter campaign the correct primary ratio is 1.58.

13.2. Comparison of SOC derived from EC tracer method and the PMF model

Receptor models estimate the amount of pollutants from different sources through statistical interpretation of ambient data and reasonably imposed constrains. The source categories were identified by the explained variation of the species in the different sources and from source profiles, as well as the temporal trend of sources contribution. OC concentrations in the two secondary aerosol source categories, i.e. secondary sulphate and organics and secondary nitrate, were summed up to obtain SOC; on the contrary, primary OC values were obtained summing up OC contents of the 4 primary sources (traffic, resuspended dust, construction work and industry).

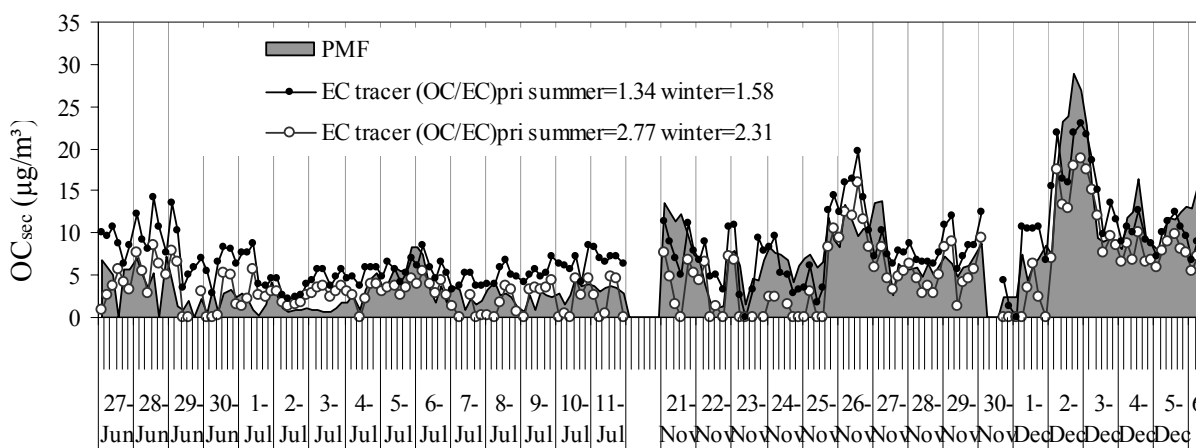


Figure 13-13: comparison between SOC estimation by EC tracer method (using two different primary ratio for both season) and by PMF model

In the literature this method has been used to estimate SOC by Yuan et al. (2006); the data have been elaborated from Institute of Applied General Physics, University of Milan.

The average SOC percentages obtained by the two methods are comparable in both seasons (Table 13-5).

During summertime, PMF estimations are in good agreement with the results obtained using a primary OC/EC ratio of 2.77, while during the winter campaign a good comparability is obtained with 1.58 ratio.

Table 13-5 compares PMF results to EC tracer method results obtained with the two different approaches.

	(OC/EC) _{pri}	EC tracer method	PMF model
Summer	2.77	31%	28%
	1.34	57%	
Winter	2.31	38%	46%
	1.58	50%	

Table 13-5: percentage of SOC in the two season obtained with EC tracer method and PMF model

Figure 13-14 and Figure 13-15 show the ratio between OC_{pri} resulting to PMF model and EC concentration in summer and in winter, in the same figures we have compared this ratio with the (OC/EC)_{pri} calculated used in the EC tracer method and explained previously. In the summer time the ratio between OC_{pri} by PMF and EC is 2.68, this value is consistent with to 2.77; it is noteworthy the 1.34 ratio (dotted line in Figure 13-14) represents the lowest value of primary ratio.

During the winter time the ratio between OC_{pri} by PMF and EC is the same value (1.58) that we have obtained as the average OC/EC ratio in three selected samples characterized from low presence of secondary compounds. The 2.31 ratio appears to represent the highest value (dotted line in Figure 13-15) of OC and EC primary ratio.

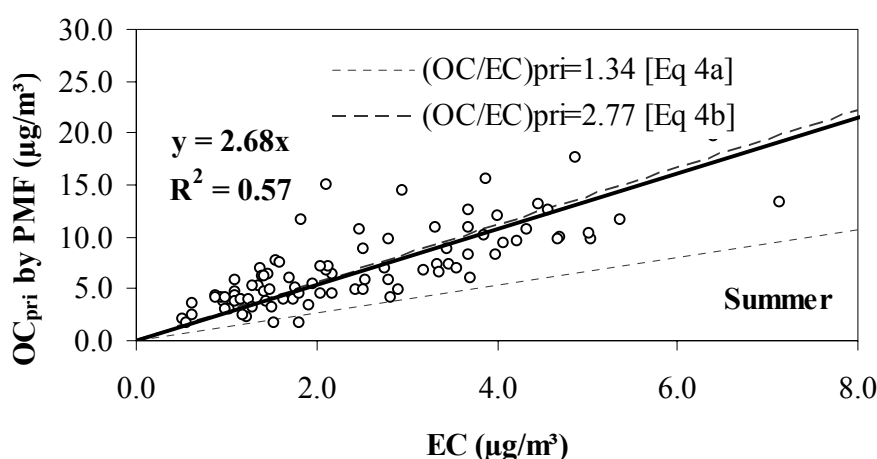


Figure 13-14: scatter plot of EC and OC_{pri} resulting by PMF, during summer season, in comparison to OC/EC ratio used to estimate OC_{pri} in EC tracer method

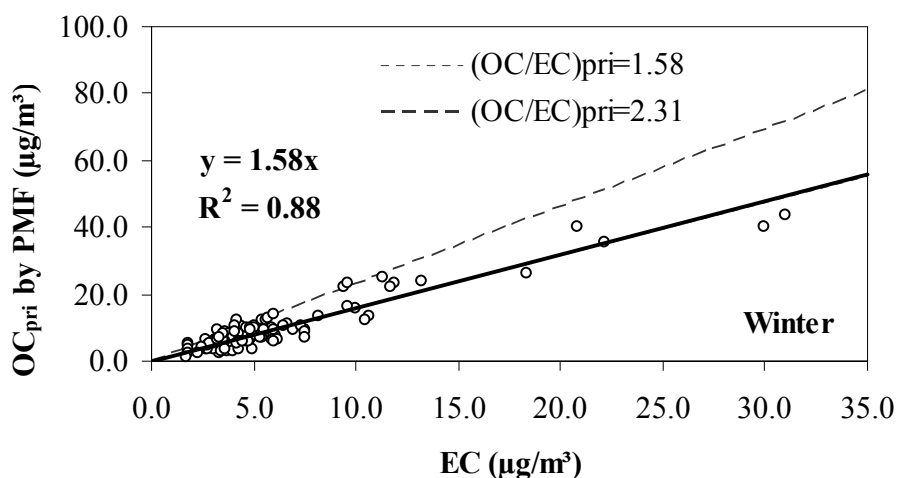


Figure 13-15: scatter plot of EC and OC_{pri} resulting by PMF, during winter season, in comparison to OC/EC ratio used to estimate OC_{pri} in EC tracer method

13.3. Secondary aerosol

In addition to SOC, the principal compounds of secondary origin in urban particulate matter is nitrate, sulphate and ammonium, the atmospheric concentration and the percentages of this compounds in PM are reported in chapter 1 and summarized in table Table 13-6. Here we used in the EC tracer method for the summer season $(OC/EC)_{pri}=2.77$ and for the winter $(OC/EC)_{pri}=1.58$.

		summer			winter		
		average	min	max	average	min	max
nitrate	$\mu\text{g}/\text{m}^3$	2.97	0.59	16.9	14.99	1.96	38.34
	%	5.2%	1.6%	27.8%	13.9%	31.2%	34.9%
sulphate	$\mu\text{g}/\text{m}^3$	3.99	1.25	9.91	6.4	1.88	6.61
	%	7.0%	2.8%	13.4%	5.8%	1.5%	14.3%
ammonium	$\mu\text{g}/\text{m}^3$	2.36	0.47	9.08	5.38	0.74	14.07
	%	4.3%	0.9%	10.3%	5.0%	1.1%	9.3%
OC_{sec}	$\mu\text{g}/\text{m}^3$	4.61	0.18	13.21	10.60	1.28	29.80
	%	9.0%	0.3%	20.6%	9.8%	0.8%	21.8%
total	$\mu\text{g}/\text{m}^3$	13.06	3.29	30.01	37.14	8.56	92.76
	%	23.9%	6.8%	40.7%	34.3%	8.4%	58.3%

Table 13-7: average, minimum and maximum of concentration and percentage of secondary compounds in summer and winter seasons

The analysis of season of data points out cold season concentration higher than hot season ones for all the species considered. In particular, for nitrate the seasonal difference can be explained by the larger availability of gaseous precursor in winter, due to the additional NO_x emissions from domestic heating not operating in summer. Moreover, the reaction between gas-phase ammonium and nitric acid to form particulate phase ammonium nitrate is favored by wintertime low ambient temperature of winter (Stelson and Seinfeld, 1982; Park and Kim, 2004). Moreover, as we already mentioned, it must be considered that also the correct estimation of atmospheric nitrate concentration is difficult because of the well-known problem of sampling artifacts, in the hot season mainly a negative artifact related to volatilization, and in the cold season likely positive artifact due to condensation (Henning et al. 2003).

Sulphate percentage is higher in summer than in winter, as its formation is favored from photochemistry activity.

Low temperature and a larger number of sources increase the concentration and the percentage of OC_{sec} during the winter time. Also for OC we should have a sampling positive or negative artifact (Henning et al. 2003).

In Figure 13-16 we report the concentration of secondary compounds in both seasons, compared to PM concentration and EU limit fixed to $50\mu\text{g}/\text{m}^3$.

During summertime, the average secondary contribution was 24%. It was noticed that during summertime the two contributions were quite comparable, while during wintertime episodes were detected in which primary or secondary contributions strongly dominated. Moreover, during wintertime secondary contribution was estimated to be 34% on average.

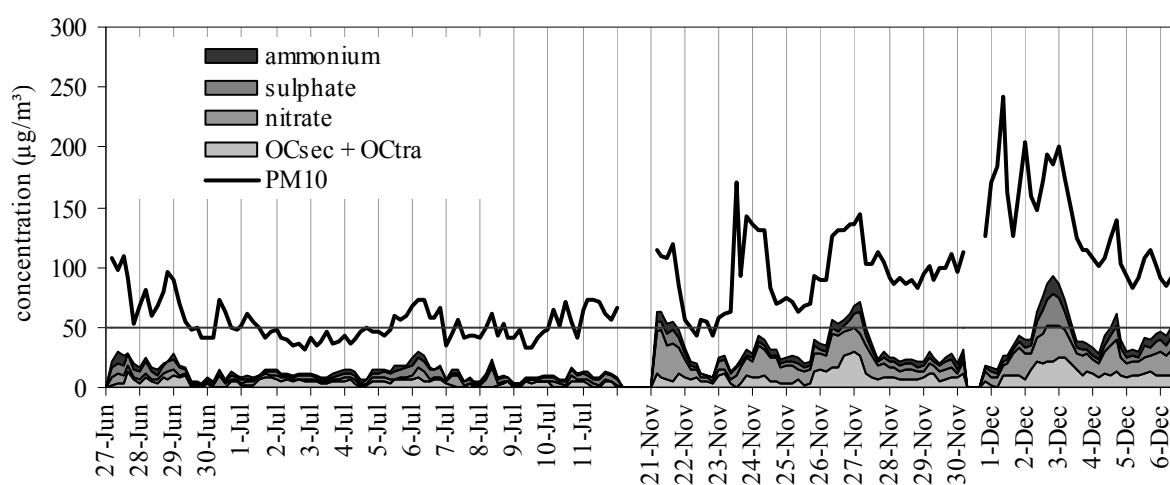


Figure 13-16: concentration of secondary compounds in summer and winter campaign. The grey line shows the EU limit fixed to $50\mu\text{g}/\text{m}^3$

Separating working days data from Sundays data, it was observed that from the evaluation of primary and secondary OC, that during Sundays the secondary OC is higher than during working days (summer: 59% secondary OC respect total OC during Sundays and 35% during working days; winter: 56% during Sundays and 28% during working days). To explain these data, we suppose that during Sundays the primary contribution is lower and so the air mass contains a higher proportion of aged OC.

Another important consideration, concerning future abatement strategies, can be done: if we consider the possibility to completely eliminate primary contribution and using the EU daily limit of $50\mu\text{g}/\text{m}^3$ (grey line in Figure 13-16) as reference limit, it was noticed that during summertime the number of exceedances on 24 hour basis would decrease from 60% to 19%; on the contrary during wintertime, this reduction would be lower (from 100% to 75%), due both to higher PM10 concentration and secondary contribution. This means that it will not be enough to decrease primary emissions in future abatement strategies, but these will have to include also programs for gaseous (secondary-precursors) pollutants emissions reduction.

13.4. Conclusions

Secondary OC gives strong contribution to total OC mass (summer 31%-64% winter 38%-50% of total OC), in both seasons the secondary PM is about one third of total PM (Table 13-7) and this contribution can not be likely reduced with abatement strategies on particulate emission.

Especially during wintertime secondary PM concentration is frequently higher than the UE daily limit.

In this work we have compared two independent methods (EC tracer method, PMF model) for secondary OC estimation.

In the EC tracer method positive and negative sampling artifacts for OC, as well as the inherent arbitrary nature of the operational definition of OC and EC, introduce additional uncertainties in the SOA estimates (Strader et al., 1999), because they depend on OC/EC ratio experimentally obtained. Furthermore, according to some authors (Strader et al., 1999; Yu et al., 2004) one of the major problems with this method is that the $(\text{OC}/\text{EC})_{\text{pri}}$ ratio may not be constant at a site but may vary with sources and meteorological conditions, especially when OC is derived from several different important sources. Although the values used in this study are statistically robust, the SOA concentration estimates remains uncertain.

Moreover, it must be considered that also the correct estimation of atmospheric nitrate concentration is difficult because of the well-known problem of sampling

artifacts, in the hot season mainly a negative artifact related to volatilization, and in the cold season likely positive artifact due to condensation (Henning et al., 2003). A not artifact-free data set might produce an error in the identification of sources and in their apportionment by PMF. For this reason we think that during summertime the separation between primary and secondary OC may be partially influenced by problems in nitrate estimation.

Acknowledgment

I would like to acknowledge V. Bernardoni (General Applied Physics Institute, University of Milan) for the helpful suggestions and D. Cristicchio her contribution to PMF analyses

References

- Castro (1999) *Atmos. Environ.*, 33, 2771-2781
Henning et al. (2003) *J. Geophys. Res.*, 108(D1), 4030,
Park and Kim (2004) *Atmos. Environ.*, 38, 1459-1471
Plaza J. et al. (2006) *Atmos. Environ.*, 40, 1134-1147.
Salma I. et al. (2004) *Atmos. Environ.*, 38, 27-36
Stelson and Seinfeld (1982) *Atmos. Environ.*, 16, 983-992
Strader R. et al. (1999) *Atmos. Environ.*, 33, 4849-4863
Turpin, B. J. et al. (1995) *Atmos. Environ.*, 29, 3527-3544.
Yu, S. et al. (2004) *Atmos. Environ.*, 38, 5275-5268.

14. Chemical and physical measurements for indoor air quality assessment at the Ca' Granda historical archive, Milan (italy)

The effects of air pollution on indoor cultural heritage are the subject of numerous studies reported in the literature.

The aim of this study was to estimate the air quality, by means of both chemical and physical studies, at the Ca' Granda Historical Archive (Milan, Italy) that houses an important collection of documents from 12th century. Temperature and relative humidity were measured in the rooms. Particulate matter (PM_{2.5}) concentrations were quantified and the chemical composition, in terms of ionic components, elements and carbonaceous fraction (total, organic and elemental carbon) were determined. The gaseous pollutants NO₂, SO₂ and O₃ and indoor acidity were also measured.

In this paper we present our findings and propose some guidelines for a better preservation of the documents.

14.1. Introduction

Libraries and archives have been used for centuries to preserve a wide variety of materials and to store precious information. The effect of air pollution on objects stored in museums and archives has recently received an increased awareness from museum and conservation staff. Actually, numerous studies have been carried out to assess the complexity of the risks, which can be chemical and physical, in museums, galleries and all the environments where works of art are exhibited and stored (Brimbecomble, 1990; Camuffo et al., 2001).

Atmospheric pollution is one of the most relevant threat to the preservation of cultural heritage. Studies comparing libraries under different environmental pollution conditions (urban sites and rural areas) demonstrated that degradation is more consistent in polluted areas (Pavlogeorgatos, 2003). Looking at indoor air quality from a chemical point of view, it is important to focus on components that have a potential deterioration effect on the building interiors such as some gases (e.g. CO, NO_x, SO₂ and O₃) and particulate matter (PM). Indoor pollution can be due to external penetration. Outdoor particles are brought indoor via ventilation, or, on the contrary, indoor sources might be present. The indoor sources are numerous

and can be ascribed to different processes such as room heating, soil dust, dust from visitors, human bio-effluent, cleaning materials, deterioration of the walls, etc. One of the main problems caused by indoor aerosols is the deposition on surfaces of dirt called soiling (Owen et al., 1992) or the chemical damage (Nazaroff et al., 1990) depending on their size and chemical composition.

Pollutants, such as O₃, NO_x and SO₂, are hazardous for cellulose-based materials since they can cause embrittlement and discoloration (Shanani et al., 1987). For example, ozone is a powerful oxidant and is deleterious for paper since it induces the formation of peroxide groups in the presence of moisture. Ozone can break any double bond in every carbon chain causing the formation of vertical cracks on a wide range of materials (Pavlogeorgatos, 2003). Ozone concentration within buildings is usually very low because it is rapidly destroyed by contact with the organic materials, though these can, of course, include the art works themselves. As regards nitrogen oxide and sulfur oxide, with the presence of humidity they can easily turn into the powerful nitric acid and sulfuric acid, which are both responsible for cellulose hydrolysis.

Few studies have been carried out in libraries for the assessment of total dust concentration together with indoor exposure to volatile organic compounds (VOCs) (Fantuzzi et al., 1996; Righi et al., 2002; Schieweck et al., 2005). The latter, potentially hazardous for both stored materials and libraries users, can have been generated from products used in previous conservation treatments (Schieweck et al., 2005; Mills et al., 1994). Particulate matter in the indoor atmosphere can be also generated by photo-oxidative processes (Brimblecombe, 1990). In addition, hydrocarbons from outdoor air can be oxidized contributing to the amount of dust deposited on indoor surfaces.

It has been demonstrated that the environmental parameters temperature and relative humidity are critical for organic materials preservation. When organic materials-based objects – like paper and parchment - release humidity, they become fragile and the fibers are easily broken (Pavlogeorgatos, 2003). In contrast, high temperature and relative humidity favour microbial growth. Actually, as with other objects, documentary heritage is susceptible to biological damage (Cappitelli et al., 2005).

In the year 2001 a major program of improvements in conservation, access and collections management was begun at the Ca' Granda Historical Archive (Milan, Italy) that houses an important collection of documents (e.g. parchments, maps and codes) dealing with the local hospital administration, and dated from the 12th century, together with other precious objects such as paintings. Air quality monitoring was included in the framework of this diagnostic investigation project whose major goal was the total restoration and functional recovery of the building

(investigations on mortars, plasters, and wooden parts, thermography of the vaults and topography reliefs were also planned).

Although some joint chemical and physical studies aiming at air quality monitoring have been carried out in museums (Camuffo et al., 1999, 2001; Gysels et al., 2004), to the best of our knowledge no studies considering both physical and chemical have ever been performed in archives and libraries.

The aim of this work was to study indoor pollutants at the Ca' Granda Historical Archive and to assess the relationship between the indoor and the outdoor environment in order to plan sound preventive strategies. Two different locations were monitored: the Archive's main hall (Capitolo d'Estate) and the basement where the oldest historical documents are stored. For this purpose particulate matter (PM_{2.5}, i.e. particles with aerodynamic diameter smaller than 2.5 μm) concentration and composition and criteria gaseous pollutants assessment have been carried out.

Simultaneously at this study carried out an aerobiological monitoring in the archive rooms and their data have been compared with chemical and physical results. This work is not reported in this paper but only mentioned in the conclusion.

14.2. Materials and Methods

14.2.1. Monitored site and sampling location description

The Historical Archive of Ca' Granda is located in the center of Milan (Italy) near major traffic axes. Milan is a large city characterized by a high density of residential and commercial premises and a very high volume of vehicular traffic (1-2 millions of vehicles per day in Milan and surroundings). Moreover, it is located in the most industrialized area of Northern Italy.

Physical-chemical samplings were carried out indoor and outdoor in parallel during an intensive field campaign in 2004, April 21st–30th (just before the beginning of refurbishment works in the Archive) aiming at the characterization of particulate matter concentration and composition as well as at the assessment of criteria gaseous pollutants levels. All the rooms have a tile floor and painted walls covered with wooden or metal bookcases.

Passive samplers (Passam®) were used for the determination of integrated concentration levels of SO₂, NO₂, and O₃ (CEN, 1997). These diffusive monitors (Hangartner, 2006) were located in parallel outdoor and at the ground floor for 1 week for O₃ measurement and for 2 weeks for SO₂ and NO₂ (the monitoring with

passive samplers needs longer times to collect a detectable quantity of the latter investigated gases).

The PM sampler location for outdoor measurements (see Fig. 1) was in the garden of the Archive next to main hall. Owing to the large difference in traffic intensity on this road on Sundays, it was decided not to sample on April 25th.

Indoor particulate matter samplings were performed for four consecutive days (April, 21st-24th) in the Capitolo d'Estate room and subsequently in the basement (April, 27th-30th). The samplers were moved from the ground floor to the basement on April 26th so that measurements are not available for that day.

The particulate matter fine fraction was selected because the Capitolo d'Estate hall is three-floor high and wooden bookcases cover the walls so that smaller particles with long residence times might play a major role in degrading objects.

24-hour (from 00:00 to 24:00) PM_{2.5} samplings have been performed using CEN-equivalent samplers (CEN = Comité Européen de Normalisation) operating at a flow rate of 2.3 m³/h and equipped with a size-selective inlet to collect particles with aerodynamic diameter smaller than 2.5 μm. The samplers were checked for comparability during previous campaigns showing a fair agreement (Chiari et al., 2005). Particles have been collected on pre-fired quartz fiber filters and on PTFE filters every other day. The use of both PTFE and quartz fiber filters was requested to achieve the full chemical characterization of the sample. According to the European norm EN12341, before and after the samplings the filters were exposed for 48 hours on open but dust-protected sieve-trays in an air-conditioned weighing room (T=20±1°C and R.H.=50±5%). The gravimetric determination of the mass was carried out using an analytical microbalance (precision 1μg), which is installed and operates in the weighing room. PM₁₀ concentration values here reported have been normalized to standard conditions (0°C and 101.3kPa). Relative humidity and temperature were also monitored using the sensors integrated with the PM samplers.

14.2.2. Analytical Techniques

Elemental analysis. Elemental concentrations were determined by Energy Dispersive X-Ray Fluorescence (ED-XRF) technique that allowed the simultaneous detection of Al, Si, S, Cl, K, Ca, Ti, V, Cr, Mn, Fe, Ni, Cu, Zn, Br, Pb in all samples. Minimum Detection Limits (MDL), at 3σ level, ranged between 2 and 20 ng/cm² (for elements with Z>22) and between 200-300 ng/cm² (for elements with 11<Z<22), corresponding to about 1-10 ng/m³ and 100-150 ng/m³ respectively for a

standard 24-hour sampling. The ED-XRF system and irradiation conditions are described in detail elsewhere (Marcazzan et al., 2004).

Reference thin films (Micromatter, US) were used for the quantitative calibration of the system. A check of the calibration was periodically performed analyzing the NIST standard SRM2783. A program on a personal computer supervised the data acquisition, storage, and reduction; the analysis of X-ray spectra was performed using the Axil code (Van Espen et al., 1977). Experimental overall uncertainties were estimated to be about 10 %.

Analysis of the carbonaceous fraction. Aerosol organic carbon (OC) and elemental carbon (EC) were determined by means of a Thermal-Optical Transmittance (TOT) instrument and by a Thermo-gravimetric Analysis coupled with Fourier Transformed Infrared Spectroscopy (TGA/FT-IR) system. These two techniques are based on the analysis of thermal evolved gases (see chapter 3 and 4).

In the present work a fair agreement was achieved for OC quantified by the two systems, i. e. TGA/FT-IR (chapter 3) and TOT (chapter 4). A good correlation between PM values and OC data is also observable and it is an evidence of OC important contribution to particulate matter mass.

Analysis of ionic components. The water-soluble inorganic fraction was determined by ion chromatography (IC). Major ionic species (NO_3^- , SO_4^{2-} , F^- , Cl^- , NO_2^- , Br^- , $\text{C}_2\text{O}_4^{2-}$, NH_4^+ , Na^+ , K^+ , Ca^{2+} , Mg^{2+}) were quantified.

Anions were analyzed using an instrument obtained by coupling a Perkin Elmer Binary LC Pump 250 and a suppressor by Alltech (Suppressor Module 335). Anions analysis was carried out by means of an Alltech Anion column HC27410 (length 150 mm, internal diameter 4.6 mm) using a solution 1 mM Na_2CO_3 / 3.5 mM NaHCO_3 as eluent at 1mL/min flow rate.

Cations were determined using an ICS-1000 Ion Chromatograph (Dionex) and a Dionex Cation column Ion Pac CS12A (length 250 mm, internal diameter 4 mm). The mobile phase was a 20 mM solution of methane sulphonic acid at 1mL/min flow rate. The solutions for the analysis were obtained after extraction of inorganic ions from particulate matter in an ultrasonic bath. Half of each quartz fiber filter (Pall, 2500QAO-UP) was submitted to three subsequent extractions using Milli-Q (MQ) water. All the solutions (samples, standards, blanks and eluents) were prepared using MQ water. Calibration curves were constructed for each ion. Reagent and filter blanks were analyzed for quality assurance.

More details on analysis and sample preparation are given in chapter 2 and Fermo et al. (2006c) where technique precision and detection limits were also evaluated.

14.3. Results

During the sampling campaign values of temperature (T) and relative humidity (R. H.) were assessed as follows: basement T $22^{\circ}\text{C}\pm 1$ and R.H.= $46\text{-}50\%\pm 1$; and Capitolo d'Estate hall T = $19\text{-}21^{\circ}\text{C}\pm 1$ and R. H. = $35\text{-}36\%\pm 1$ (see Table 14-1).

	Day (April 2007)	T ($^{\circ}\text{C}$)	R. H. (%)
Capitolo d'Estate hall	21	19 ± 1	36 ± 1
	22	20 ± 1	35 ± 1
	23	20 ± 1	35 ± 1
	24	21 ± 1	35 ± 1
Basement	27	22 ± 1	46 ± 1
	28	22 ± 1	47 ± 1
	29	22 ± 1	50 ± 1

Table 14-1: Recorded temperature (T) and relative humidity (R. H.) in the Capitolo d'Estate and the basement

PM2.5 average mass concentration values were $18.2\pm 3.6\mu\text{g}/\text{m}^3$ and $31.3\pm 4.2\mu\text{g}/\text{m}^3$ in the main hall and in the basement hall, respectively; indoor mass concentrations were generally lower than those registered outdoor as can be seen in

Table 14-2. In particular, in the main hall PM2.5 concentration was about one-half than the values registered outdoor, while in the basement PM2.5 levels were high and comparable to outdoor ones.

PM2.5	INDOOR	OUTDOOR	Indoor/Outdoor
Capitolo d'Estate hall	18.2 ± 3.6	37.4 ± 10.6	0.49
Basement	31.3 ± 4.2	38.6 ± 4.4	0.81

Table 14-2: PM2.5 ($\mu\text{g}/\text{m}^3$) indoor and outdoor

As can be seen in Figure 14-2, the PM2.5 composition indoor was dominated by organic matter (here defined $\text{OM}=\text{OC}\cdot 1.6$ as suggested by Turpin et al., 2001) which accounted for 68.5% and 40.9% of the mass measured in the main hall located at ground floor and in the basement, respectively.

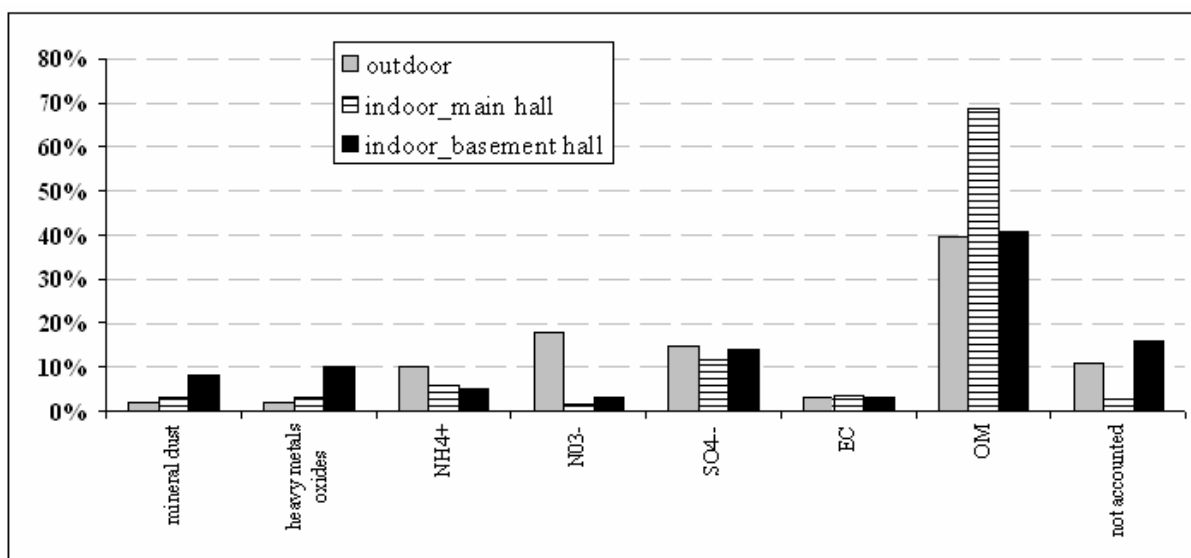


Figure 14-1: Chemical mass balance related to indoor (basement and main hall) and outdoor PM2.5 measurements.

Important contributors to indoor PM2.5 were ions like SO_4^{2-} (11.8% in the main hall and 14% in the basement hall) and NH_4^+ (5-6% in both rooms); in contrast, indoor NO_3^- concentrations were generally low, accounting for 1.5% of the PM mass in the main hall and 3.2% in the basement hall. The ionic component represented one of PM major fractions. Interestingly, indoor concentrations of the mineral component (i.e. oxides of elements with mineral origin like Al, Si, Ca, and Ti) and of the heavy metals oxides component were not negligible. Together these two components explained another 18% of the PM2.5 mass in the basement hall while their contribution in the main hall was limited to 6 % (Figure 14-2).

Another contribution to the chemical composition taken into account was elemental carbon, which was 3.9% in the main hall and 2.9% in the basement hall.

Comparing chemical indoor and outdoor composition, the largest differences were observed for nitrates, whose percentage on PM2.5 outdoor mass was 17.9%.

The elemental concentrations in the main hall were lower than those measured outdoor in agreement with the mass concentration behaviour. In the basement hall both absolute and relative elemental concentrations were enriched in respect to the outdoor environment (Table 14-3 in parts per million and in ng/m^3).

Sulfate concentrations determined by IC were compared with sulfur determined by XRF. For this purpose SO_4^{2-} , IC values were converted into S concentrations. Taking into account both techniques limits and the standard deviations, which in this case represent the variability among the samples, the mean values were in good

accordance suggesting that, in these PM samples, sulfur was present as soluble species.

Gaseous pollutants concentration indoor (main hall, ground floor) and outdoor are reported in Table 14-4.

	ng/m ³			ppm		
	outdoor	indoor main hall	indoor basement	outdoor	indoor main hall	indoor basement
Al	46 ± 8	29 ± 1	54 ± 16	1253 ± 365	1863 ± 566	2109 ± 480
Si	182 ± 97	92 ± 3	523 ± 139	5038 ± 3155	5847 ± 1852	20759 ± 6789
S	1372 ± 473	889 ± 334	1371 ± 544	36084 ± 10266	53028 ± 5006	53300 ± 17987
Cl	53 ± 37	14 ± 4	18 ± 13	1380 ± 854	912 ± 476	720 ± 550
K	160 ± 82	98 ± 5	510 ± 116	4438 ± 2704	6156 ± 1473	20223 ± 5861
Ca	105 ± 20	133 ± 10	250 ± 223	2865 ± 830	8443 ± 3016	9567 ± 8167
Ti	9 ± 9	7 ± 5	56 ± 14	261 ± 268	400 ± 182	2238 ± 703
Cr	3 ± 1	2 ± 1	5 ± 4	83 ± 39	128 ± 10	202 ± 176
Mn	55 ± 82	13 ± 1	325 ± 158	1616 ± 2470	808 ± 249	13007 ± 7046
Fe	507 ± 339	304 ± 12	1680 ± 630	14229 ± 10773	19255 ± 6255	66947 ± 29050
Cu	22 ± 7	12 ± 4	48 ± 10	594 ± 244	729 ± 12	1911 ± 517
Zn	80 ± 27	60 ± 11	113 ± 56	2154 ± 682	3657 ± 409	4375 ± 1923
Br	5 ± 2	4 ± 1	4 ± 1	136 ± 34	256 ± 10	173 ± 36
Pb	27 ± 8	20 ± 1	56 ± 21	722 ± 240	1254 ± 354	2159 ± 690

Table 14-3: Elemental concentration (ng/m³ and ppm) indoor (main hall, ground floor) and outdoor

Gaseous Pollutant	INDOOR	OUTDOOR	Sampling period
NO₂	28.5	71.3	14 days
SO₂	< 0.4	1.6	14 days
O₃	< 2	32	7 days

Table 14-4: Gaseous pollutants concentration (µg/m³) indoor (main hall, ground floor) and outdoor

Another important parameter to be considered is the aerosol acidity. In order to evaluate PM acidity, it was verified if ammonium concentration (expressed in nmol in 1 mg of PM) was enough to neutralize both nitrate and sulfate. The correlation curve obtained considering all the filters is shown in Figure 14-2. The high slope indicated that there was some acidity not neutralized by ammonium. For each single filter, the outdoor samples were characterized by higher acidity values than indoor filters.

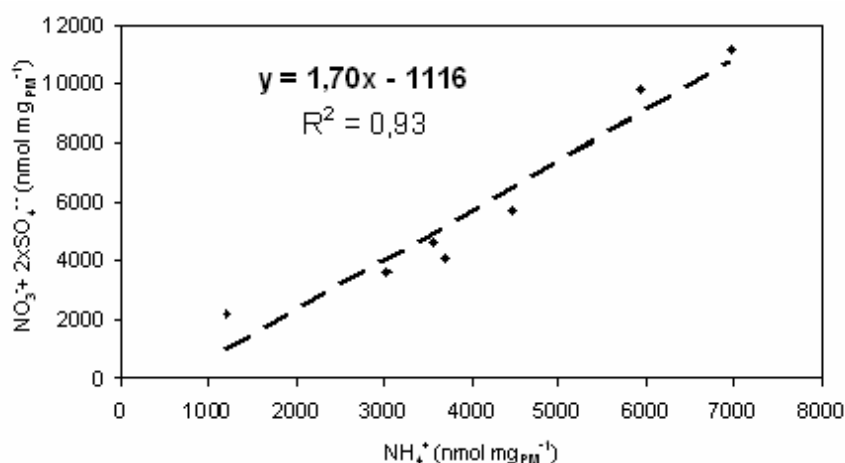


Figure 14-2: Correlation between NH_4^+ and $(\text{NO}_3^- + 2\text{SO}_4^{2-})$ to assess acidity in PM_{2.5} samples

14.4. Discussion

The legislation in force in Italy (MIBAC, 2001) refers to total suspended particulate (TSP) and PM₁₀ limit values are suggested to be in the range 20-30 $\mu\text{g}/\text{m}^3$. Results obtained during PM monitoring campaigns carried out in Milan (Lonati et al., 2005; Marcazzan et al., 2001) gave an average PM₁₀ to PM_{2.5} ratio of 0.6-0.8 (depending on the season). In this work only PM_{2.5} was measured because of its longer residence times in air. In the Historical Archive many documents, like books, are stored at the upper levels and can be damaged by PM_{2.5}. Considering these experimental results, it was possible to make the hypothesis that the limit value was likely exceeded in the basement while in the Capitolo d'Estato the particulate matter concentration was near the limit.

The higher OM concentration measured in the Capitolo d'Estato was likely due to the presence of archival materials made of paper, which are stored in this hall, as the debris of these paper documents might have been responsible for this.

The unaccounted mass, also reported in Figure 14-2, was likely explained by minor components and water; this hypothesis was enforced by the higher percentage of unaccounted mass in the basement (15.9%) where high relative humidity levels were registered. It is noteworthy that the EC percentage was comparable in the two halls and it was also similar to the outdoor concentration. As well known, this pollutant in urban environments can be considered as a marker for traffic and therefore it has a prevalent outdoor source. The interest for elemental carbon was due to its role in soiling/blackening of surfaces (Ghedini et al., 2006).

Looking at the indoor composition of traffic-related pollutants, it seemed that pollutants were transported from outdoor and subsequently accumulated indoor. In the basement hall, two small windows at street level are kept open to help air penetration and this allows pollutants entrance from outdoor. It is worth noting that metals such as iron and copper showed higher concentrations indoor (in both halls) than outdoor. It is reported in the literature (Shahani et al., 1987) that trace concentrations of metal catalysts, such as copper and iron, can decompose peroxide groups due to O_3 and initiate oxidation reactions that can lead to cellulose chain scission.

Unlike the other components, nitrate concentration did not increase in the basement hall; this result might be due to the abundance of coarse ($2.5\mu m < d_{ac} < 10\mu m$) nitrate particles instead of fine particles. In the coarse mode, nitrate generally originates from the reaction on pre-existing particles (e.g. reaction of HNO_3 and $CaCO_3$ as described in Yao et al., 2003). Moreover, the high humidity level measured in the basement hall might also cause the hygroscopic increase in size of particles containing NO_3^- . If nitrates particles, after their increasing in size, are included in the coarse mode, they are not anymore detected in $PM_{2.5}$ (only $PM_{2.5}$ fraction was measured in this work).

PM ionic component has been recently deeply studied in an archaeological museum (Mouratidou et al., 2004) where sulfate was also found to be the dominant ion. In our case high SO_4^{2-} indoor concentrations were probably due to external penetration but also to some indoor sources such as the deterioration of the interior plaster walls (De Bock et al., 1996; Mouratidou et al., 2004).

Recently, the U.S. Environmental Protection Agency (EPA) has evaluated the possibility of listing acid aerosols as criteria pollutants. Acids, together with other catalysts that can be present in particulate matter (i. e. metal ions) can mediate ionic reactions of hydrolytic nature that lead to the material deterioration. As regards libraries, some scientific investigations aimed at highlighting how the technology used to produce paper can also influence its conservation (Shanani et al., 1987). Actually, a paper formulated for stability should contain an alkali filler, such as calcium carbonate, in order to neutralize acidity. In this research some acidity in the

aerosol was found that was not neutralized by ammonium. Together with other pollutants this acidity can favour the degradation of the paper.

The gaseous pollutants measured in this campaign were the same suggested as indicators of the air quality in the museums (MIBAC, 2001); SO₂ and O₃ indoor concentrations were very low and only NO₂ exceeded the provisional threshold limit set at 5-10 ppb (see Table 4). It is worth noting that high indoor concentration of NO₂ might be produced during the decomposition of pyroxylin in book bindings (Brimblecombe, 1990).

14.5. Conclusions

On the base of the experimental results we can conclude that the air quality in the Capitolo d'Estate hall is fairly good and it is not so influenced by the outdoor pollution. On the contrary the ambient conditions in the basement hall are quite worrying because of high relative humidity and PM concentration. Actually, in this hall the air stagnation favours pollutants accumulation. Our data evidenced that the microflora can potentially be the main cause of damage in the Ca' Granda Historical Archive and that the outdoor environment can be a source of contamination. The situation can be greatly improved by monitoring and controlling the ambient conditions (Laguardia et al., 2005a; 2005b).

Acknowledgment

I'm grateful to Francesca Capitelli, Claudia Sorlini and Elisabetta Zanardini (University of Study of Milan) for the aerobiological data

References

- Brimblecombe (1990) *Atmos. Environ.*, 24B, 1-8.
- Camuffo et al. (1999) *Sci. Total Environ.*, 236, 135-152
- Camuffo et al. (2001) *Atmos. Environ.*, 35, S127-140
- Cappitelli et al. (2005) *Crit. Rev. Microbiol.*, 31, 1-10
- Chiari et al. (2005) *X-Ray Spectrom.*, 34, 323-329
- De Bock et al. (1996) *Environ. Sci. Technol.*, 30, 3341-3350
- Fantuzzi et al. (1996) *Sci. Total Environ.*, 193, 49-56
- Fermo et al. (2006a) *Atmos. Chem. Phys.*, 6, 255-266.
- Fermo et al. (2006b) *Chem. Engineering Trans.*, 10, 83-88.

- Fermo et al. (2006c) *Chem. Engineering Trans.*, 10, 203-208.
- Ghedini et al. (2006) *Environ. Sci. Technol.* 40, 939-944
- Gysels et al. (2004) *J. Cult. Heritage*, 5, 221-230
- Hangartner (2006) *Gefahrstoffe Reinhaltung der Luft*, 66, 58-61
- Yao et al. (2003) *Atmos. Environ.*, 37, 2991-3000
- Laguardia et al. (2005a) *Appl. Surf. Sci.*, 252, 1159-1166
- Laguardia et al. (2005b) In 14th Triennial Meeting ICOM-CC, The Hague, 12-16 September 2005, Preprints. James & James (Science Publishers) Ltd., London, Vol. I, pp. 193-198.
- Lonati et al. (2005) *Atmos. Environ.*, 39, 1925-1934
- Marcazzan et al. (2001) *Atmos. Environ.*, 35, 4639-4650
- Marcazzan et al. (2004) *X-Ray Spectrom.*, 33, 267-72
- MIBAC, 2001 *Atto di indirizzo sugli standard museali*, Ministero per i Beni e le Attività Culturali (DL 10/05/2001 N 238)
- Mills et al. (1994) *The organic chemistry of museum objects* Butterworth-Heinemann, Oxford
- Mouratidou et al. (2004) *Atmos. Environ.*, 38, 4593-4598
- Nazaroff et al. (1990) *Environ. Sci. Technol.*, 24, 66-77
- Owen et al. (1992) *Atmos. Environ.*, 26A, 2149-2162
- Pavlogeorgatos (2003) *Build. Environ.*, 38, 1457-1462
- Righi et al. (2002) *Sci. Total Environ.*, 286, 41-50
- Schieweck et al. (2005) *Atmos. Environ.*, 39, 6098-6108
- Shanani et al. (1987) *American Scientist*, 75, 240-251
- Turpin et al. (2001) *Aerosol Sci. Technol.*, 35, 602-610
- Van Espen et al. (1977) *Nucl. Inst. Meth.*, 142, 243-250

15. Particulate matter in Pietà Rondanini (by Michelangelo) storage room - Castello Sforzesco Museum, Milan

15.1. Introduction

During their long-term stay in museums, galleries, churches or in microenvironments, such as showcases and storage boxes, the exhibited artworks are threatened by a number of different factors such as physical, chemical and biological (Brimblecombe, 1990; Nazaroff et al., 1993). Particulate matter is harmful for works of art because it may cause soiling and/or chemical damage, depending on its size and chemical composition. The deposition of fine particles onto surfaces is comparably significant with the deposition of coarse particles (Nazaroff et al., 1990). The difference is that coarse particles settle onto upward facing surfaces under the influence of gravity, whereas fine particles deposit on surfaces of any orientation by a combination of advective diffusion and thermophoresis (Nazaroff and Cass, 1989). Further damage can be caused when chemical reactions occur involving gases or components of the deposited particles, such as Fe- and Mn-catalyzed oxidation of S(IV)-compounds to sulfates or sulfuric acid (Brandt and van Eldik, 1995), ammonium sulfate formation, etc. Therefore, high particle concentrations should be avoided in museums (Camuffo, 1998).

Atmospheric particles composition is of unquestionable importance in the study of the damage produced on building materials of artistic interest, since it directly influences the specific characteristics and entity of the degradation mechanism occurring on the cultural heritage.

The main environmental damage effect on the carbonate structural components and binders used in ancient masonry is the transformation of calcium carbonate into gypsum due to wet and dry deposition of SO₂ (Camuffo et al., 1983). Grey-to-black crust formation is produced by gypsum crystals and atmospheric deposition, including carbonaceous particles which, because of their high specific surface and heavy metal content, act as catalytic support to the heterogeneous oxidation of SO₂ (Benner et al., 1982).

In Figure 15-1 it is given an overview (Schieweck et al. 2005) about influences and interactions between human health and works of art, respectively, and indoor and outdoor pollutants as well as climatic parameters.

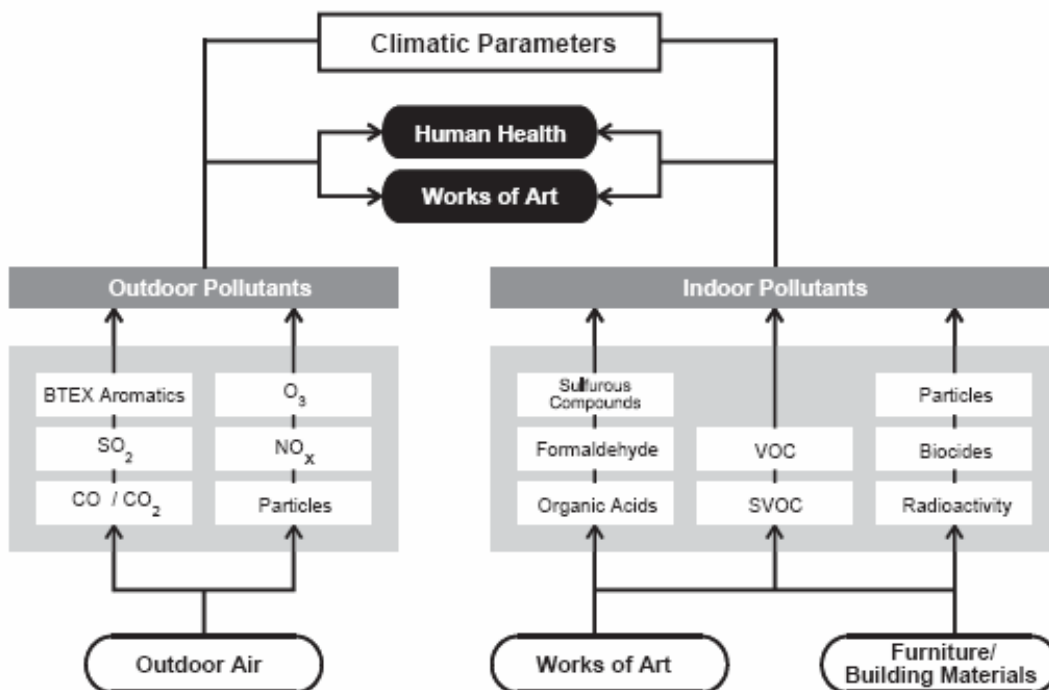


Figure 15-1. Outdoor and indoor emission sources affecting human health and works of art in cultural institutions (Schieweck et al. 2005)

In this work we have monitored and characterized the particulate matter in Pietà Rondanini (by Michelangelo) storage room - Castello Sforzesco museum.

Recently (June 2004) the statue has been cleaned. In order to identify the link between air quality and risk for the work of art, we have sampled the particulate matter in the storage room in order to defined the air quality parameters.

To identify the main sources of particulate matter simultaneously with indoor sampler we have monitored the outdoor air quality.

15.2. Experimental

15.2.1. Sampling and chemical characterization

We have sampled from July 20th 2004 to February 2nd 2005, in two sites, the first one placed in the storage room near the statue, the second one placed outdoor.

According to the European norm EN12341, before and after the samplings the filters were exposed for 48 hours on open but dust-protected sieve-trays in an air-conditioned weighing room ($T=20\pm 1^{\circ}\text{C}$ and $R.H.=50\pm 5\%$). The gravimetric determination of the mass was carried out using an analytical microbalance

(precision $1\mu\text{g}$), the uncertainty of gravimetric measurements was $\pm 2\mu\text{g}/\text{m}^3$ equivalent and the limit of detection was $2\mu\text{g}/\text{m}^3$.

The determination of ionic compounds was carried out by ion chromatography technique, the detail of this technique and the samples preparation are reported in chapter 2.

The carbon analyses was carried out by Thermo Gravimetric Analysis (TGA) coupled with Spectrophotometer Infrared (FT-IR), the details of this analyses are reported in chapter 3 and in Fermo et al. 2006.

The morphological characterization coupled with chemical composition analyses was carried out with Secondary Electron Microscopy (SEM, Stereoscan 420, Leika) coupled with microanalyses X energy dispersive (EDS, QX200, Oxford).

15.3. Results and discussion

15.3.1. Mass concentration

In both seasons (summer: from July to September, winter: from October to January), indoor concentrations of PTS were higher than the outdoor concentrations. During the daytime (when the museum is open) this difference is greatest than during the night time (Figure 15-2).

Outdoor during winter time the concentrations of PTS were higher than during summer time. PTS average concentrations during the winter increase about of $20\mu\text{g}/\text{m}^3$ (summer: daytime $44\mu\text{g}/\text{m}^3$ nighttime $68.6\mu\text{g}/\text{m}^3$, winter: daytime $64.1\mu\text{g}/\text{m}^3$ nighttime $84.7\mu\text{g}/\text{m}^3$). We have observed an equivalent increment in the museum room too, indeed during daytime the concentration has been $95.5\mu\text{g}/\text{m}^3$ during the summer and $116.0\mu\text{g}/\text{m}^3$, while in the night time the concentrations have passed from $47.6\mu\text{g}/\text{m}^3$ to $70.9\mu\text{g}/\text{m}^3$.

In both sites we observe the same PTS concentration increase, the outdoor air pollution influences the indoor concentration, because room is not sufficiently isolated. The air exchange is strongly favored from one window not perfectly closed and from one door that sometime is open.

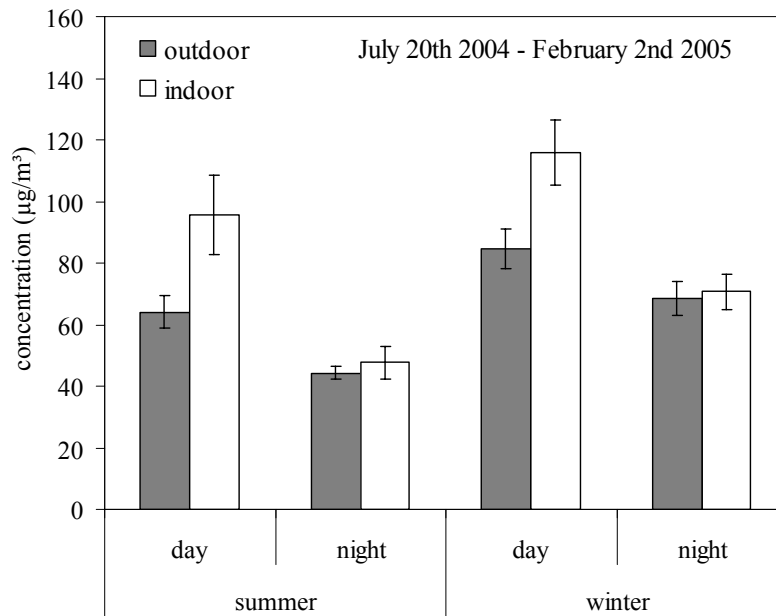


Figure 15-2: PTS concentration ($\mu\text{g}/\text{m}^3$) season average during the daytime and nighttime, indoor and outdoor.

Indoor the difference between the concentration during the daytime and the concentration during the nighttime is higher than the difference observed outdoor (Figure 15-3). The presence of the visitors contributes to the grow of the PTS concentration for two reasons: 1) they carry in the particles through their clothes and shoes and 2) re-suspended the particles from the floor.

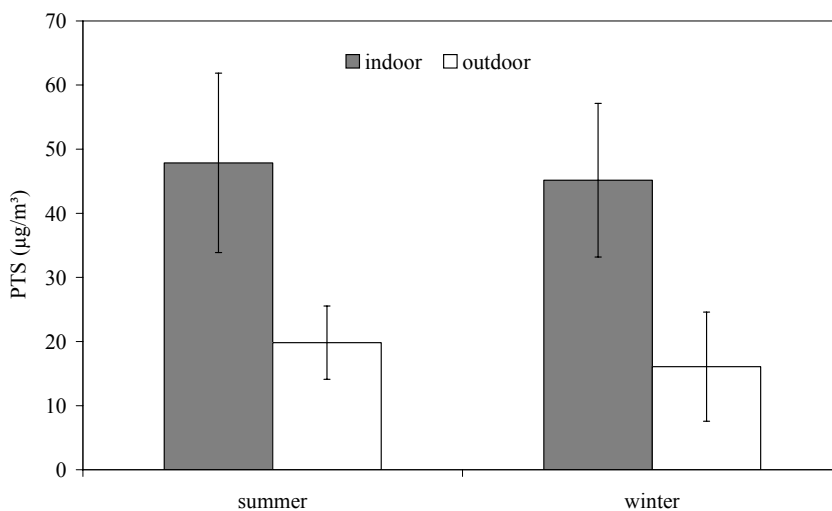


Figure 15-3: Differences of PTS concentration ($\mu\text{g}/\text{m}^3$) between nighttime and daytime, in outdoor and in indoor

15.3.2. Chemical composition

Through the knowledge the particulate matter chemical composition it is possible to identify the main sources and the transport and diffusion processes.

The main component of particulate matter are ions, particularly ammonium nitrate and sulphate, and carbonaceous compounds. Sulphate is particularly dangerous for cultural heritage, indeed the surfaces adsorb the *soot* (a complex mixing of black carbon and organic compounds) so favor the deterioration, known as *soiling* (Brimblecombe 1990).

The knowledge of the nitrate, sulphate and ammonium concentration allow the pH estimation and consequently the risk for the material. The main ions (nitrate, sulphate, ammonium, calcium and sodium) explain about the 45% of the total mass (Figure 15-4, Figure 15-5).

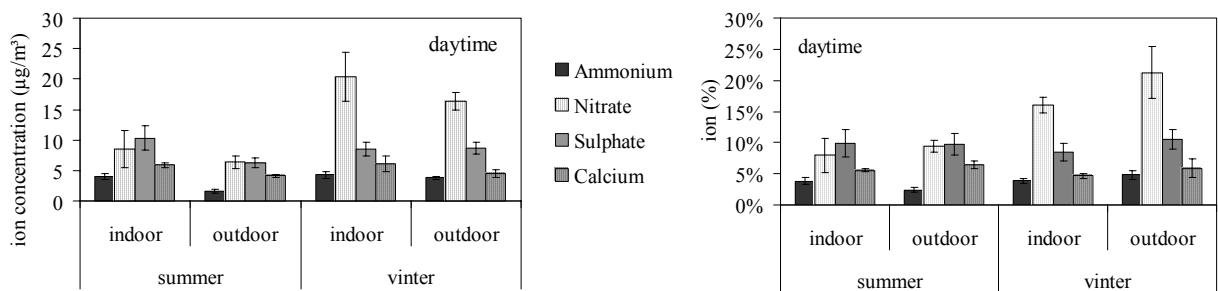


Figure 15-4: main ions average season concentration (in $\mu\text{g}/\text{m}^3$ and in %) during daytime

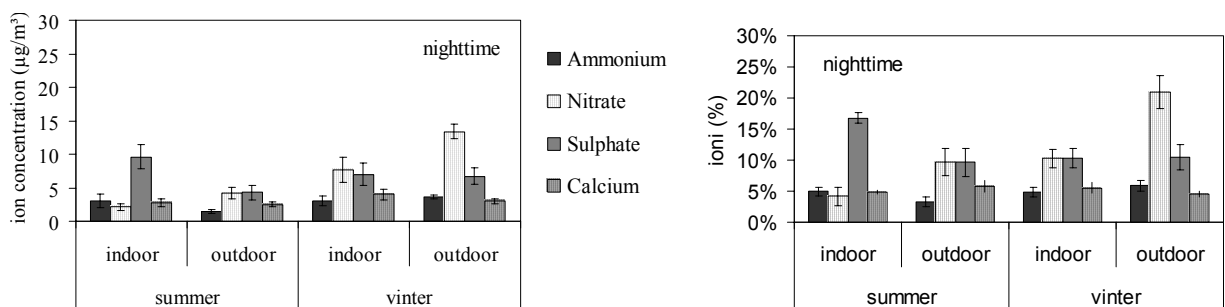


Figure 15-5: main ions average season concentration (in $\mu\text{g}/\text{m}^3$ and in %) during nighttime

Sulphate, ammonium and calcium, in indoor, show highest concentrations than outdoor, but the higher mass concentration in the room is probably due to the increase of the carbonaceous particles.

In both site (outdoor and indoor) the percentage compositions are similar, the outdoor air is the main source of the indoor particulate matter.

The ratio between the indoor and outdoor concentration (I/O) can allow to individuate the PTS additional sources in the room (Wallace, 1996). During summer the I/O for ammonium is 1.58. Probably there is an additional source of ammonium or ammonia gas in the room (this source can be the visitor).-The higher concentration of ammonium in the room decreases the pollution acidity. Outdoor pH is lower than outdoor, especially during winter time.

The analyses of carbonaceous particles is very important in the degradation process of cultural heritage study. The *soiling* process is due to a *soot* particle and the high specific surface of the carbonaceous particle and heavy metal content, act as catalytic support to the heterogeneous oxidation of SO₂ (Benner et al., 1982).

The more detail of the carbonaceous particle origin is describe in to this volume introduction and in chapter 3 and 4 .

The Organic Carbon (OC) value can be converted Organic Material (OM) using an average mean molecular-to-carbon ratio of 1.6 as proposed by Turpin and Lim (2001) for urban aerosol.

In Table 15-1: OC and EC average concentration (in µg/m³ and in %) in the two sampling site we have reported the OC and EC concentration measured in outdoor and in indoor; the carbonaceous data is available only for winter season.

	OC				EC				OC/EC
	µg/m ³		%		µg/m ³		%		
Outdoor daytime	22.3	(±2.9)	22.3%	(±1.0%)	3.6	(±0.7)	3.7	(±0.5%)	6.0
Outdoor nighttime	21.7	(±3.2)	29.4%	(±2.5%)	2.8	(±0.2)	4.5%	(±0.8%)	6.5
Indoor daytime	43.6	(±7.25)	21.7%	(±1.4%)	7.5	(±0.9)	5.6%	(±0.3%)	5.6
Indoor nighttime	29.4	(±4.8)	38.5%	(±2.9%)	4.3	(±0.3)	6.2%	(±0.6%)	6.2

Table 15-1: OC and EC average concentration (in µg/m³ and in %) in the two sampling site, during the winter season.

Indoor concentration is higher than outdoor (Figure 15-6), this trend confirm that in the room there is a particulate accumulation.

In the Figure 15-6 and Figure 15-7 we have reported the mass closure of particulate matter for winter time; the not explained mass is due to metal oxide not determined and waters.

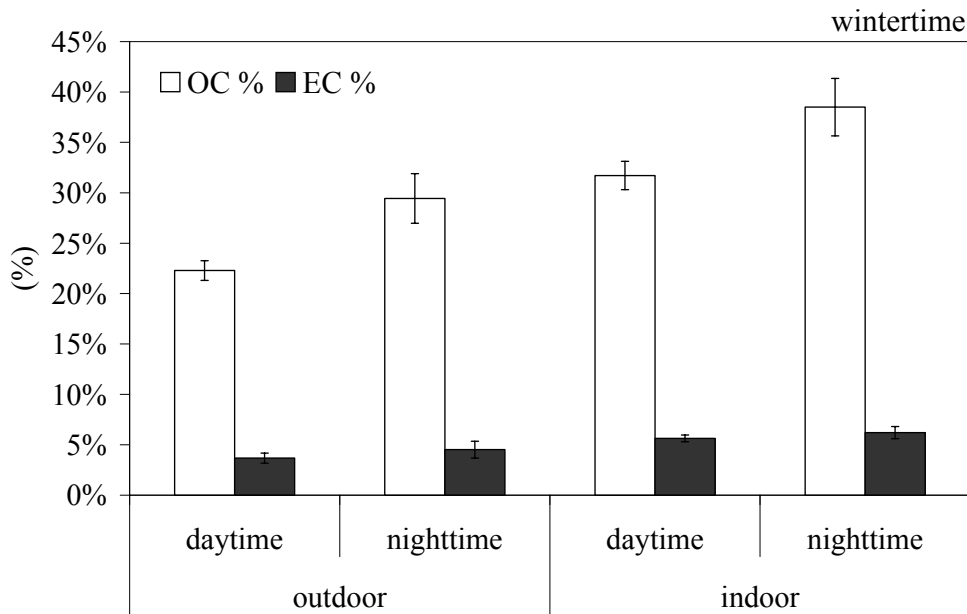


Figure 15-6: OC and EC average percentage outdoor and indoor

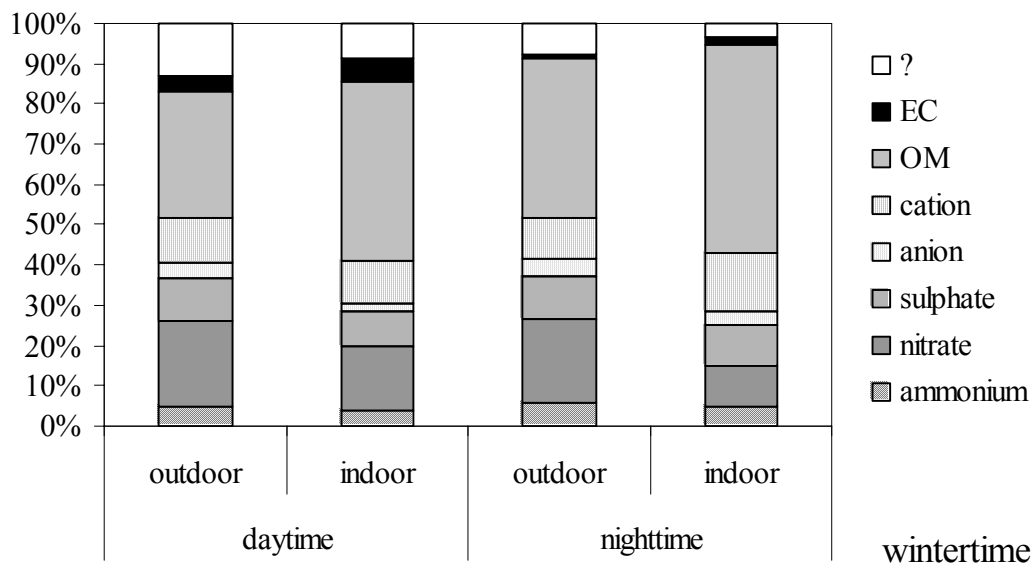


Figure 15-7: particulate matter composition during the winter season indoor (up) and outdoor (down)

15.3.3. Electronic microscopic analyses

The electronic microscopy analyses (SEM) coupled with microanalyses have pointed out the presence of carbonaceous nano-particles (diameter less of $0.5\mu\text{m}$) both indoor and outdoor. A lower number of particles, typically coming from combustion processes, are characterized by high mobility and higher persistence time in the atmosphere, so it is easy that this particulate can be transported indoors. The nano carbonaceous particles in the room confirm the air exchange with outdoor.

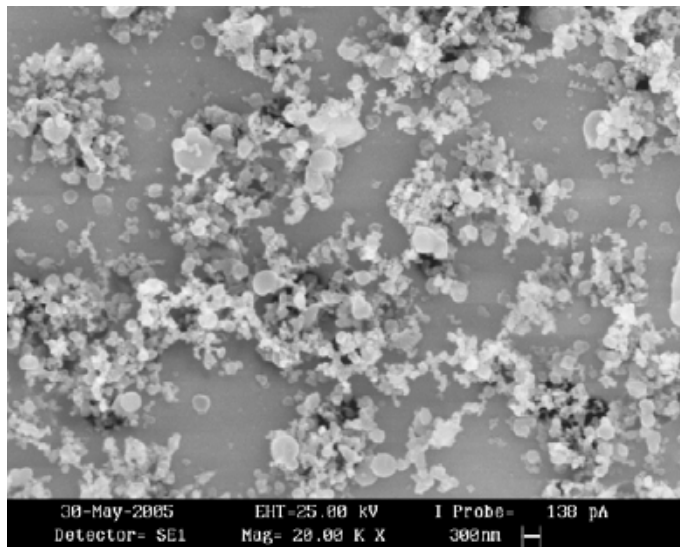


Figure 15-8: carbonaceous particles observed indoors (source ARPA Lombardia)

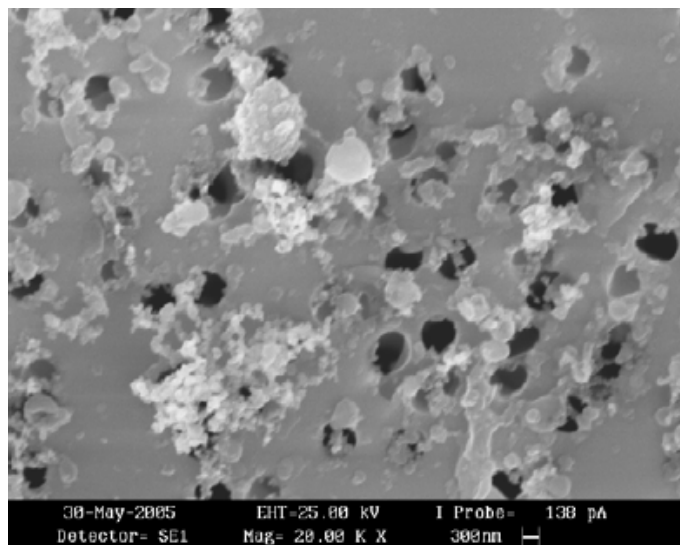


Figure 15-9: carbonaceous particles observed outdoors (source: ARPA Lombardia)

We have been observed the mineral and biological particles (Figure 15-10, Figure 15-11, Figure 15-12).

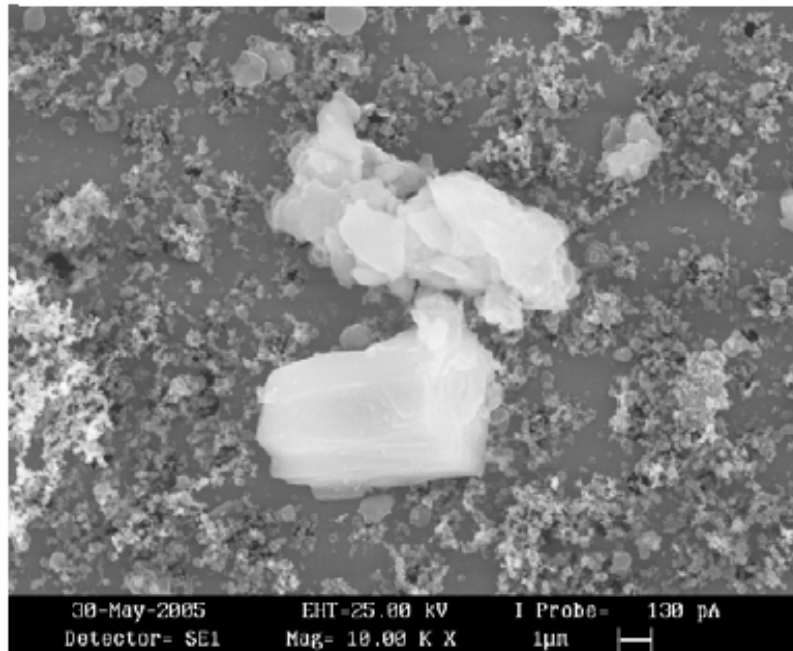


Figure 15-10: mineral particles in indoor samples (source: ARPA Lombardia)

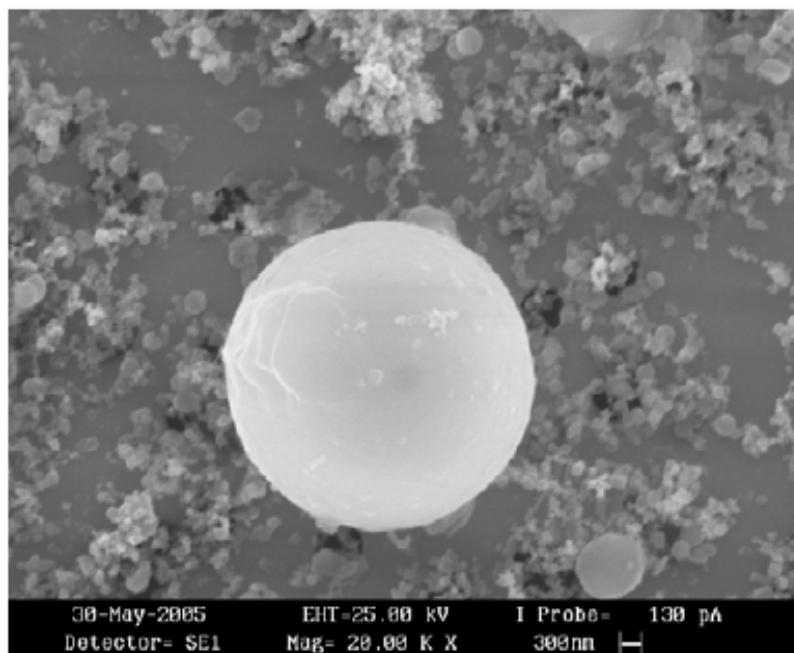


Figure 15-11: anthropogenic particle containing iron, observed in indoor sample (source ARPA Lombardia)

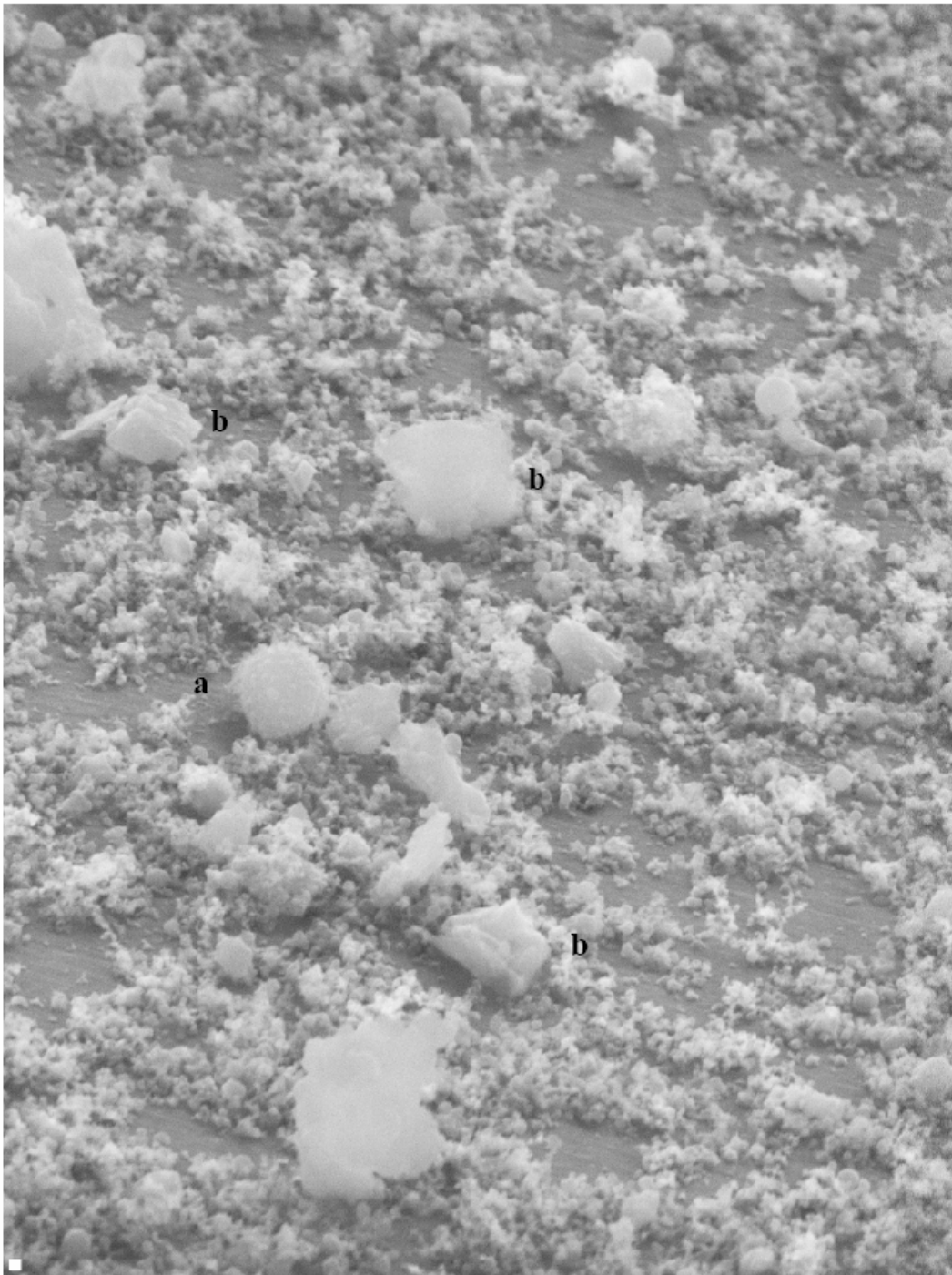


Figure 15-12: particles observed indoor sample. In the background there are much sub micronic carbonaceous particles. (a) biological particles, (b) mineral particles (source ARPA Lombardia)

15.4. Conclusion

The Pietà Rondanini storage room is strongly influenced from outdoor ambient. The air exchange is strongly favored from one window not perfectly closed and from one door that sometime is open.

The presence of the visitors favors the grow of PTS concentration. Is the visitors presence and not the number of visitor to influence the air quality in the room. We have not observed a correlation between a visitor number and PTS concentration.

The indoor particulate matter composition is similar to outdoor composition. The higher value of indoor particulate concentration is explained with a grow of the ammonium and carbonaceous particle. In both sites (in and outdoor) the particles are acid, so this is a potential risk for the statue material.

The high concentration of carbonaceous particles has been observed with the carbon fraction analyses and with electron microscopy analyse. The carbon particulate can represent a potential risk for the statue mainly because it generates the *soiling* process.

Acknowledgment

I would like to acknowledge V.Gianelle (ARPA Lombardia) for the helpful suggestions

References

- Brimblecombe (1990) *Atmos. Environ.*, 24B, 1-8.
- Fermo et al. (2006a) *Atmos. Chem. Phys.*, 6, 255-266.
- Turpin et al. (2001) *Aerosol Sci. Technol.*, 35, 602-610
- Wallace (1996) *J. air & waste management association* 46 (2): 98-126

16. Conclusions

Aerosol is of central importance for atmospheric chemistry and physics, for the biosphere, the climate and public health.

The primary parameters that determine the environmental and health effects of aerosol particles are their concentration and chemical composition.

In this work we have developed the analytical techniques to study particulate matter composition. The knowledge of PM composition can be useful to identify the main PM sources, the health risk and the formation or deposition/removal processes.

These analytical techniques have been applied in some field campaign: we have studied the urban particulate matter, the main transport processes sampling in remote sites, the PM concentration and composition in the rural site to estimate the background levels. At the moment EU limits concern only PM₁₀ fraction, but the interest for sub-micron sized particles (PM₁) is increasing for their effects on human health and on the environment. We have carried out the first national campaign to study this fraction in three urban sites in Italy. Moreover, for a good comprehension of the complex atmospheric phenomena we have sampled at high resolution time.

In the chapter 2 we reported the extraction procedure for ion quantification, to obtain the good recovery of all ions, the lowest detection limits and to use less portion of sample as possible, to have the possibility to make a large number of analyses on the same sample.

The carbonaceous fraction analysis is still object of the discussion in the scientific community, indeed there is not a reference method for this analysis. The key point of this analysis is to separate the main components of carbonaceous particles: organic carbon (OC) and elemental carbon (EC). In the chapter 3 we proposed a new analytical method based on the couple between Thermo Gravimetric Analysis (TGA) with Spectrophotometer Infrared (FT-IR) and in chapter 4 we have reported the intercomparison between this techniques and other analytical method, TOT method by Sunset Instrument. A good comparability is achieved for TC and OC while the agreement is poorer for EC, in accordance with what previously observed by other authors.

In the recent years the studies involving the Water Soluble Organic Compounds (WSOC) are increasing because they represent an important portion of OC and can

be an important marker of the origin of organic compounds (i.e. biomass burning, ageing). In the chapter 5 the new analytical technique for WSOC quantification using TOT method is reported; the validation of this analytical procedure with a most diffused technique (TOC analyses) is still in progress.

In the same chapter we discuss around an hypothetical error in the OC and EC quantification using TOT method: indeed removing the soluble compounds from the sample the contribution of pyrolytic carbon (PyC) decreases and this allows a good determination of the elemental fraction.

Nowadays, very few data on the possible contribution of particles emitted by residential wood combustion in Italy are available. In the chapter 7 we proposed a new analytical technique for levoglucosan quantification. Levoglucosan is an anhydrosugar specific marker for this source. Usually the anhydrosugar in atmospheric aerosol samples is performed by gas chromatography - mass spectrometry (GC-MS), while we have used High Performance Anion Exchange Chromatography coupled with amperometric detection (HPAEC-PAD). This technique was shown to be a high sensitive, relatively simple analytical technique for separation and quantification of anhydrosugars in aqueous extract of aerosol particle from biomass combustion. The intercomparison with GC-MS has shown a good comparability for the two techniques. Unlike traditional methods, there is not need for prior chemical derivatization or other complex sample preparation, the extraction procedure for ions quantification is suitable also for this method.

The field campaigns were performed thanks to the collaboration between different partners, the Physics Department (University of Genoa), the General Applied Physics Institute (University of Milan), the Physics Department (University of Florence), the National Institute of Nuclear Physics (Florence) and the ARPA Lombardia are the most important.

In Lombardy region atmospheric pollution due to airborne fine particles is an environmental issue of great concern: air quality standards for PM₁₀ are frequently exceeded, especially in Milan. In the ParFiL project by Regione Lombardia we have determined the carbonaceous fraction in about 1000 samples coming from ten different sites (chapter 8) in the Lombardy Region. The carbonaceous compounds are the main constituent of the particulate matter. During the summer the concentrations is quite similar in all urban sites, the average of the concentrations are for the OC 7.4 $\mu\text{g}/\text{m}^3$ and for EC 1.9 $\mu\text{g}/\text{m}^3$. During the winter the concentrations are doubled: OC is 15.3 $\mu\text{g}/\text{m}^3$ and EC is 4.2 $\mu\text{g}/\text{m}^3$. Milano and Mantova concentration result more correlated in both seasons and the background concentrations measured at Mantova BF resulted strong correlated with the urban concentrations.

Using the EC tracer method and the EC concentration in Como (the traffic site) we

have estimated that, in the urban site, about the 50% of OC is due to secondary formation; only Milano and Como show a percentage of primary OC higher than the secondary OC. An exhaustive discussion of this method for secondary OC estimation and its comparison with another method (PMF model) is reported in chapter 13).

Using levoglucosan as a marker for wood combustion we have estimated the percentage of OC due to this source. In four urban sites, taken as example (Milano, Cantù, Mantova and Sondrio), during the winter time Milan show the lowest value of the OC due to wood combustion (25%), while Sondrio show the highest value (50%) (section 8.3). This preliminary study points out that the magnitude of this source is strong.

The transport phenomena have been studied sampling in two remote sites: Monte Cimone, located in the Apennines (2165m asl) (chapter 10) and Bormio S.C. located in the Alps (2200m asl) (chapter 9). With the APCA model we have estimated that the main percentage (60%) of particle on the Monte Cimone site is due to anthropogenic sources.

The physical-chemical characterization of PM₁₀ with high temporal resolution campaign (chapter 12) allowed the individuation of the variation of the composition of the PM in the different hours of the day, and also the different magnitude of the sources during the day. The high time resolution sampling allows the study of the atmospheric phenomena (i.e. secondary formation, transport) otherwise hardly appreciable.

Sub-micron sized particles (PM₁) are of increasing concern owing to their effects on human health and on the environment. To perform the first large scale assessment of sub-micron sized aerosol concentrations, composition and sources, two monitoring campaigns (summer and winter) at three urban sites in Italy (Milan, Florence and Genoa) with different characteristics were performed (chapter 11). The major contributions are due to organic matter (about 30% in summer and 50 % in winter) and ammonium sulphate (about 10 % in winter and 40 % in summer). During the cold season nitrates also contribute up to 30 % in Milan (lower contributions were registered at the other two urban sites).

The interest for the effects of air pollution on indoor cultural heritage is increasing. We have studied two different sites: the Ca' Granda Historical Archive (chapter 14) and the Pietà Rondanini (by Michelangelo) storage room. In one of the two room monitoring in the Ca' Granda resulted that the air quality is fairly good and it is not so influenced by the outdoor pollution. On the contrary the ambient conditions, in the second one, are quite worrying because of high relative humidity and PM concentration.

The Pietà Rondanini storage room is strongly influenced from outdoor ambient. The presence of the visitors favours the growth of pollutants concentrations, the indoor particulate matter composition is similar to outdoor composition. The particulate matter acidity represents a potential risk for the statue.

ANDREA PIAZZALUNGA

[publications]

- 1. Chemical-physical and microbiological measurements for indoor air quality assessment at the Cà Granda historical archive, Milan (Italy)**
Capitelli F., Fermo P., Vecchi R., Piazzalunga A., Valli G., Zanardini E., Sorlini C
Indoor Air, submitted
- 2. The impact of fireworks on airborne particles: results of a case study.**
Vecchi R., Bernardoni V., Cricchio D., D'Alessandro A., Fermo P., Lucarelli F., Nava S., Piazzalunga A., Valli G. (2007).
Atmospheric Environment, in press
- 3. A mass closure and PMF source apportionment study on the sub-micron sized aerosol fraction at urban sites in Italy**
Vecchi R., Chiari M., D'Alessandro A., Fermo P., Lucarelli F., Mazzei F., Nava S., Piazzalunga A., Prati P., Silvani F., Valli G..
Atmospheric Environment, under second revision
- 4. A TGA/FT-IR study for measuring OC and EC in aerosol samples.**
P. Fermo, A. Piazzalunga, R. Vecchi, G. Valli, M. Ceriani,
Atmospheric Chemistry and Physics, 6, 255-266, 2006
- 5. Characterization of atmospheric aerosols at Monte Cimone, Italy, during summer 2004: source apportionment and transport mechanisms.**
F. Marengo, P. Bonasoni, F. Calzolari, M. Ceriani, M. Chiari, P. Cristofanelli, A. D'Alessandro, P. Fermo, F. Lucarelli, F. Mazzei, S. Nava, A. Piazzalunga, P. Prati, G. Valli and R. Vecchi
Journal of Geophysical Research, 111, D24202, 2006
- 6. PM mass concentration and chemical composition in the alpine remote site Bormio – San Colombano (N. Italy; 2,200 m a.s.l.)**
C. A. Belis, P. Vannini, G. Moraschetti, P. Fermo, A. Piazzalunga, G. Mognaschi, V. Gianelle and R. Vecchi
Chemical Engineering transaction vol. 10, 65 – 70, 2006
- 7. Assessment of Organic and Elemental Carbon in Atmospheric Aerosol Samples**
P. Fermo, A. Piazzalunga, F. Martino, R. Vecchi, G. Valli, A. D'Alessandro
Chemical Engineering transaction vol. 10, 83-88, 2006
- 8. Set-up of Extraction Procedures for Ions Quantification in Aerosol Samples**
P. Fermo, A. Piazzalunga, R. Vecchi, G. Valli,
Chemical Engineering transaction vol. 10, 203-208, 2006
- 9. Monitoraggio e caratterizzazione del particolato nella sala**
Fermo P., Piazzalunga A., Gianelle V., Mognaschi G., Rindone B., Bolzacchini E., Ferrero L., Perrone M.G.,
in *La Pietà Rondanini: Il Michelangelo di Milano*, edito da Museo d'arte antica del castello Sforzesco di Milano, (2006) cap. 13, pp. 159-176

10. Caratterizzazione del particolato urbano milanese: risultati preliminari relativi alla frazione carboniosa ed alla distribuzione dimensionale di alcuni metalli

P.Fermo, A. Piazzalunga, S. Gilardoni

La rivista dei combustibili Vol. 60 , fasc. 3-4 230-233, 2006

ANDREA PIAZZALUNGA

[congress comunactions]

1. **Concentration and the chemical characterization of PM10 and PM2.5 in all the Italian territory**
E. Bolzacchini, L. Ferrero, C. Lo Porto, M. G. Perrone, G. de Gennaro, P. Bruno, M. Caselli, P.R. Dambruoso, B.E. Daresta, C.M. Placentino, M. Tutino, M. Amodio, D. Baldacci, M. Stracquadano, L. Tositti, S. Zappoli, D. Gullotto, V. Librando, Z. Minniti, G. Perrini, G. Trincali, S. Becagli, A. Mannini, R. Udisti, C. Paradisi, A. Tapparo, P. Barbieri, L. Capriglia, F. Cozzi, E. Maran, E. Reisenhofer, V. Sicardi, P. Fermo, and A. Piazzalunga
European Aerosol Conference, September 11-15, 2007 – Salisburgo, Austria
2. **Identification of secondary inorganic and organic aerosol components in urban particulate matter samples**
A. Piazzalunga, P. Fermo, C. Rigamonti, R. Vecchi, G. Valli, and V. Bernardoni
European Aerosol Conference, September 11-15, 2007 – Salisburgo, Austria
3. **Fireworks as a source of PM pollution: Results of a case study**
R. Vecchi, G. Valli, V. Bernardoni, A. D'Alessandro, P. Fermo, A. Piazzalunga, S. Nava, M. Chiari, and F. Lucarelli
European Aerosol Conference, September 11-15, 2007 – Salisburgo, Austria
4. **Wood smoke contribution to aerosol concentrations in Northern Italy: Levoglucosan determination by GC-MS and HPAEC-PAD**
P. Fermo, A. Piazzalunga, R. Vecchi, G. Valli, M. A. De Gregorio, and S. Marengo
European Aerosol Conference, September 11-15, 2007 – Salisburgo, Austria
5. **PM10 physical and chemical characterisation using high-time resolved samplings in an air pollution “hot-spot” area in Europe**
R. Vecchi, G. Valli, V. Bernardoni, D. Cricchio, A. D'Alessandro P. Fermo, A. Piazzalunga, C. Rigamonti, S. Nava, F. Lucarelli F. Mazzei, and P. Prati
European Aerosol Conference, September 11-15, 2007 – Salisburgo, Austria
6. **Levoglucosan, a tracer for wood combustion in Milan particulate matter**
A. Piazzalunga, P. Fermo, R. Vecchi, G. Valli, M. A. De Gregorio
X Congresso Nazionale di Chimica dell'Ambiente e dei Beni Culturali, Lecce 11 – 15 giugno 2007
7. **Determinazione di Marker della combustione di Biomassa**
A. Piazzalunga, P. Fermo, M. Cava, R. Vecchi, G. Valli, A. De Gregorio, C. Reschiotto, F. Abballe
Particolato atmosferico dal campionamento all'analisi, Milano06 giugno 2007
8. **Il levoglucosano come tracciante della combustione delle biomasse**
A. Piazzalunga, P. Fermo, C. Leoni, R. Vecchi, G. Valli, M. Di Toro, A. De Gregorio, S. Marengo
XXII Congresso Nazionale della Società Chimica Italiana SCI2006, Firenze 10 – 15 settembre 2006

9. **La componente carboniosa del Particolato Atmosferico (progetto PARFIL 2004-2006)**
A. Piazzalunga, P. Fermo, F. Martino, R. Vecchi, G. Valli, V. Gianelle, G. Mognaschi, C. Belis, O. Cazzuli,
XXII Congresso Nazionale della Società Chimica Italiana SCI2006, Firenze 10 – 15 settembre 2006
10. **La composizione chimica del Particolato Atmosferico nella penisola Italiana, similitudini e analogie**
P. Bruno, M. Caselli, P. R. Dambrosio, B. E. Daresta, G. de Gennaro, C. M. Placentino, M. Tutino, D. Baldacci, M. Stracquadiano, L. Tositti, S. Zappoli, D. Gullotto, V. Librando, Z. Minniti, G. Perrini, G. Trincali, S. Becagli, A. Mannini, R. Udisti, E. Bolzacchini, L. Ferrero, C. Lo Porto, M. G. Perrone, C. Paradisi, A. Tapparo, P. Barbieri, L. Capriglia, F. Cozzi, E. Maran, E. Reisenhofer, V. Sicardi. P. Fermo, A. Piazzalunga
XXII Congresso Nazionale della Società Chimica Italiana SCI2006, Firenze 10 – 15 settembre 2006
11. **Campionamento e composizione chimica del particolato atmosferico (PM10, PM2.5 e PM1) per l'area urbana milanese**
M. G. Perrone, C. Lo Porto, L. Ferrero, G. Sangiorgi, Z. Lazzati, S. Petraccone, E. Bolzacchini, P. Fermo, A. Piazzalunga
SCI2006 (PM2-P-44) Firenze 10 – 15 settembre 2006
12. **Applicazione di metodiche analitiche alla quantificazione delle specie carboniose presenti nel particolato atmosferico (OC, EC, CC e WSOC)**
P. Fermo, A. Piazzalunga, F. Martino, R. Vecchi, G. Valli, A. D'Alessandro
XXII Congresso Nazionale della Società Chimica Italiana SCI2006, Firenze 10 – 15 settembre 2006
13. **Composizione chimica del particolato atmosferico nel sito alpino remoto: Bormio - San Colombano (2.200 m s.l.m.)**
C. A. Belis, P. Fermo, P. Vannini, G. Moraschetti, M. Gurini, G. De Stefani, E. Sesana, A. Piazzalunga
SCI2006 (PM2-P-56) Firenze 10 – 15 settembre 2006
14. **Il Levoglucosano come tracciante della combustione delle legna: quantificazione in campioni emissivi e in campioni di particolato atmosferico**
Andrea Piazzalunga, Paola Fermo, Cristina Leoni, Roberta Vecchi, Gianluigi Valli, Mauro Di Toro, Maria Antonietta De Gregorio, Angelo Giudici, Orietta Cazzuli, Guido Lanzani, Sergio Marengo,
VII Convention Nazionale Ambiente Ricerca Giovani, Montalto di Castro 24 – 27 ottobre 2006
15. **A comprehensive characterization on background atmospheric aerosols: results of an intensive campaign carried out at a high-altitude site in Italy**
R. Vecchi, F. Marengo, M. Chiari, A. D'Alessandro, F. Lucarelli, F. Mazzei, S. Nava, P. Prati, G. Valli, P. Bonasoni, P. Cristofanelli, P. Fermo, A. Piazzalunga
7th International Aerosol Conference September 10-15, 2006 – St. Paul, Minnesota, USA
16. **Identification and estimation of atmospheric aerosol main components: hit the target by means of a single analytical method**

- P. Fermo, A. Piazzalunga, F. Martino, R. Vecchi, G. Valli, A. D'Alessandro
7th Internation Aerosol Conference September 10-15, 2006 – St. Paul, Minnesota, USA
17. **Comparison between TOT and TGA/FT-IR carbon measurements**
P. Fermo, A. Piazzalunga, F. Martino, R. Vecchi, G. Valli, A. D'Alessandro
7th Internation Aerosol Conference September 10-15, 2006 – St. Paul, Minnesota, USA
18. **Atmospheric sampling at a remote site on Italian ALPS**
M.G. Perrone, E. Del Nevo, P. Fermo, L. Ferrero, Z. Lazzati, C. Lo Porto, F. Martino, A. Piazzalunga, F. Pedrielli, S. Petraccone, G. Sangiorgi, and E. Bolzacchini
7th Internation Aerosol Conference September 10-15, 2006 – St. Paul, Minnesota, USA
19. **Caratterizzazione di aerosol atmosferico in un sito remoto ad alta quota: risultati sperimentali di una campagna estiva.**
R. Vecchi, F. Marengo, M. Chiari, M. Ceriani, A. D'Alessandro, F. Lucarelli, F. Mazzei, S. Nava, P. Prati, G. Valli, P. Bonasoni, F. Calzolari, P. Cristofanelli, P. Fermo, A. Piazzalunga
XCII Congresso Nazionale della Società Italiana di Fisica, Torino, 18-23 Settembre 2006
20. **PM mass concentration and chemical composition in the alpine remote site Bormio – San Colombano (N. Italy; 2,200 m a.s.l.)**
C. A. Belis, P. Vannini, G. Moraschetti, P. Fermo, A. Piazzalunga, G. Mognaschi, V. Gianelle and R. Vecchi
AAAS - Advanced Atmospheric Aerosol Symposium - Milan 12-15 November 2006
21. **Set-up of Extraction Procedures for Ions Quantification in Aerosol Samples**
P. Fermo, A. Piazzalunga, R. Vecchi, G. Valli,
AAAS - Advanced Atmospheric Aerosol Symposium - Milan 12-15 November 2006
22. **Assessment of Organic and Elemental Carbon in Atmospheric Aerosol Samples**
P. Fermo, A. Piazzalunga, F. Martino, R. Vecchi, G. Valli, A. D'Alessandro
AAAS - Advanced Atmospheric Aerosol Symposium - Milan 12-15 November 2006
23. **Valutazione della componente inorganica ed organica della frazione sub-micronica del particolato atmosferico in aree urbane.**
R. Vecchi, A. D'Alessandro, P. Fermo, F. Luccarelli, F. Mazzei, S. Nava, A. Piazzalunga, P. Prati, G. Valli
Seminario: *La Cromatografia ionica nell'analisi ambientale: nuove soluzioni*, Milano, 25 gennaio 2006
24. **Determinazione del contenuto ionico nel particolato atmosferico: messa a punto di procedure estrattive**
A. Piazzalunga, P. Fermo, R. Vecchi, G. Valli, V. Gianelle, G. Mognaschi,
VI Convention Nazionale Ambiente Ricerca Giovani, Montalto di Castro 28 novembre – 1 dicembre 2005
25. **Determinazione del contenuto ionico nel particolato atmosferico: messa a punto di procedure estrattive**
A. Piazzalunga, P. Fermo, R. Vecchi, G. Valli, M. Ceriani, V. Gianelle, G. Mognaschi
VI convention Nazionale Ambiente – Ricerca – Giovani, Bologna 28 novembre – 1 dicembre 2005

26. **Assessment of atmospheric organic and elemental carbon in different environments**
P. Fermo, A. Piazzalunga, R. Vecchi, G. Valli, M. Ceriani,
10th EuCheMS International Conference on Chemistry and the Environmental (Rimini – Italy) 4 – 7 settembre 2005
27. **Determinazione della frazione carboniosa (OC ed EC) e del contenuto anionico nel particolato urbano milanese**
A. Piazzalunga, P. Fermo, M. Ceriani, G. Valli, R. Vecchi,
V Convegno Nazionale Ambiente – Ricerca – Giovani. Campobasso 20 – 22 ottobre 2004
28. **Indoor air quality monitoring of particulate matter and aerobiological components: measurements at the Ca' Granda historical archive, Milan (Italy)**
P. Fermo, A. Piazzalunga, R. Vecchi, G. Valli, M. Ceriani, C. Sorlini, E. Zanardini, F. Capitelli
10th EuCheMS International Conference on Chemistry and the Environmental (Rimini – Italy) 4 – 7 settembre 2005
29. **Inquinamento da particolato atmosferico in ambiente museale: il caso della Pietà Rondanini al Castello Sforzesco di Milano**
P. Fermo, A. Piazzalunga, V. Gianelle, G. Mognaschi, M.G. Perrone, E. Bolzacchini, L. Ferrero
10th EuCheMS International Conference on Chemistry and the Environmental (Rimini – Italy) 4 – 7 settembre 2005
30. **Secondary aerosol components contribution in PM₁₀, PM_{2.5} and PM₁: results of a winter time monitoring campaign in Milan (Italy)**
P. Fermo, A. Piazzalunga, M. Ceriani, G. Valli, R. Vecchi,
EAC 2004 – European Aerosol Conference (Budapest, Hungary) 6 - 10 settembre 2004
31. **A TGA/FT-IR study for OC and EC quantification applied to Milan Particulate Matter**
P. Fermo, S. Gilardoni, A. Piazzalunga, M. Ceriani, G. Valli, R. Vecchi, V. Gianelle, E. Bolzacchini, M.G. Perrone, M.L. Lasagni
8th International conference on Carbonaceous Particles in the Atmosphere, 14 - 16 settembre 2004
32. **SPM analysis as a key point in monitoring and assessment of damages to Iranian cultural heritage due to Kuwaiti oil wells fire**
Shahrazad Amin Shirazi, Reza Rahmani, Alberto Ventura, Vorne Gianelle, Paola Fermo, Andrea Piazzalunga
PM 2004 – 1° Convegno Nazionale sul Particolato Atmosferico (Milano –Italia), 12 - 14 maggio 2004
33. **Determinazione del carbonio organico ed elementare a Milano durante due campagne invernali**
Paola Fermo, Andrea Piazzalunga, Stefania Gilardoni, Ezio Bolzacchini, M. Grazia Perrone, Marina Lasagni, Vorne Gianelle, Michela Ceriani, Roberta Vecchi, Gianluigi Valli
PM 2004 – 1° Convegno Nazionale sul Particolato Atmosferico (Milano –Italia), 12 - 14 maggio 2004

Acknowledgment

I would like to acknowledge:

Who has driven this work:

Paola Fermo, Roberta Vecchi, and Gianluigi Valli

Who has joined this work:

Vera Bernardoni, Eleonora Delnevo, and Alessandra D'Alessandro

Claudio Reschiotto

All the colleagues I have met during these years

The students: Chiara Abate, Federico Bianchi, Maria Cava, Cristina Leoni, Fabiola Martino, Carmen Morreale, Mauro Paris, Clara Rigamonti, Francesca Tuccillo

Who helped me

Ferrari Emilio and Ferrari & Nervi s.n.c

Luca Mancini and Noknok s.n.c.

Franco Abballe, Luca Casagrande, Giampiero Ferracin and Dionex s.p.a.